# DIFFERENTIATION OF HUMAN PLURIPOTENT STEM CELLS INTO CORNEAL EPITHELIAL LIKE CELLS

**TATY ANNA BINTI KAMARUDIN**

Doctor of Philosophy

Institute of Genetic Medicine

School of Medical Sciences

Newcastle University

April 2018

# ABSTRACT

Cornea is the clear outermost protective layer of the eye which enables transmission of light onto the retina. The corneal epithelium is regenerated by limbal stem cells (LSCs), whose loss/dysfunction results in limbal stem cell deficiency (LSCD). Transplantations of *ex vivo* expanded autologous LSCs from patient's healthy eye onto the affected eye have provided a successful treatment for unilateral LSCD. This however is not applicable to patient with total bilateral LSCD, whose both eyes are affected. This thesis investigated the potential of human induced-pluripotent stem cell (hiPSCs) to differentiate into corneal epithelial-like cells as a source of autologous stem cell treatment for patients with total bilateral LSCD, and tested the engraftment of the differentiated cells in LSCD mouse model. Combined addition of bone morphogenetic protein 4 (BMP4), all trans-retinoic acid (RA) and epidermal growth factor (EGF) for the first nine days of differentiation followed by cell-replating on collagen-IV coated surfaces with a corneal-specific-epithelial cell media for an additional 11 days, resulted in step wise differentiation of human embryonic stem cells (hESCs) to corneal epithelial progenitors and mature corneal epithelial-like cells. Differences in the ability of hiPSCs lines to undergo differentiation to corneal epithelial-like cells were observed. These were dependent on the level of endogenous BMP signalling and could be restored via activation of this signalling pathway by a specific TGFβ inhibitor (SB431542). The hESC and hiPSCs-derived corneal epithelial cells were transplanted into a LSCD mouse model where they survived up to 14 days, but failed to provide long term engraftment and corneal surface regeneration. The findings showed a differential ability of hESCs and hiPSCs lines to generate corneal epithelial cells which is underlined by the endogenous BMP signalling pathway activity. However, the engraftment and functionality of the differentiated cells in the LSCD animal model has yet to be improved.

To my dearest pillars of strength Mak & Abah

and the beloved diamonds of my heart, lillahi Ta'ala.

Alhamdulillahi robbil aalamin.

# ACKNOWLEDGEMENTS

In the name of God, the most Compassionate, the most Merciful. All the praises and thanks be to God. Deep from my heart I would like to express my endless gratitude for the great time, wisdom, strength and patience granted upon me during the learning process and thesis completion. The whole PhD work was made possible with the opportunity given by the Ministry of Education Malaysia and my employer, Universiti Kebangsaan Malaysia in a form of financial assistance and sponsorship. I would also like to acknowledge the Fund for Women Graduates (FfWG), UK organisation for awarding me with financial assistance during the final stage of my study. Apart from the financial support, the completion of my PhD is largely ascribable to continuous guidance and motivation from my supervisors, my family, my colleagues and friends.

Hereby I would love to thank my supervisors; Professor Majlinda Lako and Professor Francisco Figueiredo who have shared their priceless knowledge and wisdom as guidance, advice, support, encouragement and inspiration to help me learn new things and towards the completion of my study. I am also grateful to have Professor Che Connon and Dr. Annette Meeson for their reviews and feedbacks on my works from time to time. I will always be in debt to Dr. Alex Shortt and Harley Buck from University College London for their skillful and resourceful help in the translation experiments. A huge thank you also goes to the School of Medical Sciences and the Institute of Genetic Medicine, Newcastle University as well as the staffs for the provision of all the useful help and training needed for my project.

I would also like to express my appreciation to all the stem cell research group members, especially Irina Neganova, Min Yu, Sanja Bojic and Joseph Colin for helping me around in the lab from the first day and not to forget, those who have left the stem cell group; Georgios Anyfantis, Gustavo Figueiredo, Chunbo Yang and Lili Zhu. My thankfulness also goes to my fellow PhD students in the group and the institute, especially Minjin Jeong, Nani Latar and Majed Felemban for sharing the wonderful productive PhD years with me.

Last but not the least, my most indebtedness goes to my husband; Muhammad Hafidz Abdul Malik, my sons; Muhammad Ikhwan, Muhammad Luqman and Muhammad Furqan for all the sacrifices they have made during this three and a half year abroad. My special gratitude goes to my beloved parents and family for their inspirational support, my friends and also my dearest family members who have left the world too soon.

# CONTENTS

## LIST OF FIGURES

## LIST OF TABLES

## DECLARATION AND COPYRIGHT STATEMENT

Parts of the material offered have been presented at conferences or submitted and/or published as acknowledged or cited. Some contents of this thesis were taken from published materials where the writer was the first author. Material from the work of others has been acknowledged, and quotations and paraphrases suitably indicated.



Signature:

Date: April 2018

## PUBLICATION, ABSTRACTS AND SEMINARS

### Publication

Kamarudin TA, Bojic S, Collin J, Yu M, Alharthi S, Buck H, Shortt A, Armstrong L, Figueiredo FC, Lako M. Differences in the Activity of Endogenous Bone Morphogenetic Protein Signaling Impact on the Ability of Induced Pluripotent Stem Cells to Differentiate to Corneal Epithelial-Like Cells. Stem Cells. 2018; 36:337–348. https://doi.org/10.1002/stem.2750.

### Abstracts and Seminars

'Differentiation of human-induced pluripotent stem cell into limbal and corneal epithelial lineages'. Oral presentation at North East Postgraduate (NEPG) Conference, Newcastle, 2016.

'Differentiation of hESCs and hiPSCs into corneal epithelium'. Oral presentation at Institute of Genetic Medicine (IGM) Internal Seminar, Newcastle University, 2016.

'Differentiation of human pluripotent stem cells to corneal epithelial lineages'. Oral presentation at Institute of Genetic Medicine (IGM) Internal Seminar, Newcastle University, 2017.

'Differentiation of human-induced pluripotent stem cell into limbal and corneal epithelial lineages'. Sent and accepted for poster presentation at Centre for iPS Cell Research and Application (CiRA) International Symposium, Kyoto, 2017.

## ABBREVIATIONS

| | |
|---|---|
| 0d | 0 day |
| 1d | 1 day |
| 2d | 2 days |
| 2i/3i | two or three types of differentiation inhibiting molecules |
| 2-ME | 2-mercaptoethanol |
| 3D | Three dimensional |
| 3d | 3 days |
| 5i/L | 5 inhibitors/human LIF |
| 5i/L/FA | 5 inhibitors/human LIF/FGF/Activin A |
| A | Adenine |
| ABCB5 | Adenosine tri-phosphate binding cassette B5 |
| ABCG2 | Adenosine tri-phosphate binding cassette G2 |
| Allo-CLET | Allogeneic CLET |
| AM | Amniotic membrane |
| AMD | Age-related macular degeneration |
| AMT | Amniotic membrane transplant |
| ANOVA | Analysis of variance |
| APC | Antigen presenting cells |
| APLM | Acellular porcine limbal matrix |
| ASCs | Adult stem cells |
| BD | Best disease |
| BDNF | Brain-Derived Neurotrophic Factor |
| bFGF | Basic fibroblast growth factor |
| BIOCOSHH | Biological Control of Substances Hazardous to Health |
| BLAST® | Basic Local Alignment Search Tool |
| BMP | Bone morphogenetic protein |
| BMPR | BMP receptor |
| bp | Base pair |
| BSA | Bovine serum albumin |
| C | Cytosine |
| $Ca^{2+}$ | Calcium |
| $CaCl_2$ | Calcium chloride |

| | |
|---|---|
| CAOMECS | Cultured Autologous Oral Mucosal Epithelial Cell-Sheet |
| CCL | C-C Ligand |
| CD | Cluster of differentiation |
| CDM | Corneal differentiation medium |
| cDNA | complementary DNA |
| CECs | Corneal epithelial cells |
| CEM | Corneal epithelium maintenance medium |
| CEPCs | Corneal epithelium progenitor cells |
| CESCs | Corneal epithelial stem cells |
| CFE | Colony forming efficiency |
| CFE | Colony forming efficiency |
| CK | Cytokeratin |
| CLAU | Conjunctival limbal autograft |
| CLCL-lr/lnr | Conjunctival limbal allograft-live related/nonrelated |
| CLET | Cultivated limbal epithelial tansplant |
| CM | Control medium |
| CMV | Cytomegalovirus |
| $CO_2$ | Carbon dioxide |
| Col IV | Collagen IV |
| COMET | Cultured oral mucosal epithelial transplantation |
| COSHH | Control of Substances Hazardous to Health |
| CPPs | Cell penetrating peptides |
| CRISPR–Cas9 | Clustered regularly interspaced short palindromic repeat–CRISPR-associated 9 |
| Cx43 | Connexin 43 |
| CXR | Carboxy-X-rhodamine |
| D | Difference between the two means |
| D20 | Day 20 |
| D9 | Day 9 |
| DAPI | 4',6-diamidino-2-phenylindole |
| DCM | Dilated cardiomyopathy |
| DE | Definitive endoderm |
| DKK1 | dickkopf homolog 1 |
| DKSFM | defined keratinocyte serum-free medium |

| | |
|---|---|
| DM | Differentiation medium |
| DMEM | Dulbecco’s modified Eagle’s medium |
| DMSO | Dimethyl sulphoxide |
| DNA | Deoxyribonucleic acid |
| dNTP | Deoxynucleotide phosphate |
| DPBS | Dulbecco phosphate buffered saline |
| EBs | Embryoid bodies |
| ECM | Extracellular matrix |
| ED | Ectodermal displasia |
| EDTA | Ethylene diaminetetraacetic acid |
| EEC-iPSC | Epidermal epithelium cell derived induced pluripotent stem cell |
| EGF | Epidermal growth factor |
| EGFR | Epidermal growth factor receptor |
| ER | Endoplasmic reticulum |
| ERK | Extracellular signal-regulated kinases |
| ESCs | Embryonic stem cells |
| FA | Formaldehyde |
| FACS | Fluorescence activated cell sorting |
| FBS | Fetal bovine serum |
| FCS | Fetal calf serum |
| FGF | fibroblast growth factor |
| FGFR | fibroblast growth factor receptor |
| FITC | Fluorescein isothiocyonate |
| FSC | Forward scatter |
| G | Guanine |
| GAPDH | Glyceraldehyde-3-phosphate dehydrogenase |
| GDNF | Glial-Derived Neurotrophic Factor |
| GFP | Green fluorescent protein |
| GMEM | Glasgow modified Eagle’s medium |
| GMP | Good manufacturing practice |
| GSK3 | Glycogen synthase kinase-3 |
| HAM | Human amniotic membrane |
| HCl | Hydrochloric acid |
| hESCs | Human embryonic stem cells |

| | |
|---|---|
| hiPSCs | Human induced pluripotent stem cells |
| HLEC | Human limbal epithelial cell |
| hPSC-LESCs | Human pluripotent stem cells derived limbal epithelial stem cells |
| hPSC-RPE | Human pluripotent stem cells derived retinal pigmented epithelium |
| hr | hour |
| ICC | Immunocytochemistry |
| ICM | Inner cell mass |
| IGF2 | Insulin-like growth factor 2 |
| ILV | Interleukin V |
| iPSCs | Induced Pluripotent Stem Cells |
| ISSCR | International Society for Stem Cell Research |
| KGF | Keratinocyte growth factor |
| KLAL | Keratolimbal allograft |
| KOSR | Knockout serum replacement |
| KSFM | Keratinocyte serum-free medium |
| KSR | Knockout serum replacement |
| LB | Lennox L Broth Base |
| LECs | Limbal epithelial cells |
| LESCs | Limbal epithelial stem cells |
| LIF | Leukocyte inhibition factor |
| LSC | Limbal stem cell |
| LSCD | Limbal Stem Cell Deficiency |
| LSCs | Limbal stem cells |
| MAPK | Mitogen-activated protein kinase |
| MDS | Miller-Dieker síndrome |
| MEF | Mouse embryonic fibroblasts |
| MET | Mesenchymal-to-epithelial transition |
| mEpiSCs | mouse epiblast stem cells |
| mESCs | Mouse embryonic stem cells |
| $MgCl_2$ | Magnesium chloride |
| miR-145 | microRNA 145 |
| miRNAs | microRNAs |
| MKOS | c-MYC, KLF4, OCT4 and SOX2 |
| MMC | Mitomycin C |

| | |
|---|---|
| mRNA | messenger ribonucleic acid |
| MSC | Mesenchymal stem cells |
| MSNs | Medium-sized spiny neurons |
| N/n | Number of samples/replicates |
| NCBI | National Centre for Biotechnology Information |
| NEAA | Non-essential amino acid |
| NSG | NOD/SCID/gamma |
| OCT | Optical Coherence Tomography |
| OME | Oral mucosa epithelium |
| OSKM | OCT4, SOX2, KLF4, c-MYC |
| P | Probability |
| PB | Piggyback |
| PBS | Phosphate buffered saline |
| PCR | Polymerase chain reaction |
| Pen/Strep | Penicillin/Streptomycin |
| PET | Polyethylene terephthalate |
| PFA | Paraformaldehyde |
| p-hiPSCs | protein-induced human iPSCs |
| PK | Penetrating keratoplasty |
| PLB | Passive lysis buffer |
| POS | Photoreceptors' outer segments |
| PS | Penicillin/streptomycin |
| qPCR | Quantitative polymerase chain reaction |
| qRT-PCR | Quantitative real-time reverse transcription polymerase chain reaction |
| RA | Retinoic acid |
| rh | Recombinant human |
| rhBMP4 | Recombinant human bone morphogenetic protein 4 |
| rhIGF-1 | Recombinant human insulin-like growth factor 1 |
| RiPSCs | RNA induced pluripotent stem cells |
| RLU | Relative Luminescence Unit |
| rm | recombinant mouse |
| RNA | Ribonucleic acid |
| ROCKi | Rho kinase inhibitor |

| | |
|---|---|
| RP | Retinitis pigmentosa |
| RPE | Retinal pigmented epithelium |
| rpm | Rotation per minute |
| RPMI | Roswell Park Memorial Institute |
| rsPSCs | region-selective pluripotent stem cells |
| RT | Reverse transcription |
| SAA | Severe aplastic anemia |
| SC | Stem cell |
| SCF | Stem cell factor |
| SCNT | Somatic cell nuclear transfer |
| SDIA | Stromal cell-derived inducing activity |
| SDS | Sodium dodecyl sulfate |
| SEAM | Self-formed ectodermal autonomous multi-zone |
| SEM | Standard Error Of Mean |
| Shh | Sonic Hedgehog |
| SJS | Stevens-Johnson syndrome |
| SLET | Simple limbal epithelial transplant |
| SSC | Side scatter |
| SSCE | Sequential sector conjunctival epitheliectomy |
| SSEA | Stage-specific embryonic antigen |
| T | Thymine |
| T reg | Regulatory T cells |
| T3 | Tri-iodothyronine |
| Ta | Annealing temperature |
| TACs | Transient amplifying cells |
| TAE | Tris-acetate-EDTA |
| TALENs | Transcription Activator-Like Effector Nucleases |
| TDC | Terminally differentiated cell |
| TGFβ | Transforming growth factor beta |
| Tm | Melting temperature |
| TNF-α | Tumor necrosis factor alpha |
| TSG-6 | TNF-α–stimulated protein 6 |
| UM | Unconditioned medium |
| UV | Ultra violet |

| | |
|---|---|
| VEGF | Vascular endothelial growth factor |
| VNIM | Ventral neural induction media |
| XF-Ko-SR | Xeno free knock out serum replacement |
| ZFNs | Zinc-finger nucleases |
| ZIKV | Zika virus |

# CHAPTER 1. INTRODUCTION

## 1.1 Limbal Stem Cell Deficiency (LSCD)

LSCD is a disease or condition caused by the loss or dysfunction of LSCs and the failure of limbus barrier function (Ahmad et al. 2010), leading to the loss of corneal epithelial integrity and function, resulting in neovascularisation, persistent pain and severe visual impairment that could progress to blindness (Holmes 2017) (Figure 1.1). Corneal blindness is the fourth leading cause (5.1%) of blindness and a major cause of visual impairment worldwide (Resnikoff et al. 2004, https://www.seeintl.org/corneal-blindness/). In the United Kingdom alone, it is estimated that 2.7 million people will be affected by sight loss by 2030, and LSCD is one of the contributing conditions that caused the poor vision (http://www.rnib.org.uk/nb-online/eye-health-statistics, The State of the Nation: Eye Health 2016).

In a case such as a severe trauma, the damage to LSCs niche will tip-off the balance in the growth/differentiation/survival factors as well as the changes in environment will trigger the undamaged LSCs to differentiate into early TACs. This or any events that will reduce the LSCs in the site of trauma or disrupt the maintenance of growth and survival factors may result in LSCs deficiency (LSCD) (Stepp and Zieske 2005). LSCD can be classified into diffuse or partial and unilateral or bilateral, depending on the extent of limbal involvement (Lal et al. 2016).

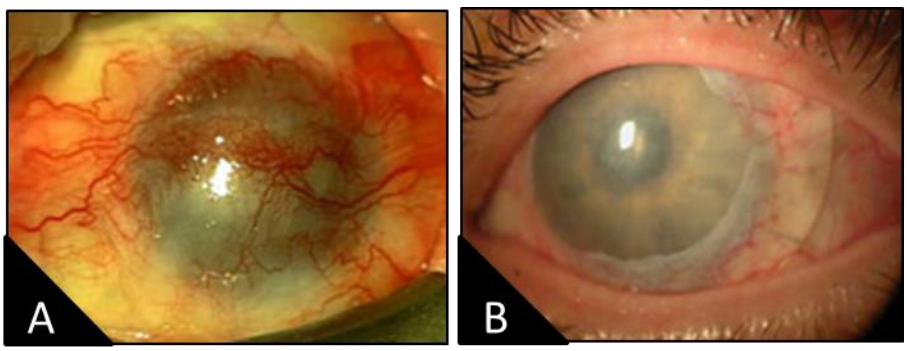


**Figure 1.1 : Bilateral limbal stem cells deficiency, before treatment (A), and after treatment (B). Photos reproduced from online source at http://www.osref.org/medical-education-materials/limbal-stem-cell-deficiency-amt.aspx.**

Partial LSCD affects only a section of limbus in an eye and the other region is spared, unlike diffuse LSCD that affect entire limbal are of the eye. Unilateral LSCD is affecting only one eye and the other eye is healthy, whilst both eyes are affected in bilateral LSCD (Dua et al. 2000). The healthy eye in partial or unilateral condition will be the main and best source for the treatment of LSCD affected eye. Bilateral total LSCD such as in Stevens-Johnson syndrome (SJS) patients could cause ocular surface diseases that lead to bilateral blindness (Gomes et al. 2003). Unlike in partial or unilateral LSCD, patients with bilateral total LSCD have both their eyes devoid of LSCs needed for *ex vivo* expansion that could subsequently used for transplantation (Osei-Bempong et al. 2013).

### 1.1.1 *Causes of LSCD*

The visual impairments resulted from LSCD alone has many common contributing factors. Those contributing factors could be classified into primary; related to hereditary and congenital abnormalities such as aniridia and epidermal dysplasia, secondary; that includes acquired factors from external environment that destroy and unable to nurture the LSCs such as chemical/thermal burns, multiple surgeries, Stevens-Johnson syndrome (SJS), ocular cicatricial pemphigoid, and idiopathic; where the exact cause of LSCD is unknown such as contact lens use and malignancy (Pfister 1994, Dua et al. 2000, Sevim and Acar 2013, Lal et al. 2016). The above factors will result in the LSCs niche destruction that in turn causes limbal dysfunction.

### 1.1.2 *Symptoms and diagnosis of LSCD*

Patients with LSCD might experience chronic eye inflammation and redness, tearing, decreased vision, photophobia and recurrent pain, present with varied corneal epithelium thickness and transparency. Those patients might also develop ingrowth of thickened fibro-vascular pannus, chronic keratitis, scarring and calcification as well as perforation of the cornea (Huang and Tseng 1991, Chen and Tseng 1991, Dua et al. 2000). The diagnosis of LSCD is mainly based on the patients' symptoms and clinical signs (such as stated above) whilst the management plans are crucially depending on its diagnosis. Impression cytology, immune-histochemical assessment and *in vivo* confocal microscopy of the corneal surface could then be performed to confirm the diagnosis of LSCD. Those techniques will allow detection of mucin containing conjunctival goblet cells on the corneal surface rather than the normal CK3 expressing corneal epithelium as well as the presence of inflammatory cells (Egbert et al. 1977, Kenyon et al. 1990, Araújo et al. 2013).

### 1.1.3 *Management of LSCD*

Inflammation of the ocular surface is a common condition accompanying LSCD at its acute stage. It is important to control the inflammatory reactions on the eye using local or systemic immune-modulation to restore the limbal microenvironment before advancing to more specialised treatment such as corneal transplant (Lal et al. 2016). Managements of LSD in general range from conservative to invasive treatment depending on the LSCD severity. Various studies have also significantly contributed to the development of new conservative as well as surgical treatments of LSCD (Haagdorens et al. 2016).

Conservative management can be applied to partial LSCD where the visual axis is not affected. The conservative treatment could range from the use of amniotic membrane patch, bandage contact lenses, topical lubricant and anti-inflammatory agents to promote corneal and limbal re-epithelialisation (Kheirkhah et al. 2008, Romero-Rangel et al. 2000). However, in the case of compromised visual axis where the corneal surface is invaded by conjunctival tissue, surgery is the treatment of choice. The conjunctival tissue needs to be removed to allow the regrowth of corneal epithelium (Dua et al. 1994) and amniotic membrane transplant (AMT) is commonly carried out to help the healing process.

Unilateral LSCD that is diffuse needs to be treated surgically by transplantation of LSCs following the removal of any fibrovascular tissue or pannus formed. This could be carried out by direct keratolimbal autograft or by expanding the autologous LSCs from the healthy other eye before transplanting them back into the LSCs deficient eye (e.g: Holoclar) (Shortt et al. 2007, Kolli et al. 2010, Behaegel at al. 2017). This treatment however is not applicable to a significant number of patients with bilateral total LSCD. In contrast, patients with bilateral total LSCD have both their eyes affected, thus could only be treated with limbal transplant from living related or cadaveric donated corneas i.e. allogeneic transplant. Unfortunately, this type of management is becoming harder as there is global shortage of donated cornea for the transplant (Gain et al. 2016) and offers poor long-term outcome due to rejection (Bhalekar et al. 2013) and failure, as demonstrated in a report of 13 cases with 100% failure after 3 years (Shortt et al. 2014). The management strategies for LSCD are summarised in Table 1.1.

| **Acute stage** | **Chronic stage** | | | |
|---|---|---|---|---|
| **Topical steroids** | **Unilateral partial** | **Unilateral diffuse/total** | **Bilateral partial** | **Bilateral diffuse/total** |
| Topical lubricants<br>AMT<br>PK | Conservative management<br>Scleral contact lens<br>SSCE<br>AMT | CLAU<br>CLET<br>SLET<br>KLAL (one eyed)<br>Allo-CLET | CLET<br>Allo-CLET<br>KLAL | CLAL-lr/lnr<br>KLAL<br>Allo-CLET<br>Keratoprosthesis |
| PK=penetrating keratoplasty, SSCE=sequential sector conjunctival epitheliectomy, AMT=amniotic membrane transplant, CLAU=conjunctival limbal autograft, SLET=simple limbal epithelial transplant, CLET=cultivated limbal epithelial tansplant, Allo-CLET=allogeneic CLET, KLAL=keratolimbal allograft, CLAL-lr/lnr=conjunctival limbal allograft-live related/nonrelated | | | | |

**Table 1.1 : Strategies of LSCD management. Adapted from Lal et al. 2016.**

While other autologous epithelial cell sources were explored for corneal trans-differentiation for bilateral total LSCD treatment, oral mucosa epithelium (OME) was found to be one of the best sources, as it shares various characteristics with the corneal epithelium (Kolli et al. 2014). The surgical procedure that uses OME to treat LSCD is called the cultured oral mucosal epithelial transplantation (COMET) (Ma et al. 2009, Eslani et al. 2012). Nishida et al. used autologous OME grown on feeder cells for the treatment of bilateral LSCD in 2004. However, mild opacity and persistence of blood vessels was still observed in all transplanted corneas at 13 – 15 months follow up, thus necessitating new scientific and clinical approaches (Nishida et al. 2004).

A decade later, Kolli et al. reported successful transplantation of *ex vivo* expanded autologous multi-layered OME using a fully compliant good manufacturing practice, feeder- and animal product-free method on two patients with bilateral LSCD (Kolli et al. 2014). Although the above mentioned studies reported some degree of patients' visual improvement during the early follow-ups, both teams still observed neovascularisation at later follow-ups. More recent studies with longer follow-up durations reported high success rate of LSCD treatment via COMET, despite some graft rejection and additional surgery needed post-transplant (Baradaran-Rafii et al. 2017, Prabhasawat et al. 2016). A summary of previous clinical studies that used COMET for LSCD treatment is shown in Table 1.2.

| Reference | Eye diseases / conditions treated | Follow-up duration | Outcome |
|---|---|---|---|
| Baradaran-Rafii et al. 2017 | Bilateral total LSCD due to chemical burn | 14 - 40 months | Following COMET, the overall and rejection-free graft survival rates are 92.9 and 69.2%, respectively. 13 from 14 eyes had stable ocular surface covered by transparent epithelium without significant neovascularization |
| Prabhasawat et al. 2016 | Bilateral LSCD of any cause | 8 – 50 months | 14 from 20 eyes (70 %) exhibited improvement in visual acuity after COMET, and some eyes required subsequent cataract surgery, penetrating keratoplasty, or keratoprosthesis implantation. |
| Dobrowolski et al. 2015 | Aniridia patients who underwent autologous cultivated epithelium transplantation | 12 – 18 months | At the end, 76.4% of the eyes had regular transparent epithelium and 23.5% had developed epithelial defects or central corneal haze; in 88.2% of cases visual acuity had increased. (13 patients; 17 eyes) |
| Gaddipati et al. 2014 | Alkali burn-induced bilateral total LSCD | 11 to 13 months | Transplanted OME cells survived and reconstructed the ocular surface, transformed into stratified epithelium with vasculatures and acquire some of the corneal epithelial-like features. |
| Kolli et al. 2014 | Bilateral total LSCD | 24 months | Successful reversal of LSCD within the follow up period |
| Kocaba et al. 2014 | Bilateral LSCD | 18 to 48 months | Cultured Autologous Oral Mucosal Epithelial Cell-Sheet (CAOMECS) technology demonstrated the presence of a functional epithelium over the long term for 62.5% of the patients. |

| | | | |
|---|---|---|---|
| Burillon et al. 2012 | Bilateral total LSCD | 15, 30, 60, 90, 180 and 360 days | Following a CAOMECS graft, 5 of 23 patients showed reconstructed corneal epithelium without ulcers or neovessels |
| Dobrowolski et al. 2011 | Aniridia or chemical burn related LSCD | 6 to 12 months | 76.4 % of eyes showed stable epithelium and 23.5 % of eyes corneas remained cloudy due to recurrent conjunctival neovascularization or stromal haze |
| Ma et al. 2009 | Alkaline or thermal burn LSCD | 26 to 34 months | Cornea surface was completely reepithelialized in 3–10 days in all but one patients. |
| Chen et al. 2009 | Alkaline or thermal burn LSCD | 10 to 22 months | Cultivated OMECs exist for long term on the cornea after COMET |
| Inatomi et al. 2006 | SJS and chemical eye injury | 22.5 months | The surviving OME consisted of irregular, nonkeratinized, stratified epithelium without goblet cells expressing K3 but not K12. |
| Nishida et al. 2004 | Bilateral LSCD | 13 to 15 months | Mild opacity and persistence of blood vessels observed in all transplanted corneas |

**Table 1.2 : Several clinical studies on LSCD treatment with COMET.**

### 1.1.4 *The need of alternative cellular source for LSCD treatment*

Various limitations in bilateral total LSCD treatment using COMET or allogeneic cells have made researchers to turn to human embryonic stem cells (hESCs) and human induced-pluripotent stem cells (hiPSCs) as potential alternative treatment sources. To date there are a handful of papers on corneal epithelium differentiation using both hESCs and hiPSCs. Those two PSCs were cultured in different conditions and supplements given at different time points during the specially defined differentiation condition and period to produce high percentage of corneal epithelial lineages cells or 3D corneal organoids (Zhang et al. 2017, Foster et al. 2017). There is however no good manufacturing practice (GMP) compatible protocols for robust hESCs and hiPSCs derived corneal epithelium differentiation that reflects in functional corneal epithelium or LSCs to be used clinically to date. The following Table 1.3 summarises the *in vitro* PSC differentiation studies that were referred to while designing our project.

| Differentiation method | Medium & supplements | Cell line(s) | Outcomes & Authors | Remarks / Points taken |
|---|---|---|---|---|
| Monolayer on collagen IV coated dish | Limbal fibroblasts conditioned epithelial medium supplemented with fetal calf serum (FCS) | hESCs lines (hES-NCL1, H1) | CK3/12 were expressed in the first and second week after differentiation induction, and declined thereafter. Ahmad et al. 2007 | Monolayer differentiation method and collagen IV coated surfaces and time points used |
| Monolayer on feeder | Cells were grown in DMEM/F-12, 15% KOSR, NEAA, mercaptoethanol. BMP4 was added for 3 days and cells were cultured in 90% DMEM/F-12, FBS, NEAA, and mercaptoethanol or in 60% DMEM, 30% Ham's F-12 medium, and FBS supplemented with insulin, hydrocortisone, ascorbate, and EGF. | mESCs | Ectodermal cell (K8/K18+) are produced in large numbers, some of them become keratinocytes (K5/K14+) after addition of serums. Aberdam et al. 2007 | BMP4 supplementation drives cells differentiation away from neural |
| hiPSCs were grown on collagen-IV coated plates | Corneal fibroblasts or limbal fibroblasts conditioned | hiPSCs from hair follicle keratinocy | Expression of ΔNP63 and K14 peaked at day 8, while markers of | Monolayer differentiation method and collagen IV |

| | | | | |
|---|---|---|---|---|
| | medium added with epithelial media contained DMEM/F12, FCS, insulin, hydrocortisone, EGF, adenine, and cholera toxin. | tes and dermal fibroblasts | terminally differentiated corneal epithelium (K3, K12) peaked at day 14. 20%–25% of the cell population was K14+ progenitor cells, while most (>90%) cells expressed K3 at day 14. Shalom-Feuerstein et al. 2012 | coated surfaces, markers (ΔNP63, K3, K12) and time points used |
| Monolayer on Matrigel coated plates | Cells were cultured for preplacodal ectoderm, neural and epidermal differentiation using various conditions. | hESCs (H9) | Seeding density (1.7–2.0 $\times 10^4$ cells/cm$^2$) with a 3-day pre-differentiation to reliably produce about 70% of pre-placodal (SIX1+) cells in the cultures. Leung et al. 2013 | Cell density for seeding, Matrigel coated plates, cell disassociation using Accutase, differentiation start point and ROCKi used in for replating |
| Three dimensional cell aggregates and replating on collgen IV coated plates | Induction: CnT-30, serum-free and xeno-free RegES-, RegES− medium supplemented with SB-505124, IWP-2, human bFGF | hiPSCs and hESCs lines | Up to 95% of cells were p63+ after 5 weeks of differentiation. Corneal epithelial-like cells were obtained upon further maturation. Mikhailova et al. 2014 | hiPSCs used, SB505124 and IWP-2 supplementation |
| Cell spheres formation and single- | Ectodermal induction: low glucose DMEM, | SSEA4+ and SSEA4- | During ectodermal induction, mRNA levels of p63 and | BMP4, RA and EGF supplementation |

| | | | | |
|---|---|---|---|---|
| cell suspensions on matrigel coated plates | RA, BMP4, EGF. Corneal epithelial differentiation medium: low glucose DMEM/F12 (3:1), FCS, PS, hydrocortisone, insulin, tri-iodothyronine, adenine, EGF | limbal fibroblasts or bone marrow mesenchymal stem cells | CK8 were highest levels between days 3 and 5. By day 9 of corneal epithelial differentiation, the majority of SSEA4+ cells exhibited epithelial morphology and CK3 and CK12 were expressed only in the SSEA4+ subgroups. Katikireddy et al. 2014 | with low glucose DMEM/F12 medium and markers (K8) used |
| Monolayer on LN511E8-coated dishes with serial pipetting during each differentiation stages | Differentiation medium (DM); GMEM supplemented with KOSR, sodium pyruvate, NEAA, l-glutamine, PS and 2-ME or monothioglycerol and Noggin or LDN-193189. Corneal differentiation medium (CDM); DM and Cnt-20 or Cnt-PR (w/o; EGF and FGF2) (1:1), KGF, Y-27632 and PS. | hiPSCs lines 201B7, 253G1, 454E2, 1231A3 and 1383D2 | Ocular cells were generated from a self-formed ectodermal autonomous multi-zone (SEAM). At day 40 of differentiation, cells in zone 3 were unique with its PAX6/p63-double-positive phenotype, representative of ocular surface ectoderm as well as K18, and E-cadherin. Approximately 99% of the cells expanded from zone 3 were stratified K14+ | Monolayer differentiation method and CnT-PR medium for corneal differentiation |

| | | | | |
|---|---|---|---|---|
| | Corneal epithelium maintenance medium (CEM); DMEM/F12 (2:1), B27, PS, KGF and Y-27632. | | epithelial cells, 95% were of corneal epithelial lineage (SSEA-4+), and 70% were differentiated corneal epithelial cells (K12+). Hayashi et al. 2016. | |

**Table 1.3 : Summary of various studies on corneal and limbal epithelial differentiation using human stem cells.**

### 1.2 Human stem cells

Stem cells are undifferentiated cells with potential to differentiate into specialized cells and with extended self-renewal capacity (Walia et al. 2012). There are three broad types of stem cells: i) embryonic stem cells (ESCs), which are isolated from the inner cell mass (ICM) of a blastocyst; ii) adult stem cells (ASCs), that are found in various tissues such as bone marrow, blood and adipose tissue; and iii) induced-pluripotent stem cells (iPSCs), that are reprogrammed from adult differentiated somatic cells such as fibroblasts (Yu et. al. 2007).

ESCs can differentiate under defined *in vitro* and *in vivo* conditions, into the cells of all the three germ layers; namely the ectoderm, endoderm and mesoderm hence they fall under the category of pluripotent stem cells. In an adult, the ASCs act as a repair system for the body, replenishing the adult specialized tissues and also maintaining the normal turnover of regenerative organs, such as blood, skin, or intestinal tissues (Wobus and Boheler 2005). However, the differentiation potential of ASCs is more limited when compared to ESCs, and for this reason they are named multipotent, or unipotent depending on the number of cell types they can differentiate to make up our organs. iPSCs, on the other hand, are reprogrammed to become pluripotent. This pluripotency allows these reprogrammed cells to differentiate into various cells based on the conditions and factors that are supplemented to the iPSCs (Sugawara et al. 2012).

Potency of stem cells specifies the cells' differentiation potential. It ranges from totipotent down to unipotent, which can be seen in progenitor cells (Figure 1.2). Totipotent stem cells can differentiate into both embryonic and extraembryonic cell types. Such cells can form a complete,

viable organism. These cells are produced from the fusion of an egg and sperm cell: e.g. fertilised zygote. Pluripotent stem cells are the descendants of totipotent cells and can differentiate into nearly all cells that derived from any of the three germ layers, such as human embryonic stem cells (Baker and Pera 2018). Multipotent stem cells can differentiate into a number of cell types, but only those of a closely related family of the cells, for example the haemopoietic stem cells. Unipotent cells however, can produce only one cell type, their own, but have the property of self-renewal, which distinguishes them from non-stem cells. Some examples of these cells are progenitor cells, corneal epithelial stem cells and muscle stem cells (Wobus and Boheler 2005).

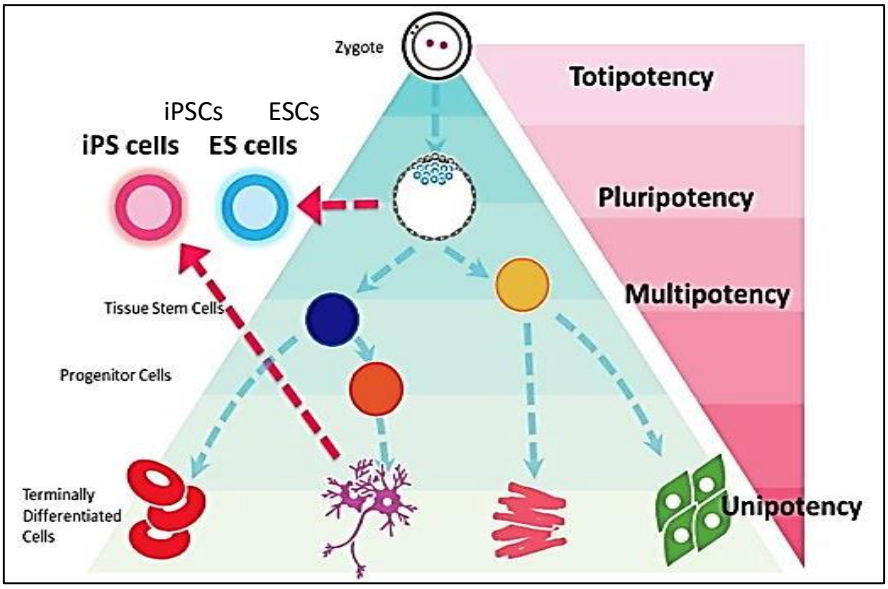


**Figure 1.2 : Hierarchical potential of stem cells. Adapted from Sugawara et al. 2012.**

The ESCs lines have been used in a wide range of medical research. However, there are always some ethical issues that come with the human ESCs (hESCs) studies especially in its conventional acquisition methods that involved the destruction of developing human embryos (Thompson et al. 1998). Despite that, they are still considered as one of the promising candidates for future therapies especially in regenerative medicine based on several previous and on-going clinical trials such as the Geron study on spinal cord injury and the Advanced Cell Technology trials on Stargardt's Macular Dystrophy, wet and dry age-related macular degeneration, diabetes type 1 and heart failure (Wobus and Boheler 2005, Schwartz et al. 2012, Schulz 2015, Ilic et al. 2015).

Advancement in medical research have enabled the culture of ASCs and their differentiation into cells with specialized characteristics, which is consistent with cells of various tissues such

as muscles, skin or nerves. The resulting autologous stem cell therapy has a great potential without the issues of rejection (Walia et al. 2012). ASCs are now extensively used in research and medical therapies, for example in bone marrow and cornea transplantation as well as wound healing (Koizumi et al. 2001, Sasaki et al. 2008). Since ASCs are only multipotent or unipotent, its differentiation potential and applications are more limited compared to the hESCs.

Since the publication of Yamanaka team's work in 2007, an increasing number of publications have focused on reprogramming the adult differentiated somatic cells from human to produce human iPSCs (hiPSCs). Other than its easily available source, the hiPSCs method avoids the debatable ethical issues for its acquisition despite its remarkable similarities to hESCs (refer to Table 1.4) (Yamanaka 2012).

| **Features** | **hESCs** | **hiPSCs** |
|---|---|---|
| Cells of origin | Inner cell mass (ICM) cells of an embryo | Differentiated somatic cells |
| Characteristic morphology | High nuclear to cytoplasm ratio, prominent nucleoli | High nuclear to cytoplasm ratio, prominent nucleoli |
| Cell culture growth | Compact flat colonies with distinct edges | Compact flat colonies with distinct edges |
| Gene expression | *NANOG, OCT4, SOX2, LIN28, c-MYC, hTERT, KLF4, GDF3, REX1, FGF4, TDGF1, NODAL, DPPA4, EBAF, GRB7, LEFTB, ESG1* | *NANOG, OCT4, SOX2, LIN28, c-MYC, hTERT, KLF4, GDF3, REX1, FGF4, TDGF1, NODAL, DPPA4, EBAF, GRB7, LEFTB, ESG1* |
| Acquisition method | Derived from the ICM of fresh or frozen embryos at the blastocyst stage, somatic cell nuclear transfer (SCNT) | Derived by reprogramming of somatic cells to a pluripotent state through overexpression of a key set of transcription factors, cell lines can be easily derived from cells with variety of genetic backgrounds |
| Surface markers | SSEA-1, SSEA-3, SSEA-4, TRA-1-60, TRA-1-81 | SSEA-3, SSEA-4, TRA-1-60, TRA-1-81, TRA-2-49/6E |
| Epigenetic memory | Not applicable, as it is derived from embryo | May retain the epigenetic marks from the cells of origin after differentiation |

| | | |
|---|---|---|
| Self-renewal capacity | Highly efficient, show high telomerase activity | Highly efficient, show high telomerase activity |
| Developmental potential | Able to form embryoid bodies (EBs) and differentiate into all the three germ layers tissues, form teratomas if injected into immune compromised mice, also could form interspecies (with mouse) chimaera *in vivo* | Able to form EBs and differentiate into all the three germ layers tissues, form teratomas if injected into immune compromised mice, also could form interspecies (with mouse) chimaera *in vivo* |
| Function / Aplication | Development and differentiation of human tissue, new drug discoveries, but difficult to generate patient-specific cells for transplantation and patient specific therapies | Research on human tissue/organ development and differentiation, patient specific cell lines generated easily, personalised cell transplants with no immune rejection problems, new and personalised drug development, disease modelling |

**Table 1.4 : The characteristic features of hESCs and hiPSCs (Adapted from Mascetti and Pedersen 2016, Narsinh et al. 2011, Takahashi et al. 2007 and Yu et al. 2007).**

The most exciting quality of hiPSCs is that it could escape the immune matching or rejection problems when it comes to therapeutic application (Wang et al. 2011). Although the hESCs and hiPSCs hold promises for various medical innovations, there is a phenomenon that could affect their basic cellular manipulation, called dissociation-induced apoptosis (Ohgushi and Sasai 2011). This condition was found to be related to Rho kinases (ROCK) activity that regulates apoptosis via myosin hyperactivation in dissociated PSCs while maintaining their metastable states of pluripotency (Ohgushi et al. 2010). This problem was solved by Watanabe in 2007, via the inhibition of ROCK and allowing the dissociated PSCs to be maintained in adherent and suspension cultures (Watanabe et al. 2007).

### 1.2.1 *Human embryonic stem cells (hESCs)*

Human embryonic stem cells (hESCs) are pluripotent stem cells derived from the ICM of an early-stage embryo (Baker and Pera 2018). Human embryos reach the blastocyst stage 4–5 days post fertilisation, at which time they consist of 50–150 cells. hESCs can give rise to all the derivatives of the three primary germinal layers; they have the potential to differentiate into more than 200 cell types of the adult body when given sufficient and necessary stimulation for

a specific cell type. They are also capable of unlimited proliferation in vitro (Thomson et al. 1998). However, these cells are conventionally derived from embryos produced by *in vitro* fertilisation and allowed to proceed to blastocyst stage, thus the acquisition process involved the disruption of otherwise living embryo (Thompson et al. 1998). Due to this acquisition method, the ethical debates on the hESCs related research are still going on to date (King and Perrin 2014). In line with this issue, recent research advancements have made it possible to acquire hESCs via somatic cell nuclear transfer (SCNT) method (Figure 1.2). A mature somatic cell is fused to an enucleated oocyte to generate a one-cell embryo which then is allowed to develop into blastula stage (Condic and Rao 2008, Wang and Gurdon 2013). Recently, this SCNT method had successfully applied to clone monkeys that could be used for future animal and disease modelling in primates (Liu et al. 2018).

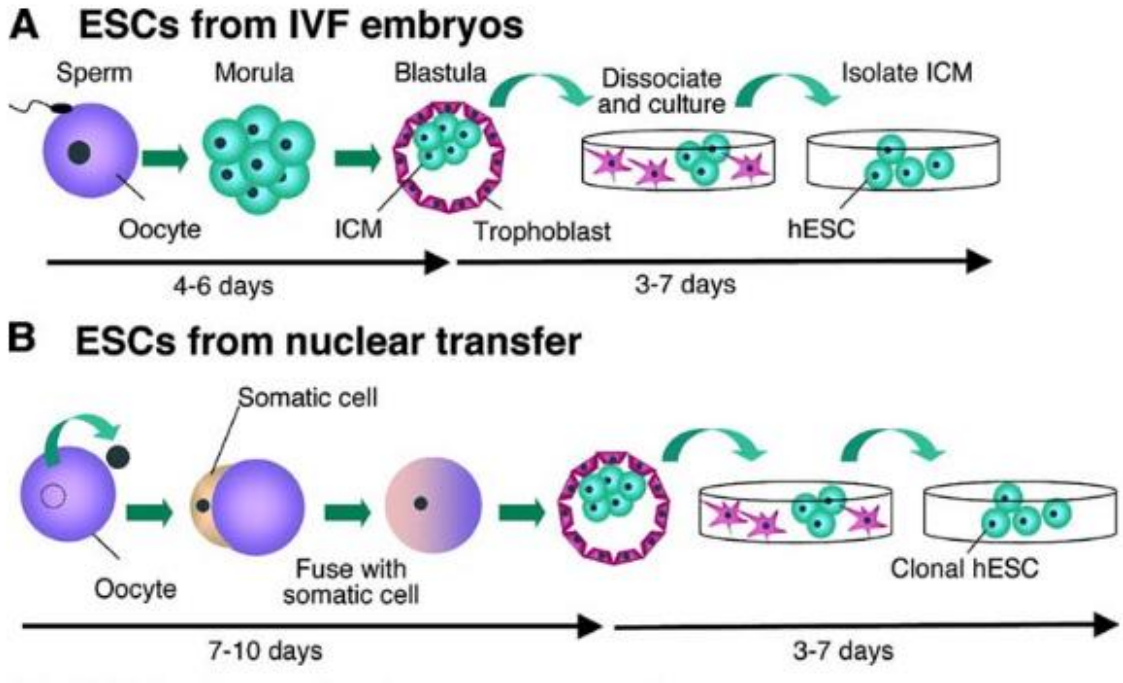


**Figure 1.3 : Methods for the derivation of hESCs. Adapted from Condic and Rao 2008.**

Mouse embryonic stem cells (mESCs) were derived more long before the naïve pluripotent state of ESCs was discovered (Martin 1981, Nichols and Smith 2009). mESCs could either derived from the ICM of pre-implantation or post-implantation mouse embryo and these methods of acquiring ESCs will produce a naïve pluripotent (i.e: mESCs) or a primed state of stem cells respectively (Figure 1.4). The mESCs in the primed pluripotent state which is more differentiated compared to the naïve are called the mouse epiblast stem cells (i.e: mEpiSCs) (Brons et al. 2007, Tesar et al. 2007). The naïve state of mESCs is maintained *in vitro* via the use of two or three types of differentiation inhibiting molecules (2i/3i) to inhibit fibroblast

growth factor receptor (FGFR), mitogen-activated protein kinase/extracellular signal-regulated kinases (MAPK/ERK) and glycogen synthase kinase-3 (GSK3) (3i) or MAPK and GSK3 (2i) in combination with or without leukocyte inhibition factor (LIF) (Olariu 2013).

Nearly two decades later, hESCs were successfully derived using the preimplantation method (Thomson et al. 1998). Although the hESCs were derived during pre-implantation stage, their pluripotent state was found to be more similar to those of mEpiSCs, which is primed pluripotency (Nichols and Smith 2009). hESCs share more similarity to mEpiSCs rather than mESCs in term of their colony morphology, growth-factor responses, gene expression pattern and inactivation status of the X chromosome (Ohgushi and Sasai 2011).

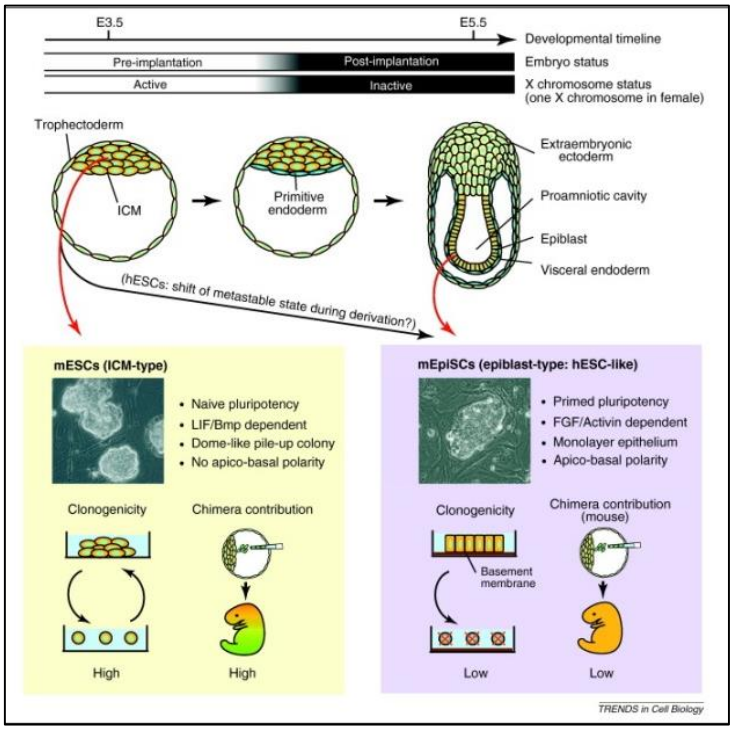


**Figure 1.4 : Schematic picture of the origins and properties of the mouse pluripotent stem cell lines, mESCs and mEpiSCs. Adapted from Ohgushi and Sasai 2011.**

However, the primed pluripotency status of hESCs can be reverted back to the naïve state by ectopic induction with the combination of *OCT4, KLF4, KLF2, LIF, GSK3β* inhibitor and mitogen-activated protein kinase pathway inhibitor (Hanna et al. 2010) or provision of 5i/L supplemented with fibroblast growth factor (FGF) and Activin A (5i/L/FA) (Theunissen et al. 2014). Unfortunately, this interconversion of primed and naïve states has a time limitation of about 24 - 48 hours for safeguarding the DNA methylation integrity of the cells (Martello and Smith 2014, Weinberger et al. 2016). Recently, the two pluripotent states of hESCs were

defined via specific molecular markers that could determine the human PSC state (Collier et al. 2017).

During terminal differentiation process, the lineage-specific markers for naïve hESCs were upregulated, but their ability to undergo terminal differentiation towards functional cell types is limited compared to primed hESCs (Warrier et al. 2016). The naïve hESCs could also differentiate into primed hESCs by supplementation of medium containing serum and FGF (Theunissen et al. 2014). The hESCs in the primed state was also reported to be efficiently changed into another alternative pluripotent state called region-selective pluripotent stem cells (rsPSCs) via changes in the culture conditions. These alternative rsPSCs unlike hESCs, are capable of forming post-implantation interspecies chimaeric embryos (Wu et al. 2015). The different characteristics of the naïve and primed pluripotency, based on murine cells are summarised in Table 1.5 below.

| **Naïve pluripotent stem cells** | **Primed pluripotent stem cells** |
|---|---|
| Efficiently repopulate the host's ICM and contribute to chimaeric embryos | Form differentiated teratomas, inefficient in repopulating the ICM when injected into host blastocysts |
| Maintain both x-chromosomes in active state (XaXa) in female cells | Predominantly undergone x-chromosome inactivation (XiXa) |
| Refractory potential to differentiate into primordial germ cells in vitro | Readily differentiate into primordial germ cells in vitro |
| Can be cloned with high efficiency | Intolerance to single cells passaging |
| Grow as packed domed colonies | Grow as flattened colonies |
| Stabilised by LIF/Stat3 and destabilised by bFGF and TGFβ/Activin signalling | Depend on bFGF and TGFβ/Activin signaling |
| Showed better differentiation into endoderm and mesoderm | Better ability to differentiate into neuroectoderm |

**Table 1.5 : The characteristics of naïve and primed pluripotent stem cells (Nichols and Smith 2009, Hanna et al. 2010).**

The hESCs, being pluripotent, require both paracrine and autocrine signals to proliferate and maintain their pluripotency (Pyle et al. 2006, Schatten et al. 2005, Amit et al. 2000). Specific signals and conditions are also pertinent for efficient differentiation of hESCs into specific

differentiated cells lineages. Their differentiation outcome is influenced by various endogenous factors such as its growth, methods of handling, epigenetic modifications (Hoffman et al. 2005), transcriptional profiles (Abeyta et al. 2004, Bhattacharya et al. 2004), and sensitivity to various conditions of hESCs population itself, as well as exogenous factors, for example the culture media composition and the method of differentiation induction (Kitsberg 2007, Bauwens et al. 2008). Some exogenous factors (noggin and bFGF) were reported to maintain the hESCs pluripotency, while others (miR-145, BMP) repress pluripotency and induce differentiation process (Xu et al. 2005, Xu et al. 2009). Some of the hESCs differentiation experiments are listed in Table 1.6 below.

| **Culture conditions** | **Differentiated cells / tissue** | **References** |
|---|---|---|
| hESC colonies were transferred into petri dishes precoated with collagen IV (coll-IV) in medium containing Dulbecco's modified Eagle's medium (DMEM)/Ham's F12 (F12), fetal bovine serum (FBS), non-essential amino acid (NEAA), penicillin, streptomycin (PS), SCF, vascular endothelial growth factor (VEGF), and basic fibroblast growth factor (bFGF). Differentiation was performed with similar efficiency in knockout serum replacement (KOSR) with the addition of heparin, bone morphogenetic protein 4 (BMP4), stem cell factor (SCF), VEGF, activin A, bFGF followed at day 4 by TGFβ1. | Endothelial cells expressing immunological markers (vWF, CD105), specific genes (VE-cadherin, KDR, GATA-2, GATA-3, eNOS), and formed cord-like structures on collagen matrix | Lagarkova et al. 2008 |
| Differentiation induction with combinations of activin A, BMP4, bFGF, VEGF and dickkopf homolog 1 (DKK1) in serum-free media | Cardiovascular progenitor cells that differentiate further to generate greater than 50% contracting cardiomyocytes | Yang et al. 2008 |
| hESCs derived endoderm cells were cultured on mouse embryonic fibroblasts (MEF), treated with Wnt3a + activin A in advanced RPMI supplemented with L- | Pancreatic lineage cells | Chen et al. 2009 |

| | | |
|---|---|---|
| glutamine and PS for 1 d, then activin A in advanced RPMI supplemented with L-glutamine, PS and FBS. Medium was changed 2 d later to FGF10 + KAAD-cyclopamine in advanced RPMI supplemented with L-glutamine, PS and FBS, and maintained for 2 d. Cells were transferred to FGF10 + KAAD-cyclopamine + retinoic acid in DMEM supplemented with L-glutamine, PS and B27 and cultured for 4 d. Differentiation to endocrine or exocrine cells: the ILV-treated populations were cultured in DMEM/F12 supplemented with N2, albumin fraction V and bFGF for the first 4 d. Nicotinamide was added and maintained for 8 d, changing the medium every 3 d. | | |
| Nanoscale ridge/groove pattern arrays constructed using UV-assisted capillary force lithography. The dimension and alignment were finely controlled over a large area. hESCs seeded onto the 350-nm ridge/groove pattern arrays in the absence differentiation-inducing agents and maintained for 5 days. | Neuronal lineage cells | Lee et al. 2010 |
| Undifferentiated hESCs were cultured in mesoderm-inducing medium for 1 week. Adherent cells were expanded in monolayer for 3–4 week and seeded on decellularized bone scaffolds in osteogenic medium for 3 days to allow cell attachment. Cell-seeded constructs were then cultured in osteogenic medium for 5 week in either perfusion bioreactors or static dishes. Tissue development was evaluated after 3 and 5 week. | Bone tissue | Marolt et al. 2012 |
| hESCs were plated on a Matrigel-coated 96-well plate. After overnight culture, cells were exposed to BMP4 and activin A or CHIR99021 in a previously established serum-free media APEL for 2–3 days, then FGF9 and heparin in APEL media for 4 days to induce IM cells. Subsequently cells were exposed to FGF9, BMP7, retinoic acid (RA) and heparin for 4–11 days in case of | Renal lineage cells that form self-organizing structure, including nephron formation | Takasato et al. 2014 |

| | | |
|---|---|---|
| BMP4/activin A induction. In case of CHIR99021 induction, cells were exposed to FGF9 and heparin for 6 days then cultured in APEL basal media for another 6 days. | | |
| hESCs were preplated on gelatin for 45 min to remove feeder cells and then plated on Matrigel in feeder conditioned media. Feeder-free cultured hESCs were plated directly on Matrigel in TeSR$^{TM}$1. When cells reached >80% confluence, differentiation was initiated by switching to DMEM-F12/Neurobasal media (2:1) supplemented with N2 and retinol-free B27 (N2B27). For the first 10 days, cultures were supplemented with SB431542, LDN-193189 and dorsomorphin. Some initial experiments were performed with noggin instead of LDN. Where indicated, Shh or cyclopamine was added to the cultures. Cells remained in basal N2B27 or were supplemented with activin A from day 9. BDNF and GDNF were added from day 28 to aid neuronal maturation and survival. | GABAergic striatal medium-sized spiny neurons (MSNs) | Arber et al. 2015 |
| Confluent hESC cultures were scraped and cultured in low-attachment plates with NutriStem to form EBs with Rock inhibitor during the first 24 hr. At week 5, pigmented structures were cut out with a scalpel and dissociated into single cells. Cells were plated on different substrates and cultured until homogeneous pigmentation is reached (week 9). | Retinal pigment epithelial cells | Reyes et al. 2016 |
| hESCs were plated into 24-well plates in mTesR1 with Y-27632. Definitive endoderm (DE) differentiation started by adding Activin A, NEAA, FBS in RPMI 1640 medium for 3 days. BMP4 was added on the first day. DE was differentiated to posterior foregut endoderm by exposure to FGF4, and noggin for 3 days in RPMI 1640 supplemented with NEAA and FBS. RA was added on day 6. The resulting posterior foregut spheroids were | 3D foregut spheroids-gastric organoids | McCracken et al. 2017 |

| | | |
|---|---|---|
| collected and transferred to a 3D culture system until day 34. | | |

**Table 1.6 : Differentiation of hESCs into various cell lineages/tissues.**

Additionally, extensive work has been carried out to differentiate hESCs into eye lineages. In view of treating visually disabled patients, researchers have tried to obtain fully compatible *in vitro* differentiated cells to treat those patients. Differentiation protocols developed for several eye lineages were summarised in Table 1.7.

| **Supplements / Conditions** | **Differentiated cells / tissue obtained** | **References** |
|---|---|---|
| RPE differentiation: embryonic bodies (EBs) were subjected to neuroectodermal induction with SB-505124 and IWP-2. Then the EBs were transferred onto well plates coated with LN-521 and coll-IV in XF-Ko-SR medium. Pigmented foci were manually separated, and disasssociated with TrypLE™ Select enzyme, and the resulting single-cell suspension replated to culture wells coated with LN-521 and col IV. For the final passage, the RPE cells were plated to similarly coated polyethylene terephthalate (PET) hanging cell culture inserts.<br>LESC differentiation: EBs were subjected to surface ectodermal induction with XF-Ko-SR medium supplemented with SB-505124 and bFGF, followed by XF-Ko-SR medium with BMP4. Then the EBs were transferred onto well plates coated with LN-521 and col IV in a defined and serum-free medium CnT-30 at a density of approximately 15 EBs per $cm^2$. The cells were thereafter maintained in CnT-30. | 1) hPSC-RPE cells with mature tight junctions, expression of RPE genes and proteins, and phagocytosis and key growth factor secretion capacity.<br>2) hPSC-LESCs expressing LESC markers such as p40/p63α | Hongisto et al. 2017 |
| Differentiation: DMEM/F12 and defined keratinocyte serum-free medium (KSFM) (1:1). Airlifting: DMEM/F12 and DMEM (1:1) with PS, FBS, epidermal growth factor (EGF), insulin, hydrocortisone, cholera | ABCG2+ cells from 7% $CO_2$ group isolated as CEPCs formed 3 - 4 layers | Zhang et al. 2017 |

| | | |
|---|---|---|
| toxin, and 3,3',5-triiodo-L-thyronine. Different carbon dioxide ($CO_2$) levels in culture. | of epithelioid cells by airlifting and expressed ABCG2, p63, CK14 and CK3. | |
| Human limbal fibroblast conditioned medium | Cells similar to epithelial progenitor cells, undergo trans-differentiation and exhibit squamous metaplasia | Brzeszczynska et al. 2014 |
| Vitro HES, 5% FBS and 10ul/ml Hygromycin for 16 days and transplanted onto Bowman's membrane | Cells that expressed corneal-related markers: *PAX6* and *CK3* | Hanson et al. 2013 |
| Induction: 90% BHK21-medium/Glasgow modified Eagle's medium (GMEM), glutamine, KOSR, pyruvate, NEAA, β-mercaptoethanol, PS, co-cultured with murine PA6 cell line | Corneal keratocytes | Chan et al. 2013 |
| hESCs were differentiated with ventral neural induction media (VNIM) that was supplemented with recombinant mouse (rm) Noggin, recombinant human (rh) Dickkopf-1 (Dkk1), rhIGF-1, rhLefty A, Human Sonic Hedgehog (Shh) and 3,3′,5-triiodo-L-thyronine (T3) until day 37. KOSR-free media was then supplemented with rmNoggin, rhDkk1, rhIGF-1, rhbFGF, retinoic acid, T3, taurine, and Shh until day 60. During days 37-41, PR-induction medium was supplemented with human Activin-A, to encourage the photoreceptor progenitor cells maturation | Retinal photoreceptor cells | Mellough et al. 2012 |
| Cells were cultured on Matrigel-coated plate in DMEM/F-12 supplemented with bovine serum albumin (BSA), NEAA, PS, N2, B27, bFGF. | Progenitor and mature lens cells | Yang et al. 2010 |

| | | |
|---|---|---|
| Cells were grown in 85% DMEM/F-12, 15% KOSR, NEAA, mercaptoethanol. At day 4, BMP4 added for 3 days. At day 7, BMP4 was removed, and cells were cultured in 90% DMEM/F-12, FBS, NEAA, and mercaptoethanol or in 60% DMEM, 30% Ham's F-12 medium, and FBS supplemented with insulin, hydrocortisone, ascorbate, and EGF. | Ectodermal cells | Aberdam et al. 2008 |
| Cells were cultured on a layer of irradiated MEF in unconditioned medium (UM): DMEM/F-12 containing KSR, MEM, NEAA, L-glutamine, mercaptoethanol, and bFGF. Alternatively, hESCs were plated on Matrigel in medium conditioned by MEF. EBs were cultured in UM without bFGF or N2 medium: DMEM/F12 containing N2 supplement and MEM NEAA. After 1–2 days, EBs were transferred to a new vessel to remove adherent MEF. Differentiated EBs were plated onto gelatin-coated plates in defined keratinocyte serum-free medium (DKSFM). Direct differentiation: hESC colonies were grown on Matrigel in MEF-conditioned hESC medium before switching to differentiation medium, which contained UM or N2 and a combination of DMSO, RA, BMP4, or Noggin. | Keratinocytes | Metallo et al. 2008 |
| Cells were maintained on MEF before manually passaged and transferred onto col IV coated plate and supplemented with medium containing low-glucose DMEM/F12 (3:1), FBS, PS, hydrocortisone, insulin, tri-iodothyronine, adenine, cholera toxin and EGF. | Corneal epithelial-like cells | Ahmad et al. 2007 |

**Table 1.7 : Differentiation of hESCs into several eye lineages.**

### 1.2.2 *Human-induced pluripotent stem cells (hiPSCs)*

Human induced-pluripotent stem cells (hiPSCs) are derived from somatic cells which have undergone reprogramming process to return to the pluripotent stem cell stage. Unlike hESCs, hiPSCs derivation does not require the destruction of human embryos, therefore avoids the ethical debate as that on the conventional way of hESCs derivation (Narsinh et al. 2011). The reprogramming process generally comprise three phases; initiation, maturation and stabilisation

(Mikkelsen et al. 2008, Buganim et al. 2014). Mesenchymal-to-epithelial transition (MET) was prominent in the initiation phase (Li et al. 2010) while the *OCT4, SOX2, KLF4, c-MYC* (OSKM) transgene repression was vital during the transition of maturation to the stabilisation phase (Golipour et al. 2012). This multi-step process also involved both transcriptome and proteome resetting (Sancho-Martinez and Izpisua Belmonte 2013). Apart form those transcriptional changes there are epigenetic alterations that allow the conversion of somatic cells into stem cells. The changes include histone modifications during early reprogramming process, chromatin reorganisation, DNA demethylation of promoter regions and X reactivation during late reprogramming process (Takahashi et al. 2007, Maherali et al. 2007, Wernig et al. 2007, Fussner et al. 2011).

The first hiPSCs were produced by Yamanaka lab in 2007 by reprogramming adult human dermal fibroblasts using viral vectors (Takahashi et al. 2007). During the reprogramming process, the genome of somatic cell is reprogrammed to a pluripotent state *in vitro* by the introduction and forced expression of genes that are important for pluripotency maintenance equivalent to that of hESCs. Those genes include *OCT4, SOX2, NANOG, KLF4, c-MYC* and *LIN28* (Takahashi and Yamanaka 2006, Takahashi et al. 2007, Yu et al. 2007). The resulting hiPSCs have similar characteristics to primed hESCs. These cells have similar characteristics to hESCs in their characteristic morphology, surface antigens gene expression profiles, epigenetic status, self-renewal capacity, differentiation potential and function as described previously (Chin et al. 2009, Narsinh et al. 2011). They are characterised *in vitro* by their ability to give rise to cells belonging to all three germ layers *in vitro* and *in vivo* (Walia et al. 2012). A recent report stated that it is possible to generate naïve hiPSCs via directly reprogramming the somatic cells (Kilens et al. 2018). Thus similar to hESCs, there will be naïve and primed states of hiPSCs.

There are various reprogramming methods developed for hiPSCs derivation (Figure 1.5). Viruses such as retrovirus, adenovirus and sendai virus (Sendai) were initial vectors used to introduce the reprogramming factors into somatic cells (Fusaki et al. 2009, Sommer et al. 2009, Zhou and Freed 2009). These viral transduction processes need to be carefully controlled and tested before the technique can lead to useful treatment for humans. This is because, in animal studies, the virus used to introduce the stem cell factors may cause genomic insertion of viral transgenes leading to tumour formations (Okita et al. 2007). The integrative retroviral reprogramming methods stated above used genetic material in the process, hence they are

unreliable for clinical therapeutic purposes because of increased risk of tumorigenesis associated with uncontrolled gene integration into the cell's genome (Medvedev et al. 2010). However, other DNA free methods for hiPSCs induction that directly delivering the reprogramming proteins attached to the cell penetrating peptides (CPPs) have been developed. Although this method is simpler, more economical and avoids the risk of genomic integration, it has much lower efficiency and kinetics, and a much longer time is needed to produce viable hiPSCs after its induction (Walia et al. 2012).

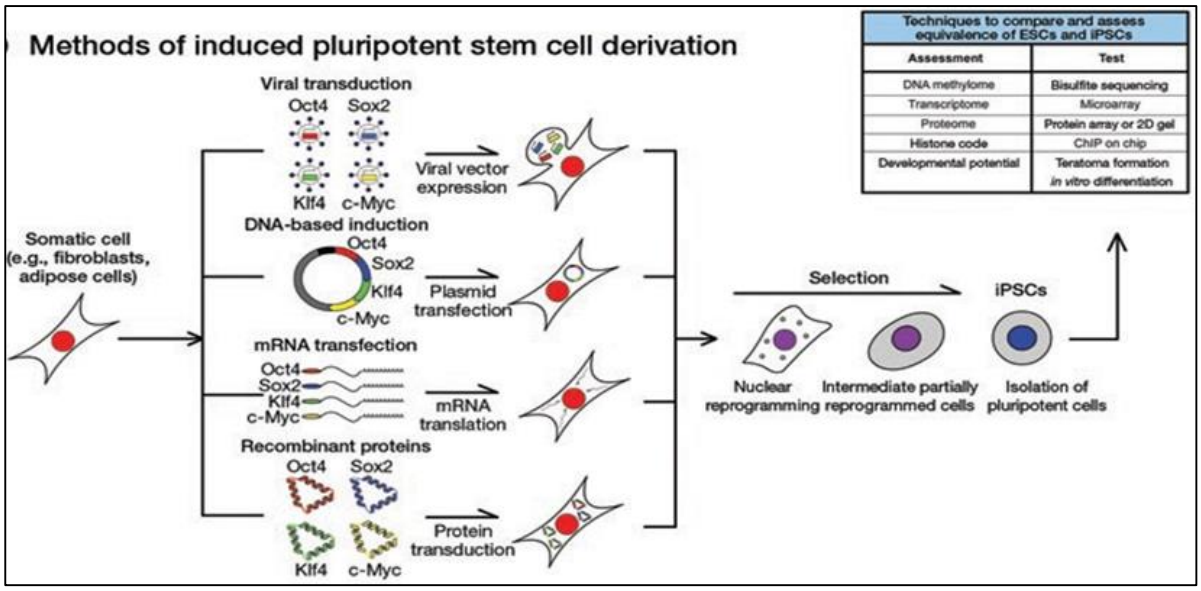


**Figure 1.5 : Methods for derivation of hiPSCs. Adapted from Narsinh et al. 2011.**

The use of adenovirus has successfully produced hiPSCs without the transgene integration but this method was more effective in only certain types of cells such as hepatocytes (Fusaki et al. 2009, Zhou and Freed 2009). The use of Sendai based RNA virus has also avoids transgene integration as virus does not integrate into the human cells' gene and will be removed by sequential dilution every time a cell divides. This Sendai method was successfully used to reprogram fibroblasts and blood cells (Jin et al. 2012, Chen et al. 2013, Hunihan et al. 2017).

Investigations have also been done on non-viral vectors, such as repeated nucleofection of a non-viral polycistronic plasmid containing reprogramming gene sequences and the use of non-integrating episomal vectors (Abujarour and Ding 2009). But these methods showed lower level of transgenes expression and lower efficiency compared to viral reprogramming. One of the most efficient (0.1 - 1% efficiency) non-viral gene delivery system uses excisable piggyback (PB) transposon carrying the coding of c-MYC, KLF4, OCT4 and SOX2 (MKOS cassette)

which is excised from its integration site without changing the original DNA sequence (Woltjen et al. 2009, Somers et al. 2010, Gonzalez et al. 2011, Robinton and Daley 2012).

The most recent DNA free technique for hiPSCs reprogramming involves the use of synthetically modified messenger ribonucleic acid (mRNA) and CPPs to deliver the reprogramming proteins (Kim et al. 2009). The resulting iPSCs are called RNA induced pluripotent stem cells (RiPSCs) and protein-induced human iPSCs (p-hiPSCs) respectively. These are to date the most efficient (1 - 4.4%), non-mutagenic, with high cell survival and safe non-integrating cell reprogramming method (Kim et al. 2009, Warren et al. 2010, Robinton and Daley 2012).

Another method of hiPSCs reprogramming is via the application of microRNAs (miRNAs). MicroRNAs are short RNA molecules that bind to complementary sequences on messenger RNA and block gene expression (Bao et al. 2013). This reprogramming method was shown to be highly efficient as reported by Anokye-Danso et al. stating that a single miRNA cluster (miR302/367) can reprogram fibroblasts four-fold more efficiently than the standard *OCT4, SOX2, KLF4, c-MYC* expression (OSKM) method (Anokye-Danso et al. 2011, Hu et al. 2013). These findings may also lead to non-viral, non-transcription factor mediated procedure for generating hiPSCs for use not only in basic stem cell biology studies, but also for high throughput hiPSCs generation for large patient populations. The various methods of cell reprogramming and their efficiencies are summarised as below.

| **Vector types** | **Delivery methods** | **Efficiency for human cells (%)** | **Multiple cell types reprogrammed** |
|---|---|---|---|
| Retroviral | Integrating | 0.02 – 0.08 | Yes |
| Lentiviral | Integrating | 0.02 - 1 | Yes |
| Lentiviral (miRNA) | Non-integrating | 10.4 – 11.6 | No |
| miRNA (direct transfection) | Non-integrating, DNA-free | 0.002 | Yes |
| Adenoviral | Non-integrating | 0.0002 | No |
| Sendai | Non-integrating | 0.5 – 1.4 | Yes |
| mRNA | Non-integrating, DNA-free | 0.6 – 4.4 | No |
| Protein | Non-integrating, DNA-free | 0.001 | No |

| | | | |
|---|---|---|---|
| Episomal | Non-integrating | 0.0006 – 0.02 | Yes |
| PiggyBac | Integrating, excisable | 0.02 – 0.05 | No |
| Plasmids | Non-integrating | 0.005 | No |

**Table 1.8 : Various published methods of reprogramming and their efficiencies. Adapted from Rao and Malik 2012 and Stadtfeld and Hochedlinger 2010.**

### 1.2.3 *Human ESCs and iPSCs for regenerative medicine, drug discovery and disease modelling*

In regenerative medicine, it is most important to establish robust, cost effective systems for culturing and differentiating the pluripotent cells and eliminating the need to use of animal-derived substances or feeder cells to meet the clinical grade standard (Skottman and Hovatta 2006). It has also been shown that their self-renewal and differentiation capacity are the two inherent aspects influenced by its pluripotency status and initial culture conditions (Lee et al. 2014, Lee et al. 2017). Differentiating hESCs into usable cells while avoiding transplant rejection are just a few of the hurdles still faced by researchers. Many nations currently have special law on either hESCs research or the production of new hESCs lines. This is because that conventional way of hESCs retrieval involved the destruction of otherwise alive human embryos. Thus this raised significant concerns on ethical and religious ground (Rao and Condic 2008). However, because of their combined abilities of unlimited expansion and pluripotency, embryonic stem cells remain a theoretically potential source for regenerative medicine and tissue replacement after injury or disease.

Immune rejection is a more serious challenge that could be faced by patients following stem cells transplantation should the immune issue arise. This is due to the dispersed integration of the stem cells after transplantation which will either require immune suppression drug treatment for lifetime or the removal of the transplanted cells (Condic and Rao 2008).The recently discovered capacity of human somatic cells, for example fibroblasts to be relatively easily reprogrammed into embryonic stem cell-like cells, named hiPSCs and their differentiation capability to almost any cell type in the adult organism (Takahashi et al. 2007) offers new approaches to avoid immune rejection issues. Amongst others, hiPSCs have started to be used for the generation of autologous cells for patient-specific transplantation that avoid post-transplantation rejection by patient's immune system (Tucker et al. 2014). Tissues derived from hiPSCs will be a nearly identical match to the donor's cell and thus more likely to avoid

rejection by the immune system following an autologous transplant (Guha et al. 2013, Morizane et al. 2013).

However, an increasing number of data demonstrated that hiPSCs derived cells could induce immune reactions following autologous treatment (Kruse et al. 2015). The risks of autologous immune reactions towards hiPSCs could arise from the abnormal epigenetic signature (Lister et al. 2011, Ruiz et al. 2012) and somatic coding mutations that will result in the formation of fusion proteins (Gore et al. 2011) as well as the genomic instability that could lead to cancer (Yoshihara et al. 2017). Although additional research is still needed, hiPSCs have already been useful tools for drug development and modelling of diseases, and scientists hope to use them in transplantation medicine and drug discovery (Condic and Rao 2008).

These new avenues for personalised cell transplantation using hiPSCs and hESCs, however still need further consideration and clarification especially on the effects of subtle differences between the two stem cell types on their therapeutic applications (Robinton and Daley 2012). The *in vivo* efficacy and safety following transplantation of these cells have yet to be established. One of the unfavourable effects of immune matching feature of patient specific stem cell transplant is the lack of immune reactions that naturally detect tumour formation. Thus, tumour formation might be enhanced after transplantation of impure or unstably differentiated hiPSCs and hESCs (Condic and Rao 2008).

Despite the small window of uncertainty in the long term outcome of stem cell therapy, there are a few recently approved human stem cell therapy trials for spinal cord injury and macular degeneration and diabetes. Those trials use differentiated cells derived from hESCs or hiPSCs for treating the respective conditions (Lu et al. 2009, Sharp et al. 2010, Schulz 2015, Ilic et al. 2015, Garber 2015). Another on-going trial for age-related macular degeneration (AMD) treatment in Japan uses *in vitro* differentiated retinal pigment epithelium (RPE) from allogeneic hiPSCs (Riken Press Releases 2013, Cyranoski 2014, Hildreth 2016, Mandai et al. 2017).

Drugs development costs were also significantly increased due to delayed detection of side effects in clinical settings. This cost could well be saved with the use of hESCs or hiPSCs that can be induced to differentiate into various tissues for the evaluation of the drug clearance, absorption and side effects. These tissues could be generated from cells of different donors, thus each will carry different genotypes that may reflect the variation in the drug metabolisms in different individuals (Pouton and Haynes 2007, Wilmut 2007, Zuba-Surma et al. 2012, Ko

and Gelb 2014). Apart from cost saving, the application of stem cells in drug discovery will also minimise the need of human or patient involvement in the clinical trial, which to some degree pose an unknown risk to the patient (Rubin and Haston 2011).

Human disease modelling research field is aiming to generate models of human diseases using disease specific pluripotent stem cells as summarised in Table 1.9. This may sound feasibly possible to achieve and will give a valuable insight into various life-threatening diseases for example common genetic diseases such as the cardiovascular diseases and also inherited diseases that will affect the vision (Liang and Du 2014, Nguyen et al. 2015). However, there are still various points that need to be considered in the choice of disease to be modelled, such as availability of animal model, sources of somatic cells for reprogramming, availability of both healthy and affected tissues from patients (Colman and Dreesen 2009, 2009a).

| **Disease model & Authors** | **Methods** | **Findings** |
|---|---|---|
| Severe aplastic anemia (SAA). Melguizo-Sanchis et al. 2018 | hiPSCs were derived from unaffected controls and SAA patient and differentiated into hematopoietic progenitors. | The *in vitro* model mimics 2 key features of SAA: (1) the failure to maintain telomere length during reprogramming process and hematopoietic differentiation resulting in SAA-iPSC and iPSC-derived-hematopoietic progenitors with shorter telomeres than controls; (2) the impaired ability of SAA-iPSC-derived hematopoietic progenitors to gave rise to erythroid and myeloid cells. |
| Miller-Dieker síndrome (MDS). Bershteyn et al. 2017 | MDS patients derived hiPSCs and hiPSCs lines and were differentiated into cerebral organoids | Cell migration defect in the patient-derived organoids was rescued when the MDS causative chromosomal deletion were corrected |
| Zika virus (ZIKV) infection. Qian et al. 2016 | hiPSCs lines were differentiated into forebrain, midbrain and hypothalamic organoids | The organoids recapitulate key features of human cortical development, including progenitor zone organization, neurogenesis, gene expression, and a distinct humanspecific outer radial glia cell layer. |

| | | |
|---|---|---|
| | | The forebrain organoid model of ZIKV exposure revealed preferential, productive infection of neural progenitors with either African or Asian ZIKV strains. ZIKV infection leads to increased cell death and reduced proliferation, resulting in decreased neuronal cell-layer volume resembling microcephaly. |
| Dilated cardiomyopathy (DCM). Hinson et al. 2015 | Normal and DCM patient T cells were reprogrammed into hiPSCs via lentiviral delivery method and differentiated into cardiomyocytes | Titin mutations in hiPSCs from DCM patients define sarcomere insufficiency as a cause of dilated cardiomyopathy |
| Age-related macular degeneration (AMD). Chang et al. 2014 | T cells from patients with dry AMD were reprogrammed into hiPSCs via integration-free episomal vectors and differentiated into retinal pigmented epitelial (RPE) cells | The RPE cells derived from AMD patients have decreased antioxidative defense and are more susceptible to oxidative damage leading to AMD formation. Curcumin was found to effectively restore the neuronal functions in AMD patient-derived RPE. |
| Ectodermal dysplasia (ED). Shalom-Feuerstein et al. 2013 | Fibroblasts from healthy donors and ED patients carrying two different point mutations in the DNA binding domain of p63 were reprogrammed into hiPSC via lentiviral infections and differentiated into epidermal cells | EEC-iPSC from patients showed early ectodermal commitment into K18+ cells but failed to further differentiate into K14+ cells (epidermis/limbus) or K3/K12+ cells (corneal epithelium). APR-246 (PRIMA-1MET), a small compound that restores functionality of mutant p53 in human tumor cells, could revert corneal epithelial lineage commitment and reinstate a normal p63-related signaling pathway. |

| | | |
|---|---|---|
| Retinitis pigmentosa (RP). Tucker et al. 2013 | Normal and patient's skin fibroblasts and keratinocytes were reprogrammed into hiPSCs via infection with Sendai viruses. The hiPSCs were allowed to form EBs which then differentiated into multi-layer eye cup-like structures with features of human retinal precursor cells | Patient's hiPSCs were differentiated into multi-layer eye cup-like structures with features of human retinal precursor cells. Analysis showed the disease is caused through protein misfolding and endoplasmic reticulum (ER) stress. Transplantation of the cells into 4-day-old immunodeficient mice resulted in the formation of morphologically and immunohistochemically recognizable photoreceptor cells, suggesting that the mutations in this patient had caused post-developmental photoreceptor degeneration. |
| Best disease (BD). Singh et al. 2013 | Normal and patient's skin fibroblasts were reprogrammed into hiPSCs via lentiviral infection. The hiPSCs were differentiated into RPE cells | Impaired photoreceptors' outer segments (POS) handling was ssen in the pathophysiology of the disease using the RPE from mutant hiPSCs and contribute to the clinical picture of BD and studies on maculopathies. |
| Retinitis pigmentosa (RP). Jin et al. 2012 | Patient's dermal fibroblasts were reprogrammed into hiPSCs by using a Sendai-virus vector. hiPSCs were differentiated into RPE-like cells | RP patient-specific rod cells recapitulated the disease feature and revealed evidence of ER stress and rod degeneration. |
| Dystrophic epidermolysis bullosa. Itoh et al. 2011 | Normal and patient's dermal fibroblasts were reprogrammed into hiPSCs by retroviral transduction. The hiPSCs | 3D skin equivalents was generated using hiPSCs-derived keratinocytes, suggesting that the keratinocytes were fully functional. Autologous hiPSCs have the potential to provide a source of cells for |

| | | |
|---|---|---|
| | were differentiated into keratinocytes | regenerative therapies for specific skin diseases. |

**Table 1.9 : Various disease modelling experiments using hiPSCs.**

Recent advances in genetic editing created ways for the generation of complex genetic disease models. The application of genomic editing methods such as zinc-finger nucleases (ZFNs), transcription activator-like effector nucleases (TALENs) or clustered regularly interspaced short palindromic repeat–CRISPR-associated 9 (CRISPR–Cas9) substantially increases the efficiency of gene editing to correct the gene mutations afflicted by the diseases (Sterneckert et al. 2014) as well as inserting mutation in vitro to model a pathology (Hinson et al. 2015, Avior et al. 2016). Additionally, a more recent approach allowed RNA to be transiently edited by using CRISPR-Cas13 method (Abudayyeh et al. 2017). These techniques will offer a new hope for the patients with genetic disease through a treatment called genetic therapy (Niu et al. 2016, Maeder and Gersbach 2016).

### 1.3 Anatomy of the Cornea and Limbus

In an adult human, cornea is the transparent tissue layer located at the anterior part of eyeball. It covers the outermost surface of the iris, serving as a protective layer, refracting as well as allowing light to pass through to reach the retina (Zieske 2004). Unlike its peripheral neighbouring conjunctiva, it is devoid of blood vessels (Figure 1.6). Cornea consists of six layers (Dua et al. 2013) with three different types of cells (Figure 1.7). The outermost epithelial layer of cornea consists of 5 to 6 layers of non-keratinized stratified corneal epithelial cells, which express both cytokeratin 3 (CK3) and cytokeratin 12 (CK12) (Moll et al. 1982).

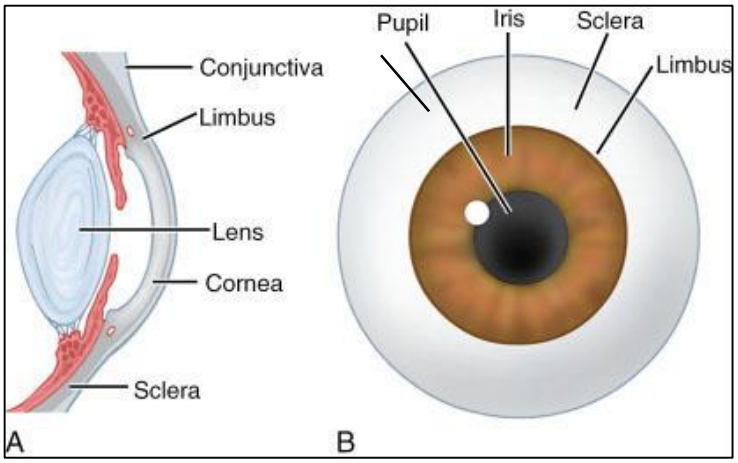


**Figure 1.6 : The cornea and limbus or corneoscleral junction in horizontal section (A), and anterior view (B). Adapted from http://medicine.academic.ru/137051/limbus_corneae**

The cuboidal basal epithelial cells express cytokeratin 14 (CK14) (Merjava et al. 2011) and are called the corneal epithelial stem cells (CESCs). Unlike the basal cells, the suprabasal cells are flatter and express the corneal cytokeratins (CK3 & CK12) (Merjava et al. 2011). The corneal epithelium is resting on a basement membrane that connects the epithelium to the Bowman's layer. This basement membrane component includes collagen-IV and laminin, where at adult stage the collagen-IV was found to be absent from the central cornea (Cleutjens et al. 1990). The Bowman's layer beneath the basement membrane separates the epithelium and the corneal stroma that makes up 90% of the total corneal thickness (Figure 1.7).

The corneal stroma comprises mainly extracellular matrices such as collagen I and V bundles and different types of proteoglycans with fibroblast-like keratocytes, dendritic cells and macrophages/monocytes scattered within it (Hamrah et al. 2003, Katikireddy et al. 2014). The keratocytes are neural crest-derived mesenchymal cells that could respond to injury by resuming repair phenotypes (West-Mays and Dwivedi 2006). The most anterior part of the corneal stroma has a specific architecture which is important in preserving the corneal smooth curvature even during extreme hydration (Müller et al. 2001, Bron 2001). The sub-basal region of the stroma contains the corneal nerve plexuses (Patel and McGhee 2005). Corneal stroma is supported by a strong well-defined layer (Dua's layer) and Descemet's membrane, which separate the stroma from a single layered endothelium on the innermost corneal layer (Dua et al. 2013).

The corneal endothelium originates from neural crest cells, forms a monolayer posterior to Descemet's membrane and controls corneal hydration and nutrition (Waring et al. 1982). It was reported that the adult, corneal endothelium express cytokeratins 8 and 18 (Merjava et al. 2009). It also forms a barrier between the corneal stroma and anterior chamber that maintains corneal transparency by regulating corneal hydration (Joyce 2003). These cells were also reported to be arrested in G1-phase that causes its non-replicative state. The non-replicative state is age-relatedly reversible and important for the cells' functional importance as a barrier and 'pump' (Joyce 2003). The corneal endothelial cells function and integrity is maintained by its own secreted Descemet's membrane (Lwigale 2015).

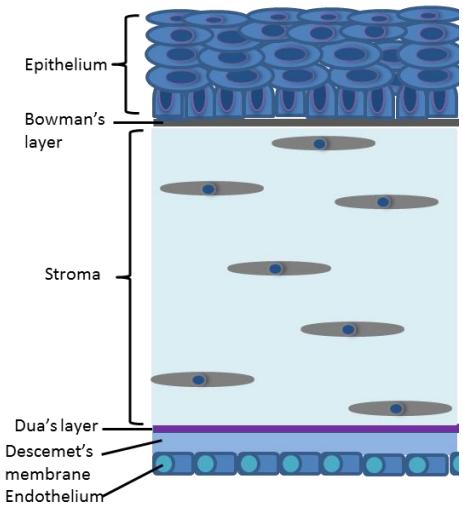


**Figure 1.7 : Representative histological diagram of cornea, showing the six different layers, based on Dua et al. 2013 and Lwigale 2015.**

Limbus is a junctional annular zone between the cornea and conjunctiva or sclera (Figure 1.6). It is also called the corneoscleral junction separating the avascular cornea from the surrounding conjunctiva, and is lined basally by the limbal stem cells (Ahmad 2012). Limbus was suggested to serve as an area where the corneal epithelial precursors with stem cell properties can be found, by Davenger and Evensen early in 1971 (Davenger and Evensen 1971). These stem cells reside on the basal epithelial layer of the limbus (Menzel-Severing 2011) in the highly pigmented areas called the Palisades of Vogt, as shown in Figure 1.8 (Higa et al. 2005, Li et al. 2007). These cells are called the limbal stem cells (LSCs) and have an important role in maintaining the homeostasis of the corneal epithelium, especially in response to injury (Cotsarelis et al. 1989, Stepp and Zieske 2005). These basally located LSCs express cytokeratin 14 (CK14), cytokeratin 15 (CK15), ABCG2 and ΔNp63 (Watanabe et al. 2004, Kawasaki et al. 2005, de Paiva et al. 2005, Di Iorio et al. 2005, Figueira et al. 2007, Lyngholm et al. 2008).

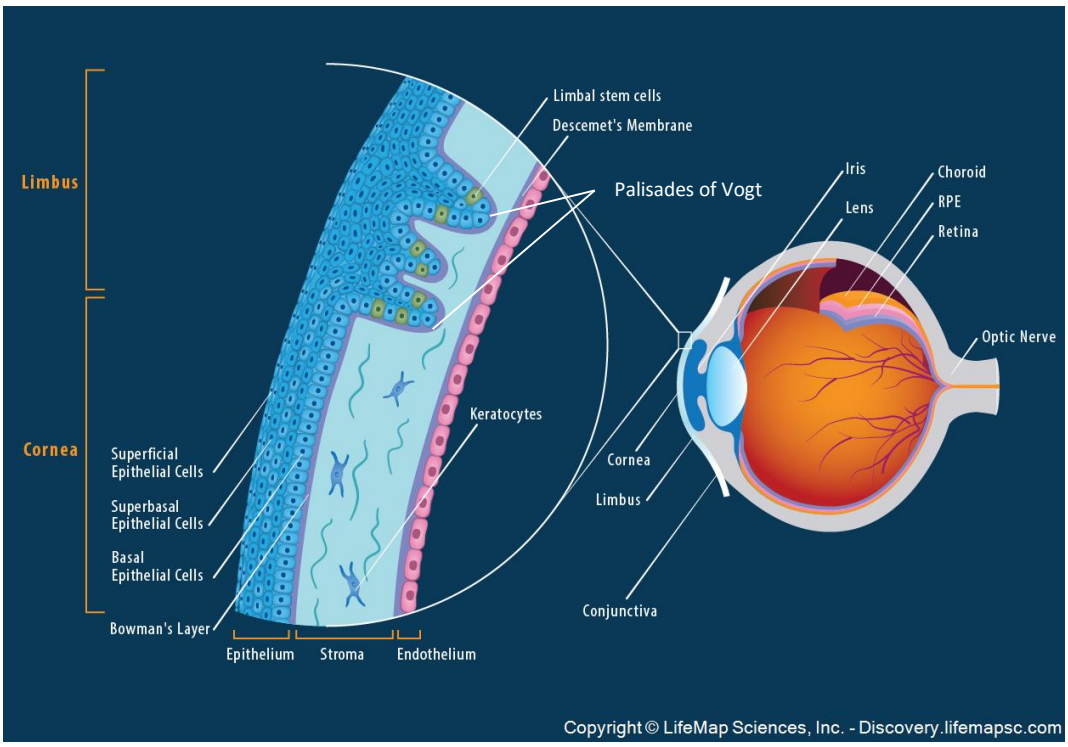


**Figure 1.8 : The cornea (image from https://discovery.lifemapsc.com/in-vivo-development/eye/corneal-epithelium).**

In adult eyes, corneal epithelial cells are normally lost in the tear film. Homeostasis is maintained by the migration of the transient amplifying cells (TACs) centripetally from the limbus to central cornea, and they differentiate while moving from the basal to superficial layer of the cornea, to give rise to differentiated corneal epithelial cells (Figure 1.9). This pattern of movement of corneal cells is described as: x + y = z hypothesis by Thoft and Friend in 1983. Where x is the proliferation of basal cells, y is the centripetal movement of cells and z is the cell loss from the corneal surface (Thoft and Friend 1983).

The LSCs niche is maintained by several intrinsic and extrinsic factors comprises a combination of anatomical and biochemical events that occurred during development as well as factors released by neighbouring cell populations (Espana et al. 2003, Kawakita et al. 2005). This niche is vital to protect the LCSs from unnecessary differentiation and apoptosis that compromise the stem cells reserve (Li and Xie 2005, Moore and Lemischka 2006). The LSCs are more abundant in superior and inferior limbus, compared to the nasal and temporal side (Wiley et al. 1991). Following a minor corneal injury, LSCs will undergo asymmetrical mitosis and replicate to produce daughter cells, some of which will remain as stem cells and the rest are called TACs. These TACs are the progenitors that will differentiate to ultimately generate the terminally

differentiated corneal epithelium to replace the damaged cells (Schlötzer-Schrehardt and Kruse 2005).

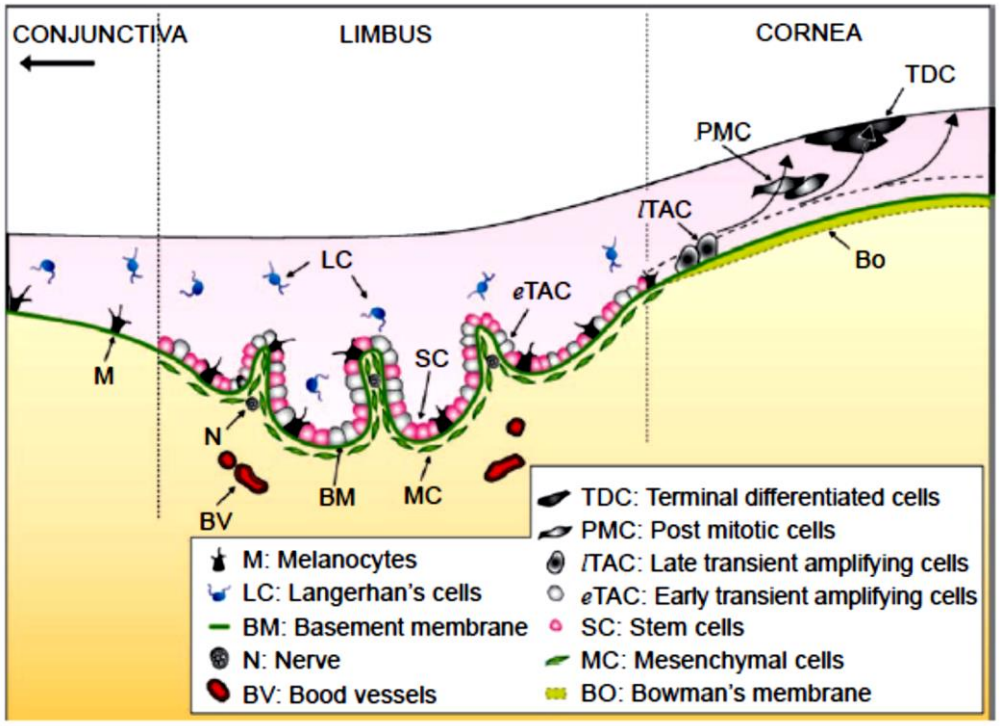


**Figure 1.9 : The different cells in limbus and cornea. Adapted from Li et al. 2007.**

## 1.4 The Human Embryonic Development

### 1.4.1 *The TGFβ signalling pathways*

Embryonic development in human is largely regulated by the transforming growth factor β (TGFβ) superfamily of cytokines (Gordon and Blobe 2008). This superfamily includes more than 30 growth factors such as TGFβs, activins, inhibins, bone morphogenetic proteins (BMPs), growth differentiation factors including myostatin, nodal, leftys and Mullerrian-inhibiting substance (Heldin et al. 1997, Miyazono et al. 2005, Caestecker 2004). The TGFβ superfamily signalling pathways consist of type I and type II receptors where the TGFβ superfamily ligandscould bind. Activated receptors will interact with intracellular mediators (SMADs), either BMP (SMAD 1/5/8) or TGFβ (SMAD 2/3) responsive SMADs that will later form a complex with a common SMAD4 (Wrana and Attisano 2000). The complex will then be translocated into the nucleus where it could interact with other transcription factors to regulate cellular responses such as proliferation, differentiation, migration and apoptosis (Gordon and Blobe 2008). Nodal/Activin and BMP subfamilies have also been shown to be important during the formation of the three germ layers of vertebrates, where low BMP activity in vertebrate ectoderm indicates neural tissue (Wu and Hill 2009). Any alterations in the TGFβ superfamily

pathways or its members could result in human diseases and developmental disorders (Massague et al. 2000). A schematic diagram showing the TGFβ signalling pathways is shown below.

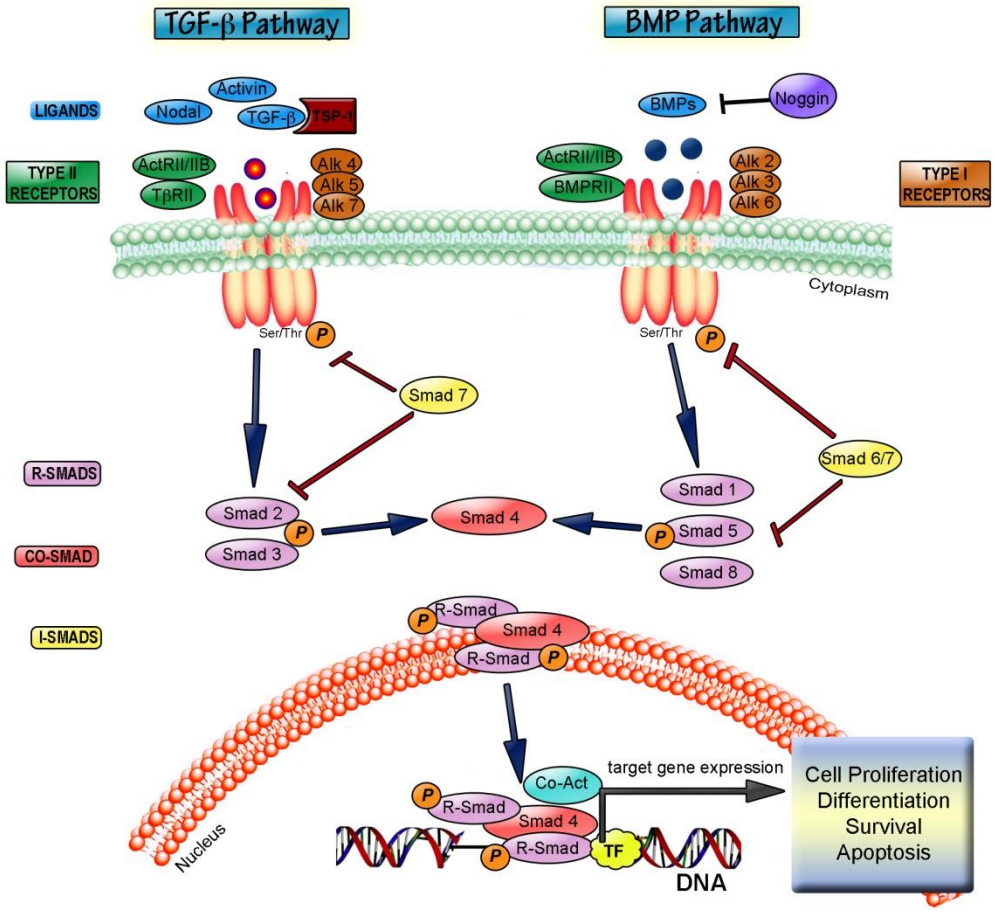


**Figure 1.10 : The TGFβ and BMP signalling pathways. Adapted from Villapol et al. 2013.**

### 1.4.2 *The development of eye and cornea*

Human eye development in utero begins as early as 3 weeks post-gestation with the formation optic grooves followed by optic vesicles at either sides of the forebrain. The process starts with the formation of its major structures that originated from four main embryonic sources; neuroectoderm, optic neural crest, mesoderm and surface ectoderm (O'Rahilly 1975, 1983, Jean et al. 1998). The development of the eye in the anterior neural plate of prosencephalon region (Figure 1.11A and B) involved complex interactions and mechanisms (reviewed by Jean et al. 1998, Sinn and Wittbrodt 2013).

The early stages of eye development are mainly regulated by *PAX6* (Collinson et al. 2003, Graw 2010), a key gene that has also been shown to induced ectopic eyes and ectopic expression of other early eye development genes such as *OTX2*, *RX*, and *SIX3* when misexpressed (Chow et al. 1999, Chow and Lang 2001). Initially, *PAX6* induces a single eye field formation in the anterior neural plate. Later, *SHH* overexpression causes *PAX2* expression and represses *PAX6* during the separation of the eye field as shown in Figure 1.11 C (Litwack 2012).

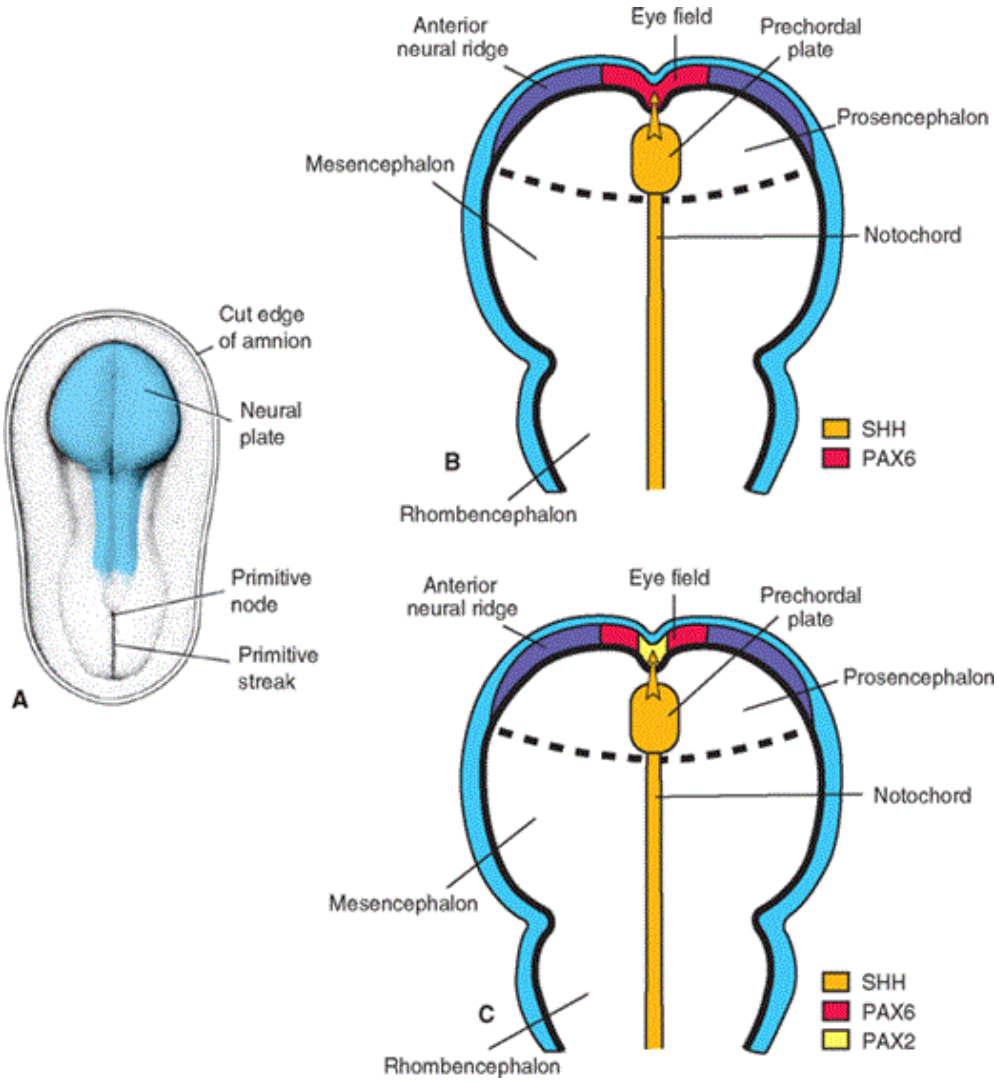


**Figure 1.11 : Formation and separation of eye field in the anterior neural plate. External view of a neural plate at 3 weeks (A). Sectional views of the developing brain, prosencephalon region (B and C). Figures taken from Sadler 2014.**

At 3 weeks after gestation, the two eye fields are the first to appear, and soon the optic vesicles start to form as shown in Figure 1.12 B – D (Sadler and Langman 2010). Evagination of the eye primordia on either sides of the forebrain tube lead to the formation of optic vesicles that extend toward overlying surface ectoderm. During this process, inductive signals are exchanged

between the optic vesicles and its adjacent ectoderm resulting in the formation of lens placode and early optic cup (Chow and Lang 2001, Martinez-Morales and Wittbrodt 2009). During the fourth and fifth weeks, the lens placodes and optic vesicles become invaginated to form the lens pits/vesicles and optic cups respectively (O'Rahilly 1975).

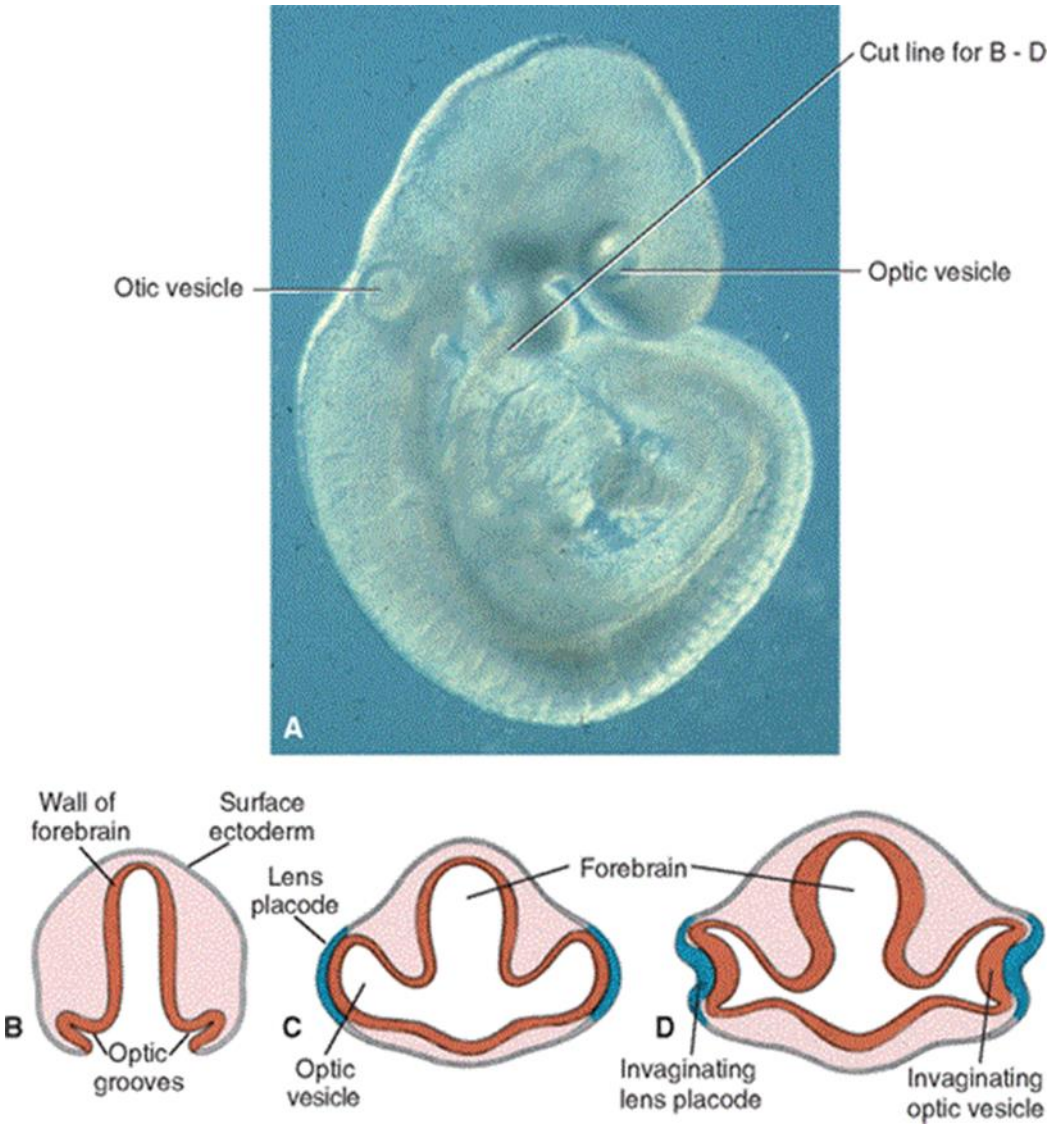


**Figure 1.12 : Development of optic vesicles. External view of 5 – 6 weeks embryo (A). Sections from developing embryos at different time points (B, C, D). Adapted from Sadler and Langman 2010.**

During the optic vesicles formation process, TGFβ and FGFs are released by surrounding mesenchyme and surface ectoderm respectively (Figure 1.13A), enhancing optic vesicle cells' migration and differentiation during the morphogenesis (Sanford et al. 1997). Retinoic acid (RA) was also reported to have an influence in the peri-ocular mesenchyme migration in mice eye morphogenesis (Matt et al. 2005). Then *MITF* and *CHX10* expression were detected and

localised in the invaginating optic cup regions, where the pigmented and neural retina will later develop from respectively (Nguyen and Arnheiter 2000). As development proceeds, the expression of *PAX2* is maintained in the optic stalk and *PAX6* in the lens placode (Figure 1.13 C) (Sadler 2014). At this stage *PAX6* regulates the lens formation, while the optic vesicles express *BMP4* (Chang et al. 2001). BMP4 improves and maintains the expression of *SOX2* and *LMAF*, the genes that act together with *PAX6* to initiate lens crystallin formation (Matsushima et al. 2011). The crystalline formation gene is in turn regulated by *SIX3* (Goudreau et al. 2002) during lens morphogenesis.

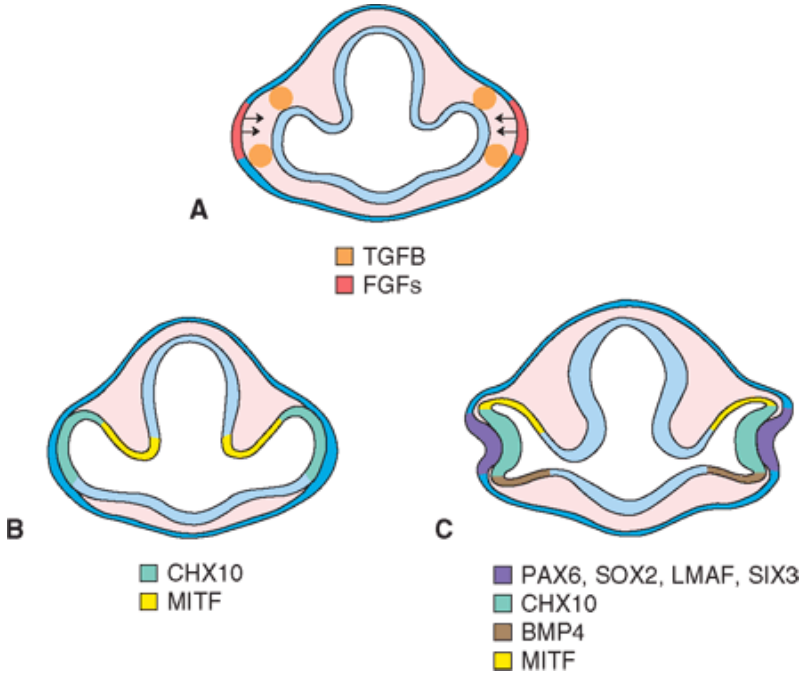


**Figure 1.13 : Molecular regulation in early stages of eye development (3 – 4 weeks). Adapted from Sadler 2014.**

At around 5 – 6 weeks of gestation, cornea starts to develop as the surface ectoderm closes following the formation of lens vesicles. Corneal development is also regulated by a complex process involving interactions between the surface ectoderm and the adjacent developing tissues such as the lens (Cvekl and Tamm 2004). During this period, the space between the lens vesicles and surface ectoderm is filled with mesenchymal cells from the neural crest. These cells later differentiate into corneal stroma and endothelium (Figure 1.14). The surface ectoderm that covers the anterior side of the mesenchyme will develop into corneal epithelium (Graw 2010, Zavala et al. 2013). At the same time the eyelids develop covering the external surface of the cornea.

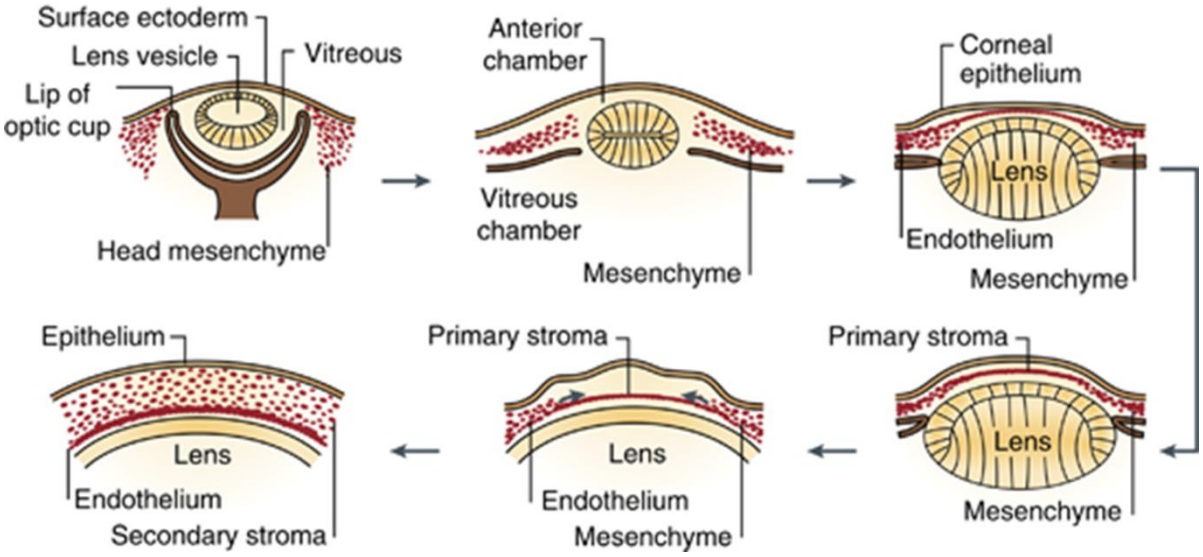


**Figure 1.14 : Formation of the cornea. Adapted from Zavala et al. 2013.**

Although the cornea as a whole comprises three closely located main components; corneal epithelium, its stroma and the endothelium, those components actually developed from different embryological origins. The corneal epithelium developes from surface ectoderm (Hay 1980) and the stroma and the endothelium developed from the mesenchymal tissue and neural crest cells (Amano et al. 2006, Graw 2010, Swamynathan 2013). The corneal epithelium shares the same characteristics as other non-keratinised stratified squamous epithelia, with an exception of being transparent. New epithelial cells are continuously regenerated by the limbal stem cells (LSCs) which are thought to reside at the Palisades of Vogt in the limbus (Schlotzer-Schrehardt & Kruse 2005, Li et al. 2007).

Those cells progressively migrate from peripheral to central region of the cornea, and ascend from basal to superficial layer to form a new stratified layer of non-keratinised squamous epithelium (Lu et al. 2001). These new epithelia compose of intermediate filaments that ensure them to anchor each other and stay firmly on the cornea, namely cytokeratins 3 and 12 (CK3 and CK12*).* Thus making CK3 and CK12 as useful markers for differentiated human corneal epithelium (Auw-Haedrich et al. 2011). Markers for the various stages of human corneal epithelial differentiation from pluripotent stem cells (PSCs) are listed in the following table.

| **Development stages** | **Markers** | **Function / location** |
|---|---|---|
| PSCs | OCT4, NANOG | Pluripotency markers / embryonic stem cells |
| Eye field | PAX6, SIX2, SIX3 | Eye development master genes / neural plate & adult corneal stroma progenitor cells |

| | | |
|---|---|---|
| Ectoderm | BMP4 | Non-neural ectoderm marker / pre-placodal ectoderm |
| Epithelium | K8, K18 | Simple epithelium / superficial corneal cells |
| | ECadherin | Cell adhesion / cornea and limbus |
| Corneal progenitors | ΔNp63, ABCG2 | Putative limbal stem cells marker / basal limbus |
| | CK14, CK15 | Structural proteins / basal limbal and basal corneal cells |
| Corneal epithelium | CK3, CK12 | Structural proteins / superficial cells of central cornea |
| | CK19 | Structural protein / peripheral cornea, limbus and conjunctiva |
| Conjunctiva | CK13 | Structural protein / conjunctiva |

**Table 1.10 : Markers of various corneal epithelial differentiation stages. Adapted from Funderburgh et al. 2005, Moll et al. 2008, Merjava et al. 2011 and Mort et al. 2012).**

Based on the eye and corneal development process together with the outcomes of various studies in the corneal epithelial differentiation and LSCD treatment fields, it is evident that there is still no robust and efficient protocol that could differentiate both hESCs and hiPSCs towards functional corneal epithelium lineages. Furthermore, successful engraftment of hESCs or hiPSCs-derived corneal epithelial cells in animal model of LSCD has also not been reported to date. Thus our project was planned and aimed to address those needs.

## 1.5 Project Aims

1. To define efficient protocols for hESCs differentiation to corneal epithelial lineages.
2. To assess the efficiency of the hESCs derived protocols on hiPSCs.
3. To investigate the engraftment of hESCs and hiPSCs derived corneal epithelial-like cells in a mouse model of LSCD.

# CHAPTER 2. GENERAL MATERIALS AND METHODS

## 2.1 General Laboratory Practice

All experiments were carried out according to the Control of Substances Hazardous to Health (COSHH and BIOCOSHH) regulations. Cells and tissue culture experiments were performed in compliance with regulations for containment of Class II pathogens. All experimental procedures were in compliance with Newcastle University current safety policies.

## 2.2 Cell Culture

Human embryonic stem cell (hESC) line, H9 was purchased from WiCell (WiCell Research Institute, Inc. USA) and human induced-pluripotent stem cells (hiPSCs), SB-Ad2 and SB-Ad3 were generated and fully characterised in our group (Baud et al. 2017). All cell culture experiments were performed in a Class II biosafety cabinet laminar air flow tissue culture hood. Cells between passages 18 to 50 were used.

### 2.2.1 *Preparation of mTeSR™1 medium (STEMCELL Technologies, Cambridge, MA)*

A bottle of 5 x Supplement for mTeSR™1was thawed overnight at 2 - 8°C. The thawed 100 mL supplement was aseptically added to 400 mL mTeSR™1 Basal Medium to make a total volume of 500 mL. 5.0 mL of Penicillin/Streptomycin (Pen/Strep)(Gibco, UK) was added and the medium was well mixed. The complete mTeSR™1 medium is stable when stored at 2 - 8°C for up to 2 weeks.

### 2.2.2 *CORNING Matrigel matrix (Corning, USA) coated plates preparation*

A working solution of CORNING Matrigel (hESC-qualified) was the solution prepared for actual use by adding cold 240 µL Matrigel stock aliquot (thawed from -20°C on ice) to 15 mL of cold knock-out DMEM (Gibco, UK) to coat two and a half 6-well plates. 1.0 mL of the Matrigel working solution was pipetted onto each well of a cold 6-well plate. Formation of air bubbles was avoided by carefully pipetting the liquid into the wells. Matrigel solution was evenly spread by carefully swirling the solution across the surface. A chilled pipette tip was used to break any trapped air bubbles in the plate. Plates were incubated at room temperature (15-25°C) for at least 1 hour before use. Excess coating solution was aspirated carefully prior to adding 1.0 mL of mTeSR™1 medium into each coated well, before plating in cells. Coated plates were stored at 4°C for up to a week. The plates were sealed to prevent dehydration (e.g. using parafilm).

### 2.2.3 *Thawing cryopreserved hESCs or hiPSCs*

The hESCs/hiPSCs vial was removed from the liquid nitrogen storage tank. The vial was rolled between gloved hands for about 10-15 seconds to remove the frost. The vial was immersed and gently swirled in a 37°C water bath using long forceps without submerging the cap. The vial was removed from the water bath once only ice crystal remained in it. The outer surface of the vial was sterilised by spraying the tightly capped vial with 70% ethanol. The cells were then transferred gently into a sterile 15 mL conical tube using a 5.0 mL pipette. 11 mL of mTeSR™1 medium was added drop-wise to cells in the 15 mL conical tube. At the same time the tube was gently moved back and forth to mix the pluripotent stem cells and to reduce osmotic shock to the cells. The cells were then centrifuged at 1000 rpm for 5 minutes. The supernatant was aspirated and the cell pellet was resuspended 0.5 mL mTeSR™1 medium for every well that will receive cells. The cells were then gently pipetted up and down in the tube.

A 6-well plate coated with Matrigel was labelled with the cell line name, the passage number from the vial, the date and initials. Excess Matrigel coating solution was removed from the wells and 1.5 mL mTeSR™1 medium containing 10 µM Rho kinase inhibitor (ROCKi) (Y27632) (Chemdea, NJ, USA) was added to each well. Then 0.5 mL of the cell suspension was added drop-wise into each well. The plate was gently shaken back and forth and side to side to evenly distribute the cells. Circular motion was avoided to prevent pooling of cells in the centre of the well. Cells in each well were examined under a microscope and the plate was gently placed in the incubator. Spent medium was replaced daily from the wells.

### 2.2.4 *Feeding pluripotent stem cells*

The hESCs/hiPSCs were observed using a microscope to monitor cell growth or for any differentiating cells. The spent medium was aspirated and 2.0 mL of fresh mTeSR™1 medium was added into each well. This procedure was repeated daily until the cells require passaging.

### 2.2.5 *Passaging hESCs or hiPSCs on Matrigel with EDTA*

Cells were passaged every 3 to 4 days using 0.02% ethylene diamine tetraacetic acid (EDTA)(Versene, Belgium) solution. Initially, spent medium was aspirated and each well of a 6-well plate was washed with 2.0 mL of calcium and magnesium free Dulbecco phosphate buffered saline (DPBS) (Gibco, UK). The DPBS was aspirated and 1.0 mL of EDTA 0.02% solution was added to the well. The cells were incubated in a tissue culture incubator in a dark at 37°C and 5% $CO_2$ for 3 – 5 minutes. After the incubation period, cells were observed under

a microscope to check if the cell colonies were detaching from the plastic surface. The EDTA was aspirated and 3.0 mL of mTeSR™1 medium (1:3 passaging ratio) was added. The cell colonies were detached mechanically by pipetting and the resulting cells suspension from one well was added drop-wise into three wells of pre-warmed 6-well plate coated with Matrigel and supplemented with 1.0 mL mTeSR™1 medium per well. The plate was gently shaken back and forth and side to side to evenly distribute the cells. Cells in each well were examined under the microscope and the plate was gently placed in the incubator.

### 2.2.6 *Cryopreservation of hESCs or hiPSCs grown on Matrigel*

Spent medium was aspirated and each well of a 6-well plate containing 90% confluent cells was washed with 2.0 mL of calcium and magnesium free DPBS (Gibco, UK). The DPBS was aspirated and 1mL of warm StemPro Accutase (Gibco, UK) solution was added to the well. The cells were incubated in a tissue culture incubator in dark at 37°C and 5% $CO_2$ for 3 – 5 minutes. After the incubation period, cells were observed under a microscope to check if the cell colonies could easily be detached from the plastic surface. 3.0 mL of cold mTeSR™1 medium was added to each well. The cell colonies were detached mechanically by pipetting to produce a single cells suspension. The cell suspension was then being centrifuged at 1000 rpm for 3 minutes. Supernatant was discarded and the cell pellet was resuspended in 1.0 mL of filter-sterilised freezing medium consisting of 90% fetal bovine serum (FBS, Gibco, UK), 10% dimethyl sulfoxide (DMSO, Sigma Aldrich, Germany) and 10 µM ROCK inhibitor. The cell suspension in freezing medium was then transferred to a cryovial labelled with cell name, passage number, date and initial. The cell vial was transferred to a pre-cooled isopropanol-containing freezing container and stored in -80°C freezer for 1 or 2 days before being transferred into a liquid nitrogen storage container for long-term storage.

### 2.2.7 *Preparation of 3T3 fibroblasts medium*

3T3 fibroblast medium was prepared by mixing 89% high glucose Dulbecco's Modified Eagle's Medium (DMEM) + GlutaMAX, 10% FBS and 1% Pen/Strep. The resulting medium was filter-sterilised and stored at 2 - 8°C for 2 to 4 weeks.

### 2.2.8 *Thawing and culturing 3T3 fibroblast cells*

The fibroblast medium was warmed up to room temperature. A volume of 5.0 mL of the fibroblast medium was transferred to a 15 mL falcon tube. Cryovial containing 3T3 cells was quickly defrosted in a hot bath, until only small crystals of ice were left in the vial. A volume of 1 mL of fibroblast medium was added drop by drop to the cryovial containing the cells. The cells suspension was then transferred drop by drop to the falcon tube containing 5.0 mL of fibroblast medium. The falcon tube with cell suspension was then being centrifuged at 1000 rpm for 3 minutes. While the centrifuge is running, 5.0 mL of fibroblast medium was added to a labelled T25 flask. After centrifugation, the supernatant was discarded and the cell pellet was resuspended in 1.0 mL fibroblast medium. The cell suspension was then transferred to the T25 flask and the flask was gently rotated in order to uniformly spread the cells. The flask containing cells was incubated at 37°C in 5% $CO_2$.

### 2.2.9 *Passaging of 3T3 fibroblasts*

Spent medium was aspirated from the 80% confluent T75 culture flask. The flask was briefly washed with PBS. A volume of 5.0 mL of 0.05% Trypsin-EDTA (Gibco, UK) was transferred into the T75 flask to cover the surface of the flask. The flask was incubated for 5 minutes at 37°C. A double quantity (10 mL) of 3T3 fibroblast medium was added to the flask to inactivate the trypsin. The cell suspension was transferred into a 50 mL falcon tube. The falcon tube was centrifuged at 1000 rpm for 3 minutes. While the centrifugation was taking place, 15 mL of fibroblast medium was transferred into each of the new T75 flasks. The supernatant was aspirated and the cell pellet was resuspended in 1.0 mL of fibroblast medium. The cell suspension was split in the ratio desired (e.g:1:4), and transferred into new labelled flasks. The flasks were incubated at 37°C in 5% $CO_2$. Medium was changed on the third day and every other day from then on.

### 2.2.10 *Cryopreservation of 3T3 fibroblasts*

Freezing medium was prepared as follows: 90% FBS and 10% DMSO. The medium was then filter sterilised and stored at 4°C. Cryovials were labelled with the cell line, passage number, and cryopreservation date and name initials. Spent medium was aspirated from the T75 culture flask with the 80% confluent 3T3 fibroblasts. The flask was then briefly washed with PBS. 5.0 mL of 0.05% Trypsin-EDTA was added to the T75 flask to cover the surface of the flask. The flask was then incubated at 37°C for 5 minutes. A double quantity (10 mL) of 3T3 fibroblast medium was added to the flask to inactivate the trypsin. The cell suspension was transferred

into a 50 mL falcon tube. The falcon tube was centrifuged at 1000 rpm for 3 minutes. Supernatant was discarded and the cell pellet was resuspended in 2.0 mL of freezing medium. The resulting suspension was transferred into two cryovials. The cryovials were then stored in -80°C and then transferred to a liquid nitrogen storage 24 – 48 hours later.

### 2.2.11 *Inactivation of 3T3 fibroblasts using mitomycin C*

2.0 mg of mitomycin C (MMC) from *Streptomyces caespitosus* (Sigma-Aldrich, Germany) powder was dissolved in 2.0 mL of knock-out DMEM to make a stock concentration of 1 mg/mL mitomycin C solution. The stock solution was kept at 4°C in the dark. Spent medium from a T75 flask containing 80% confluent 3T3 fibroblasts was aspirated. The flask was briefly washed with DPBS. Then, 7.5 mL of fresh fibroblast medium was added to the flask. 7.5 µL of 1 mg/mL mitomycin C was added to the medium in the flask making up a final concentration of 1.0 µg/mL mitomycin C in the mixture. The mixture was mixed well and allowed to cover all the growing cells in the flask. The flask was incubated for 2 hours in the incubator at 37°C in 5% $CO_2$.

### 2.2.12 *Preparation of gelatine coated plates*

2.04 g of porcine gelatine powder was dissolved in 100 mL distilled water in a glass bottle. The solution mixture was autoclaved. The autoclaved 2% gelatine solution was aliquoted in 15 mL falcon tubes and stored in -20°C as long term stocks. The 2% gelatine solution was diluted in PBS to make up 0.2% gelatine/PBS solution. The 0.2% gelatine in PBS was filter sterilised and kept at 37°C before being used to coat the plastic plates. A volume of 1.5 mL of 0.2% gelatine/PBS was added into each well of a 6-well plate. The plate was incubated at 37°C for 1 hour or for 2 hours at room temperature in a laminar flow cabinet. The excess gelatine was aspirated from the wells. The wells were allowed to dry briefly before 2.0 mL 3T3 fibroblast medium is added.

### 2.2.13 *Preparation of 3T3 fibroblasts feeder plates*

After 2 hours of incubation, the fibroblast medium with added mitomycin C was removed from the 3T3 cells in T75 flask. The cells were then washed three times with PBS. Then 5.0 mL of 0.05% Trypsin-EDTA was added to the flask and the cells were incubated with trypsin for 5 minutes at 37°C. After 5 minutes, 10 mL of fibroblast medium was added to the flask. The cell suspension was then transferred to a 50 mL falcon tube and centrifuged at 1000 rpm for 3 minutes. Supernatant was discarded and the cell pellet was resuspended in 5.0 mL of fibroblast

medium. Cell count was performed using dual-chamber haemocytometer and a light microscope. 24.03 x $10^3$ cells were added into each well of the 6-well gelatine coated plates containing fibroblast medium. The plates were gently rocked forward and backward, and from side to side to spread the cells evenly on the plate. The plated cells were incubated at 37°C. The feeder plate will be ready to use on the following day.

### 2.2.14 *Preparation of limbal epithelium medium (Yu et al. 2016)*

The limbal epithelium medium was prepared by mixing together and filter-sterilising the following reagents: for a 500 mL epithelial medium: 75% low-glucose Dulbecco's modified Eagle's medium (DMEM) and 25% Ham's F12 medium (both Gibco, UK). This composition was supplemented with the following: 10% fetal bovine serum (FBS), 1% penicillin/streptomycin (both Gibco, UK), 500 µL hydrocortisone (0.4 mg/mL), 250 µL insulin (5 mg/mL), 35 µL triiodothyronine (1.4 ng/mL), 300 µL adenine (24 mg/mL), 84 µL cholera toxin (8.4 ng/mL) and 50 µL EGF (10 ng/mL) (all Sigma-Aldrich, UK).

### 2.2.15 *Seeding cells on 3T3 fibroblasts feeder plates for colony forming efficiency (CFE) assay*

Cell suspensions from different experimental groups on day 9 and day 20 were mixed well in their respective vial. Cell counts were performed for each group using a dual-chamber haemocytometer and a light microscope. Fibroblast medium was removed from the feeder plates and it was replaced by the limbal epithelial medium. 500 – 1000 cells were added to each well containing the feeder cells and the limbal epithelial medium. Three wells of CFE were set for each group in each biological replicate. The limbal epithelial medium was replaced after three days and every other day thereafter. The CFE plates were regularly observed and kept in culture for 14 days.

### 2.2.16 *Staining the cell colonies with rhodamine-B (Sigma-Aldrich, Germany)*

After 14 days, spent medium was aspirated from the CFE plates and the wells were washed with PBS once. Then 1.0 mL of 3.7% formaldehyde (VWR chemicals, UK) was added into each well. The cell colonies were fixed in formaldehyde for 10 minutes at room temperature. Then the formaldehyde was discarded. The wells were washed with PBS once before enough volume of 1% rhodamine-B in absolute methanol (VWR chemicals, UK) was added to each well. The colonies were stained for 10 minutes before the stain being washed three times with PBS. Stained cell colonies (shown by the arrows) in cell culture plates (Figure 2.1) were

observed and counted with the aid of a dissection microscope. Adult human limbal epithelial cells were used as positive control for all CFE.

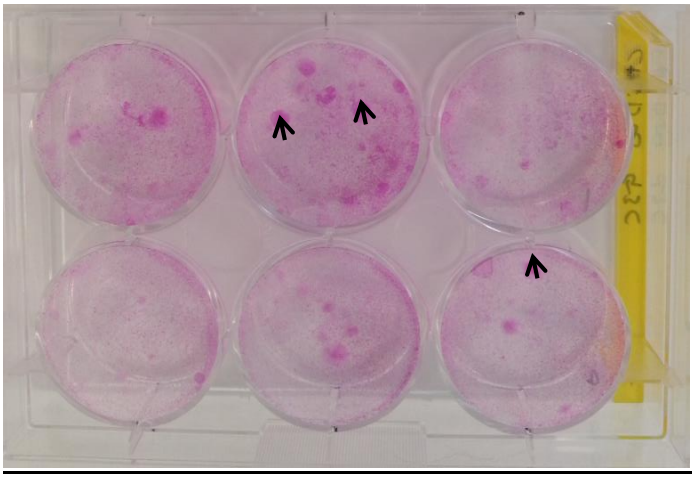

**Figure 2.1 : A representative photo of cell colonies stained with rhodamine-B in a cell culture plate from differentiating hESC (H9) in a 6-well plate. Black arrows showing some of the stained cell colonies.**

### 2.3 RNA Isolation From Cells

RNA was extracted from the cells collected from experimental hESCs and iPSCs and at days 0, 3, 6, 9, 14, 20 of the monolayer experiment. This was achieved using the ReliaPrep$^{TM}$ RNA Cell Miniprep System (Promega, WI) following methods as described in the instruction manual.

In brief, cell pellets were mixed with 500 µL BL buffer with added 1-Thioglycerol to lyse the cells. Then sample tubes were briefly centrifuged. A collection tube and a mini column for each sample were prepared and the mini column was labelled accordingly. 170 µL of 100% isopropanol (VWR chemicals, UK) was added to the sample cell lysate and the solution was carefully mixed by pipetting. The sample mixture was then transferred into the mini column and being centrifuged for 30 seconds at 12,000 – 14,000g at 20 – 25°C. The mini column was removed and the liquid in the collection tube was discarded before the mini column was placed back into the collection tube.

500 µL RNA wash solution (diluted with ethanol) was added to the mini column and then being centrifuged for 30 seconds at 12,000 – 14,000g at 20 – 25°C. The collection tube was emptied as before. DNase I incubation mixture was prepared by combining 24 µL of Yellow Core Buffer, 3.0 µL of $MnCl_2$ (0.09M) and 3.0 µL of DNase I enzyme to make up the total of 30 µL of solution mixture. This mixture was mixed gently by pipetting.

30 µL of freshly prepared DNase I incubation mix was directly applied to the membrane inside the mini column to thoroughly cover the membrane. The DNase 1 mixture on the mini column membrane was allowed to incubate for 15 minutes at room temperature. Then, 200 µL column wash solution (added with ethanol) was added to the mini column before being centrifuged for 15 seconds at 12,000 – 14,000g at 20 – 25°C. 500 µL of RNA wash solution (ethanol added) was added and the mini column was centrifuged again for 30 seconds at 12,000 – 14,000g at 20 – 25°C. The mini column was transferred into a new collection tube and 300 µL of RNA wash solution (ethanol added) was added. The mini column was centrifuged at high speed for 2 minutes and then the mini column was transferred to a labelled elution tube. 15 µL of nuclease free water was added to the mini column membrane to completely cover the membrane surface with water. The mini column in elution tube was then being centrifuged for 1 minute at 12,000 – 14,000g at 20 – 25°C. Then the mini column was discarded and the elution tube was capped. The purified RNA was stored at -80°C.

### 2.3.1 *RNA quantification*

The RNA concentration was measured using a Nanodrop Spectrophotometer 2000 (Thermo Fisher, MA) machine. Initially the spectrophotometer was calibrated with 1.0 µL nuclease free water as a blank solution and followed by 1.0 µL of the RNA sample. A260/280 is the absorbance ratio to determine the purity of RNA or DNA. A value of 1.5 – 2.5 is acceptable for DNA or RNA purity.

## 2.4 Reverse Transcription

GoScript™ Reverse Transcription System (Promega, WI) was used to convert 1.0 µg of extracted RNA into cDNA following the method described in the instruction manual. Experimental RNA, Primer Oligo (dT)15 (0.5 µg/reaction) and Nuclease-Free water were briefly centrifuged and mixed to make up a total volume of 5.0 µL. The mixture was then heated in a 70°C heat block for 5 minutes. It was then immediately chilled in ice water for at least 5 minutes before being centrifuged for 10 seconds and stored on ice. The reverse transcription mix was prepared on ice by mixing 4.0 µL of GoScript 5x Reaction buffer, 3.0 µL of $MgCl_2$ (final concentration (1.5 – 5.0 mM), 1.0 µL of Oligo (dT)15 primer, 1.0 µL of GoScript Reverse Transcriptase and 6.0 µL of nuclease-free water to a final total volume of 15 µL for each cDNA reaction. 15 µL of reverse transcription mix was combined with the 5.0 µL of RNA and primer mix prepared earlier. Then the reaction mixture was annealed in a heat block at 25°C for 5

minutes, extended in a heat block at 42°C for up to 1 hour using a thermal cycler machine (Eppendorf, UK), and then stored at -20°C.

## 2.5 Quantitative Real-Time Reverse Transcription Polymerase Chain Reaction (qRT-PCR)

### 2.5.1 *Primer design*

Gene sequences were obtained from National Centre for Biotechnology Information (NCBI) and Basic Local Alignment Search Tool (BLAST®) databases specified for human species. NCBI/Primer-BLAST was used to design forward and reverse primers for all the genes. Designed primers were generally 17-25 nucleotides in length within the 100-200 bp product size and both the forward and reverse primers are spanning an exon-exon junction so that genomic contamination can be avoided. The melting temperature (Tm) was determined for both the forward and reverse primers using the formula:

Tm = 4(G+C) + 2(A+T). The initial annealing temperature (Ta) used for each PCR reaction was generally 5°C below the lowest Tm of the primer pair (forward and reverse primers).

### 2.5.2 *Quantitative real-time reverse transcription polymerase chain reaction (qRT-PCR) and analysis*

For quantification of genes expression in the control and experimental hESCs and hiPSCs, qRT-PCR was used. For each of qRT-PCR reaction mixture, 1.0 µL of cDNA produced from 1.0 µg of RNA was amplified in a 384-well plate using the 2x GoTaq® qPCR Master Mix (consisting of Hot Start Polymerase, $MgCl_2$, dNTPs and reaction buffer) with carboxy-X-rhodamine (CXR) reference dye (both by Promega, WI). In summary, Forward primer, Reverse primer and Nuclease-free water were mixed to make up 1.0 µM primers mixture solution for each target gene. The resulting solution was briefly centrifuged before being kept on ice. The cDNA samples were then diluted in micro-eppendorf tubes and kept on ice. Diluted cDNAs were then added to qPCR mastermix in 1.5 mL eppendorf tubes before nuclease-free water was added to the mixture. Then, CXR reference dye was added to the mixture and the tubes containing sample mixtures were centrifuged briefly then kept on ice. A qPCR plate was labelled before 7.5 µL of each sample mixtures was loaded to each well. Unopened stickers were used as guide and to avoid cross contamination during sample loading.

The qPCR plate was then centrifuged briefly and checked to ensure that all the wells were loaded with sample solution. 2.5 µL of primer mix was added to each sample containing wells.

The plate was centrifuged again for 1 minute and checked for any missing reaction solution. A sticker sheet was then applied on the plate and properly pressed down onto the plate. The sticker edges were trimmed. The plate was then centrifuged for 5 minutes. The qPCR machine was turned on and the qPCR program was started, a new experiment was set up and the programme was set to 'RUN' after the qPCR plate was placed on the machine tray.

The reactions analyses were carried out using The Applied Biosystems 7900HT Fast Real-Time PCR System by Life Technologies in a similar sequence to that of standard PCR. Following completion of the PCR program, the data was analysed using SDS v2.4 software (Applied Biosystems) for ΔΔCt and $2^{-\Delta\Delta Ct}$ calculations (Livak and Schmittgen 2001).

### 2.6 Immunocytochemistry (ICC)

Cells were dissociated and kept as suspension in 2% FBS/PBS on ice. Cell count was manually performed using dual-chamber haemocytometer and a light microscope prior to cytospin step.

#### 2.6.1 *Cytospining cells suspensions for slides preparation*

Slides were initially labelled, and then the slides and filters were correctly placed into appropriate slots in the cytospin with the cardboard filters facing the center of the cytospin. Each filter and slide pair is clipped with each other and the hole in the filter is in proper position so that cells will be able to reach the slide. 100 µL of cell suspension with known number of cells per µL (1000 cells/µL) was quickly aliquoted into a cyto-funnel chamber corresponding to a correctly labelled slide. The lid of the cytospin was carefully placed over the samples and spun at 1000 rpm for 3 minutes. The filters were removed from their slides without contacting the smears on the slides. A border line encircling the cells' area on the slide was then drawn using an ImmEdge Hydrophobic Barrier Pen (Vector Laboratory, Burlingame, CA).

#### 2.6.2 *Antibody dilution optimisation*

Dilution optimisations for each of primary antibodies was carried out by diluting the primary antibody in antibody diluent comprising PBS, 0.1% bovine serum albumin (BSA) (Sigma Aldrich, Germany) and 0.3% Triton-X-100 (Sigma Aldrich, Germany), to make up 1:50 and 1:100 dilutions. Similar optimisation step was carried out for secondary antibodies, where the dilution factors used were 1:600 and 1:800. Dilutions that gave bright signal and less background were selected.

### 2.6.3 *Immunostaining the cytospun cells*

On the first day, cytospun cells on slides were first fixed in 4% paraformaldehyde (Sigma Aldrich, Germany) for 30 minutes at room temperature. The cells were washed with PBS for 3 times (5 minutes each time). Cells were permeabilized with 0.1% Triton X-100 for 15 minutes. A blocking solution consisting of 5% BSA, 5% goat serum (SigmaAldrich, Germany) and 0.3% triton-X-100 was added for 1 hour. For surface markers, the same blocking solution was used but without the addition of Triton-X. Primary antibody was diluted in antibody diluent to give desired working concentration. Diluted primary antibody was added to the cells and left in the fridge/cold room in a wet chamber overnight at 4°C. Control immune-labelling where only secondary antibody was added was prepared in all experiments.

On the next day, the secondary antibody was diluted in antibody diluents as for the primary antibody. The cells were washed with antibody diluent for 3 times (3 minutes each wash). Secondary antibody was then added and left at room temperature for 2 hours. The secondary antibody is photosensitive and must be kept in the dark to avoid bleaching of the fluorochromes. The wells were washed using antibody diluent for 3 times (3 minutes each time). 4',6-diamidino-2-phenylindole (DAPI) (dilution 1:10) was added to the wells to stain the cell nuclei for 5 minutes. The wells were then washed 3 times (3 minutes each) using PBS. The slides were mounted using Vectashield (Vector Laboratories, Burlingame, CA) with Hoechst 33342 Solution (2000:1) (Thermo Scientific, UK) and they were covered with cover slips in the case of plates. Plates were stored in the fridge in the dark for up to 4 weeks and imaging repeated.

## 2.7 Microscopy and Quantification Software

### 2.7.1 *Inverted microscopy*

Cells in cultures, plates, and flasks were observed using a Bioscience Axiovert 200M microscope in combination with the associated CarlZeiss software-AxioVision, which allows the performance of transmitted light bright field, phase contrast and epifluorescence technique. Images were then processed using the AxioVision40 version 4.8.2.0 software (Zeiss AxioVert 1, Germany).

### 2.7.2 *Fluorescence microscopy*

Dry slides were observed under a fluorescence microscope. Pictures were taken at different magnifications on the same day up to 2 days after fluorescence staining to keep the quality of the images all the same. The images captured at 20x magnification using the fluorescence

microscope were exported as JPEG files. Three images were captured for each slide from each of the experimental groups. ImageJ software was then used to count the stained and unstained cells from the pictures. Five fields, each containing more than 100 cells were counted for each group.

### 2.8 Statistical Analysis

Quantitative data were presented as mean ± standard error of mean. Statistical analysis and graphs generation were carried out using Microsoft Excel and GraphPad Prism 7 software. Significance differences between the data were analysed using one-way ANOVA, in which a p value less than 0.05 ($p<0.05$) was considered as statistically significant. In each figure the shown values represent the mean ± SEM ($n = 3$). * denotes $p < 0.05$; ** denotes $p < 0.01$, *** denotes $p< 0.001$ and **** denotes $p< 0.0001$.

# CHAPTER 3. DIFFERENTIATION OF HESCS AND HIPSCS INTO CORNEAL EPITHELIAL LIKE CELLS

## 3.1 Introduction

Cornea is the transparent region at the front of the eye which enables transmission of light to the retina. It comprises the corneal epithelium, stroma and endothelium. The corneal epithelium is continuously regenerated by limbal stem cells (LSCs) (Schlotzer-Schrehardt and Kruse 2005, Li et al. 2007) which migrate from peripheral to central region of the cornea and ascend from basal to superficial layer in order to differentiate and form a new stratified layer of non-keratinized squamous epithelium (Lu et al. 2001). The corneal epithelium develops from surface ectoderm (Hay 1980), whilst the stroma and endothelium developed from the mesenchymal tissue and neural crest cells (Amano et al. 2006).

Limbal stem cell deficiency (LSCD) is a disease caused by the loss or dysfunction of LSCs, leading to loss of corneal epithelial integrity and function, resulting in persistent pain and severe visual impairment (Dua et al. 2000). Work done by our group and others have shown that the transplantation of *ex vivo* expanded autologous LSCs is able to reconstruct the corneal surface and to restore vision in patients with unilateral total LSCD (Kolli et al. 2010, Rama et al. 2001, Dua and Azuara-Blanco 2000). This treatment however is not applicable to a significant number of patients with total bilateral LSCD where patient's both eyes are devoid of LSCs which are needed for the *ex vivo* expansion and subsequently used for transplantation. Hence alternative sources of cells that could be used to replace the missing LSCs in total bilateral LSCD are being sought after by many researchers.

Of those, transplantation of *ex vivo* expanded oral mucosa epithelial (OME) cells has been the most used cell source in clinical studies of bilateral LSCD treatment with a reported 'success' rate of 48-75% within follow up times up to 34 months (Inatomi et al. 2006, Nishida et al. 2004, Burillon et al. 2012, Hirayama et al. 2012, Sotozono et al. 2013, Chen et al. 2009, Ma et al. 2009, Sheth et al. 2015, Kolli et al. 2014). Our group also showed that cultured oral epithelial cells retained a gene expression profile that was attributed to epithelial stem cells in general, but they did not acquire a typical limbal expression pattern after 10-14 days in culture (Kolli et al. 2014), thus indicating that the transplanted cells did not fully transdifferentiate into corneal epithelium.

Recent advances in somatic cell induced reprogramming have shown that it is possible to reprogram somatic cells back to an “embryonic like cells” through overexpression of four key pluripotency factors. These are named induced pluripotent stem cells and like human embryonic stem cells (hESCs) they are characterised by unlimited self-renewal and potential to differentiate into any cell type of the adult organism (Takahashi et al. 2007, Lewitzky and Yamanaka 2007). The most important advantage of human induced pluripotent stem cells (hiPSCs) is the ability to avoid post-transplantation rejection by patient’s immune system (Tucker et al. 2014).

Previous studies in the field have replicated early developmental mechanisms by blocking the transforming growth factor β (TGFβ) and Wnt-signaling pathways with small-molecule inhibitors and activating fibroblast growth factor (FGF) signaling (Mikhailova et al. 2014) to generate corneal epithelial-like progenitor cells capable of terminal differentiation toward mature corneal epithelial-like cells within 44 days. TGF-β pathway has been shown to play multiple roles in maintenance of pluripotency and early cell fate decisions. Work done by other groups (Vallier et al. 2004) and ours (Zhu et al. 2016) has shown that low activity of this pathway (either through application of inhibitors or low endogenous activity) results in neuroectodermal default pathway which skews pluripotent stem cells away from non-neural ectoderm and corneal epithelial differentiation.

For this reason, we designed our differentiation protocol to include growth factors and morphogens (BMP4, RA, EGF) that have been shown to promote non-neural ectodermal commitment (Gambaro et al. 2006, Aberdam et al. 2007, Metallo et al. 2008, Li and Lu 2005) and proliferation of corneal epithelial progenitors. In the second window of differentiation, we attempted to replicate the LSC niche by coating the cell culture surfaces with collagen-IV shown to be the key component of limbal stroma and (Schlotzer-Schrehardt et al. 2007, Blazejewska et al. 2009) and feeding the cells with a defined media (CnT-Prime) which is used to maintain the ex vivo expansion of human corneal epithelial progenitors (Gonzalez et al. 2017).

Traditionally, differentiation of hESCs and hiPSCs to corneal epithelial cells has relied on usage of feeder cells, undefined conditioned media or amniotic membrane (Ahmad et al. 2007, Hanson et al. 2013, Hayashi et al. 2012, Hewitt et al. 2009, Shalom-Feuerstein et al. 2012). More recently, small molecule driven protocols have become available resulting in generation

of corneal epithelial–like cells within six weeks (Mikhailova et al. 2014). However, no protocols for robust hESCs and hiPSCs derived corneal epithelium differentiation that reflects in fully functional corneal epithelium or LSCs has been reported to date. Thus this chapter describes the development of a defined feeder-free monolayer differentiation method which results in differentiation of hESCs and hiPSCs to corneal epithelial like cells within 20 days.

## 3.2 Specific Objectives

The specific objectives of this chapter are:

a - to define efficient protocols for robust hESCs differentiation to corneal and limbal epithelial cells using monolayer culture methods.

b - to apply and assess the efficiency of hESCs-derived protocols on hiPSCs.

## 3.3 Materials and Methods

### 3.3.1 *Cell culture*

All cell culture was performed in a Class II biosafety cabinet laminar air flow tissue culture hood as detailed in Chapter 2. Cells were between passage 18 and 50, and maintained in mTeSR™1 medium. Every 3 to 4 days, cells were passaged using 0.02% ethylene diamine tetraacetic acid (EDTA) (Versene, Lonza, Belgium) solution.

### 3.3.2 *Plating the human pluripotent stem cells (hPSCs) for monolayer experiment*

a. Plating pluripotent cells on day0

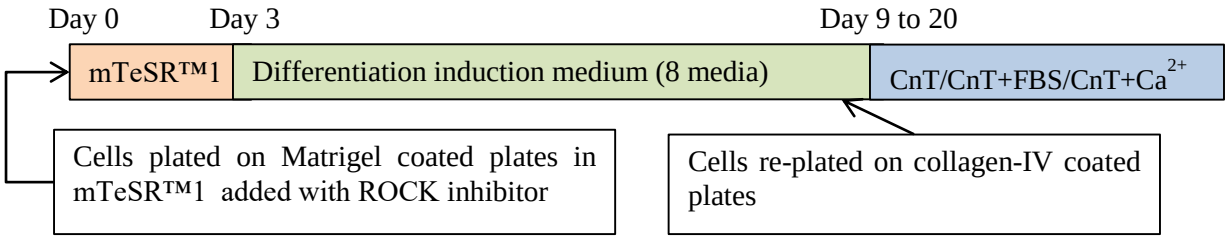


**Figure 3.1 : A schematic of the monolayer differentiation method.**

Used mTeSR™1 media was aspirated from the wells and the wells were gently washed with 2.0 mL calcium and magnesium free Dulbecco phosphate-buffered saline (DPBS). The DPBS was aspirated and 1.0 mL of warm StemPro Accutase (Gibco, UK) was added to each well. The cells in accutase were incubated for 2 – 3 minutes at 37°C before 3.0 mL cold mTeSR™1 medium per well was added to inactivate the accutase. Cells were collected from all wells and transferred into a 50 mL falcon tube. The cells were then centrifuged at 800 rpm for 4 minutes.

Supernatant was removed and cell pellet was resuspended in 5.0 mL of warm mTeSR™1 medium. The cells were counted using a dual chamber haemocytometer and a light microscope.

Cells were plated at the density of 1.7 – 2.0 x $10^4$ cells/$cm^2$ in each well of a 6 well plate with mTeSR™1 media supplemented with ROCK inhibitor at concentration of 10 μM. The ROCK inhibitor was added only on the day of plating cells to aid the stem cells survival as single cells (Watanabe et al. 2007). Fresh mTeSR™1 medium without ROCK inhibitor was used to replace the used medium on days 1 and 2. The remaining cells were collected as day 0 cell pellet for qPCR. Three wells were assigned for every experimental group and two additional wells of cells were plated for qPCR cell sample at day 3. The mTeSR™1 medium was changed every day until day 3. At day 3, the mTeSR™1 medium was replaced with prepared and filter sterilised eight different serum free differentiation media according to the experimental groups. The basic supplements such as N2 (Lifetech, Thermo Fisher Scientific, UK), B27 (Lifetech, Thermo Fisher Scientific, UK), non-essential amino acids (NEAA), glutamine and penicillin/streptomycin solution were all added into the basal medium of low glucose DMEM/F12 (1:1) to provide the essential nutrients needed for the optimal cell growth as a substitute to serum. The resulting medium was called the "control medium" (CM).

Photos of growing cells were taken at days 3 (before adding differentiation media), 6 and 9 using Bioscience Axiovert 200M microscope in combination with the associated CarlZeiss software-AxioVision as detailed in Chapter 2. Medium change was performed daily from day 3 to day 9 for all groups. One well of cells from each group was collected for qRT-PCR on day 6 and day 9. RNA extraction and complementary DNA (cDNA) generation was done before real-time quantitative PCR (qRT-PCR) to assess the expression of *ΔNp63, ECadherin, CK8, BRACHYURY, PAX6, BMP4* and *OCT4* was performed at days 0 and 9.

b. Replating differentiating cells under limbal epithelial culture conditions (day 9 - 20)

Collagen IV coated 12-well plates were prepared based on method by Ahmad et al. 2007 and detailed in section 3.2.4 of this chapter. Cells from the remaining well of each experimental group in stage 1 were disassociated with TrypLe express (Gibco, UK). Cells were plated at the density of 1.7 – 2.0 x $10^4$ cells/$cm^2$ in three different media prepared using CnT-Prime 2D Diff. (CellnTec, Switzerland) media with or without the addition of 10% FBS and 0.07 mM calcium supplement ($CaCl_2$) (Sigma-Aldrich, Germany).

Photos of cells were taken every 3-5 days using Bioscience Axiovert 200M microscope in combination with the associated CarlZeiss software-AxioVision as detailed in Chapter 2. Cell samples were collected at days 14 and 20 for RNA extraction, cDNA generation and qRT-PCR for all conditions. Real-time qRT-PCR was performed for the limbal and corneal epithelial cell, epithelial cell junction proteins and neuro-ectodermal markers: *ΔNp63, ABCG2, CK3, CK12, ECadherin*, and *PAX6*.

### 3.3.3 *Preparation of the differentiation media and supplements*

The supplements needed for the differentiation media was prepared first prepared as follows:

a. Reconstitution of rhBMP4 (RnD Systems)

50 µg rhBMP4 powder needed to be dissolved in sterile 4 mM HCl (Sigma-Aldrich, Germany) in at least 1% bovine serum albumin (BSA)(Sigma-Aldrich, Germany). Initially the 4 mM hydrochloric acid (HCl) was prepared by diluting 3.0 µL of 12 M HCl in 10 mL of sterile $dH_2O$. 0.1 mg of BSA was then dissolved in the diluted HCl. 2.0 mL of the resulting solution was then used to dissolve the rhBMP4 powder to make up a 25 µg/mL stock solution. The stock solution was then being aliquoted in micro centrifuge tubes and stored at -20°C.

b. Preparation of all trans retinoic acid (Sigma-Aldrich, Germany) solution

3 mg of all trans retinoic acid (RA) powder was dissolved well in 10 mL DMSO (Sigma Aldrich, Germany) to make up 10 mL of 1 mM RA stock solution. The solution was then aliquoted in micro centrifuge tubes and stored in -20°C.

c. Reconstitution of IWP-2 (Merck Milipore)

10 mg of IWP-2 powder was dissolved in 2.14 mL DMSO to make up a 10 mM stock solution. The resulting stock solution was aliquoted and stored in -20°C.

d. Reconstitution of SB505124 (Sigma-Aldrich, Germany)

5 mg of SB505124 powder was dissolved in 1.49 mL DMSO to make up a 10 mM stock solution. The resulting stock solution was aliquoted and stored in -20°C.

e. Reconstitution of LDN 193189 (Stemgent)

2 mg of LDN 193189 powder was dissolved in 4.52 mL of DMSO to make up a 1 mM stock solution. The resulting stock solution was aliquoted and stored in -20°C.

f. Reconstitution of human EGF (Sigma-Aldrich, Germany)

500 µg EGF was dissolved in 1000 µL sterile $dH_2O$ to make up a 0.5 mg/mL stock solution. The resulting stock solution was aliquoted and stored in -20°C.

g. Preparation of eight differentiation media

The eight differentiation media were prepared by adding the appropriate csupplements and filter-sterilising the resulting medium. Each medium comprise the components listed in the following cluster of tables.

| **Group 1** | **Materials / final concentration** |
|---|---|
| | DMEM-F12 (1:1) |
| | N2 supplement (100x); 1 % (v/v) |
| | B27 supplement (50x); 2 % (v/v) |
| | Non-essential amino acids (100x); 1 % |
| | L-glutamine (100x); 1 % |
| | Pen/strep; 1 % |

| Group 2 | Materials / final concentration |
|---|---|
| | Group 1 medium |
| | rhBMP4; 25 ng/mL |

| Group 3 | Materials / final concentration |
|---|---|
| | Group 1 medium |
| | All trans retinoic acid; 1 µM |

| Group 4 | Materials / final concentration |
|---|---|
| | Group 1 medium |
| | EGF; 10 ng/mL |

| Group 5 | Materials / final concentration |
|---|---|
| | Group 1 medium |
| | rhBMP4; 25 ng/mL |
| | All trans retinoic acid; 1 µM |

| | |
|---|---|
| | EGF; 10 ng/mL |

| Group 6 | Materials / final concentration |
|---|---|
| | Group 1 medium |
| | SB-505124; 10 µM |
| | IWP-2; 10 µM |

| Group 7 | Materials / final concentration |
|---|---|
| | Group 1 medium |
| | rhBMP4; 25 ng/mL |
| | SB-505124; 10 µM |
| | IWP-2; 10 µM |

| Group 8 | Materials / final concentration |
|---|---|
| | Group 1 medium |
| | LDN193189; 100 nM |

**Table 3.1 : List of components for each differentiation media.**

### 3.3.4 *Collagen-IV coated plates preparation (Ahmad et al. 2007)*

A 0.25% acetic acid (VWR chemicals, UK) in sterile distilled water ($dH_2O$) was prepared to reconstitute the lyophilized collagen IV from human placenta (Sigma-Aldrich, Germany) to a concentration of 0.5 mg/mL. The solution mixture was placed at 4°C for 3 hours with intermittent swirling once the acetic acid was added. The reconstituted collagen aliquots can be stored at -20°C for 1 - 3 years. A 2 $cm^2$ tissue culture well was coated with collagen-IV by adding 200 µL of the collagen solution into each well and then the culture plates were then sealed and placed at 4°C overnight. Excess collagen-IV solution was removed and the wells were briefly washed with DPBS before plating of cells on day 9.

### 3.3.5 *RNA isolation and cDNA synthesis*

RNA was extracted from the cells collected from experimental hESCs and hiPSCs and at days 0, 9, and 20 of the monolayer experiment. This was achieved using the ReliaPrep™ RNA Cell Miniprep System (Promega, WI) following methods as described in the manufacturer's instruction manual. RNA was quantified before cDNA synthesis was performed using Promega

GoScript™ Reverse Transcription System following the manufactures instructions and as previously detailed in Chapter 2.

### 3.3.6 *Quantitative PCR (qRT-PCR)*

Quantification of endogenous pluripotency and differentiation genes expression in the control and experimental hESCs and hiPSCs was assessed by qRT-PCR as previously detailed in Chapter 2. The sequences of the primers (Sigma-Aldrich, UK) used are listed in the following table.

| Gene name/Primer | Sequence (5' – 3') |
|---|---|
| ***PITX2*** | F: CCTTACGGAAGCCCGAGT<br>R: CCGAAGCCATTCTTGCATA |
| ***BMP4*** | F: TCCACAGCACTGGTCTTGAG<br>R: GGGATGTTCTCCAGATGTTCTT |
| ***CK12*** | R: GAAGAAGAACCACGAGGATG<br>R: TCTGCTCAGCGATGGTTTCA |
| ***ABCG2*** | F: CGAGTCTGTTGGTCAATCTC<br>R: TCCTGTTGCATTGAGTCCTG |
| ***CK8*** | F: GATCGCCACCTACAGGAAGCT<br>R: ACTCATGTTCTGCATCCCAGACT |
| ***OCT4*** | F: TCTCGCCCCCTCCAGGT<br>R: GCCCCACTCCAACCTGG |
| ***SOX2*** | F: GGCAGCTACAGCATGATGCAGGACC<br>R: CTGGTCATGGAGTTGTACTGCAGG |
| ***SIX1*** | F: TAAGAACCGGAGGCAAAGAG<br>R: CCCCTTCCAGAGGAGAGAGT |
| ***GATA3*** | F: CTCATTAAGCCCAAGCGAAG<br>R: TCTGACAGTTCGCACAGGAC |
| ***ECADHERIN*** | F: CCCGGGACAACGTTTATTAC<br>R: GCTGGCTCAAGTCAAAGTCC |
| ***ΔNp63*** | F: CTGGAAAACAATGCCCAGAC<br>R: GGGTGATGGAGAGAGAGCAT |
| ***BRACHYURY*** | F: CCCTATGCTCATCGGAACAA<br>R: CAATTGTCATGGGATTGCAG |

| | |
|---|---|
| ***SIX3*** | F: CCCACACAAGTAGGCAACTG<br>R: GTCCAATGGCCTGGTGCT |
| ***EN1*** | F: GCACACGTTATTCGGATCG<br>R: GCTTGTCCTCCTTCTCGTTC |
| ***RAX*** | F: GGCAAGGTCAACCTACCAGA<br>R: GCTTCATGGAGGACACTTCC |
| ***SOX10*** | F: GACCAGTACCCGCACCTG<br>R: GCGCTTGTCACTTTCGTTC |
| ***CK3*** | F: CGTACAGCTGCTGAGAATGA<br>R: CTGAGCGATATCCTCATACT |
| ***PAX6*** | F: TCTTTGCTTGGGAAATCCG<br>R: CTGCCCGTTCAACATCCTTAG |
| ***GAPDH*** | F: TGCACCACCAACTGCTTAGC<br>R: GGCATGGACTGTGGTCATGAG |

**Table 3.2 : List of primers and their sequences used for qRT-PCR.**

Analysis was carried out using The Applied Biosystems 7900HT Fast Real-Time PCR System by Life Technologies in a similar sequence to that of standard PCR. Following completion of the PCR program, the data was analysed using SDS v2.4 software (Applied Biosystems), ΔΔCt and $2^{-\Delta\Delta Ct}$ calculations.

### 3.3.7 *Immunocytochemistry (ICC)*

Excess cells from day 9 and day 20 cells' dissociation and replating process were kept in 2% FBS/PBS on ice in different vials. Undifferentiated cells were similarly prepared and stained as negative controls. Cell count was performed for each group. Cells were cytospun onto slides and stained as detailed in Chapter 2. The list of antibodies used and their dilution factor are listed in the table below.

| Antibodies | React with | Developed in | Dilution | Cat. No. / Company |
|---|---|---|---|---|
| **CK3 primary** | Rabbit, cow, human | Mouse | 1:100 | [AE5] Ab77869 / Abcam |
| **P40 (ΔNp63) primary** | Human, mouse, rat, bovine | Rabbit | 1:100 | NBP2-29467 / Novusbio |

| | | | | |
|---|---|---|---|---|
| **CK12 primary** | human | Rabbit | 1:100 | NBP2-34843/ Novusbio |
| **CK13 primary (AF 647 conjugated)** | Human, mouse | Rabbit | 1:200 | [EPR3671] Ab198585 / Abcam |
| **PAX6 primary** | Mouse, rat, sheep, cow, dog, human, rhesus monkey | Rabbit | 1:50 | Ab5790 / Abcam |
| **Anti-Mouse IgG (FITC)** | Mouse | Goat | 1:800 | F2012 / Sigma |
| **Anti-Rabbit IgG (FITC)** | Rabbit | Goat | 1:800 | F9887 / Sigma |

**Table 3.3 : List of antibodies used and their dilution factor.**

The stained slides were mounted using Vectashield (Vector Laboratories, Burlingame, CA) with Hoechst 33342 Solution (2000:1) (Thermo Fisher Scientific, UK) and they were covered with cover slips in the case of plates. Plates were stored in the fridge in the dark for up to 4 weeks and imaging repeated. Cells were viewed using a Bioscience Axiovert microscope in combination with the associated CarlZeiss software-AxioVision (Zeiss, Germany).

### 3.3.8 *Microscopy*

Dry stained slides were observed under a fluorescence microscope. Pictures were taken at different magnifications on the same day up to 2 days after fluorescence staining to keep the quality of the images all the same. The images, captured at 20x magnification using the fluorescence microscope, were exported as JPEG files. ImageJ software was then used to count three random fields of the stained and unstained cells, in which a total of at least 100 cells were counted. Three random pictures were taken per slide per group.

### 3.3.9 *Colony forming efficiency (CFE) assay*

During the second stage of the cell culture on day 9, cells were dissociated using TrypLe express (Gibco, UK), counted and replated on collagen IV coated plates, some cells were kept for colony forming efficiency assay. Limbal stem cells (LSCs) expanded from donated human limbal rings consist of a mixture of undifferentiated (60 – 80%) and differentiated LSCs were

used as a positive control. Three wells of 6-well plate were set for each experimental group in each biological replicate. The CFE assay was carried out as detailed in Chapter 2 (sections 2.2.15 and 2.2.16) and the resulting colonies were stained with rhodamine-B.

### 3.3.10 *Statistical analysis*

Statistical analysis and graphs generation were carried out using Microsoft Excel and GraphPad Prism 7 software. Z scores were calculated using the following formula: Z score = D/SEM where D is the difference between the two means and SEM is the standard error of mean (computed from the data). In each figures the shown values represent the mean ± SEM (n=3). Significance differences between the data were calculated using one-way ANOVA, in which p values less than 0.05 were considered as statistically significant.

## 3.4 Results

This monolayer experiment was designed to robustly differentiate pluripotent stem cells into corneal and limbal epithelium. HESCs and hiPSCs were initially plated as single cells on Matrigel coated plates and supplemented with mTeSR™1 medium with added ROCK inhibitor. The cells were plated at the density of $1.7 – 2.0 \times 10^4$ cells/cm$^2$, based on the previous protocols by Leung et al. 2013, which suggested this seeding density as optimal for ectodermal differentiation of hESCs and avoiding neural crest cells differentiation. ROCK inhibitor was added only on the day of plating cells to improve cells' survival as single cells (Watanabe et al. 2007).

### 3.4.1 *The differentiation induction media*

On day 3, the mTeSR™1 medium was changed to several differentiation initiation media. The basic supplements such as N2, B27, non-essential amino acids (NEAA), glutamine and penicillin streptomycin were all added into the basal medium of low glucose DMEM/F12 (1:1) to provide the essential nutrients needed for the optimal cell growth as the substitute of serum. The resulting medium was called the control medium (CM) and it was supplemented to cells in Group 1.

Specific supplements were added to the CM according to the experimental groups to observe the inter-relations between various differentiation pathways on the morphological and gene expression of the differentiating stem cells. Based on various published literatures, six specific supplements were selected out of which three were inhibitors of different pathways. Bone

morphogenetic protein-4 (BMP4) which was reported to promote ectodermal differentiation and inhibit neuronal differentiation by Aberdam et al. 2007 as well as lens formation (Furuta and Hogan 1998, Wordinger and Clark 2007) was supplemented to Group 2. Group 3 CM was supplemented with all-trans retinoic acid (RA) which has been described to prime embryonic stem cells to differentiate into ectodermal cells (Schuldiner et al. 2000).

Group 4 CM was supplemented with epidermal growth factor (EGF) which stimulates stem cells growth, proliferation and survival of corneal and limbal stem cells (Imanishi et al. 2000, Trosan et al. 2012). The CM for Group 5 was supplemented with BMP4, RA and EGF to give the combined effects of the three different supplements. Supplementation of RA together with BMP4 was previously reported by Itoh et al. 2011 to be able to direct hiPSCs towards ectodermal differentiation. Control medium for Group 6 was supplemented with SB505124, a selective TGF-β type 1 receptor inhibitor to encourage differentiation towards neuro-epithelium. Similarly, IWP-2, a Wnt/β-catenin pathway inhibitor that induces stem cells to differentiate into epithelium (Chen et al. 2009) was tested. Combination of those inbibitors should allow stem cells differentiation towards neuro-ectodermal pathways (Schuldiner et al. 2000).

Group 7 received CM with SB505124, IWP-2 and BMP4 added to observe the inter-relation between the TGF-β and the Wnt pathways inhibitors in the presence of BMP4. The three supplements in Group 7 should cause neuro-ectodermal differentiation to the stem cells as the presence of BMP4 will promote ectodermal differentiation (Aberdam et al. 2007). Group 8 was given the CM supplemented with LDN 193189, a BMP pathway inhibitor that promotes neural progenitor and neural crest cells differentiation (Boergermann et al. 2010). This group was included as a control for the BMP4 differentiation group. The eight differentiation media, its contents and references are summarised in the following table.

| Groups | Medium contents | Reference(s) |
|---|---|---|
| **Group 1 (G1)** | 1% N2, 2% B27, 1% non-essential amino acids, 1% glutamine, 1% Pen/Strep, low glucose DMEM/F12 (1:1) = control medium | Leung et al. 2013, Yao et al. 2006 |
| **Group 2 (G2)** | control medium + bone morphogenetic protein-4 (rhBMP4) (25 ng/ml) | Shalom-Feuerstein et al. 2013 |
| **Group 3 (G3)** | control medium + All trans retinoic acid (RA) (1 µM) | Metallo et al. 2008 |
| **Group 4 (G4)** | control medium + epidermal growth factor (EGF) (10 ng/ml) | Ahmad et al. 2007, Herbst 2004 |
| **Group 5 (G5)** | control medium + rhBMP4 (25 ng/ml ) + All trans RA (1 µM) + EGF (10 ng/ml) | Shalom-Feuerstein et al. 2013, Katikireddy et al. 2014 |
| **Group 6 (G6)** | control medium + SB-505124 (10 µM) + IWP-2 (10 µM) | Shalom-Feuerstein et al. 2013, Mikhailova et al. 2014 |
| **Group 7 (G7)** | control medium + SB-505124 (10 µM) + IWP-2(10 µM) + rhBMP4 (25 ng/ml) | Shalom-Feuerstein et al. 2013, Mikhailova et al. 2014 |
| **Group 8 (G8)** | control medium + LDN193189 (100 nM) | Leung et al. 2013, Boergermann et al. 2010 |

**Table 3.4 : The differentiation induction media, the contents and references for each.**

### 3.4.2 *Early differentiation stage day 3 - 9*

Similar morphological appearance was observed for both the hESCs (H9) and hiPSCs (SB-Ad2 Cl2 and SB-Ad3 Cl1) for the same experimental group on day 3. On Day 3, the plated cells in all groups formed small colonies as shown in Figure 3.2. Morphologically, both the hESCs and hiPSCs lines have the same undifferentiated appearance in term of the cells' shape and the colonies. The undifferentiated cells are small with large nucleus and scanty cytoplasm, and they grew in compact colonies on matrigel coated plates supplemented with mTeSR™1.

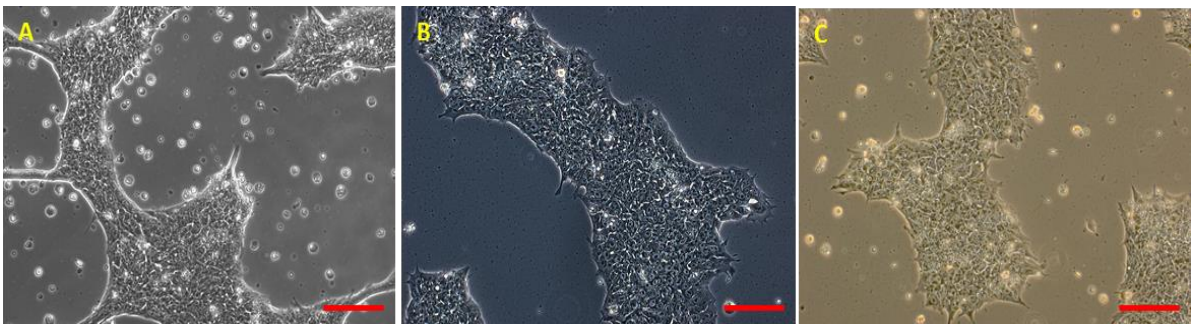


**Figure 3.2 : The morphology of undifferentiated hESC (H9) (A), and hiPSC (SB-Ad2 (B) and SB-Ad3 (C)) at day 3. Scale bar = 200 µm.**

Upon adding the differentiation induction medium on day 3, the cells in each group grew differently at least for the first three days (not shown). The colonies proliferated, became confluent and started to differentiate towards day 6 of the differentiation induction period. There were two groups, Group 4 and Group 8 that formed floating cell aggregates due to overconfluency (not shown in figure) on day 7. Groups that were supplemented with BMP4, RA and EGF showed the most differentiated morphology typical of epithelial cells on day 9 for both hESCs and hiPSCs. The differentiated cell morphology were observed by the formation of growing pockets of flatter and larger cells with higher cytoplasm to nucleus ratio (indicated by the arrows) in between the smaller undifferentiated stem cells areas, which are in similar to those reported by Xu et al. 2002. These pockets of differentiated cells could be observed as shown in Figures 3.3, 3.4 and 3.5 (day 9). Cells in Groups 1, 4, 6 and 8 on the other hand, proliferated robustly and mostly retained the stem cell appearance.

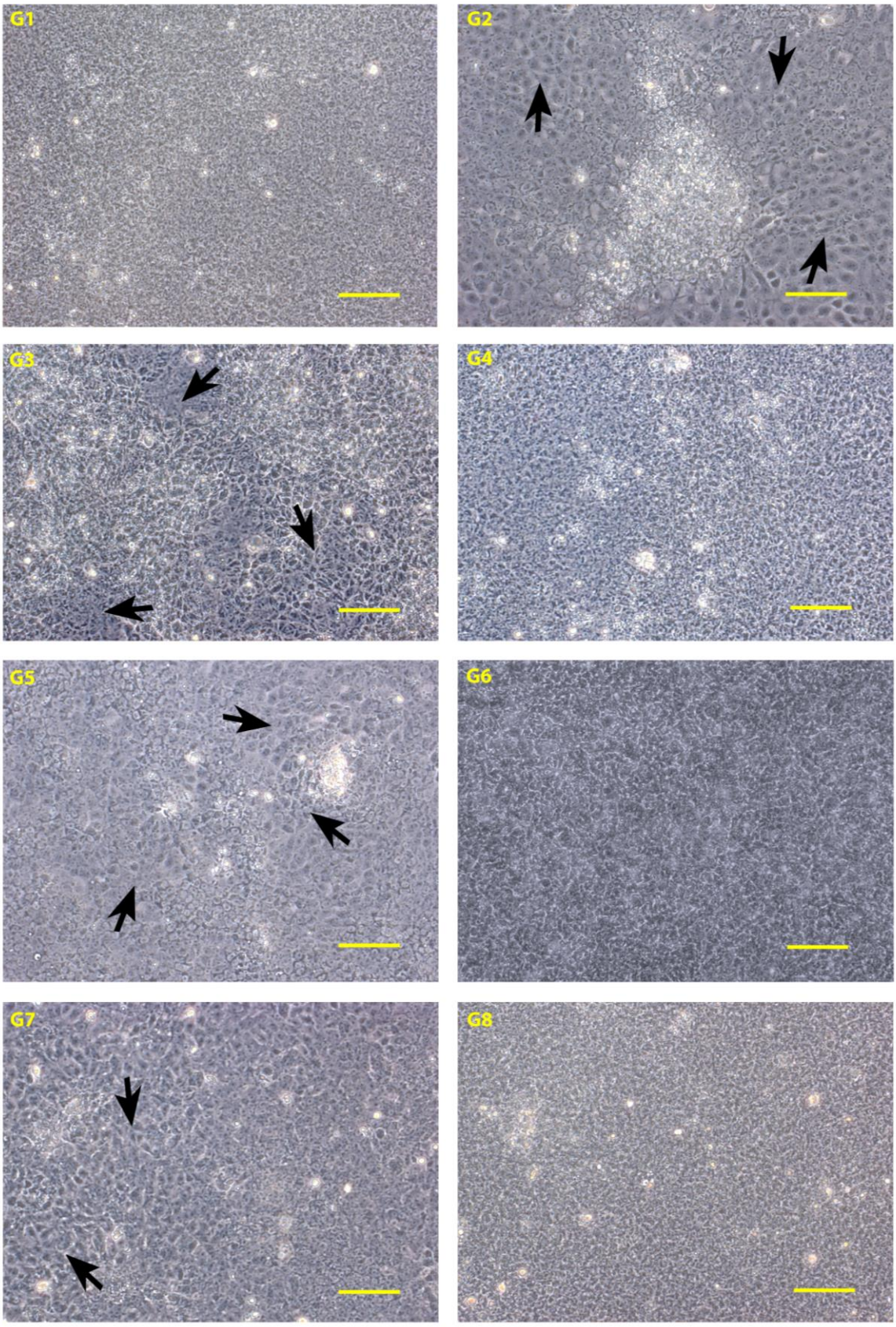


**Figure 3.3 : The morphology of hESCs (H9) at day 9. Arrows indicate the flat epithelial-like cells areas. Scale bar = 50 µm.**

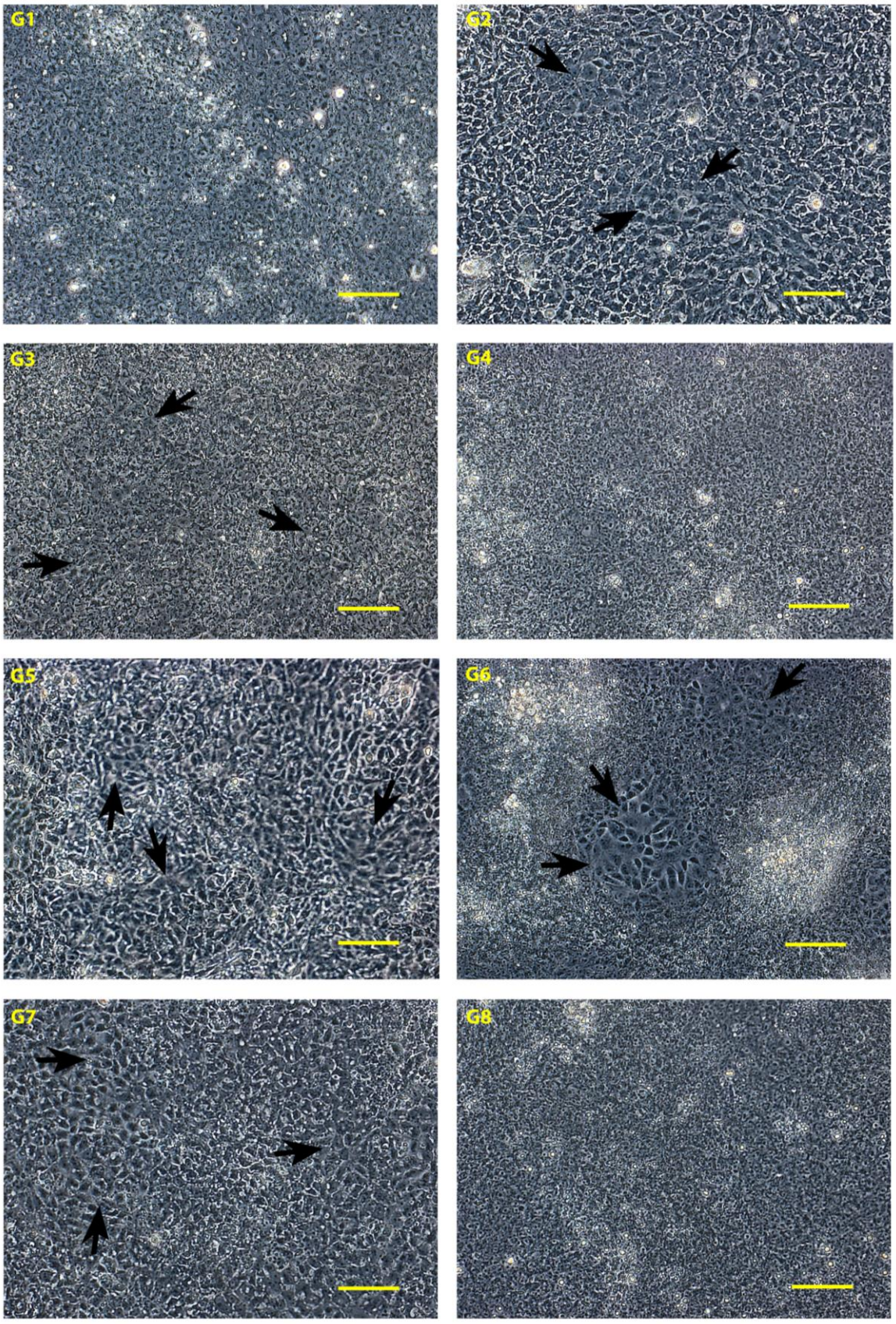


**Figure 3.4 : The morphology of hiPSCs (SB-Ad2) at day 9. Arrows indicate the flat epithelial-like cells areas. Scale bar = 50 µm.**

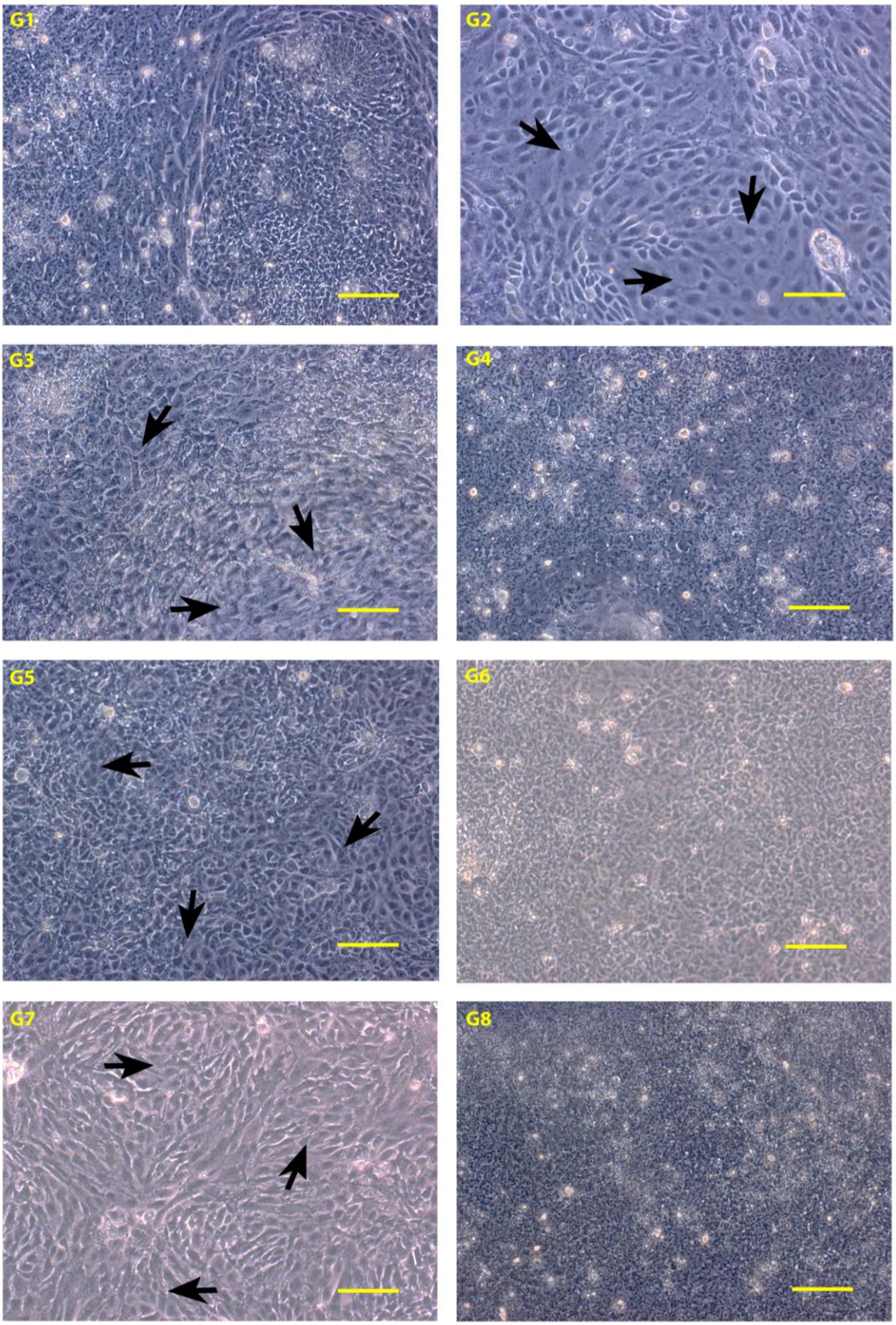


**Figure 3.5 : Morphology of hiPSCs (SB-Ad3) at day 9. Arrows indicate the flat epithelial-like cells areas. Scale bar = 50 µm.**

Gene expression profile for differentiation induction period on days 0, and 9 for hESCs and hiPSCs was assessed using several essential markers chosen for qRT-PCR analysis to match the aim for corneal and limbal epithelial differentiation in this first stage of experiment. These markers are as listed in Table 3.5 below.

| Cell lineages | qRT-PCR markers |
|---|---|
| **Ectodermal, limbal and corneal stem cells, surface pluristratified epithelium** | *ΔNp63* |
| **Ectodermal and epithelial cells cytokeratin** | *CK8* |
| **Calcium dependent cell-cell adhesion glycoprotein in basal and suprabasal corneal epithelium** | *ECadherin* |
| **Oral ectoderm and developing eye** | *PITX2* |
| **Non-neural ectoderm, developing cornea and lens** | *BMP4* |
| **Neuroectoderm, anterior placodal ectoderm, developing eye and lens** | *PAX6* |
| **Lens ectoderm and developing forebrain** | *SIX3* |
| **Retinal and early eye primordia cells** | *RAX* |
| **Non-neural ectoderm, developing endothelial/luminal epithelium** | *GATA3* |
| **Mesodermal and preplacodal ectoderm cells** | *SIX1* |
| **Mesodermal cells** | *BRACHYURY* |
| **Pluripotent and undifferentiated stem cells** | *OCT4* |

**Table 3.5 : List of gene markers for qRT-PCR on day 0 - 9.**

All the hESCs and hiPSCs groups displayed a significant decrease in the expression of the pluripotency (*OCT4*) markers by day 9 as shown in Figures 3.6, 3.7 and 3.8. This showed that all the groups lost their pluripotency and entered the differentiation process. Despite significant downregulation of pluripotency markers, G1, G4 and G8 of one of the hiPSCs (SB-Ad3) retained higher levels of *OCT4* compared to all hESCs and the other hiPSCs line. This correlated well with the morphological observations of pluripotent stem cell phenotype retention highlighted in the earlier section.

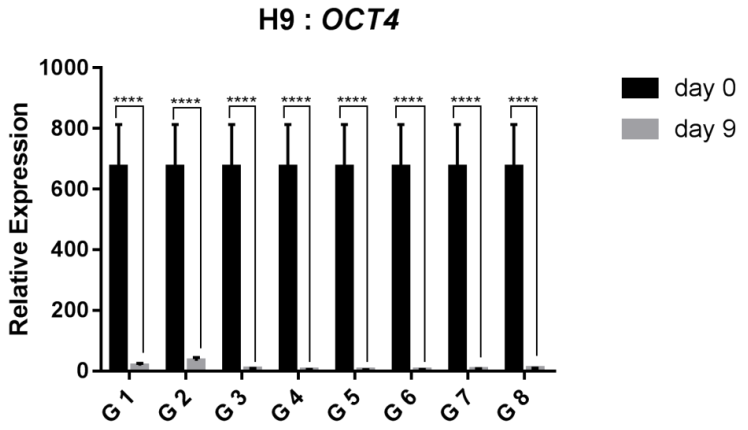


**Figure 3.6 : *OCT4* expressions for hESCs (H9). * - significantly different compared to day 0. Data presented as mean ± SEM. n = 3.**

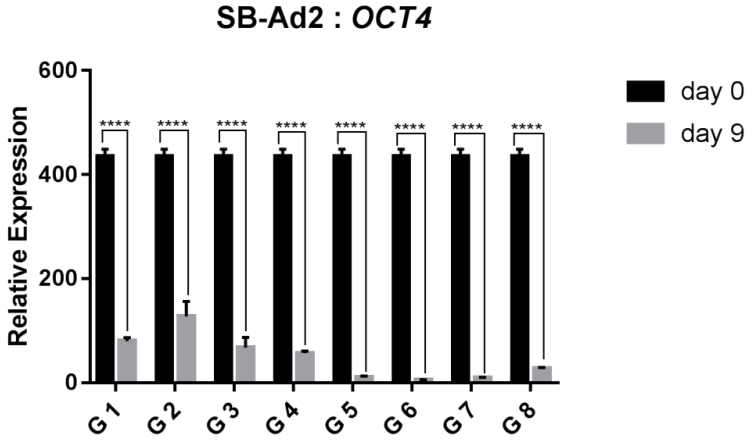


**Figure 3.7 : *OCT4* expressions for hiPSCs (SB-Ad2). * - significantly different compared to day 0. Data presented as mean ± SEM. n = 3.**

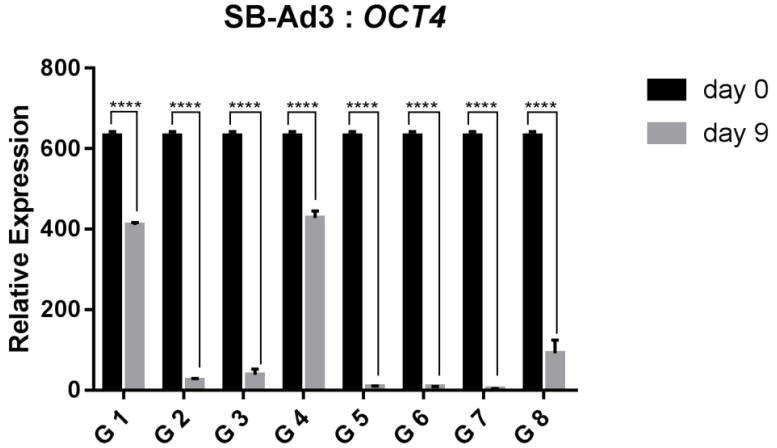


**Figure 3.8 : *OCT4* expressions for hiPSCs (SB-Ad3). * - significantly different compared to day 0. Data presented as mean ± SEM. n = 3.**

Mesodermal marker represented by *BRACHYURY* (Figure 3.9) was investigated to ensure that differentiation was not skewed towards mesoderm as a result of BMP4 supplementation. This analysis indicated a significant downregulation of this marker in most groups for both hESCs and hiPSCs with exception of G2 where BMP4 was the sole growth factor added which could have influenced differentiation process towards this lineage.

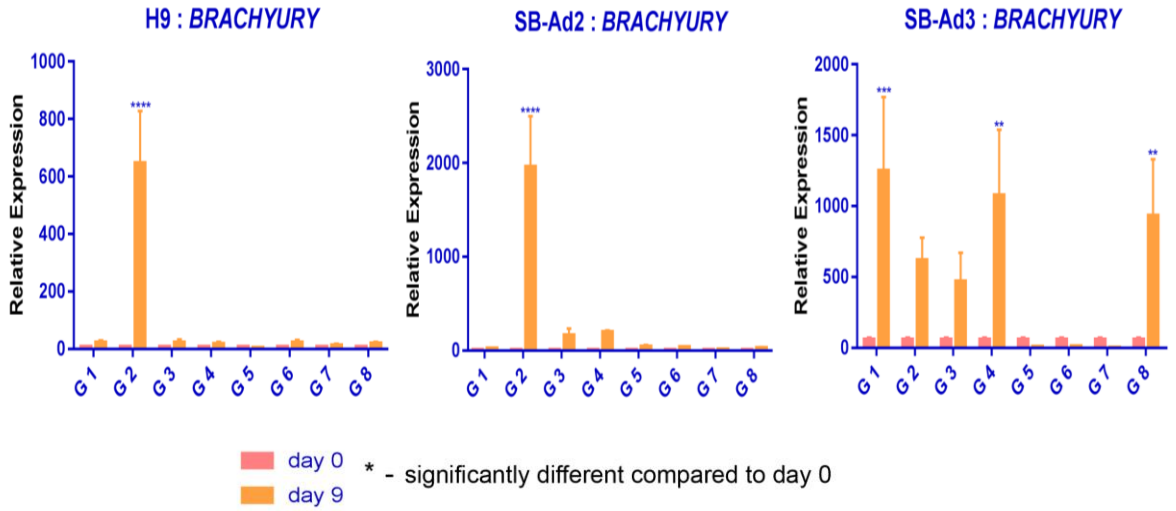


**Figure 3.9 : Relative expression of *BRACHYURY* gene on day 0 and day 9. Data presented as mean ± SEM. n = 3.**

The expression of *RAX* (early eye primordia and retinal protein), *PAX6* (anterior placodal neuroectoderm) and *SIX3* (lens ectoderm and forebrain development) were increased on day 9 compared to day 0, especially in Groups 1, 4, 6 and 8 in both hESCs and hiPSCs lines as shown in Figure 3.10. The increased expression of neuroectodermal and eye development markers by the cells in those groups suggests their differentiation towards neuroectoderm and lens.

The expression of *RAX* and *PAX6*, a marker of retinal protein and neuroectodermal, developing eye and lens respectively was significantly higher in G8 for all the cell lines (Figure 3.10). It is likely that the group has undergone lineage commitment to neural ectoderm as it was supplemented with BMP4 antagonist, which should inhibit non-neural ectodermal differentiation.

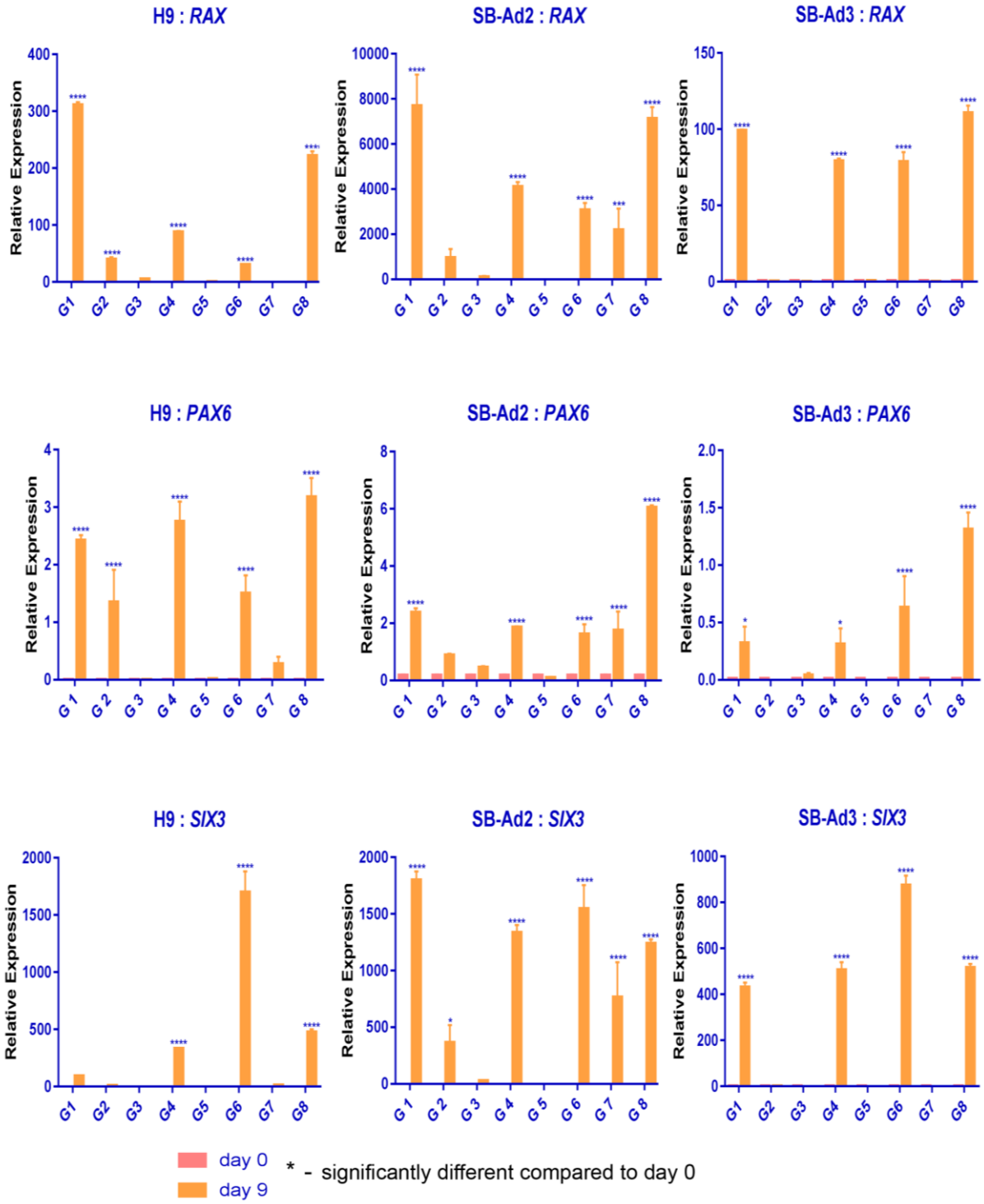


**Figure 3.10 : Relative expression of *RAX*, *PAX6* and *SIX3* genes on day 0 and day 9. Data presented as mean ± SEM. n = 3.**

In contrast, *PITX2*, *BMP4* and mostly *GATA3* expression (markers for developing eye, lens and non-neural ectoderm) on day 9 was increased in groups that were supplemented with BMP4 and/or RA or EGF (Figure 3.11). This is a promising change that suggests differentiation towards non-neural ectoderm lineages, eye development and epithelium in those groups (G2, G3, G5, G7).

*BMP4* gene which is expressed in early ectodermal tissue and helps in patterning the development of the head (Metallo et al. 2008 and Bothe et al. 2011), is often used as a marker of non-neural ectoderm, developing cornea and lens. Our qPCR analysis indicated a consistent and significant upregulation of *BMP4* in G2, G3 and G5 across hESCs and hiPSCs (Figure 3.15), suggesting that the differentiation factors added to these three groups encouraged differentiation to non-neural ectoderm which is the desired path before going further towards corneal epithelial cells.

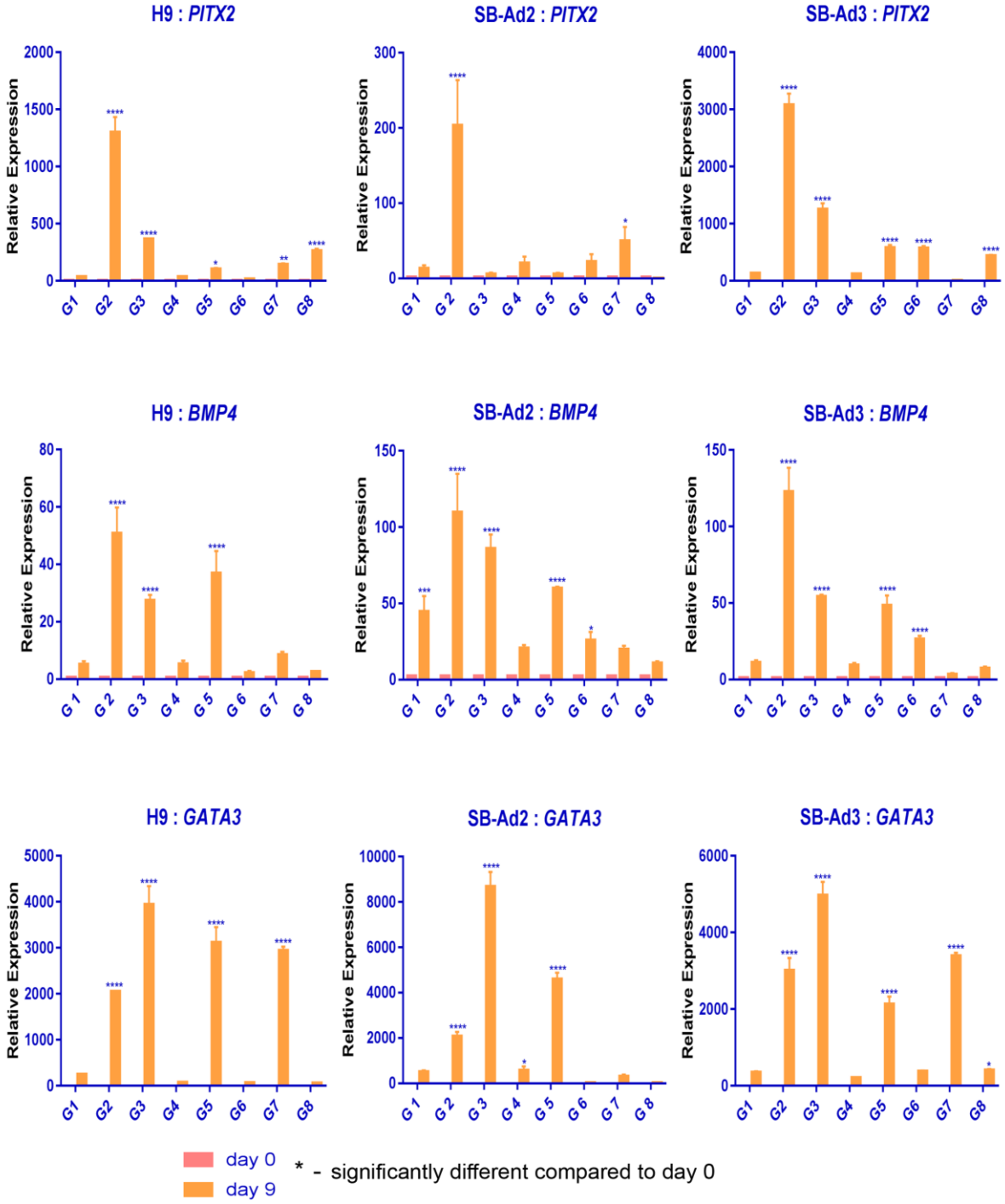


**Figure 3.11 : Relative expression of *PITX2*, *BMP4* and *GATA3* on day 0 and day 9. Data presented as mean ± SEM. n = 3.**

Finally, hESCs and hiPSCs groups that were supplemented with BMP4, RA and EGF displayed an increased expression of *ECadherin*, *ΔNp63* and *CK8*, which are the markers for epithelial cells, limbal and corneal epithelium as shown in Figure 3.12. The expression of ectodermal cytokeratin 8 (*CK8*), basal and suprabasal corneal epithelium (*ECadherin*) and putative limbal stem cells marker (*ΔNp63*) genes were all significantly increased in G2, G3 and G5 of both hESCs and hiPSCs (Figure 3.12), further suggesting cells' commitment to corneal and limbal epithelial lineages.

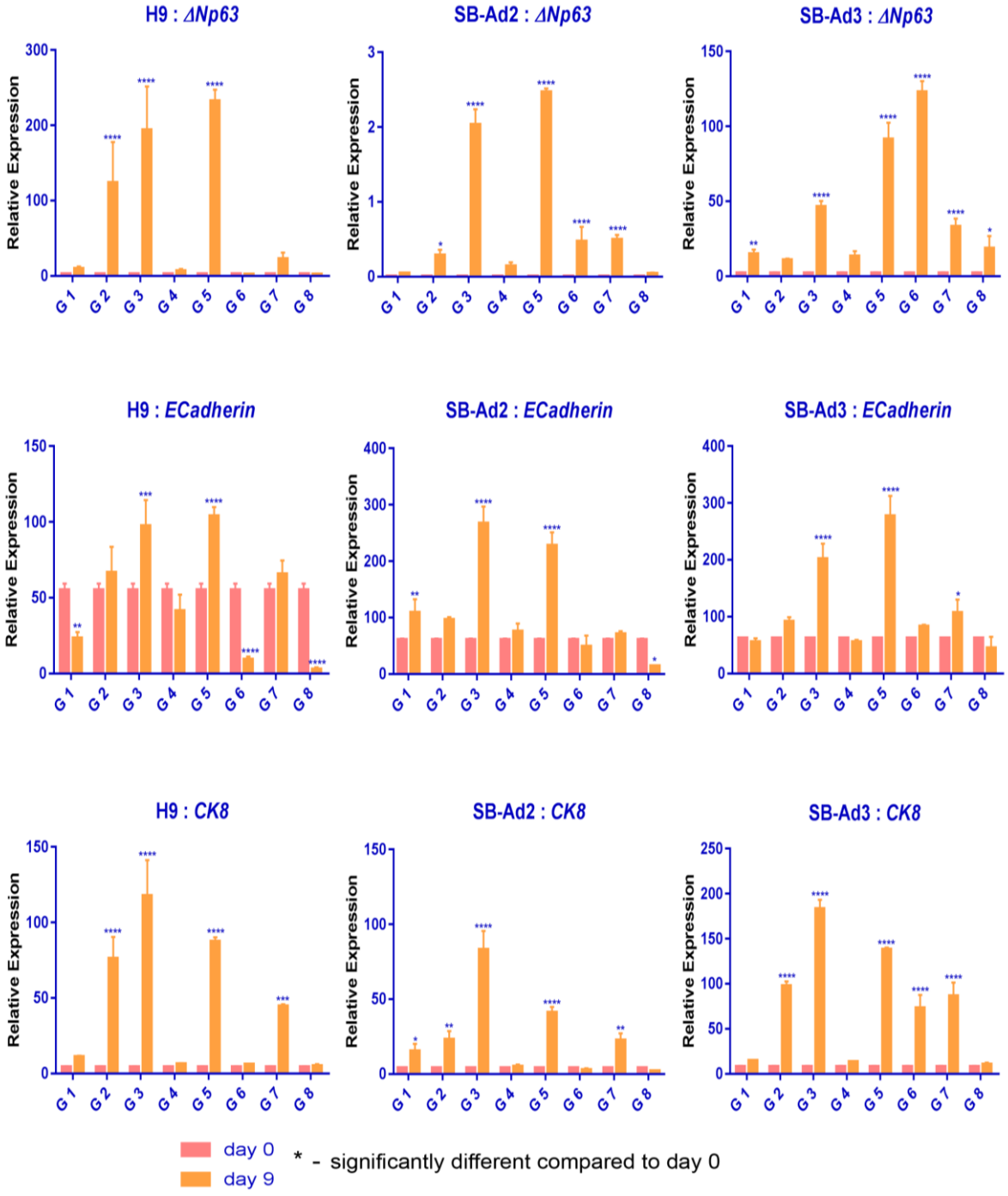


**Figure 3.12 : Relative expression of *ΔNp63*, *ECadherin* and *CK8* on day 0 and day 9. Data presented as mean ± SEM. n = 3.**

To summarise and take into account all the significant differentiation changes resulted from the different protocols, z scores were calculated. The calculated z scores were then used to assess the early corneal epithelium differentiation in the seven different groups compared to the control, G1 on day 9. Although addition of BMP4 has been associated with differentiation of hESC and hiPSC to mesodermal lineages (Ren et al. 2011, Zhang et al. 2008); a significant increase in the expression of mesodermal *BRACHYURY* was only observed in the hESC (H9) and one hiPSC line (SB-Ad2; Figure 3.13A) upon BMP4 treatment (Group 2). The expression of *RAX*, a gene expressed in the eye primordia and required for retinal cell fate determination (Furukawa et al. 1997), was significantly downregulated in Groups 2-7 for both hESC and hiPSC, thus indicating that in all these groups, the differentiation to neuroectodermal lineages was avoided (Figure 3.13B).

*BMP4* is expressed in early ectodermal tissue (Metallo et al. 2008) and is often used as marker of non-neural ectoderm, developing cornea and lens. Our qRT-PCR analysis indicated a significant upregulation of *BMP4* in experimental groups 2, 3 and 5 of hESC and two hiPSC (Figure 3.13C), suggesting that the differentiation factors added to these three groups encouraged differentiation to non-neural ectoderm (Leung et al. 2013). The expression of ectodermal cytokeratin 8 (*CK8*), basal and suprabasal corneal epithelium (*ECadherin*) and putative limbal stem cells (*ΔNp63*) markers were all significantly increased in experimental Groups 3 and 5 of both hESCs and hiPSC (Figures 3.13D, E and F), indicating a likely commitment of these groups to corneal epithelial progenitors.

At this induction stage, Groups 2, 3 and 5 were selected as these groups showed a promising morphological changes as well as gene expressions that met the favourable differentiation criteria. Those selected groups expressed increased putative corneal and limbal stem cell, and epithelial cytokeratin markers (*ΔNp63*, *ECadherin* and *CK8*), increased non-neural ectodermal marker (*BMP4*) across the lines. Therefore, those that have significantly low z scores for mesodermal (*BRACHYURY*) and retinal differentiation (*RAX*), and high ectodermal (*BMP4*), non-neural ectoderm (*CK8*), epithelial (*ECadherin*) and putative limbal epithelial (*ΔNp63*) markers from all three cell lines were selected for further differentiation experiments.

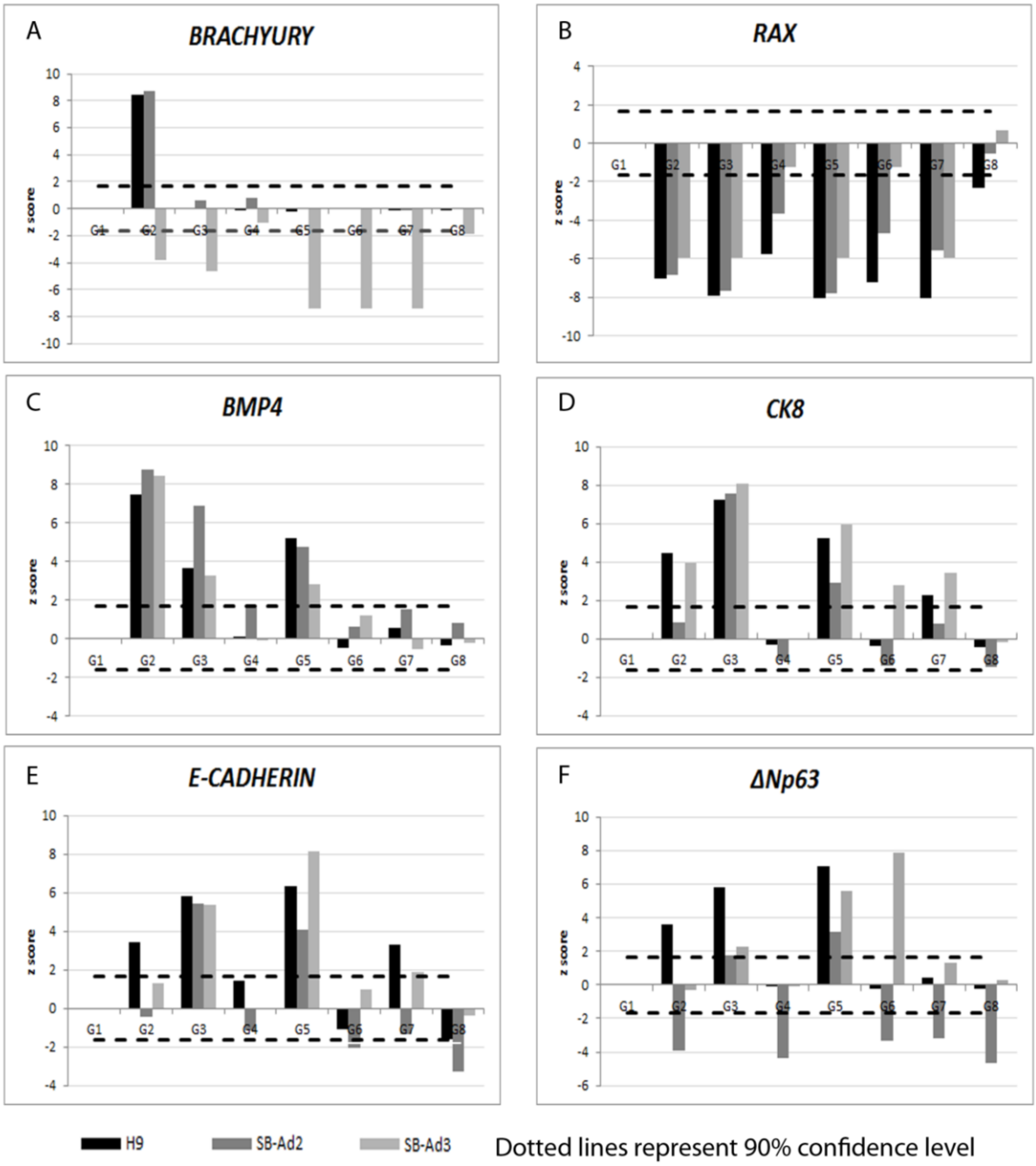


**Figure 3.13 : Z scores of corneal epithelial lineages differentiation markers on day 9.**

The z scores from the qRT-PCR analysis consistently showed that the experimental groups that were supplemented with BMP4, RA and a combination of BMP4, RA and EGF showed a significant upregulation of non-neural ectoderm, epithelial, cell junction and putative LSC markers. We therefore went on to analyse these groups by immunostaining for the expression of putative LSC protein, ΔNp63.

No significant differences between the control non supplemented groups and the ones that received BMP4, RA and a combination of BMP4, RA and EGF were found (Figure 3.14A and

B). These immunostaining results do not corroborate the qRT-PCR analysis and a possible reason for this may be the post-translational modifications already reported for the p63 protein (Li and Xiao 2014). The negative controls of stained undifferentiated cells on the other hand, did not express both PAX6 and p63 proteins (data not included).

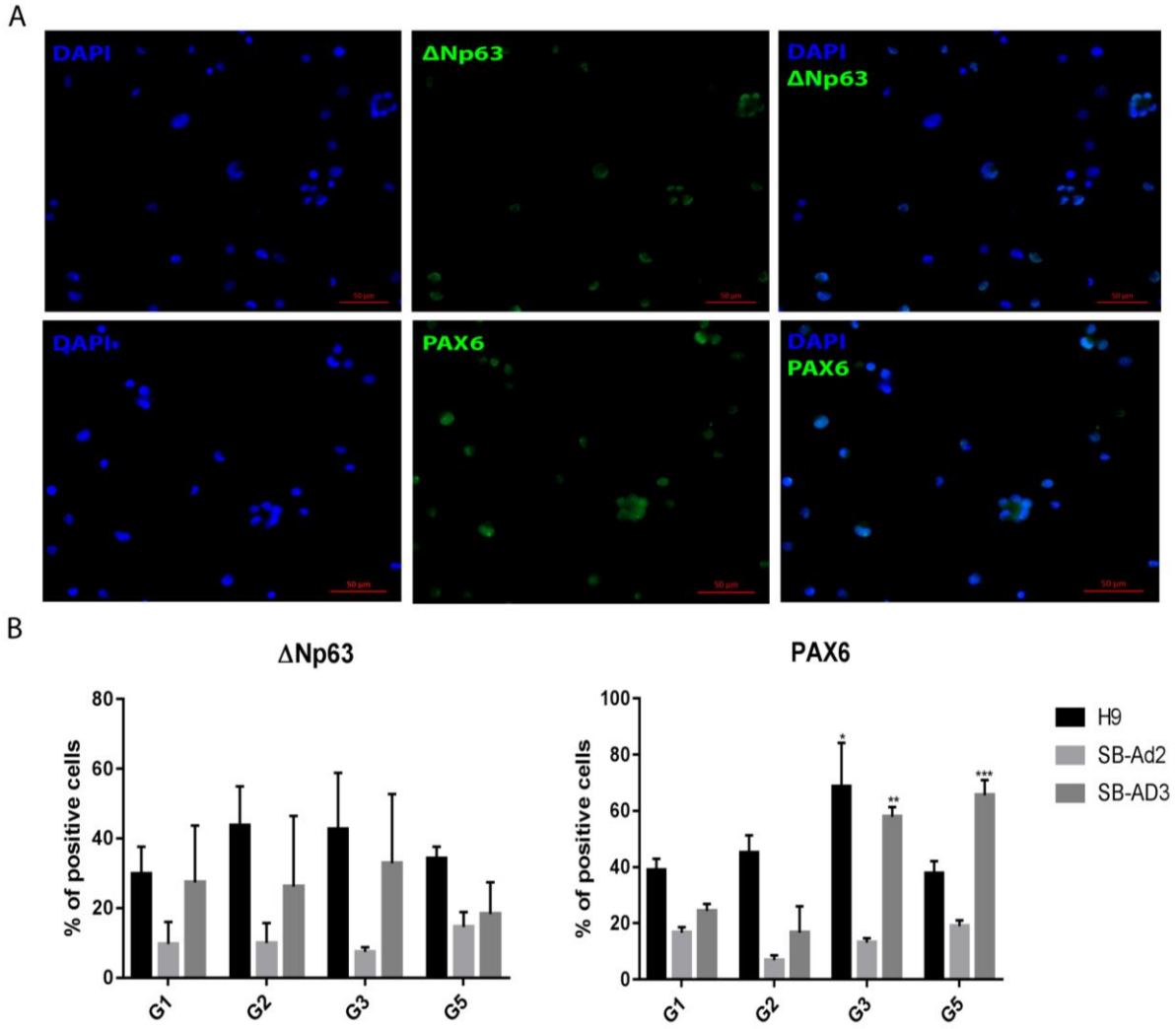


**Figure 3.14 : Representative photos of ΔNp63 and PAX6 positive immunostaining at day 9 for hESC (A). Percentages of ΔNp63 and PAX6 positive cells at day 9 in the three cell lines (B). * - significantly different compared to G1. Data presented as mean ± SEM. n = 3.**

Colony forming efficiency (CFE) was highest in experimental Groups 2 and 5 of hESCs (H9) and one of the hiPSCs lines (SB-Ad2), suggesting that supplementation of basic media with BMP4 or a combination of BMP4, RA and EGF provides an optimal combination for directing differentiation of hESC and hiPSC to corneal epithelial-like progenitor cells. Notwithstanding, no significant difference in CFE ability were observed between the four experimental groups tested in the second hiPSCs line (SB-Ad3) as shown in Figure 3.15, indicating significant differences between the hiPSCs lines in their response to our differentiation protocols and the need for further culture modifications for non-responsive hiPSCs lines.

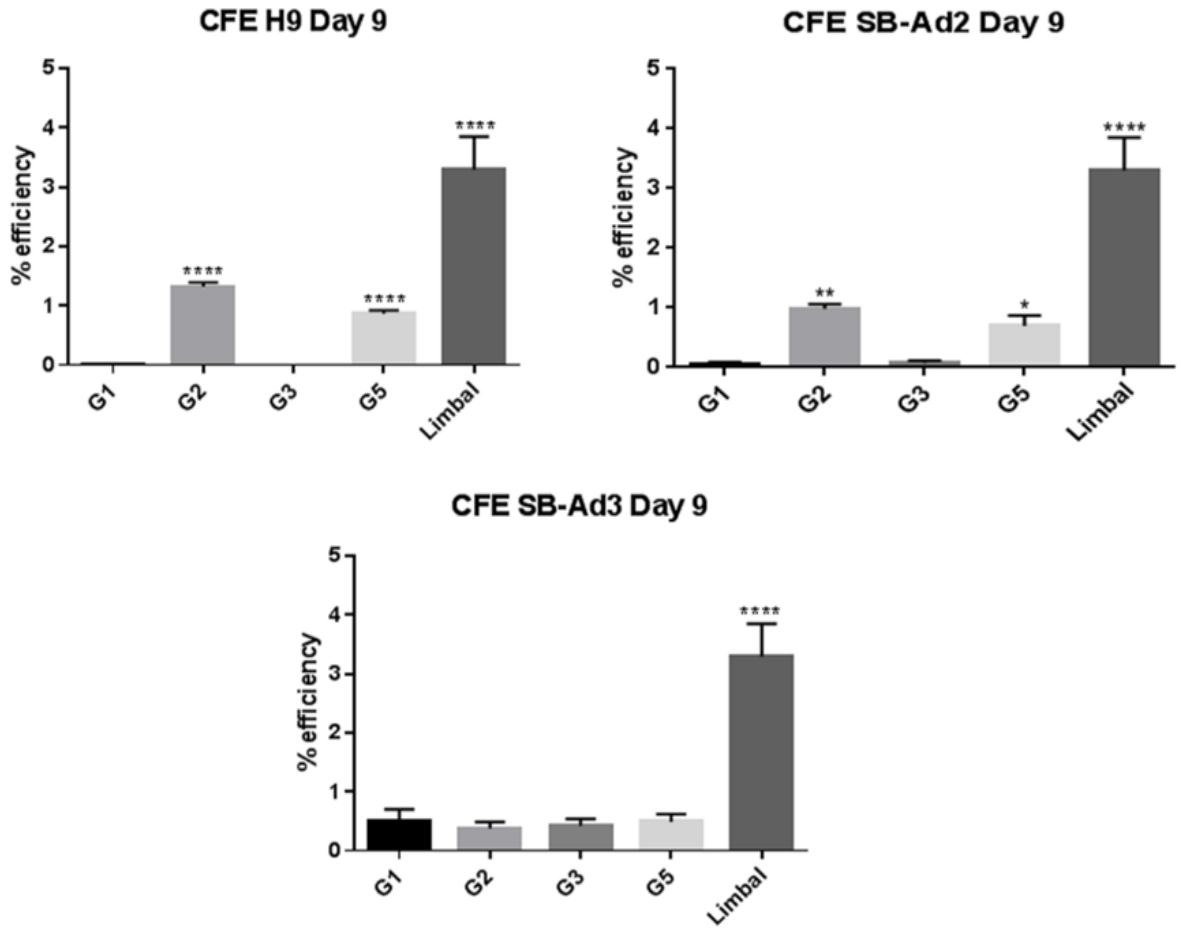


**Figure 3.15 : Colony forming efficiency for all the three cell lines on day 9. * - significantly different compared to G1. Data presented as mean ± SEM. n = 3.**

### 3.4.3 *Late differentiation stage day 10 – 20*

Figure 3.16 showed the appearance of H9 cell after 5 days being re-plated on collagen-IV coated plates at day 9. The medium was changed to a serum-free CnT-PR 2D-Diff corneal differentiation medium to provide conditions that mimic the cornea. This medium was supplemented to the cells in three ways: on its own, added with 10% fetal bovine serum (FBS) or added with 0.07 mM $CaCl_2$.

The FBS or $CaCl_2$ supplementation was decided following initial experiment findings, where the re-plated H9 cells did not survive well when supplemented with CnT-PR 2D-Diff only medium (Figure 3.16). Addition of 10% FBS was based on a report by Medawar et al. 2008 who showed improved differentiation of ectodermal cells into K5 and K14 expressing epithelial cells. The 0.07 mM calcium supplementation was based on the calcium content in the CnT-epithelial proliferation medium (http://cellntec.com/products/cnt-pr/#datasheet). A previous

study also reported that addition of calcium triggers the differentiation of mouse corneal epithelial cells (Ma and Liu 2011). The re-plated cells were left for 2 days without medium change to allow longer time for the cells to attach to the collagen-IV coated surface.

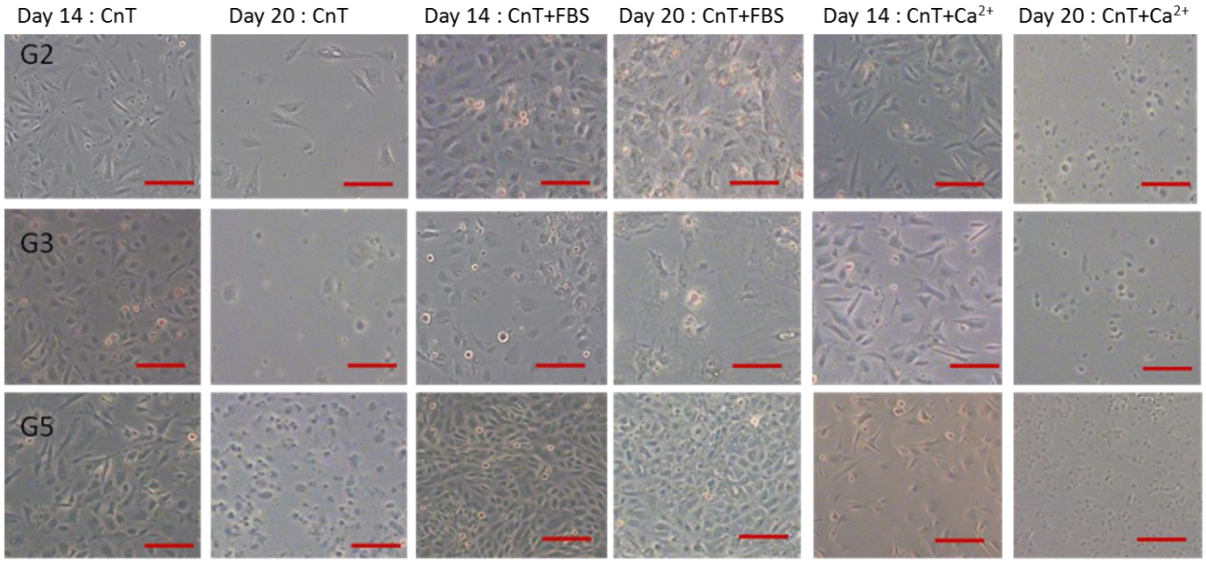


**Figure 3.16 : The hESCs on days 14 and 20 in CnT-PR 2D Diff. medium with or without supplementation of FBS and $Ca^{2+}$. Scale bar = 25 µm.**

Observations on day 14 (5 days after re-plating) showed that cells were generally did not attached well to the plate in CnT or CnT+$Ca^{2+}$ media. There were only three (Groups 2, 3 and 5) groups that survived until day 20 for H9 as shown in Figure 3.16 and these were cultured in CnT-PR + 10% FBS medium.

The replating protocols on day 9 were then further improved with the addition of 10 µM ROCK inhibitor to the CnT-PR 2D-Diff. + 10% FBS medium for the first two days to help the cell survival. More cells survived until day 20 in Groups 2, 3 and 5 for all the lines as assessed by daily culture observation. Similar morphological changes were observed in both hESCs and hiPSCs during this time window (Figures 3.17, 3.18, 3.19). Cells appeared larger and flatter and characterised by an epithelial-like morphology by the end of the experiment on day 20.

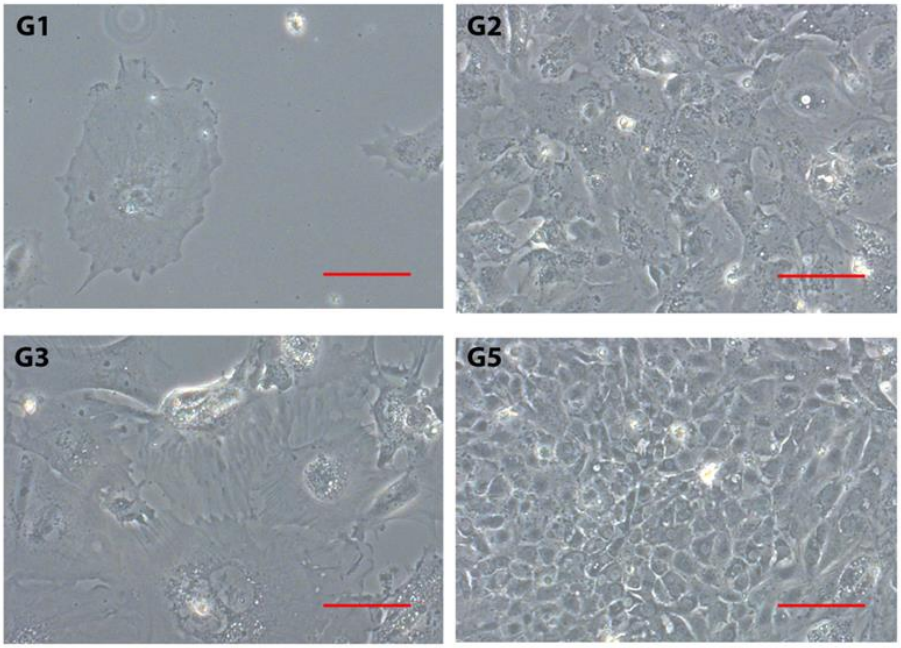


**Figure 3.17 : Morphology of hESCs (H9) at day 20. Scale bar = 50 µm.**

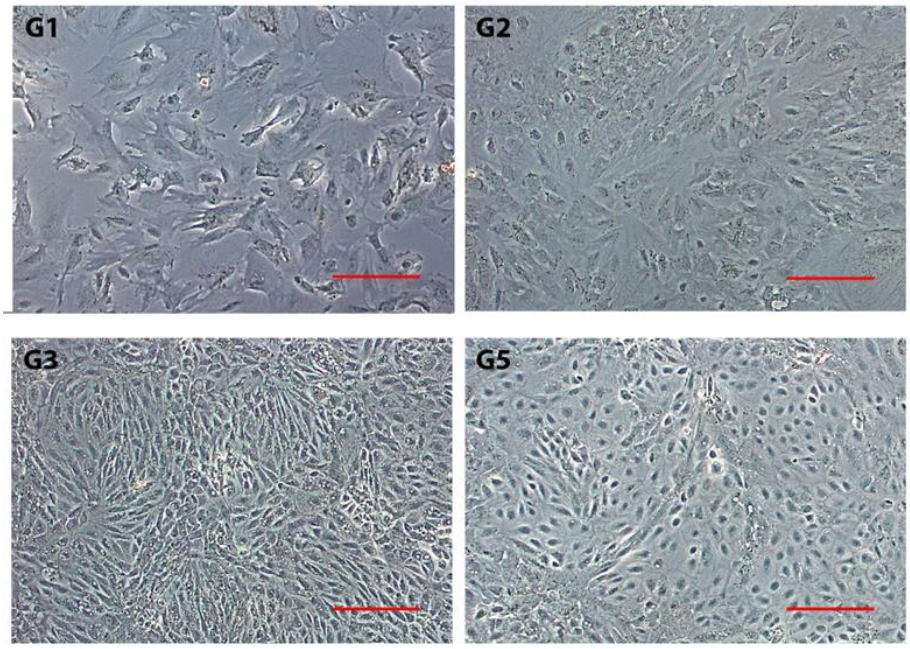


**Figure 3.18 : Morphology of hiPSCs (SB-Ad2) at day 20. Scale bar = 50 µm.**

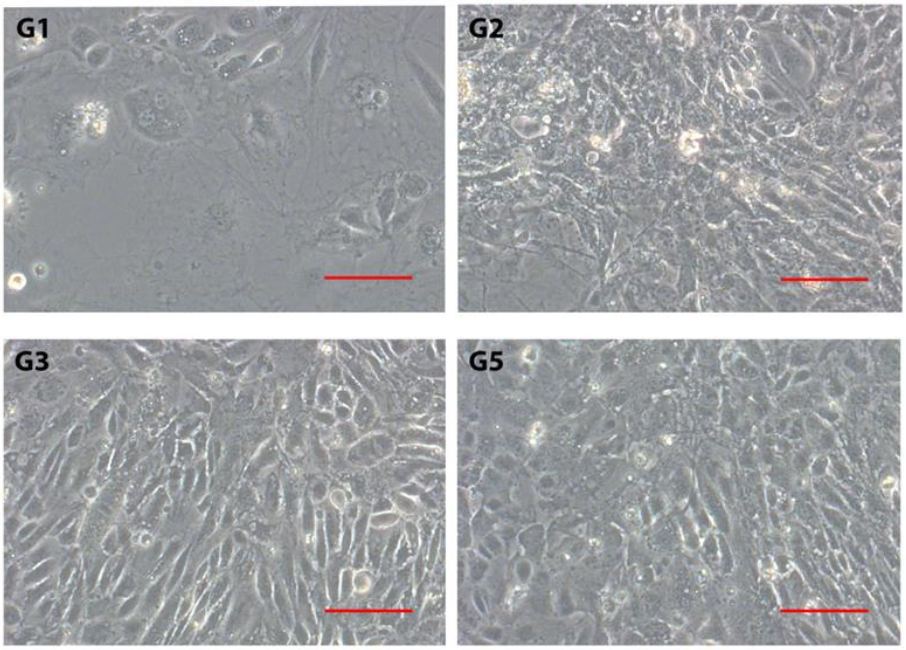


**Figure 3.19 : Morphology of hiPSCs (SB-Ad3) at day 20. Scale bar = 50 µm.**

In this second stage of the experiment, qRT-PCR analysis was carried out at day 20 for the expression of genes that are more specific to corneal and limbal epithelium. The gene markers used are as listed in Table 3.6 below.

| Cell lineages | qRT-PCR markers |
|---|---|
| **Ectodermal, corneal and limbal stem cells, surface pluristratified epithelium** | *ABCG2, ΔNp63* |
| **Differentiated human corneal epithelium** | *CK3, CK12* |
| **Ectoderm and epithelial cells cytokeratins** | *CK8* |
| **Calcium dependent cell-cell adhesion glycoprotein in basal and suprabasal corneal epithelium** | *ECadherin* |
| **Neuroectodermal, anterior placodal ectoderm and developing lens** | *PAX6* |

**Table 3.6 : List of gene markers for qRT-PCR on day 10 - 20.**

Quantitative RT-PCR analysis showed that the combination of RA, BMP4 and EGF (Group 5) was associated with the greatest upregulation of putative limbal stem cell marker (*ΔNp63)* across the cell lines (Figures 3.20, 3.21, 3.22). Expression of *ABCG2*, a putative LSC marker (Morita et al. 2015), was also consistently highest in groups supplemented with RA across the

cells lines. Differentiated corneal epithelial cytokeratin, *CK3* expression was more variable across the cell lines, with the highest expression observed in BMP4 supplemented group for hESCs, RA supplemented group for hiPSC-SB-Ad3 and RA and RA, BMP4 and EGF supplemented group for hiPSC-SB-Ad2. *CK12* expression was consistently the highest in the groups supplemented with RA, BMP4 and EGF. Together these data suggest some intra-line differences in the capacity to mature towards corneal epithelial like cells.

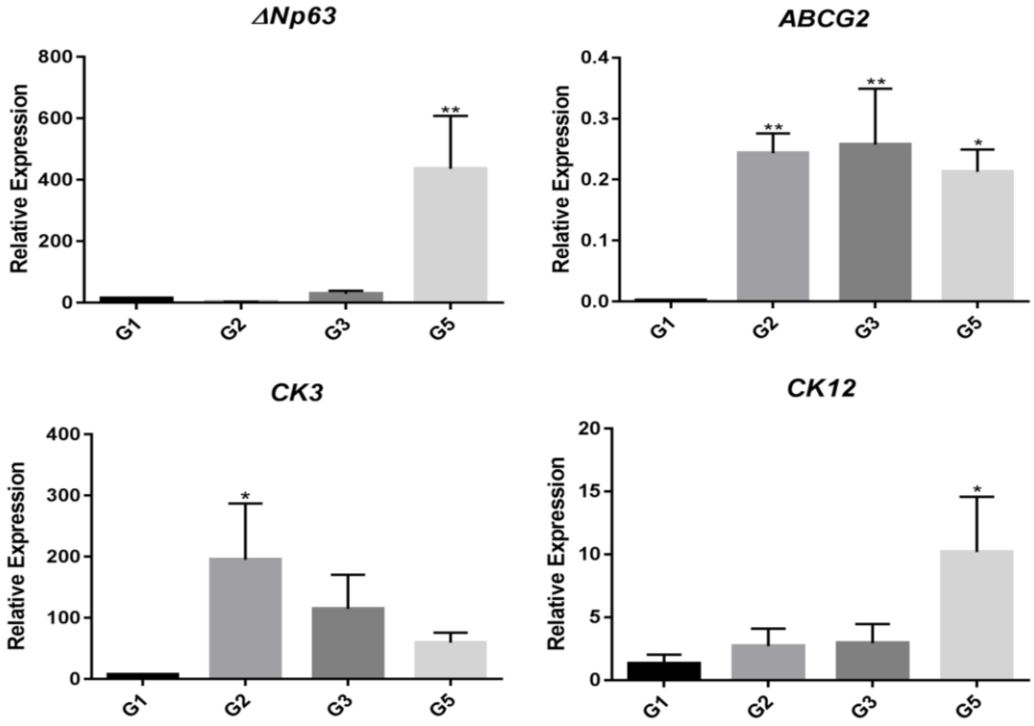


**Figure 3.20 : Relative gene expressions of hESCs (H9) on day 20. * - significantly different compared to G1. Data presented as mean ± SEM. n = 3.**

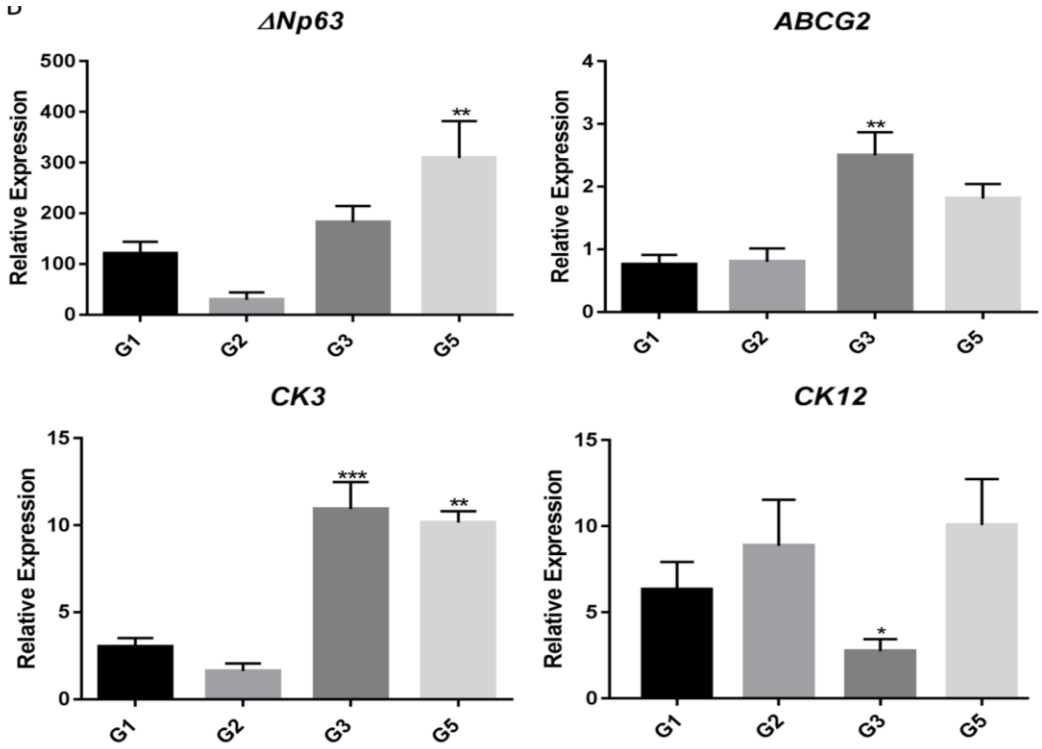


**Figure 3.21 : Relative gene expressions for hiPSCs (SB-Ad2) on day 20. * - significantly different compared to G1. Data presented as mean ± SEM. n = 3.**

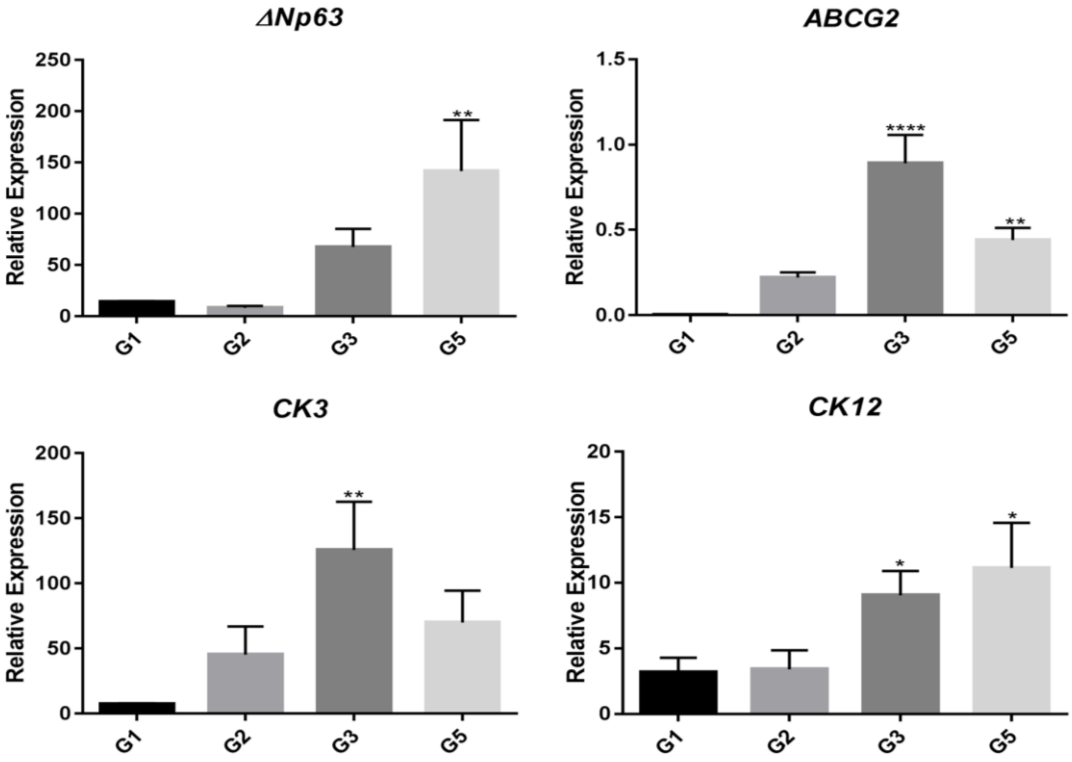


**Figure 3.22 : Relative gene expressions for hiPSCs (SB-Ad3) on day 20. * - significantly different compared to G1. Data presented as mean ± SEM. n = 3.**

Immunostaining analysis at day 20 revealed a significant upregulation of ΔNp63 expression in groups supplemented with BMP4, RA and EGF across the hESCs and hiPSCs lines compared to G1 (Figure 3.23). It needs to be noted though that the expression of this marker decreased from day 9 of differentiation, indicating further differentiation of these cells to CK3 and CK12 expressing corneal epithelial cells as shown in Figure 3.24A and B.

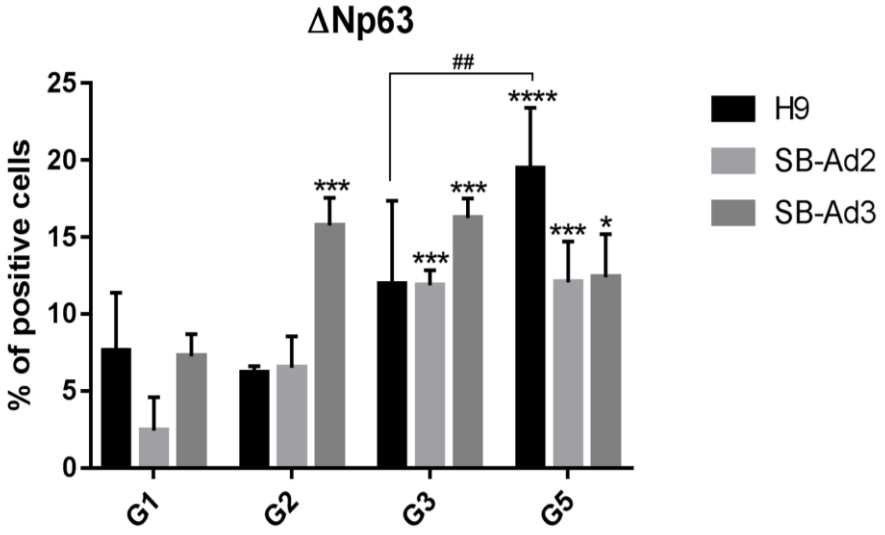


**Figure 3.23 : Expression or ΔNp63 protein at day 20 for all three cell lines. * - significantly different compared to G1 of the same cell line. # - significantly different compared to the other group. Data presented as mean ± SEM. n = 3.**

A

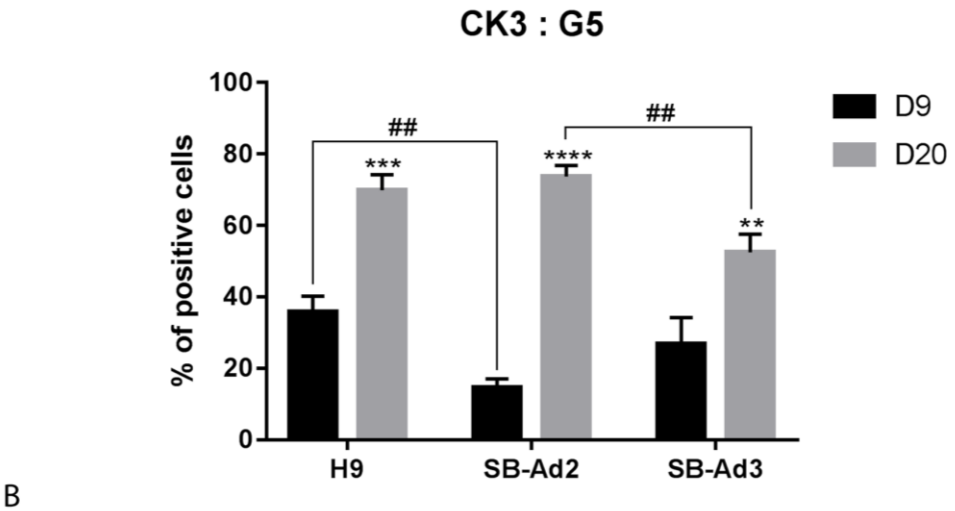


B

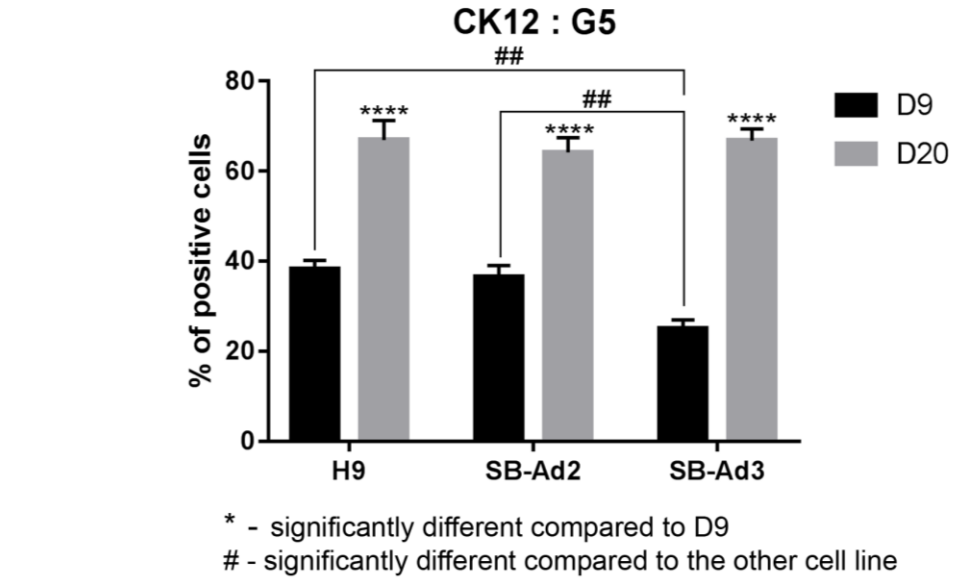


* - significantly different compared to D9
\# - significantly different compared to the other cell line

**Figure 3.24 : Expression of CK3 and CK12 proteins at day 20 in G5 for all the three cell lines. Data presented as mean ± SEM. n = 3.**

CFE assays also showed that the BMP4, RA and EGF supplemented group in hESCs resulted in the highest colony forming ability which was similar to human limbal epithelial progenitor cells (Figure 3.25). All the selected groups of one of the hiPSCs lines (SB-Ad2) showed an increased CFE ability compared to control group; however this was considerably lower than human limbal epithelial progenitor cells (Figure 3.25). In contrast, all the treated groups from the second hiPSCs line (SB-Ad3) showed a very low CFE ability and no difference to the untreated control group, indicating a lack of response from this cell line to differentiation factors added during the 20 days time window.

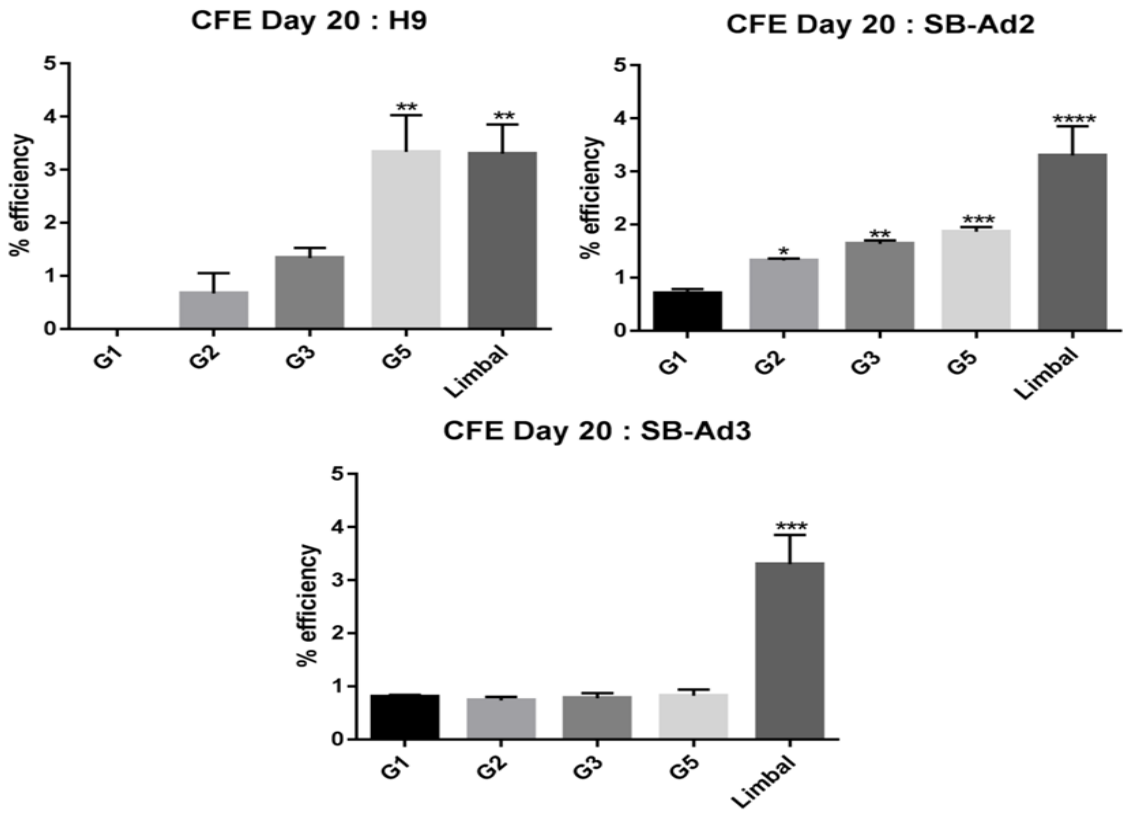


**Figure 3.25 : Colony forming efficiency of all the cell lines on day 20. * - significantly different compared to G1. Data presented as mean ± SEM. n = 3.**

### 3.5 Discussion

Efficient differentiation of a large numbers of hESCs and hiPSCs for autologous cell replacement therapies using robust and fast protocols has become an important aim for most researchers in the field. Since the main aim of our study was to design robust differentiation protocols for differentiation of hiPSCs to corneal epithelial like cells for autologous cell replacement therapies, we tested the two-step differentiation protocol in two hiPSCs lines generated and well characterized by our laboratory (Van De Bunt et al. 2016).

In this experiment, we report a feeder-free, two-step method that results in differentiation of hESCs to corneal epithelial progenitors and mature corneal epithelial cells within 20 days as evident in the related genes and proteins expressions as well as the CFE assays. One of the hiPSCs lines was able to generate corneal epithelial progenitors with comparable colony forming ability in response to BMP4, RA or combined addition of BMP4, RA and EGF, albeit at lower levels than hESCs. In contrast, the second tested hiPSCs line was not able to respond to the two-step differentiation protocol resulting in low levels of corneal epithelial progenitor generation. Although it was noted that the expression of master regulatory gene of eye development, *PAX6* was nearly absent (in groups supplemented with BMP4, RA and EGF)

during the early differentiation stage, this time point might represent the phase where PAX6 is downregulated following its upregulation phase at earlier time point (eg: day 6). However, the PAX6 protein expression was was shown to be significantly high in those groups. These findings could be rectified by testing the specificity of PAX6 antibody used for immunostaining using knockout cells and positive control cells, as well as comparing the ICC results with Western Blot analyses. Additionally, the successfully differentiated cells could be further distinguished from other ectodermal lineages such as conjunctiva or epidermal cells by assessing the expression of markers that are specific to those lineages (i.e: CK13, K1, K2, K9, K10) (Moll et al. 2008, Merjava et al. 2011).

Differences in transcriptional and epigenetic profiles between hiPSCs lines which are linked to their differentiation capacity are commonly encountered, especially during directed differentiations, where specific molecules were used to alter the pathways of interest (Narsinh et al 2011a). A study published by our group indicated that hiPSCs lines that possess higher level of mitochondrial protein CHCHD2, have a less active TGFβ signalling activity, making them more prone to neural differentiation (Zhu et al. 2016). A recent report by Nishizawa et al. also indicated that haematopoietic commitment of hiPSCs lines depends on the expression of insulin-like growth factor 2 (IGF2) (Nishizawa et al. 2016). Earlier, Fujiwara and colleagues also found variations in the basal cardiomyocyte differentiation efficiency of hiPSCs lines which was overcomed by using Cyclosporin-A (Fujiwara et al. 2011). Together, those studies and our findings suggest that differentiation protocols may need to be adjusted to take into account the endogenous expression of key transcription and growth factors as well as signalling pathways that govern early differentiation steps in hiPSCs.

# CHAPTER 4. BMP PATHWAY ANALYSIS AND OPTIMISATION OF HIPSCS DIFFERENTIATION

## 4.1 Introduction

In the earlier chapter, the two types of human pluripotent stem cells (hPSCs) used for corneal epithelial lineages differentiation responded differently towards the differentiation cues exposed to them. Supplementation of BMP4, RA and EGF had directed the hESCs with differentiation towards corneal epithelial lineages. However, the same supplementation did not result in the same change in one of the human induced-pluripotent cells (hiPSCs) used.

Endogenous BMP signalling activity is different in various hiPSCs lines and crosstalk between BMP and TGFβ signalling has also been reported (Quarto et al. 2012) affecting the propensity of each cell line during differentiation process. Given the importance of BMP4 signalling in inhibiting neural differentiation and promoting epidermal commitment of embryonic stem cells (Aberdam et al. 2008, Metallo et al. 2008, Guenou et al. 2009), we investigated the level of endogenous BMP pathway activity using a reporter based assays to confirm our quantitative RT-PCR assessment findings. Since one of the hiPSCs lines was not responsive to the differentiation method, we assessed the BMP pathway activity of the hiPSCs lines in view of improving the differentiation of less responsive hiPSCs.

An optimisation experiment was planned based on the findings of the endogenous BMP signalling assessment on the hiPSCs lines. Since there is a crosstalk between BMP and TGFβ signalling pathways, a selective TGFβ inhibitor, SB431542 which has been reported to improve the BMP pathway (Du et al. 2014) and to drive differentiation away from neuro-ectoderm (Li et al. 2015) was used to improve the corneal epithelial differentiation in the less responsive hiPSCs. This chapter will later discuss on the findings of the endogenous BMP signalling differences in the hiPSCs lines used and the outcome of differentiation optimisation in the less responsive hiPSCs line using SB431542.

## 4.2 Specific Objectives

The specific objectives of this chapter are:

- to assess the endogenous BMP pathway in H9, SB-Ad2 and SB-Ad3 cells based on their gene expressions using quantitative RT-PCR.
- to confirm the qRT-PCR findings on the endogenous BMP pathway using luciferase BMP reporter assays.

- to assess the effects of BMP4 and SB431542 supplementation on the endogenous BMP pathway in the three cell lines.

## 4.3 Materials and Methods

### 4.3.1 *Lennox L Broth Base (LB) medium and LB agar preparation*

10 g Lennox L Broth Base powder (Invitrogen, UK) was dissolved in 500 mL of distilled water in a 1.0 L glass bottle. The bottle was labelled, loosely capped and autoclaved at 121°C for 15 minutes. The autoclaved broth was allowed to cool to room temperature before use.

16 g Lennox L Agar powder (Invitrogen, UK) was dissolved in 500 mL of distilled water in a 1.0 L glass bottle. The bottle was labelled, loosely capped and autoclaved at 121°C for 15 minutes. The hot agar was then allowed to slightly cool in a 60°C water bath.

Ampicillin stock solution was prepared by dissolving 100 mg of ampicillin sodium salt powder (Sigma-Aldrich, Germany) in 1.0 mL distilled water. The resulting stock solution was kept in -20°C. 500 µL ampicillin (from 100 mg/mL stock) was added to the warm agar and mixed by swirling. Sterile 10 cm plates were laid out on the bench and the agar was carefully poured into the plates to avoid the formation of air bubbles. The agar plates were allowed to solidify at room temperature before being properly wrapped and kept in a 4°C fridge until use.

### 4.3.2 *Plasmid transformation*

pGL3-Basic (Promega, WI : E1751) and pRL-Null (Promega, WI : E2271) plasmids were transformed into chemically competent bacteria using a heat-shock transformation method. Competent cells were taken out from -80°C and thawed on ice for approximately 20 – 30 minutes. Agar plates containing 100 µg/mL ampicillin were removed from 4°C fridge and let warmed up to room temperature. 50 ng of each plasmid was mixed into 20 µL of competent cells in a micro centrifuge tube. The mixture was gently mixed by flicking the bottom of the tube with fingers a few times. Then the mixture was incubated on ice for 30 minutes. Each transformation tube was being heat-shocked by placing the bottom half of the tube into a 42°C water bath for 45 seconds. The tubes were put back on ice for 2 minutes. 250 µL LB medium (without antibiotic) was added to the bacteria and grown in 37°C shaking (225 rpm) incubator for 45 minutes.

### 4.3.3 *Mini bacterial culture*

Plasmid names, antibiotic resistance, date and initials were written down at the bottom of the warmed up plates. The lab bench area was kept sterile by working near a flame or Bunsen burner. 50 µL of the transformation was transferred onto a 10 cm agar plate containing ampicillin using a sterile pipette tip. A sterile 'L-shaped' glass rod spreader was used to spread out the transformation liquid onto the agar surface.

An *ID1* reporter plasmid, pGL3 BRE Luciferase was a gift from Martine Roussel & Peter ten Dijke (Addgene plasmid #45126) and was obtained as a bacterial stab culture. The bacteria growing within the punctured area of the stab culture was touched using a sterile pipette tip. The tip was then run lightly over a section of an agar plate to spread the bacteria over approximately one-third of the surface area of the plate to create streak #1. A fresh sterile pipette tip was used to pass through streak #1 and to spread the bacteria over the next one-third section of the plate to create streak #2. Third fresh pipette tip was used to pass through streak #2 and to spread the bacteria over the next one-third section of the plate to create streak #3.

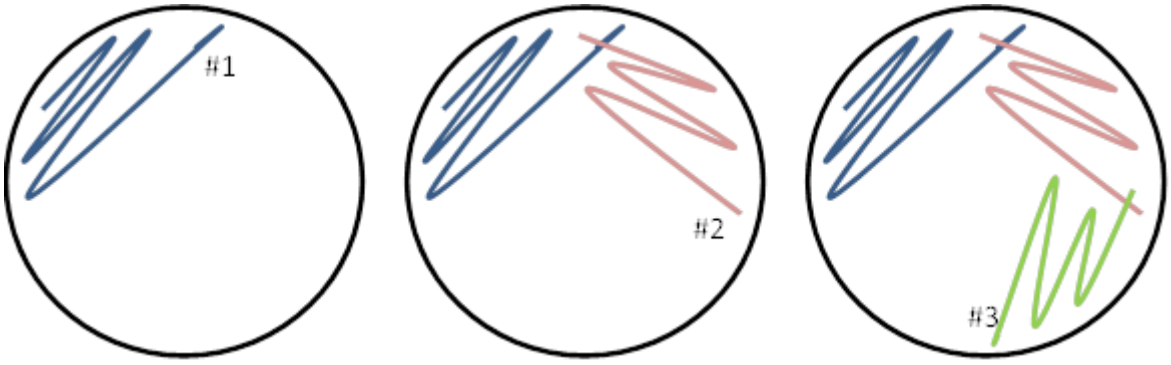


**Figure 4.1 : Bacterial streaks from a stab culture on agar plates.**

The plates were incubated at 37°C overnight with the bottom part on top. Colonies appeared as white dots growing on the solid medium. The bacterial culture plates with colonies were sealed using parafilm and stored in 4°C for a few weeks.

### 4.3.4 *Overnight liquid bacterial culture*

A single colony was picked from the streaked LB agar plate using a sterile pipette tip. The tip was then dropped into 5.0 mL of LB medium (with added ampicillin) in a 50 mL falcon tube and swirled around. The tube was then labelled with plasmid name and date. The liquid culture was loosely covered with its cap and incubated in a shaking (225 rpm) incubator at 37°C for 12

– 18 hours. Bacterial growth was checked after incubation, which is characterised by a cloudy haze in the medium. Glycerol stock could be created for long term storage of the bacteria.

### 4.3.5 *Plasmid DNA isolation by Qiagen® plasmid maxi kit*

1.0 mL of the overnight liquid bacterial culture was diluted into 100 mL selective LB medium (with ampicillin added). The culture was grown at 37°C for 12 – 16 hours with vigorous shaking (225 rpm). The bacterial cells were harvested by centrifugation at 6000 g for 15 minutes at 4°C. The used medium was discarded and the bacterial pellet could be kept in -20°C if the plasmid isolation process is not carried out immediately.

The bacterial pellet was resuspended in 10 mL of Buffer P1. The bacteria was resuspended completely by vortexing or pipetting up and down until no clumps remain. 10 mL Buffer P2 was added and mixed thoroughly by vigorously inverting the sealed tube 4 – 6 times. Do not vortex, as this will result in shearing of genomic DNA. The lysate should appear viscous. Do not allow the lysis reaction to proceed for more than 5 minutes. If LyseBlue has been added to Buffer P1, the cell suspension will turn blue after addition of Buffer P2. Mixing should result in a homogeneously coloured suspension. If the suspension contains localized colourless regions or if brownish cell clumps are still visible, continue mixing the solution until a homogeneously coloured suspension is achieved. The mixture was then incubated at room temperature for 5 minutes.

10 mL of chilled Buffer P3 was added immediately and thoroughly mixed by vigorously inverting 4–6 times, and incubate on ice for 20 minutes. If LyseBlue reagent has been used, the suspension should be mixed until all trace of blue has gone and the suspension is colourless. A homogeneous colourless suspension indicates that the sodium dodecyl sulfate (SDS) has been effectively precipitated. The sample was mixed again just before being centrifuged at 20,000 g for 30 minutes at 4°C. Centrifugation should be performed in non-glass tubes (e.g., polypropylene). After centrifugation the supernatant should be clear. Supernatant containing plasmid DNA was removed promptly and the supernatant was centrifuged again at 20,000 g for 15 minutes at 4°C. The resulting supernatant was removed promptly.

A Qiagen-tip 500 was equilibrated by applying 10 mL Buffer QBT and the column was allowed to empty completely by gravity flow. Supernatant from previous centrifuging step was applied promptly to the equilibrated tip and allowed to enter the resin by gravity flow. The Qiagen-tip

was washed with 30 mL of Buffer QC twice. The buffer was allowed to move through the Qiagen-tip by gravity flow. DNA was eluted with 15 mL Buffer QF. The eluate was collected in a 50 mL tube. DNA was precipitated by adding 10.5 mL room temperature isopropanol to the eluted DNA. The solution was mixed and centrifuged immediately at 15,000 g for 30 minutes at 4°C. Supernatant was carefully decanted as isopropanol pellets are more loosely attached to the side of the tube. DNA pellet was washed with 5.0 mL room temperature 70% ethanol and centrifuged at 15,000 g for 10 minutes. The supernatant was carefully decanted without disturbing the pellet.

The pellet was air-dried for 5 – 10 minutes and excess ethanol was carefully removed using pipette tip. The DNA was redissolved in 100 µL of TE buffer, pH 8.0. The pellet should not be overdried, as overdrying will make the DNA difficult to redissolve. DNA concentration and quality was measured using a Nanodrop spectrophotometer 2000 machine (Thermo Fisher Scientific).

### 4.3.6 *Restriction digestion of plasmid DNA*

Restriction enzyme to digest the plasmids was selected by analysing the plasmid DNA sequence. The plasmid DNA used were pGL3 Basic, pRL Null and pGL3 BRE Luciferase was cut using Nhe1 enzyme (Thermo Fisher Scientific, UK). Appropriate reaction buffer (10x Tango buffer) was determined by reading the instructions for the selected enzyme.

A restriction digestion reaction mixture was combined in a microcentrifuge tube. The mixture comprised: 1.0 µg DNA, 1.0 µL Nhe1 enzyme, 2.0 µL 10x buffer and a volume of $dH_2O$ to bring the total volume to 20 µL. The mixture was gently mixed by pipetting. The reaction tube was then incubated at 37°C for 1 hour. The products of the digest was visualised by gel electrophoresis.

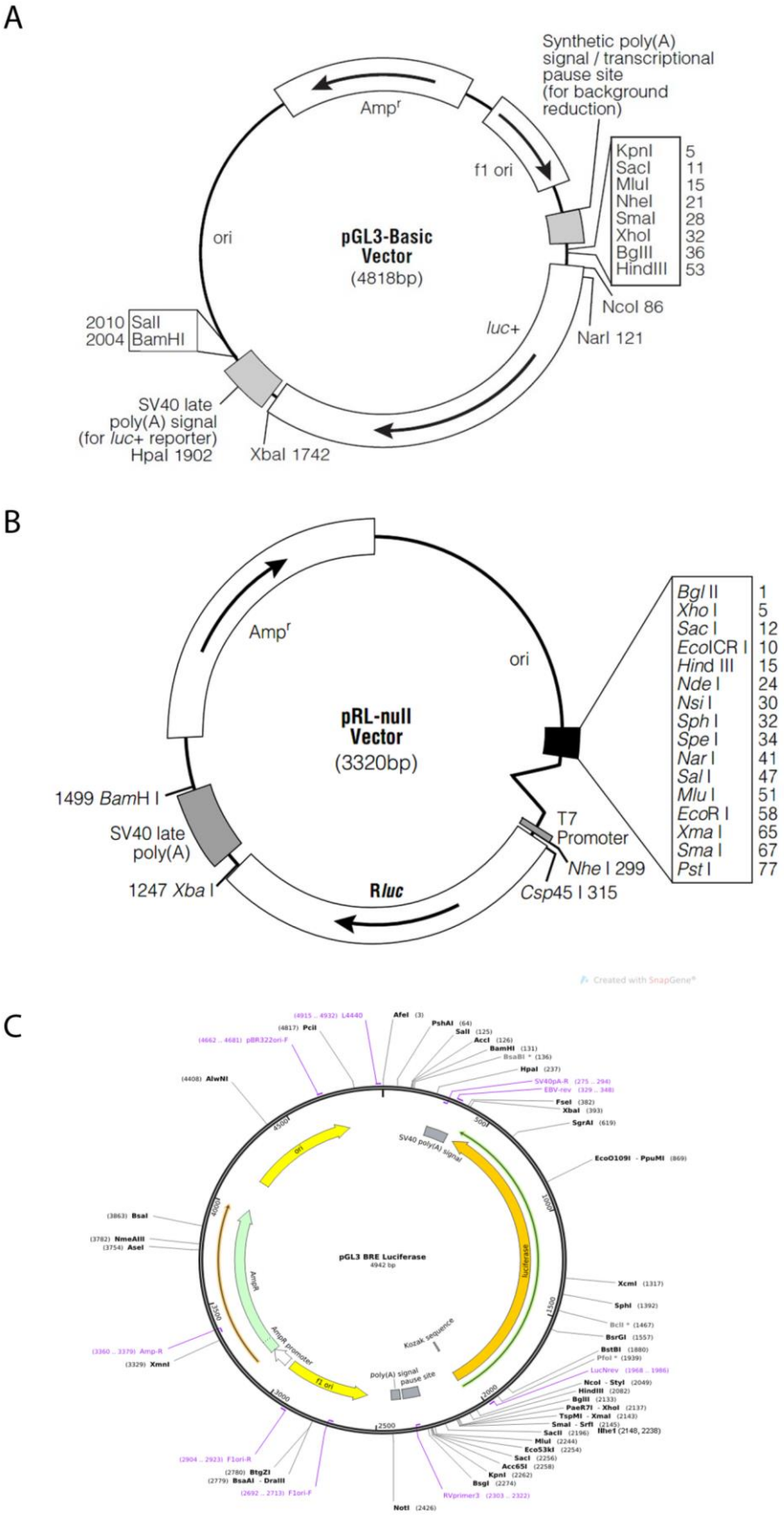


**Figure 4.2 : The sequence maps for the plasmids used; pGL3-Basic (A), pRL-Null (B) and pGL3-BRE-Luc (C). Adapted from Promega and Addgene.**

### 4.3.7 *Gel electrophoresis*

Agarose gel was prepared by dissolving agarose gel powder (Bioline.com, BIO-41025) in 1x Tris-acetate-EDTA (TAE) buffer (Formedium, UK). Agarose gel concentration to be prepared depends on the size of bands (restriction digest products) needed to be separated. The smaller the band size, the higher the agarose concentration. The restriction digest products size of the plasmid DNA used (pGL3 Basic, pRL Null and pGL3 BRE Luciferase) range from 100 - 5000 bp. Therefore, 1% agarose was prepared by mixing 1 g of agarose powder in 100 mL of 1x TAE buffer in a microwavable flask. The mixture was microwaved for about 3 minutes until the agarose is completely dissolved but not over boiled.

In the meantime, the gel tray was prepared by applying masking tapes on both ends of the tray and placing a well comb in place. The agarose solution was left to cool slightly before 10 µL GelRed (Cambridge Bioscience) was added and carefully swirled around to mix. The GelRed was added to allow the visualisation of DNA under ultraviolet (UV) light. The agarose solution was then carefully poured into the prepared gel tray to avoid bubbles formation. Any bubble formed was pushed away from the well comb or towards the edges of the gel with a pipette tip. The newly poured gel was left to set at room temperature for 20 – 30 minutes until it has completely solidified.

2.0 µL of 6x DNA loading dye (Thermo Scientific, UK) was added to 10 µL of each restriction digest samples. The loading dye provides a visible dye that helps with gel loading and it contains a high percentage of glycerol that increases the density of the DNA causing it to settle to the bottom of the gel well. Once the gel has solidified, the masking tapes and gel comb were carefully removed and the gel was placed into the gel box (electrophoresis unit). The gel box was then filled with 1x TAE buffer until the gel is covered.

10 µL of each molecular weight ladders, GeneRuler 100bp Plus and GeneRuler 1kb DNA ladder (Thermo Scientific, UK) was carefully loaded into the first and last lanes of the gel, respectively. Then 10 µL of each of the digest samples and loading dye mixture was loaded into the additional wells of the gel. The gel was run at 100V for 1.5 hours. Power was turned off and the electrodes were disconnected form the power source at the end of the run. The gel was then carefully removed from the gel box and brought to a UV DNA visualisation machine, GelDoc-It 310 imaging system (UVP, LLC Upland, CA) to visualise the DNA fragments.

### 4.3.8 *Cell culture*

Undifferentiated hESCs (H9) and hiPSCs (SB-Ad2 and SB-Ad3) were maintained in Matrigel (growth factor reduced) plates with mTeSR™1 medium (STEMCELL Technologies, Cambridge, MA) at 37°C and 5% $CO_2$. hESCs and hiPSCs were passaged every 3 – 4 days using EDTA 0.02% (Versene, Lonza, Belgium) at 1:3 - 1:6 ratios. All cells used were between passages 18 and 50.

The hESCs and hiPSCs were initially disassociated by incubating with Accutase for 5 minutes. The disassociated cells were collected and centrifuged at 500 g for 5 minutes. The cell pellet was resuspended into 2 ml of media and cell count was performed prior to replating cells at the density of 1.3 x $10^5$ cells into each well of a Matrigel coated 24 well plate. 10 µM ROCK inhibitor was added to the medium during the seeding process one day before transfection.

The remaining disassociated cells from the seeding process were lysed using BL + TG buffer and kept in -20°C for RNA extraction and qPCR. Transfected cells were cultured in mTeSR™1 medium alone or mTeSR™1 supplemented with BMP4 (25 ng/mL) or BMP4 and SB431542 (10 µM) with daily medium change for three days. Cell extracts were prepared 48 hours after transfection using a passive lysis buffer (PLB).

a. Plating the pluripotent stem cells (hESCs) for optimisation experiment at day 0

mTeSR™1 medium was aspirated from the wells of a 6-well plate and the wells were gently washed with 2.0 mL DPBS. DPBS was aspirated and 1.0 mL of warm StemPro Accutase (Gibco, UK) was added to each well. The cells in accutase were incubated for 2 – 3 minutes at 37°C before 3.0 mL cold mTeSR™1 medium per well was added to inactivate the accutase. Cells were collected from all wells and transferred into a 50 mL falcon tube. The cells were then centrifuged at 1000 rpm for 3 minutes. Supernatant was removed and cell pellet was resuspended in 5.0 mL of warm mTeSR™1 medium. The cells were count counted using a haemocytometer.

Cells were plated at the density of 1.7 - 2 x $10^4$ cells/$cm^2$ (Leung et al. 2013) in each well of 6 well Matrigel coated plate with mTeSR™1 media supplemented with ROCK inhibitor at concentration of 10 µM. Fresh mTeSR™1 medium without ROCK inhibitor was used to replace the used medium on days 1 and 2. The remaining cells were collected as day 0 cell pellet for qPCR. Three wells were assigned for every experimental group and two additional wells of

cells were plated for qPCR cell sample at day 3. The mTeSR™1 medium was changed every day until day 3. At day 3, the mTeSR™1 medium was replaced with serum free differentiation medium for Group 5 (as described in Chapter 3), which is supplemented with BMP4, RA and EGF. The SB435142 (10 µM) was gradually added to the differentiation media starting on day 3 for 1, 2 or 3 days. Schematic representation of the differentiation protocols and the list of media used during the differentiation induction period are as shown in Figure 4.3.

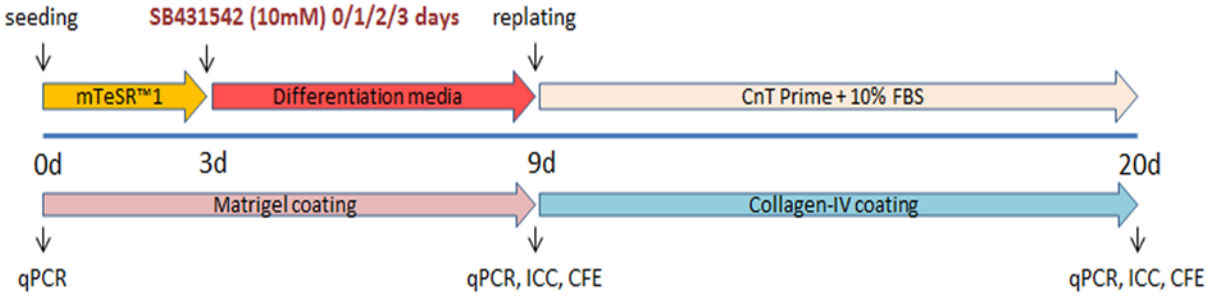


**Figure 4.3 : Schematic outline of the optimisation experiment.**

b. Replating cells onto collagen-IV coated plates at day 9

Differentiating cells were disassociated using TrypleExpress and replated at 1.7 x $10^4$ cells/$cm^2$. Cells were then supplemented with corneal differentiation medium (CnT-PR 2D Diff.) and 10% serum for the next 11 days. The culture medium was supplemented with 10 µM ROCK inhibitor for 2 days after replating. Cell morphology, gene and protein expression as well as colony forming efficiency were assessed at day 0, 9 and 20. The experiment was set for three technical and biological replicates for each group.

### 4.3.9 *qRT-PCR of endogenous BMP pathway related genes*

RNA extraction was performed on the lysed hESCs and hiPSCs samples. The extracted RNA was then measured and reverse transcription process was carried out to convert 1 µg of extracted RNA into cDNA following the method described in the instruction manual (Promega). The resulting cDNA was kept in -20°C. Endogenous BMP pathway genes expression in the hESCs and hiPSCs was assessed by qRT-PCR. The primers used are listed in the following table.

| Gene Name | Primer sequence (5' – 3') |
|---|---|
| ***BMP4*** | F: TCCACAGCACTGGTCTTGAG |
| | R: GGGATGTTCTCCAGATGTTCTT |

| | |
|---|---|
| ***GAPDH*** | F: TGCACCACCAACTGCTTAGC<br>R: GGCATGGACTGTGGTCATGAG |
| ***TGFβ1*** | F: GGCCAGATCCTGTCCAAGC<br>R: GTGGGTTTCCACCATTAGCAC |
| ***BMPR1A*** | F: TGAAATCAGACTCCGACCAGA<br>R: TGGCAAAGCAATGTCCATTAGTT |
| ***BMPR1B*** | F: TCACAAGACGTTTCCTGCGT<br>R: TGGTGGTGGCATTTACAACG |
| ***BMPR2*** | F: GGCAGCAGTATACAGATAGGTGA<br>R: ACTGCCCTGTTACTGCCATT |
| ***JUNB*** | F: ACGACTCATACACAGCTACGG<br>R: GCTCGGTTTCAGGAGTTTGTAGT |
| ***ID1*** | F: CTGCTCTACGACATGAACGG<br>R: GAAGGTCCCTGATGTAGTCGAT |
| ***ID2*** | F: CCGTGAGGTCCGTTAGGAAA<br>R: TGAGCTTGGAGTAGCAGTCG |
| ***SMAD1*** | F: CCGAGCGGCTCAACCC<br>R: AGTTTGAAGTCCAGAAGAGTAGAA |
| ***SMAD5*** | F: CGGCCGAGCTGCTAATAAAG<br>R: TTCATTGGGTCAAGTCTCGC |
| ***SMAD6*** | F: CTGAGCCGAGAGAAAGAGCC<br>R: AAAATGCAGTCCACCGATGC |
| ***SMAD 9*** | F: CACACAACGCCACCTATCCT<br>R: ACTGGTCGAAAGTCTGAGTGT |
| ***STAT1*** | F: TTACAAACCTCAAGCCAGCC<br>R: TGATAGGCAGTAACACGGGG |
| ***SOX4*** | F: GAGTTCCCGGACTACTGCAC<br>R: GCGCCCTTCAGTAGGTGAAA |
| ***OCT4*** | F: TCTCGCCCCCTCCAGGT<br>R: GCCCCACTCCAACCTGG |
| ***ECADHERIN*** | F: CCCGGGACAACGTTTATTAC<br>R: GCTGGCTCAAGTCAAAGTCC |
| ***CK8*** | F: GATCGCCACCTACAGGAAGCT |

| | |
|---|---|
| | R: ACTCATGTTCTGCATCCCAGACT |
| ***CK3*** | F: CGTACAGCTGCTGAGAATGA<br>R: CTGAGCGATATCCTCATACT |
| ***ΔNp63*** | F: CTGGAAAACAATGCCCAGAC<br>R: GGGTGATGGAGAGAGAGCAT |

**Table 4.1 : List of primers used for qRT-PCR.**

### 4.3.10 *Plasmid transfection by lipofection*

Lipofectamine 3000 reagent (Thermo Fisher, Waltham, MA, USA) was used for plasmids transfections. For plasmid lipofection, 500 ng plasmids (pGL3-Basic (Promega, Madison, WI, USA) or pGL3 BRE Luciferase (Addgene, Massachusetts USA)) were used to transfect the cells in each well of 24 well plate following manufacturer's recommendations. The optimum volume of Lipofectamine 3000 for plasmid transfection was initially determined for all cell lines and the optimised volume was used for all transfection procedures thereafter. Cells that were transfected with empty vector (pGL3-Basic) or BMP reporter (pGL3-BRE-Luciferase) were co-transfected with empty renilla vector (pRL-Null) (Promega, Madison, WI, USA).

### 4.3.11 *Dual luciferase assay*

Luciferase activities were evaluated with a Dual-Luciferase Assay System (Promega, Madison, WI, USA) according to the manufacturer's recommendations using Varioskan LUX plate reader (Thermo Fisher Scientific, Waltham, MA USA). Cells were washed with DPBS before being lysed with appropriate volume of passive lysis buffer (PLB). Lysed cells were kept at -20°C before the luciferase activity being analysed. Background luminescence was determined using untransfected cells and the background readings were then subtracted from the resulting luminescence readings before being normalised using the renilla luminescence and presented as relative luminescence unit (RLU).

### 4.3.12 *Colony forming efficiency (CFE) assay*

CFE assays were carried out on differentiating cells at days 9 and 20 of the differentiation period using the protocols described earlier in Chapter 2, subsections 2.2.16 and 2.2.17.

### 4.3.13 *Immunocytochemistry (ICC)*

ICC assessments were carried out on cells at days 9 and 20 following the protocols detailed earlier in Chapters 2, section 2.6.

## 4.4 Results

### 4.4.1 *Endogenous BMP pathway related gene expressions*

Quantitative RT-PCR analysis indicated that the non-responsive hiPSCs line (SB-Ad3) expressed higher levels of endogenous *BMP4* gene when compared to the responsive hiPSCs line, SB-Ad2 (Figure 4.4). However, the expression of key receptors (*BMPR1A*, *BMPR1B* and *BMPR2*) and receptor activated *SMAD1* and *SMAD5* genes that mediate BMP signalling were significantly lower in SB-Ad3, suggesting that this hiPSCs line may be characterised by a much lower level of endogenous BMP activity. This was further corroborated by low expression of two BMP target genes, *ID1* and *JUNB* which were also expressed at a significantly lower level in the non-responsive hiPSCs line when compared to the responsive line (Figure 4.4). Since both the receptor and effector genes expressions are lower, addition of exogenous BMP4 alone (as in our differentiation methods), is unlikely to activate the pathway in the SB-Ad3 hiPSCs line. To confirm this further, a BMP reporter plasmid was transfected in both hiPSCs lines causing a transient overexpression of BMP specific gene, *ID1* (Korchynskyi and Dijke 2002).

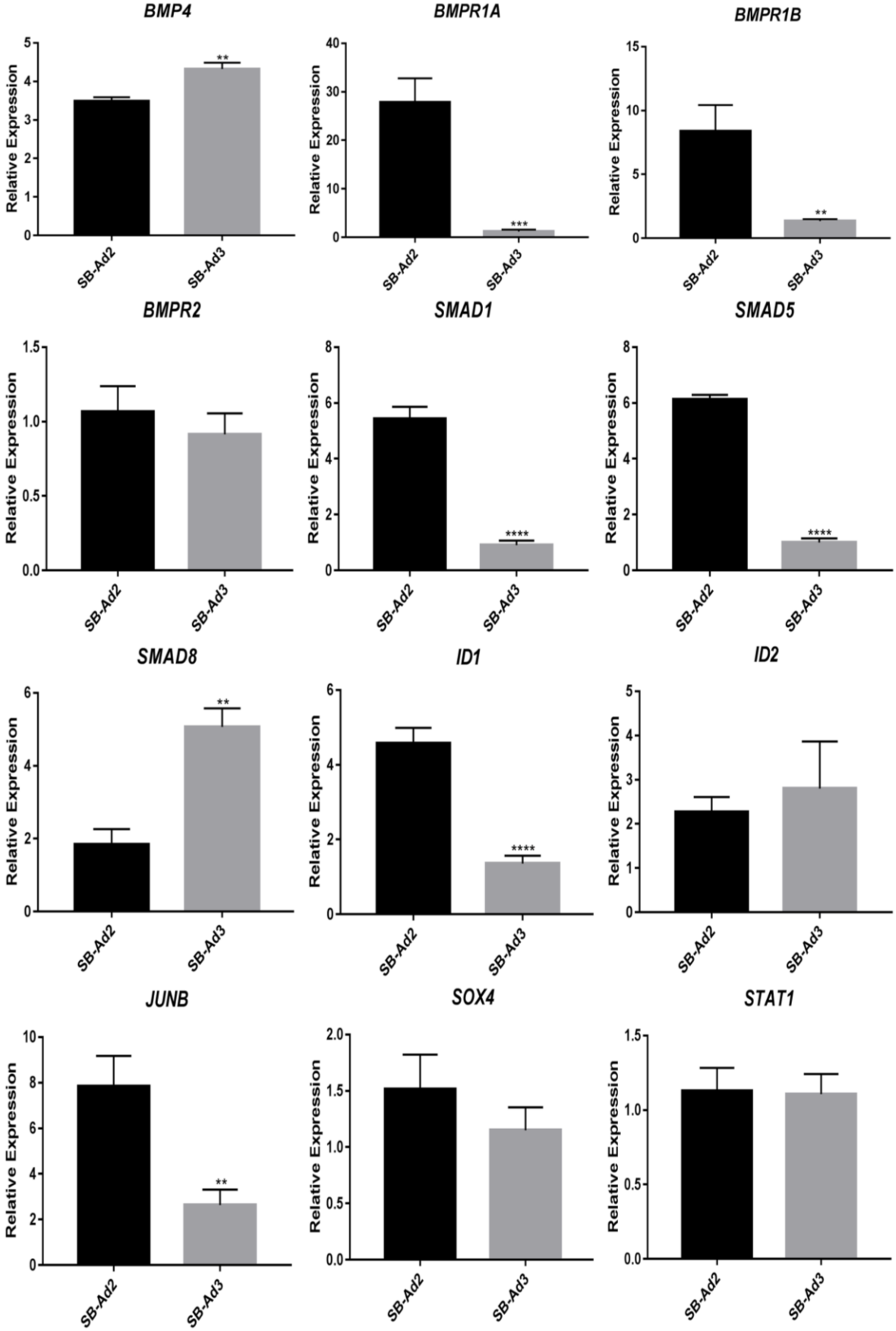


**Figure 4.4 : Relative gene expressions for endogenous BMP pathway in the hiPSCs normalised against hESCs, H9. Data presented as mean ± SEM, n = 3. * - significantly different compared to the other cell line.**

### 4.4.2 *Plasmid DNA concentration*

Purchased plasmids were transformed and and cultured overnight. The purified plasmid DNA (from mini bacterial culture) concentration and purity was assessed using Nanodrop 2000 spectrophotometer. The concentrations of each purified plasmid DNA are listed in the table below.

| | Plasmid name | Concentration (ng/µL) |
|---|---|---|
| **1** | pGL3-Basic | 436.8 |
| **2** | pRL-Null | 550.2 |
| **3** | pGL3-BRE-Luciferase | 348.5 |

**Table 4.2 : Concentrations of the purified plasmid DNA resulting from the mini bacterial culture.**

### 4.4.3 *Gel electrophoresis*

In order to verify that the purified plasmid DNA obtained from the bacterial culture are having the right size, each of the DNA was linearised by digestion using Nhe1 enzyme and the digest product was then run through gel electrophoresis together with respective control plasmid (purchased stock). The gel analysis showed that each of the plasmid DNA was having the right size which is the same as the control. In case of pGL3-BRE-Luciferase DNA, this DNA was cut at two locations by the Nhe1 enzyme. Therefore, the digestion products consist of two different sized DNA fragments. The bigger fragment contained the backbone (4852 bp) of the plasmid and the smaller fragment (90 bp) contained the BMP reporter segment (Addgene). Those different sized DNA fragments can be visualised in the gel electrophoresis images shown in Figure 4.5. The analysed plasmids DNA were then transfected into the pluripotent as well as differentiating hESCs and hiPSCs before the luciferase activity of the transfected cells were assessed using dual luciferase assay system (Promega).

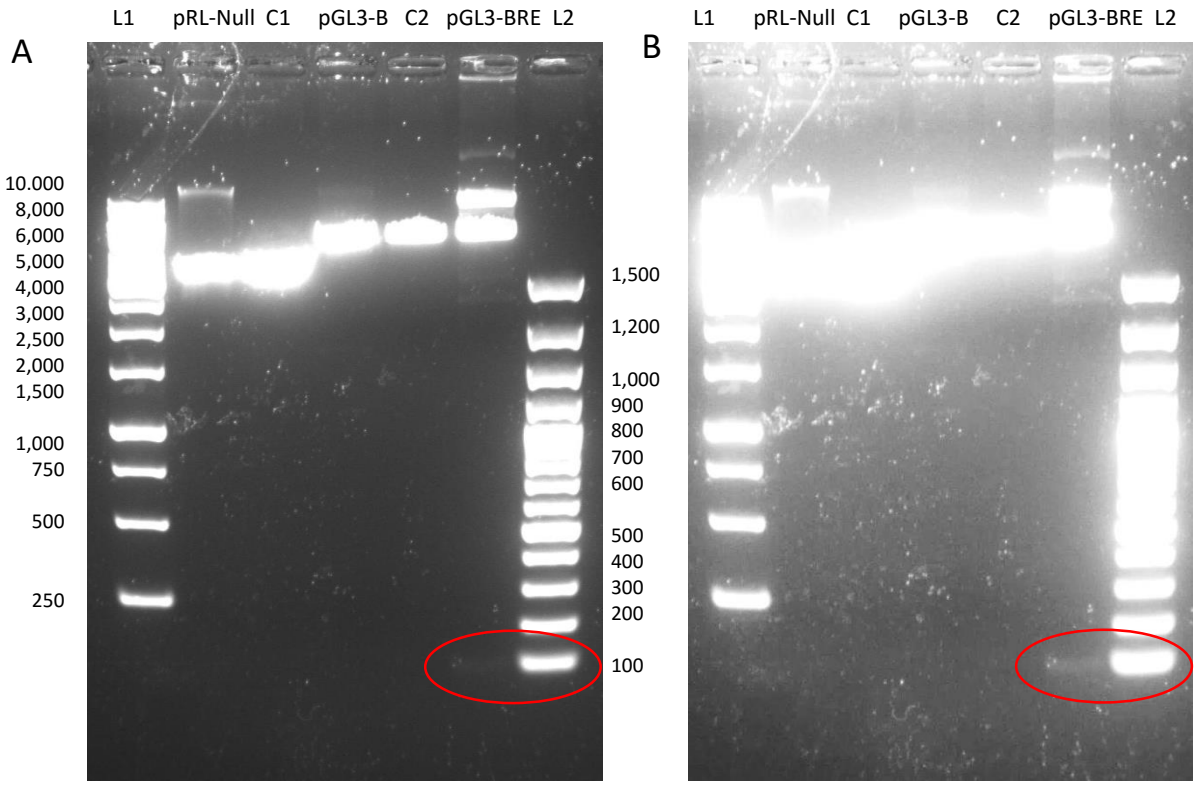


**Figure 4.5 : Gel electrophoresis analysis of the plasmid DNA. Lower exposure photo (A) and over exposed photo (B) showing the smallest DNA fragment (red circles) that contains the *ID1* reporter. L1 - GeneRuler 1kb DNA ladder, C1 – control for pRL-Null, C2 – control for pGL3-Basic, L2 - GeneRuler 100bp Plus ladder.**

### 4.4.4 *Effects of BMP4 and SB431542 on BMP reporter levels in H9, SB-Ad2 and SB-Ad3*

The BMP reporter analyses showed that the SB-Ad3 hiPSCs line has a significantly lower endogenous BMP signalling activity compared to SB-Ad2 hiPSCs (Figure 4.6A). Supplementation of BMP4 improved the BMP activity of both hiPSCs lines; however SB-Ad3 hiPSCs still lagged behind SB-Ad2 (Figure 4.6B). Interestingly, combined supplementation of BMP4 and SB431542 did not have a significant impact on SB-Ad2; but it significantly increased the BMP activity of SB-Ad3 hiPSCs to the same level as SB-Ad2 (Figure 4.6B).

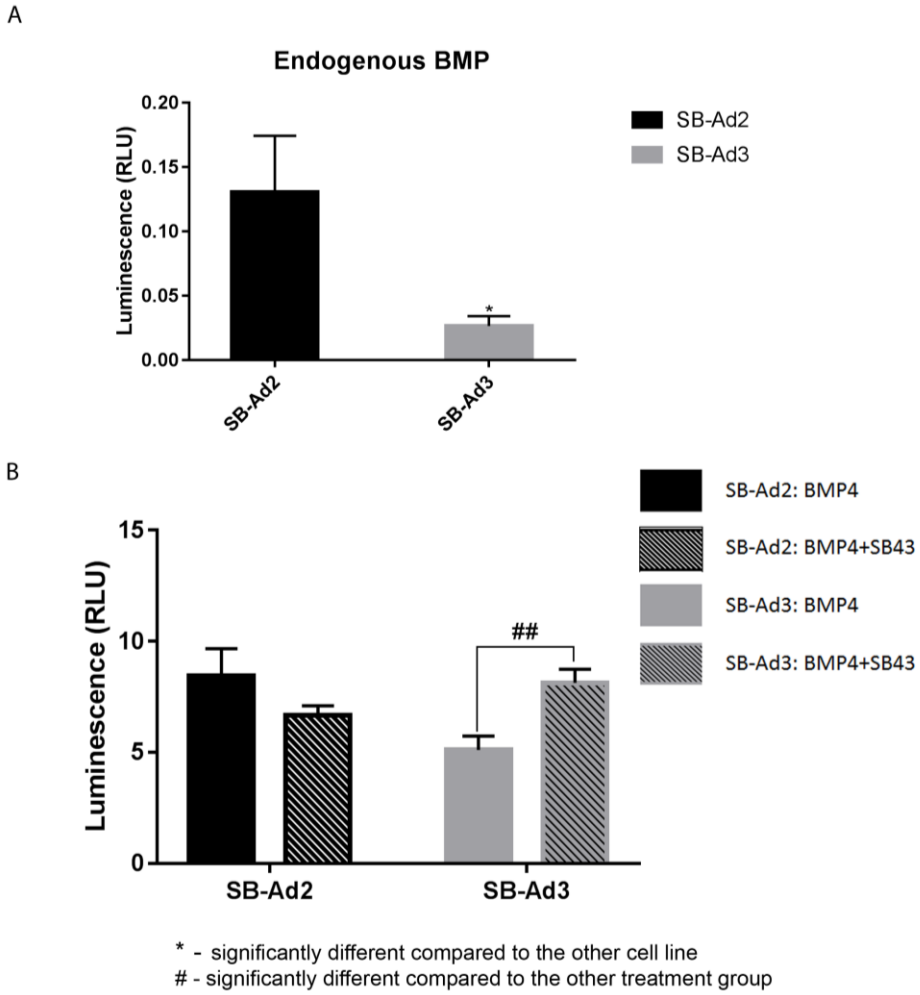


**Figure 4.6 : Endogenous BMP pathway activity levels normalised to hESCs (H9)(A), and the changes in BMP pathway activity following BMP4 and SB431542 supplementations (B) on the hiPSCs. Data presented as mean ± SEM of the relative luminescence unit (RLU). n = 3.**

### 4.4.5 *Early stage, day 0 – 9 of optimised differentiation*

The differentiation optimisation experiment had SB-Ad3 hiPSCs from groups 1 and 5 either unexposed or exposed to the TGFβ inhibitor, SB431542 for 1, 2 or 3 days (Figure 4.3). Gene expression assessment on day 9 of the optimised differentiation experiment revealed that all the hiPSCs (SB-Ad3) groups have decreased pluripotency, which can be seen in the low *OCT4* expression. Ectodermal, epithelial and putative limbal stem cell markers (*BMP4, CK8, ECADHERIN* and *ΔNp63)* expressions were significantly higher in G5 subgroup that was unexposed or exposed to SB431542 for only 1 day, compared with the control G1 with no SB431542 exposure. This finding is in agreement with our earlier results described in Chapter 3, where G5 of SB-Ad3 showed significantly high z scores at day 9 (Figure 3.17). Additionally, the terminally differentiated corneal epithelium cytokeratin, *CK3* gene expression was also

significantly higher in all the G5 subgroups at this early stage compared to the control (Figure 4.7).

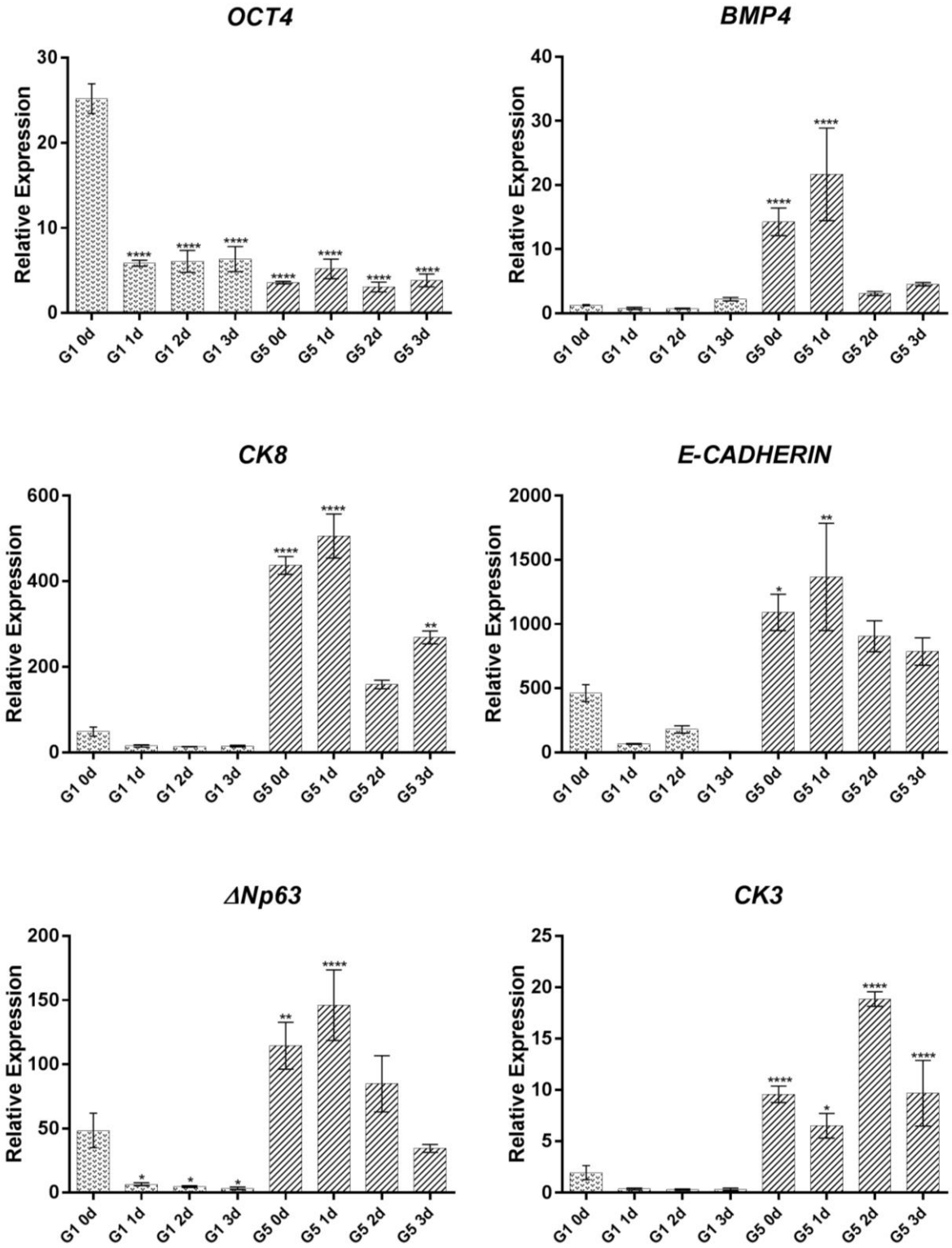


**Figure 4.7 : Relative expression of pluripotency and corneal epithelial differentiation related genes on day 9. Data presented as mean ± SEM, n = 3.* - significantly different compared to G1 0d.**

Figure 4.8 showed that during the early differentiation stage, the percentage of ΔNp63 positive cells was higher in G5 subgroups with or without SB431542 exposure than their respective G1 subgroup.

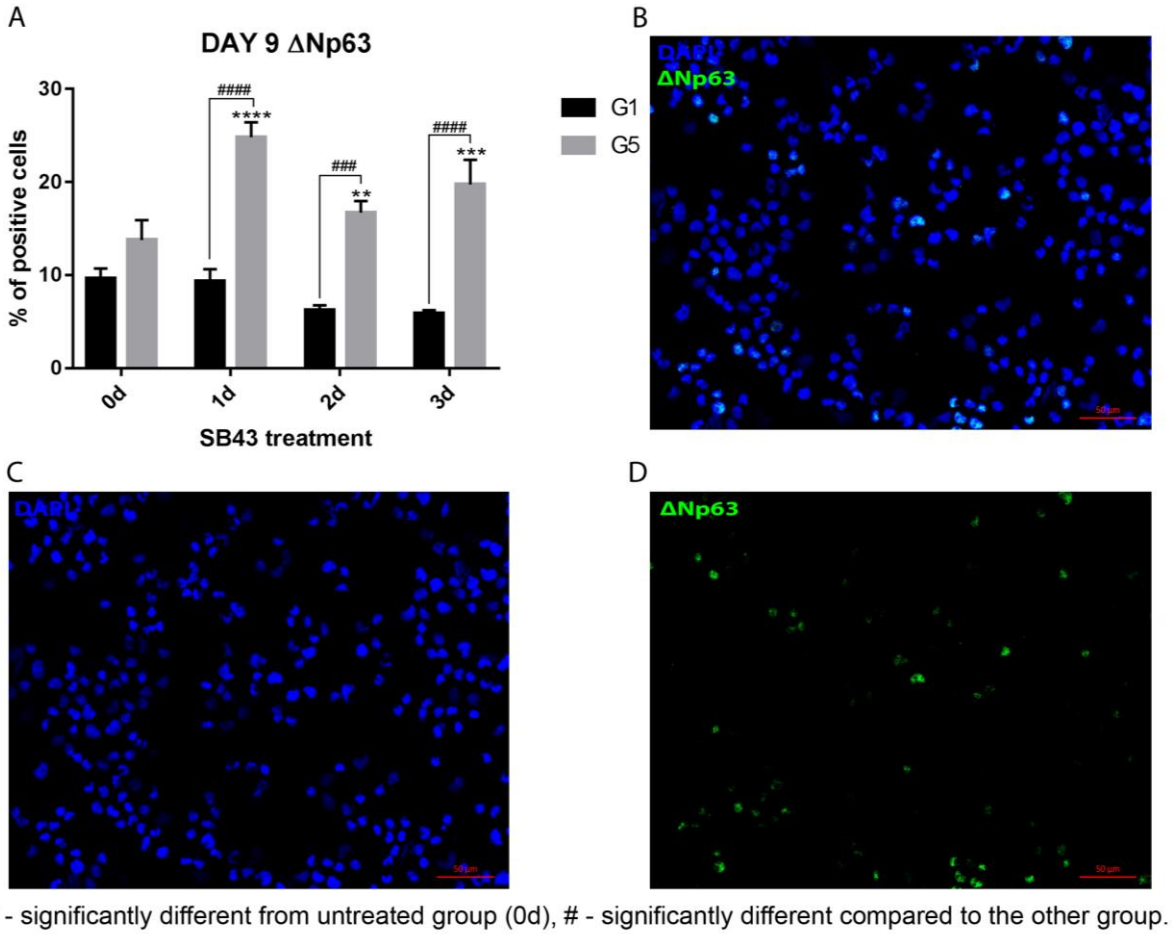


**Figure 4.8 : Immunocytochemistry analysis indicating the percentage of ΔNp63 positive cells at day 9 (A). Data presented as mean ± SEM. n = 3. Representative immunofluorescence micrographs from G5 1d (B, C and D).**

Although the gene expression and percentage of positive cells for ΔNp63 were improved with SB431542 exposure especially in the G5 subgroups that were supplemented with BMP4, RA and EGF, the colony forming ability of all groups at this early stage were still very low compared to the adult human limbal epithelial cells as shown in Figure 4.9. This suggests that cells at this early differentiation stage might need more cues and/or longer differentiation periods.

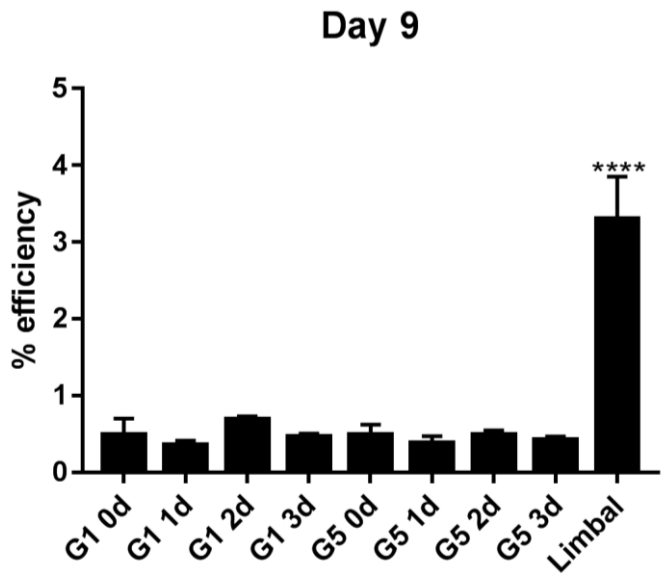


**Figure 4.9 : Colony forming efficiency at day 9. Data presented as mean ± SEM. n = 3. * - significantly different compared to G1 0d.**

### 4.4.6 *Late stage, day 10 – 20 of optimised differentiation*

At day 20, quantitative RT-PCR analysis indicated the putative limbal stem cells markers, (*ABCG2* and *ΔNp63)* and differentiated corneal epithelial marker *(CK3)* were expressed at a significantly high level compared to the control, G1 0d. It was also found that the highest expression of *ΔNp63* was in G5 subgroups treated for 2 or 3 days with SB431542 (Figure 4.10). Similarly, ICC assessment revealed that those two subgroups had higher percentage of ΔNp63 positive cells (Figure 4.11 A).

Interestingly, only the subgroups treated for 3 days with SB431542 showed significantly enhanced CFE ability compared to control G1(untreated with SB431542 and assigned as G1 0d) (Figure 4.12), suggesting that continuous inhibition of TGFβ pathway for 3 days with this specific TGFβ inhibitor can result in differentiation of non-responsive hiPSCs lines to corneal epithelial progenitor cells. Most importantly, three days SB431542 exposure to G5 cells had significantly improved the CFE to a similar levels observed in adult human limbal epithelial cell. This CFE result is in agreement with the gene and protein expressions shown by the putative limbal stem cell marker (ΔNp63) as shown in Figures 4.10 and 4.11.

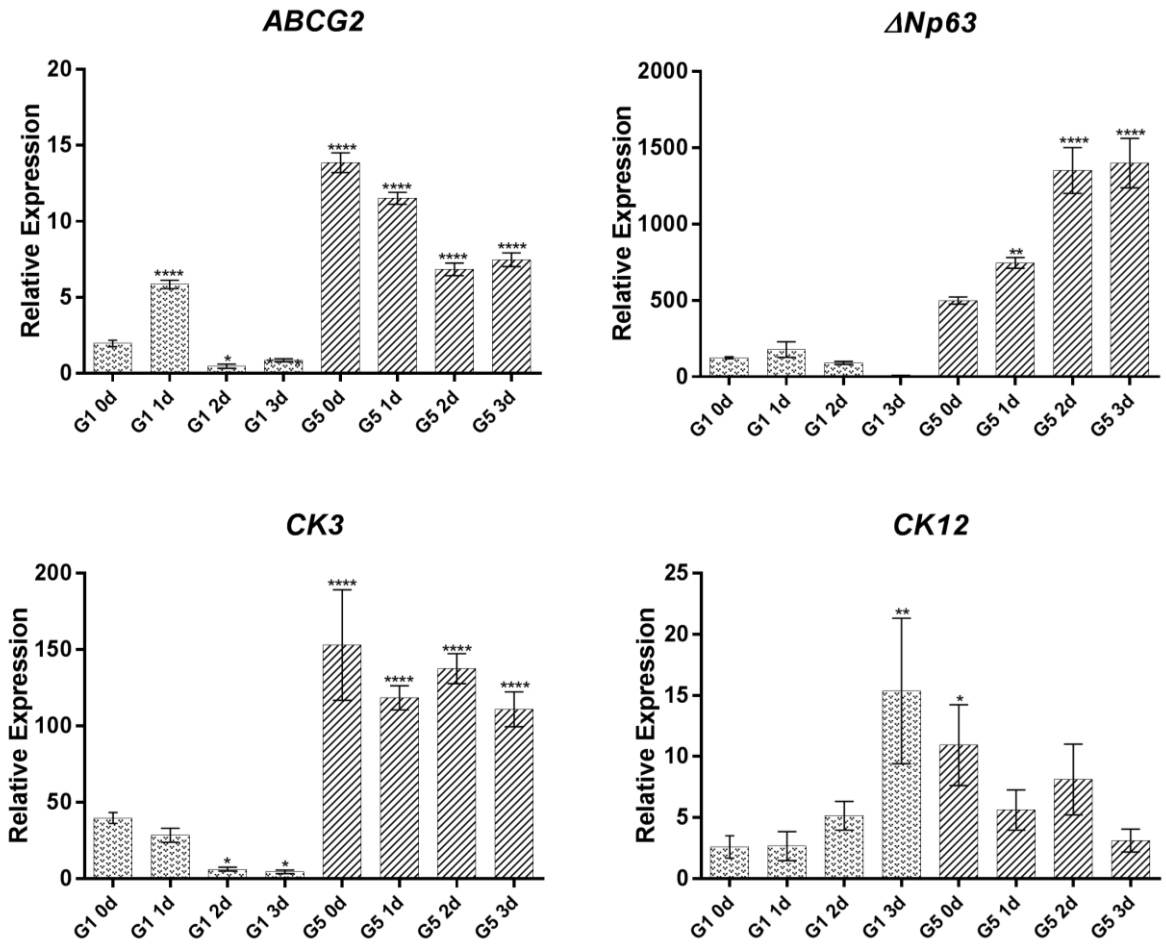


**Figure 4.10 : Relative gene expressions at day 20. Data presented as mean ± SEM. n = 3. * - significantly different compared to G1 0d.**

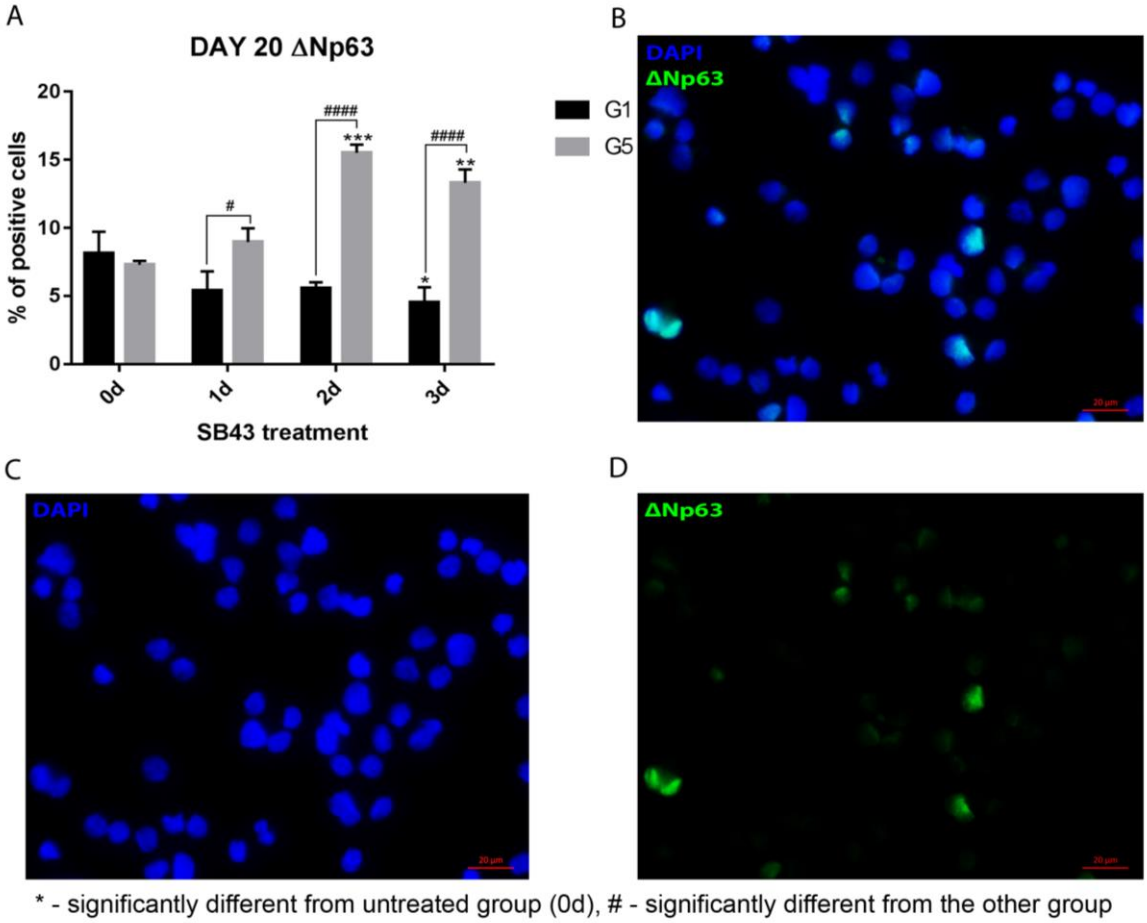


**Figure 4.11 : Immunocytochemistry analysis indicating the percentage of ΔNp63 positive cells at day 20 (A). Data presented as mean ± SEM. n = 3. Representative immunofluorescence micrographs from G5 2d (B, C and D).**

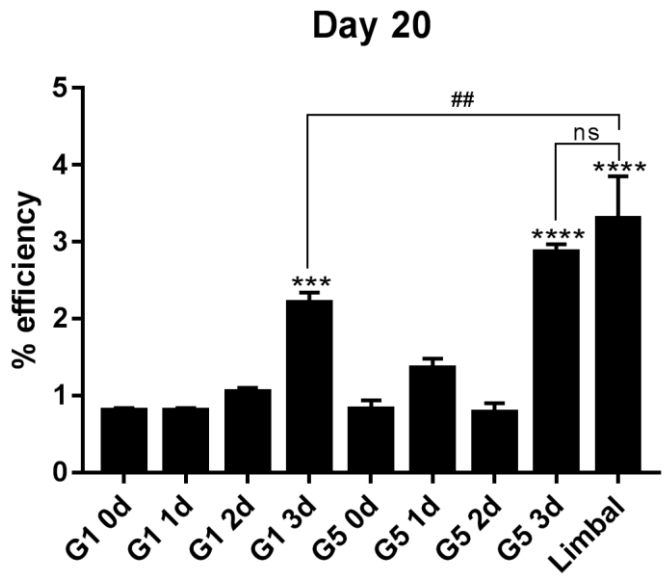


**Figure 4.12 : Colony forming efficiency at day 20. Data presented as mean ± SEM. n = 3. * - significantly different from G1 0d. # - significantly different from the other group. ns = no significant difference.**

## 4.5 Discussion

These experiments indicated that the non-responsive hiPSCs line (SB-Ad3) had a low level of BMP signalling activity which was caused by low expression of receptors and effectors. BMP reporter analysis confirmed that the two hiPSCs lines have significantly different levels of endogenous BMP signalling activity.

In view of improving the corneal differentiation potential of the less responsive line (SB-Ad3), we tried to alter the co-SMAD/r-SMAD interaction in the cytoplasm. Since co-SMAD (SMAD4) is shared between TGFβ and BMP pathways (Wrana and Attisano 2000, Wu and Hill 2009), we focused on the inhibition of the TGFβ pathway which should lead to an increase in the availability of SMAD4 for the BMP pathway. SB431542, a TGFβ inhibitor which was reported to be able to change the balance of co-SMAD (SMAD4) into the favour of BMP signalling (Du et al. 2014, Li et al. 2015) to activate the BMP pathway was used in the optimisation experiment. Our findings showed that the less responsive hiPSCs (SB-Ad3) line, but not the other needed BMP4 supplementation together with SB431542 (10 μM) for BMP signalling improvement. This closely corroborates those published by Shalom-Feuerstein et al. (Shalom-Feuerstein et al. 2013) who reported improved differentiation of hiPSCs to epidermal lineages upon addition of SB431542 to BMP4 and ascorbic acid supplemented media.

A different small molecule TGFβ inhibitor (SB505124) was used by Mikhailova et al. to guide differentiation of hiPSCs to corneal epithelial progenitor cells in combination with a Wnt inhibitor (IWP-2) and FGF (Mikhailova et al. 2014). Earlier in our setting, we also used SB505124 with IWP-2 alone or in combination with BMP4. Although SB505124 was reported to be more selective than SB431542 in TGFβ inhibition (DaCosta Byfield et al. 2004), SB505124 supplementation in our setting failed to enhance the expression of key epithelial and LSC markers, suggesting cross-talk between signalling pathways is essential for guiding differentiation of pluripotent stem cells to corneal epithelial lineages. Based on the BMP signalling improvement brought about by SB431542 supplementation on SB-Ad3 cells, we next planned for an optimisation experiment to improve the less responsive hiPSCs differentiation towards corneal epithelial like cells.

Since our earlier setting showed that supplementation of BMP4, RA and EGF (G5 protocols) to hESCs (H9) had directed the cells' differentiation towards corneal epithelial lineages, the G1 and G5 protocols were used in the optimisation experiment using SB431542 on SB-Ad3 hiPSCs.

As expected, SB431542 exposure on SB-Ad3 hiPSCs that were supplemented with BMP4, RA and EGF (G5) resulted in a significant improvement of corneal epithelial lineages differentiation as evident in the related genes and proteins expression analyses as early as the first differentiation window at day 9. However, *PAX6* gene was not assesses at this early stage in our setting. This would be a highly beneficial assessment to be carried out in future experiments, enabling the correlation between eye development and corneal epithelial differentiation genes to be understood.

This outcome also showed that the hiPSCs, especially SB-Ad3 line has an impaired directed differentiation that is 'repairable' when compared to the hESCs (Narsinh et al. 2011a). Similar to other published studies in the field, the optimised differentiation protocols generated a high percentage of CK3, CK12 and ΔNp63 positive cells in the first window of differentiation. In addition, the findings also indicated that the hiPSCs derived epithelial progenitors from the optimised protocols (G5 3d) have a high colony forming efficiency which was comparable to the limbal epithelial progenitor cells (Figure 4.12) obtained from adult human limbal ring.

# CHAPTER 5. TRANSLATIONAL STUDY USING GFP EXPRESSING DIFFERENTIATED HESCS AND HIPSCS IN ANIMAL MODEL OF LSCD

## 5.1 Introduction

*In vitro* studies are useful to define cell fates; however these cannot provide insight into cells' capacity to engraft and function *in vivo*. This capacity is vital to measure the potential of the aforementioned cells in future clinical settings. Thus translational studies using suitable animal models of the target disease have to be performed prior to clinical trials (Trounson & DeWitt 2016).

Green fluorescent protein (GFP) has been used to tag cells for various experimental applications without changing the cells' original function and characteristics (Tsien 1998). GFP reporters have been introduced into stem cells for stable GFP expression (Zaragosi et al. 2007) before the cells are differentiated towards the desired lineages. The GFP reporters thus provide an optimal *in vivo* detection especially for post transplantation observations.

This chapter aims to summarise the results obtained from transplantations of the GFP labelled hESCs and hiPSCs derived corneal epithelial-like cells in a mouse model of limbal stem cell deficiency (LSCD). LSCD induction in the mouse was established by Dr. Alex Shortt, Harley Buck and Pervinder Sagoo in the University College London and is going to be described in a publication currently being prepared (Sagoo et al. under preparation).

## 5.2 Specific Objectives

The specific objectives of this chapter are:

- to generate GFP expressing hESCs (H9) and hiPSCs (SB-Ad3) stable cell lines by nucleofection.
- to differentiate the GFP expressing cells to corneal epithelial cells using the best protocol from earlier experiments.
- to assess the engraftment of the transplanted cells on the cornea of LSCD mice.

## 5.3 Materials and Methods

### 5.3.1 *Cell culture*

Undifferentiated hESCs (H9) and hiPSCs (SB-Ad3) were maintained in BD Matrigel$^{TM}$ (growth factor reduced) plates with mTeSR$^{TM}$1 medium (STEMCELL Technologies, Cambridge, MA)

at 37°C and 5% $CO_2$. hESC and hiPSC were passaged every 3 – 4 days by using 0.02% EDTA (Versene, Belgium) at 1:3 - 1:6 ratios. All cells used were between passages 30 and 50.

a. Heat-shock transformation of competent bacteria and plasmid purification

Standard heat-shock transformation of chemically competent bacteria was carried out using a cell transformation kit by Dr. Chunbo Yang in Lako's group. Briefly competent cells were mixed with GFP expressing plasmid DNA, pmaxGFP (3.49 kb) in a falcon tube and incubated on ice for 20-30 minutes. Then, the tube was placed into a 42°C water bath for 30-60 seconds before being transferred back on ice for 2 minutes. 500 µL Lennox L Broth Base (LB) medium was added to the mixture and allowed to grow in a 37°C shaking incubator for 45 minutes. The transformed cells were then plated onto a 10 cm LB agar plate containing kanamycin and incubated overnight at 37°C. A single colony of the bacterial culture were then picked and inoculated into 10 mL LB medium and grown for about 8 hours with vigorous shaking (~300 rpm).

Qiagen plasmids purification maxi kit was used for purification of advanced transfection-grade plasmid DNA. The obtained plasmids were concentrated by centrifuging the plasmids vial at high speed for 15 minutes at 4°C. Then the supernatant was carefully removed and the plasmids pellet was air-dried in a tissue culture hood for about 10 minutes. The pellet was resuspended in filtered water and the plasmids/DNA concentration was measured using a Nanodrop 2000 machine. The plasmid DNA was linearised via restriction endonuclease (PvuI) reaction and DNA pellet was kept in -20°C before nucleofection.

b. H9 and SB-Ad3 cells' nucleofection with pmaxGFP plasmid using a Nucleofector® Kit (Amaxa GmbH)

H9 and SB-Ad3 cells at 1 or 2 days after passage were used for nucleofection. The pmaxGFP plasmid's GFP expression is driven by cytomegalovirus (CMV) promoter that allows stable transgene expression (http://www.amaxa.com, Barrow et al. 2006). The entire supplement containing 2.0 µg pmaxGFP was added to the Nucleofector® Solution together with 10 µM ROCK inhibitor (Y27632). Fresh cell culture plates were prepared by filling in 2.0 mL of mTeSR$^{TM}$1 supplemented with ROCK inhibitor (10 µM) for each well of a 6-well plate coated with Matrigel and plates were pre-incubated/equilibrated in a humidified incubator at 37°C and 5% $CO_2$.

Prior to nucleofection, the cells were detached from Matrigel plates by incubation with StemPro Accutase for 5 minutes at 37°C. The cells were dissociated into a single cell suspension by pipetting the suspension carefully up and down for 4 – 6 times. Medium was added to inactivate the Accutase. 2 x $10^6$ of the detached cells were counted and aliquoted before being centrifuged at 115 g for 3 minutes at room temperature. The cell pellets were carefully resuspended in 100 µL room temperature Nucleofector® Solution supplemented with 10 µM ROCK inhibitor per sample. Then 100 µL of cell suspension was combined with 5.0 µg DNA and transferred into a special cuvette. Nucleofector® Program B16 was selected and started after the cuvette with cell/DNA suspension was inserted into the Nucleofector® cuvette holder.

500 µL of pre-incubated culture medium was added to the cuvette and the sample was immediately gently transferred into the prepared 6-well plate using the supplied pipette. Transfected cell plates were kept in an incubator at 37°C in 5% $CO_2$. The GFP expression for each cells were checked after 24 hours using a fluorescence microscope. Puromycin (0.5 µg/mL) was added to the culture medium to select the GFP expressing cells. Individual colonies of GFP expressing cells were then carefully picked and expanded separately. Colonies with the brightest GFP intensity were chosen and expanded for the experiment. Expanded GFP cells were kept as frozen stocks for future experiments in a -80°C freezer and nitrogen storage tank.

c. Differentiation of H9 GFP and SB-Ad3 GFP

The H9 GFP and SB-Ad3 GFP cells were cultured using the best protocols described in the previous Chapter 4. Medium change was performed daily. On day 9, the cells were replated on collagen-IV coated plates or human amniotic membrane (HAM). The medium was changed to CnT-PR 2D Diff. with 10% FBS and 10 µM ROCK inhibitor for the first 2 days, and then without ROCK inhibitor thereafter up to day 20. Bright field and fluorescence images were taken at days 3, 9 and 20 and CFE assays were set on days 9 and 20. Assessment of cell pluripotency (*OCT4*), putative limbal stem cell markers (*ΔNp63, ABCG2), ECADHERIN*, *CK8*, *CK3* and *BMP4* expression was carried out by qRT-PCR on days 0, 9 and 20. The experiment was set for three technical and biological replicates for each group.

d. Human amniotic membrane (HAM) preparation

Human amniotic membrane (HAM) was removed from -80°C freezer and allowed to thaw on ice. A 6-well plate needed for washing the HAM later was prepared with 2 wells filled with 2 mL DPBS supplemented with 1% Pen-strep and 1 well filled with 2.0 mL CnT-Prime medium.

The lid of a 6-well plate was taken and placed "top-side up" on bench. HAM was unwrapped from its nitrocellulose backing using a straight tying (non-toothed) forceps, and placed flat on the top surface of 6-well plate lid, epithelial side up. One edge of the HAM was held with a non-toothed forceps with left hand (for right-handed operator). Whilst still holding the HAM with the forceps in the left hand to maintain its orientation, the HAM was sequentially washed in the pre-prepared 6-well plate - ie. twice in DPBS and once in CnT-PR 2D Diff. medium. HAM constructs were prepared by stretching out and trimming the HAM, followed by wrapping and trapping its edges between two sterile glass coverslips. The prepared HAM was then transferred into a 6-well plate and immersed with CnT-PR 2D Diff. medium until needed.

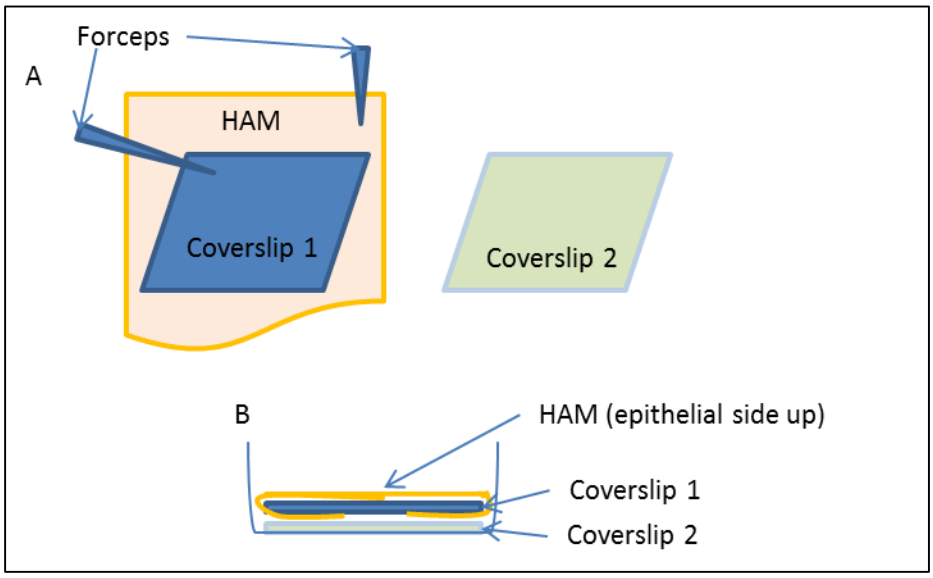


**Figure 5.1 : HAM preparation process. HAM was carefully held using a forceps and placed on top of a glass coverslip (A). The HAM was wrapped around a coverslip and the edges were secured using another coverslip and the whole construct was placed in a well of 6-well plate (B).**

e. Differentiating cells on HAM

Dissociated cells on day 9 were kept as single cells suspension after being counted. The cells were then carefully seeded at twice the density of the initial monolayer experiment onto the prepared HAM. 60 – 90 minutes were allowed for the cells to settle down well on the membrane with minimal amount of medium before more medium was added to the well. Medium change was done four days after seeding to allow enough time for the cells to attach to the membrane. Medium change was carried out every 2 days up to day 20.

f. Differentiating cells on temperature responsive plates

Normal and temperature responsive plates were coated with collagen-IV at least a day before being used and were washed briefly with DPBS before being seeded with cells. Temperature responsive plate filled with medium was warmed up (37°C) to assist cell attachment after seeding. Cells were seeded onto the plates at a predetermined cell density (1.5 or twice the density of the initial monolayer experiment). Cells were kept in CnT-PR 2D Diff. medium supplemented with 10% PBS for another 11 days before transplant.

### 5.3.2 *Mouse LSCD model for transplant*

The animal work was carried out by Dr. Alex Shortt's research team (at University College London). The induction of LSCD was performed on the eye of male adult (5 – 8 weeks old) immunocompromised NOD/SCID/gamma (NSG) recipient mice by exposing the corneal and limbal epithelium of the left eye for 3 minutes to either 20% ethanol or mitomycin-C (10 mg/mL). The right eye was kept as a normal control. Inflammatory reaction of the mice cornea was treated with 1% prednisolone eye drops for 24 hours prior to transplantation. LSCD induction via ethanol was carried out 30 minutes or 24 hours prior to transplant whilst the mitomycin-C inductions were done 3 weeks earlier. LSCD mice were deeply sedated and were treated under optimal surgical procedure during the transplant. Mice were kept on a warm 'surgical surface' during surgery and an antibiotic (chloramphenicol) cream was applied on the mouse eyelids after being sutured shut.

### 5.3.3 *Transplantation of differentiated cells onto LSCD mouse model's cornea*

The differentiated cells were detached using various methods (as detailed in Table 5.1) from culture plates/surfaces before being applied to the denuded recipient mouse cornea. One well of 6-well plate of cells were used per mouse cornea. The transplanted cells were protected by gently closing the eyelids over the graft with minimal abrasion of the surface. The eyelids were then sutured shut. Post operatively the sutures were removed at day 4 and the eye opened and examined using a fluorescent stereomicroscope. Serial imaging was performed to observe the number and distribution of GFP expressing engrafted cells on the cornea. Animals were sacrificed after 3 weeks and eyes with engrafted GFP cells were fixed in paraformaldehyde.

a. First transplant

Five mice were used for the transplant. GFP cells were differentiated on normal or temperature sensitive plates until day 20. Prior to transplant, the cells were disassociated either by using a

low temperature treatment together with a special membrane for temperature sensitive plate, or using dispase which was inactivated by CnT-Prime + 10% FBS medium before being centrifuged and resuspended in a minimal volume (20 µL) of the CnT-Prime + 10% FBS medium. The cells were transplanted as cells suspension on the mice cornea and later covered with fibrin gel. The mice eyelids were carefully closed and sutured shut.

b. Second transplant

Three mice were used for the second transplant. The GFP cells were either differentiated on HAM or normal plates until day 20. On the transplant day, cells were incubated for 2.5 hours in CnT-Prime medium + 10% FBS + Rock inhibitor (10 µM) at 37°C before disassociation. The cells were either scrapped off from plates or from the HAM using a cell scrapper and kept in CnT-Prime medium + 10% FBS + Rock inhibitor (10 µM) prior to transplant. The cells were transplanted as cells sheet onto the mice cornea and either Matrigel or amniotic membrane was applied on top to secure the transplanted cells on the cornea. The mice eyelids were then carefully closed and sutured shut.

c. Third transplant

Four mice were used in the last transplant attempt. LSCD was induced using 20% ethanol 24 hours before transplant and the corneal inflammation was treated with 1% prednisolone eye drops after the LSCD induction. Differentiated GFP cells at day 9, day 20 and day 27 were cultured on normal plates. The cells were scrapped off from plates and kept in CnT-Prime medium + 10% FBS + Rock inhibitor (10 µM) until transplantation. The cells were transplanted as cells sheet and air drying step was applied to promote cells' attachment on the cornea. The mice eyelids were then carefully closed and sutured shut.

## 5.4 Results

### 5.4.1 *Differentiation of GFP expressing cells*

The GFP cells showed similar morphology as their respective non-GFP cell lines based on the microscopy observations as shown in Figures 5.2 and 5.3.

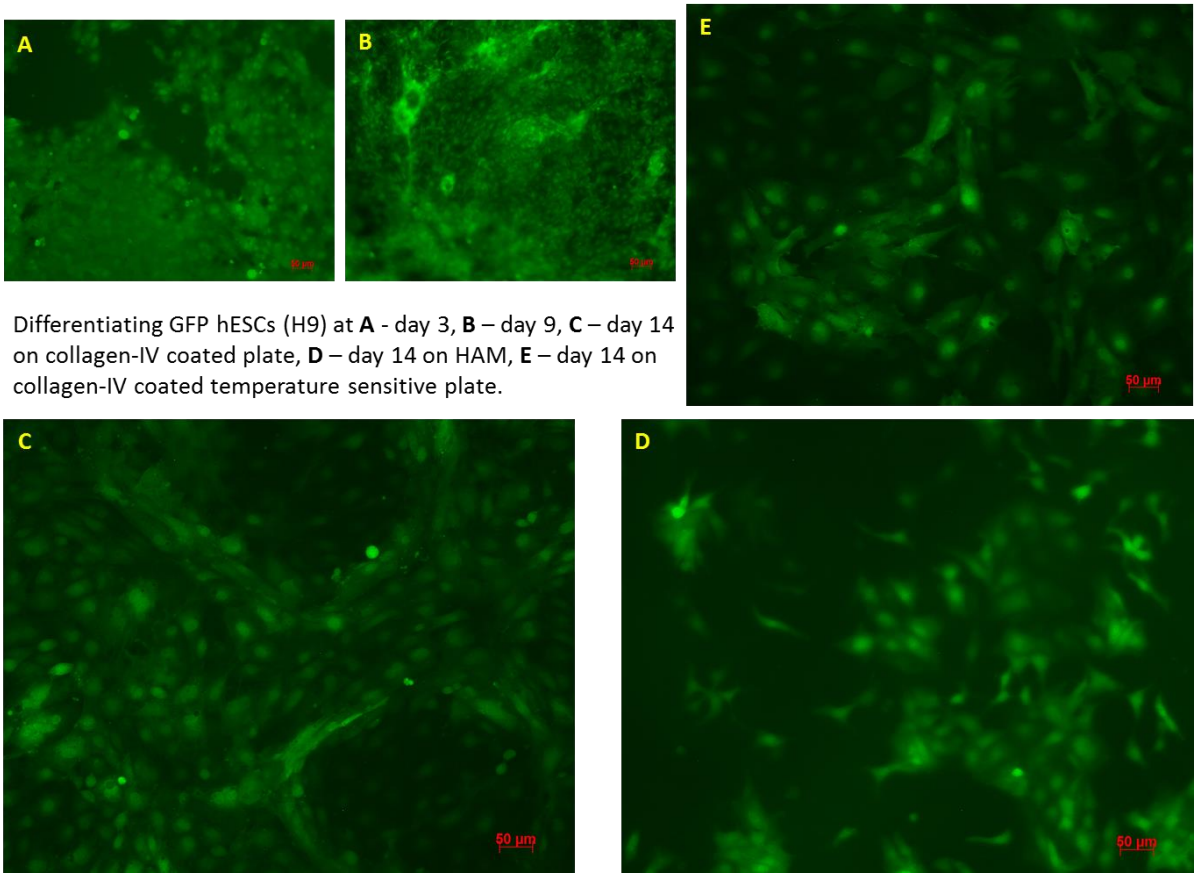


Differentiating GFP hESCs (H9) at **A** - day 3, **B** – day 9, **C** – day 14 on collagen-IV coated plate, **D** – day 14 on HAM, **E** – day 14 on collagen-IV coated temperature sensitive plate.

**Figure 5.2 : Representative photomicrographs showing the morphology of differentiating GFP hESCs (H9) at day 3 (A), day 9 (B), day 14 on collagen-IV coated plate (C), day 14 on HAM (D), and on collagen-IV coated temperature sensitive plate (E).**

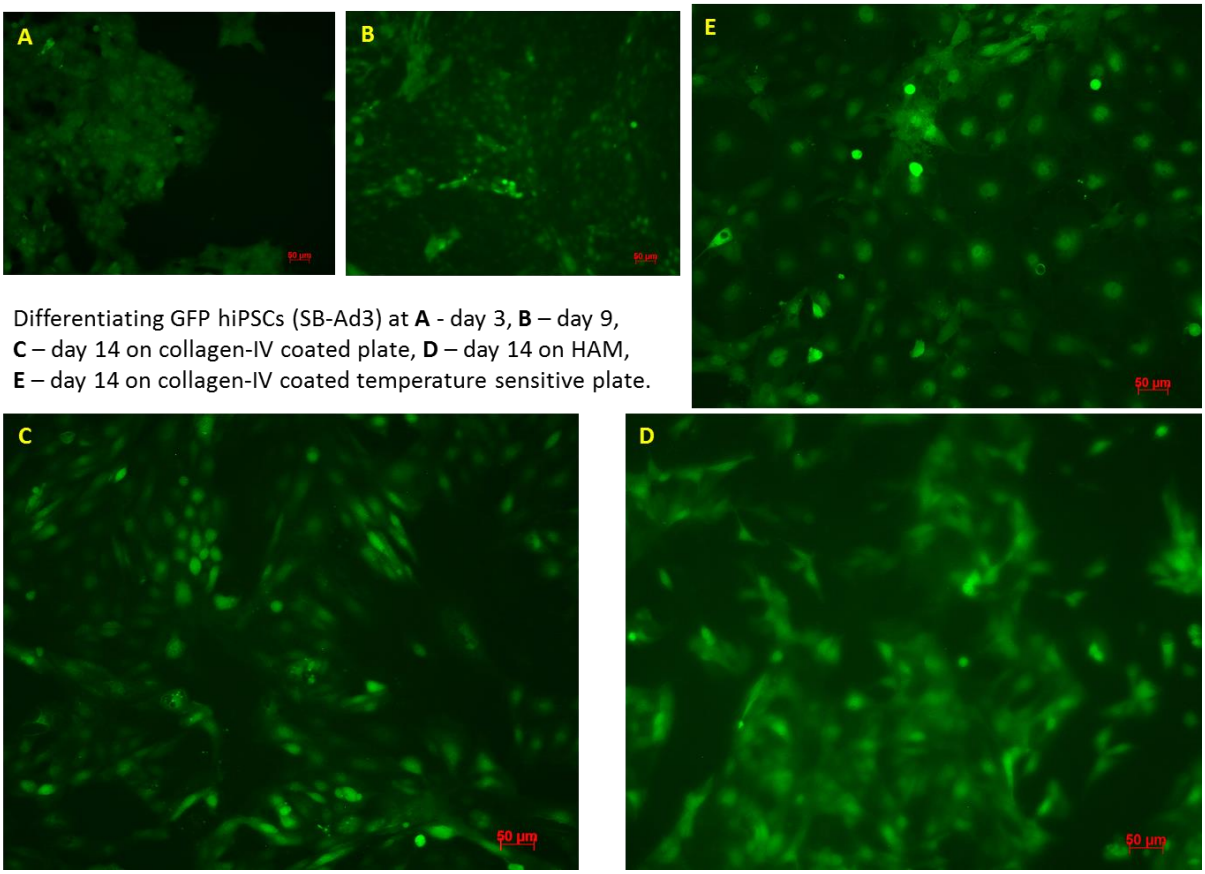


Differentiating GFP hiPSCs (SB-Ad3) at **A** - day 3, **B** – day 9, **C** – day 14 on collagen-IV coated plate, **D** – day 14 on HAM, **E** – day 14 on collagen-IV coated temperature sensitive plate.

**Figure 5.3 : Representative photomicrographs showing the morphology of differentiating GFP hiPSCs (SB-Ad3) at day 3 (A), day 9 (B), day 14 on collagen-IV coated plate (C), day 14 on HAM (D), and day 14 on collagen-IV coated temperature sensitive plate (E).**

Quantitative RT-PCR analyses showed that both GFP expressing hESCs and hiPSCs had similar early gene expression changes as those in earlier experiments on the respective non-GFP cells (Figure 5.4). Pluripotency gene (*OCT4*) was down regulated and the epithelial (*CK8*, *ECADHERIN*), non-neural ectoderm (*BMP4*), putative limbal stem cells (*ΔNp63*) and differentiated corneal epithelial cell (*CK3*) markers were all upregulated during early differentiation window in both cell lines.

Colonies of the GFP cells amongst the feeder cells in CFE assays were easily detected and observed using a fluorescence microscope. However, similar to the earlier experiment on non-GFP cells, the colony forming potential for the GFP cells (except H9 GFP) were still significantly low compared to the limbal cell (Figure 5.5) at this early differentiation stage (day 9).

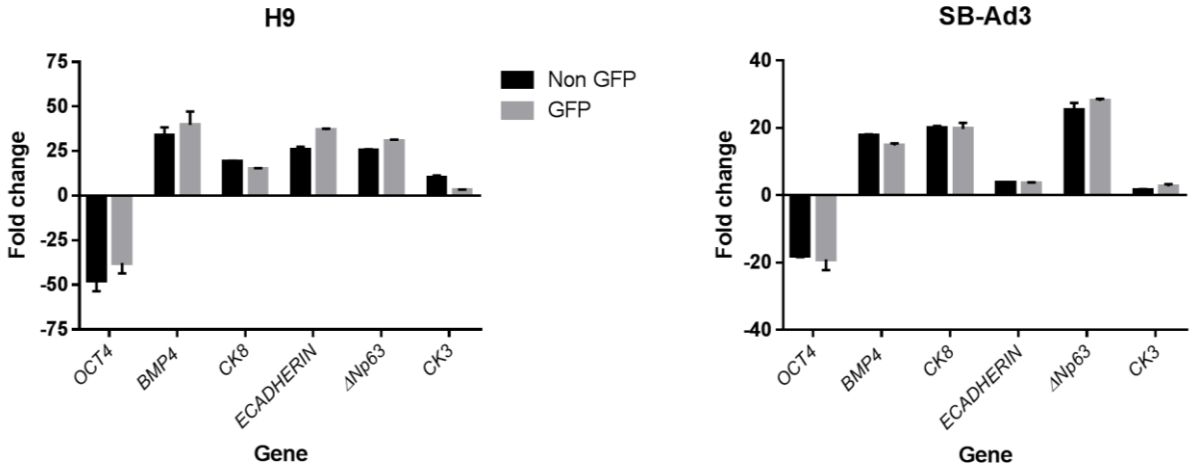


**Figure 5.4 : Gene expression assessments for both hESCs (H9) and hiPSCs (SB-Ad3) at day 9 compared to day 0. Data presented as fold change mean ± SEM of day 9 expression compared to day 0 (fold change). n = 3.**

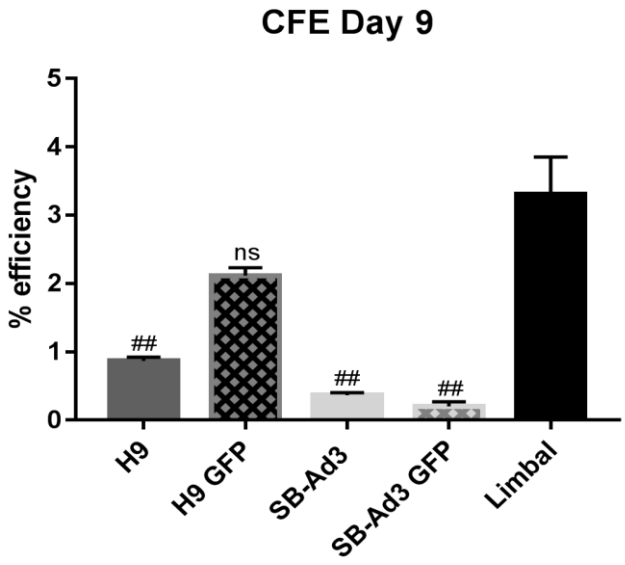


**Figure 5.5 : CFE of hESCs (H9) and hiPSCs (SB-Ad3) at day 9 of differentiation compared to adult limbal epithelial cells. Data presented as mean ± SEM. n = 3. # - significantly different compared to the limbal cells, ns – no significant different compared to the limbal epithelial cells.**

During the late differentiation period, both cell lines showed continued differentiation towards corneal epithelial lineages as observed in the fold changes of the related genes (Figure 5.6). Pluripotency marker *OCT4* was downregulated whilst the putative limbal stem cells (*ΔNp63, ABCG2*) and differentiated corneal epithelial cells (*CK3*) markers were upregulated. The colony forming ability of both GFP cell lines at this late differentiation stage was improved and was

significantly higher (i.e: H9 GFP cells) compared to that of adult human limbal epithelial cells (Figure 5.7).

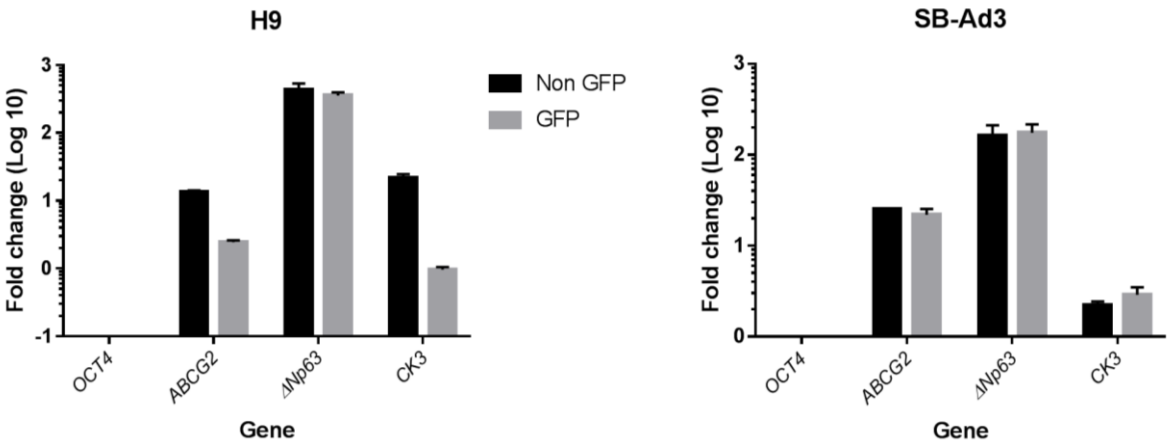


**Figure 5.6 : Gene expression assessments at day 20 compared to day 0 of both hESCs (H9) and hiPSCs (SB-Ad3). Data presented as log of fold change mean ± SEM of day 20 expression compared to day 0 (fold change). n = 3.**

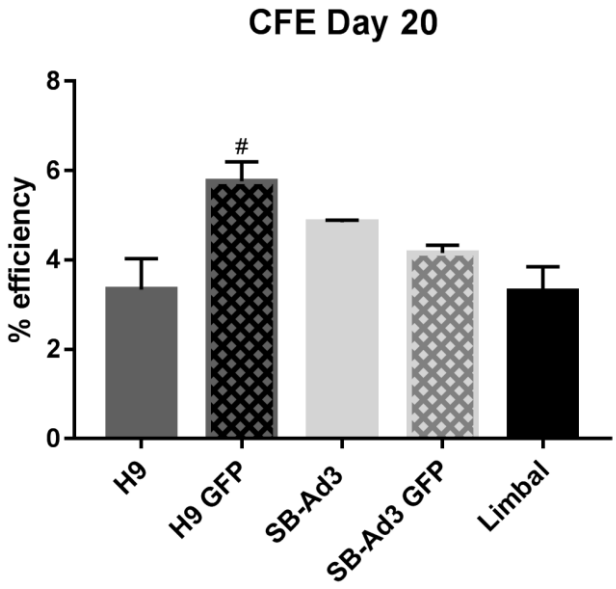


**Figure 5.7 : CFE of hESCs (H9) and hiPSCs (SB-Ad3) at day 20 compared to adult limbal epithelial cells. Data presented as mean ± SEM. n = 3. # - significantly different compared to limbal epithelial cells.**

### 5.4.2 *Transplant outcomes*

GFP expressing hESCs and hiPSCs were cultured and differentiated in Lako's lab at Newcastle University and were brought in a portable incubator to Dr. Shortt's lab at the Department of Immunology, University College London for transplantation into mouse models of LSCD.

LSCD mice were contributed and prepared by Dr. Shortt's research team, who also performed all transplantation procedures. The detailed information on the transplantation experiments are summarised in Table 5.1 below.

| **LSCD induction** | **Transplanted cells' age and preparation** | **Culture surface and pretransplant medium used** | **Method to secure cells on cornea** | **Outcome** |
|---|---|---|---|---|
| 20 % ethanol. LSCD induction was done 30 minutes before transplant. | 1. H9 D20 cells scrapped off and resuspended as single cells/clumps in 25 µL medium | Cold CnT-PR 2D + 10% FBS, coll-IV coated temperature sensitive plate | None | No cell engrafted 4 days post-transplant |
| | 2. SB-Ad3 D20 cells treated with dispase, inactivated with medium, centrifuged and resuspended in 30 µL medium | Cold CnT-PR 2D + 10% FBS, coll-IV coated temperature sensitive plate | Fibrin gel | No cell engrafted 4 days post-transplant, cornea was perforated and bleeding |
| | 3. SB-Ad3 D20 cells sheet was scrapped off and resuspended in medium | Cold CnT-PR 2D + 10% FBS + ROCKi, coll-IV coated normal plate | Matrigel | No cell engrafted 3 days post-transplant |
| | 4. H9 D20 cells sheet was scrapped off and resuspended in medium | Cold CnT-PR 2D + 10% FBS + ROCKi, coll-IV coated normal plate | Matrigel | Some cells were engrafted 3 days post-transplant |
| | 5. SB-Ad3 D20 cells grown on HAM, scrapped off as a sheet | Cold CnT-PR 2D + 10% FBS + ROCKi, HAM | HAM | No cell engrafted 3 days post-transplant |
| Mitomycin C (10 mg/mL). | 1. H9 D20 cells transferred using | Cold CnT-PR 2D + 10% FBS, coll-IV | None | |

| | | | | |
|---|---|---|---|---|
| LSCD induction was done 3 weeks before transplant. | temperature sensitive plate's membrane | coated temperature sensitive plate | | No cell engrafted 4 days post-transplant |
| | 2. SB-Ad3 D20 cells scrapped off and resuspended as single cells/clumps in 25 µL cold medium | Cold CnT-PR 2D + 10% FBS, coll-IV coated temperature sensitive plate | Fibrin gel | |
| | 3. H9 D20 cells treated with dispase, inactivated with medium, centrifuged and resuspended in 30 µL medium | Cold CnT-PR 2D + 10% FBS, coll-IV coated temperature sensitive plate | Fibrin gel | No cell engrafted 4 days post-transplant, cornea was perforated and bleeding |
| 20 % ethanol. LSCD induction was done 24 hours before transplant, 1% prednisolone was used to treat inflammation . | 1. H9 D20 cells were scrapped off as a sheet and resuspended in medium | Cold CnT-PR 2D + 10% FBS + ROCKi, coll-IV coated normal plate | Air-drying for 2 minutes | A few cells engrafted 4 days post-transplant, cells disappeared at second follow-up. |
| | 2. SB-Ad3 D27 cells were scrapped off as a sheet and resuspended in medium | Cold CnT-PR 2D + 10% FBS + ROCKi, coll-IV coated normal plate | Air-drying for 2 minutes | A few cells engrafted 4 days post-transplant, 10 days later the cells were observed near the limbus and disappeared at third follow-up. |
| | 3. H9 D9 cells were scrapped off as a sheet and resuspended in medium | Cold CnT-PR 2D + 10% FBS + ROCKi, coll-IV coated normal plate | Air-drying for 2 minutes | |
| | 4. SB-Ad3 D9 cells were scrapped off as a sheet and resuspended in medium | Cold CnT-PR 2D + 10% FBS + ROCKi, coll-IV coated normal plate | Air-drying for 2 minutes | No cell engrafted 4 days post-transplant |

**Table 5.1 : Summary table of the transplantation experiments and the outcomes.**

The cells that were transplanted to the first batch of LSCD mice did not engraft onto the cornea as observed 4 days of transplantation. Enzymatic disassociation (using dispase) resulted in eye perforation (Figure 5.8 D). These results brought about the idea of avoiding enzymatic cell disassociation, using HAM to differentiate the cells and Matrigel instead of fibrin gel application that may improve cell transfer and secure the transplanted cell on the cornea respectively, without affecting cells' viability.

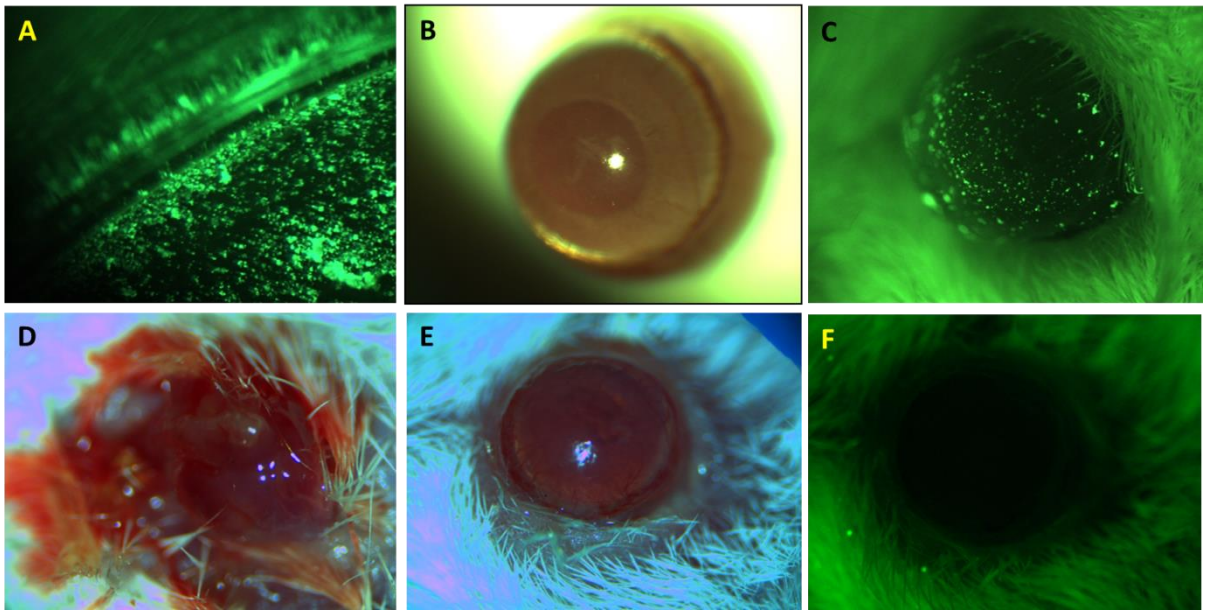


**Figure 5.8 : First transplant. Differentiated hESCs were disassociated and resuspended in a minimal volume of medium (A). An LSCD mouse cornea before transplantation (B). A mouse cornea with GFP H9 cells suspension added (C). A 'perforated'/damaged mouse cornea during the first follow-up (D). A normal mouse cornea during first follow-up with no engrafted GFP cells using bright field (E) and fluorescent (F) exposure at day 4 post-transplant.**

The second transplantation showed that some of the transplanted cells survived for 3 days on the mice cornea (Figure 5.9). This slightly improved cells survival might be due to the transplantation of cells as a sheet instead of single cells suspension and the use of Matrigel to secure the transplanted cells in place.

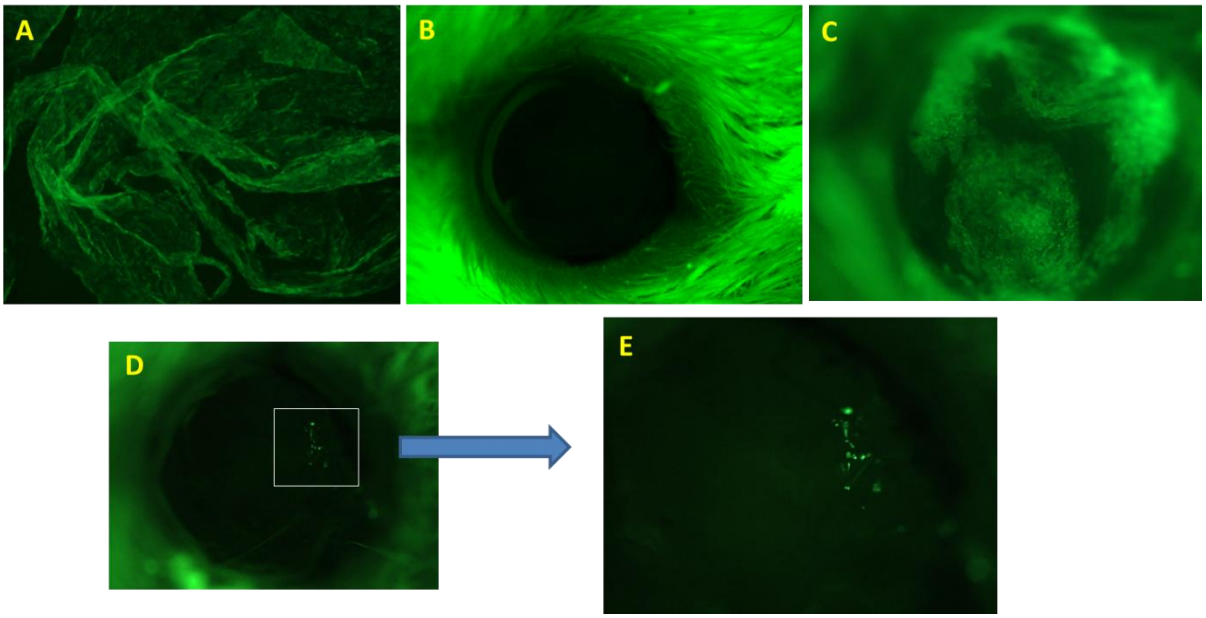


**Figure 5.9 : Second transplant. Differentiated hESCs were scraped-off from plates and resuspended in a minimal volume of medium (A). A mouse cornea before transplantation (B). A mouse cornea with GFP H9 cells sheet added (C). A mouse cornea during first follow-up with small number of engrafted GFP H9 cells during first follow-up at day 3 post-transplant (D). Engrafted GFP H9 cells at a higher magnification (E).**

The third transplant attempt resulted in a better cells' survival of up to 14 days. Unfortunately, those cells did not engraft and they disappeared from the mouse cornea after 14 days (Figure 5.10). This improvement might have resulted from the various differentiation time points when the cells were transplanted as well as the treated corneal inflammation prior to transplantation. Since there is no successful cell engraftment and proliferation observed on the mice cornea, histological analysis post-transplant was not carried out.

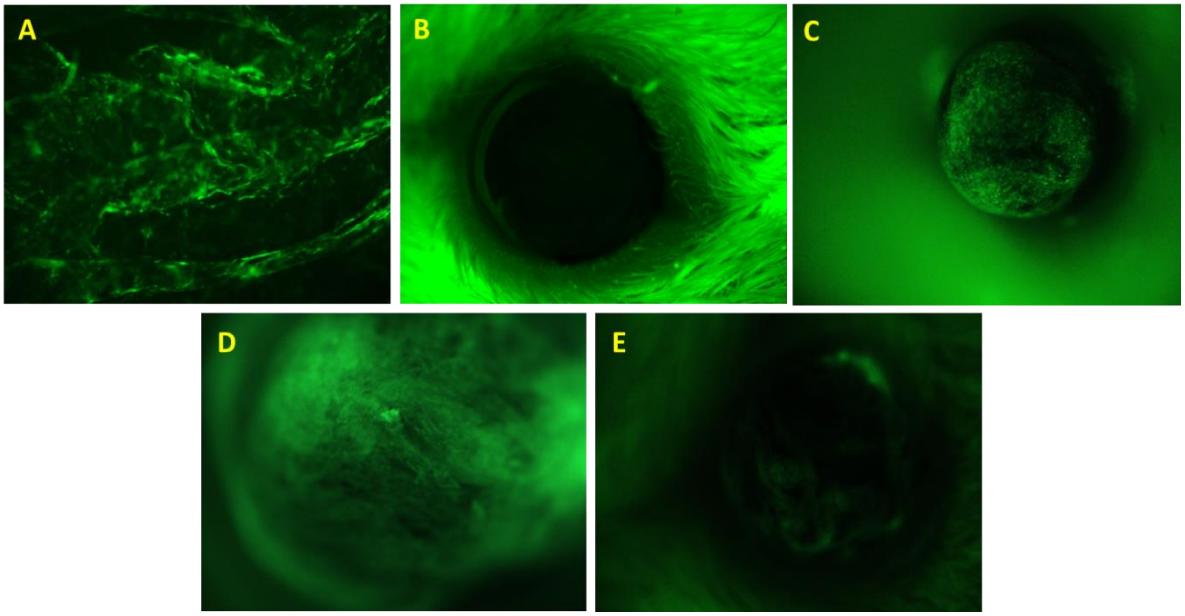


**Figure 5.10 : Third transplant. Differentiated hiPSCs were scraped-off from plates and resuspended in a minimal volume of medium (A). A mouse cornea without GFP cells before transplantation (B). A mouse cornea with GFP SB-Ad3 cells sheet added (C), at a higher magnification (D). A mouse cornea during first follow-up with a small number of engrafted GFP H9 cells at day 4 post-transplant (E).**

### 5.5 Discussion

Translational studies are important as a downstream pre-clinical step to provide important clues for future clinical therapeutic applications. Several animal models of LSCD have been used to dissect the potentials of *in vitro* differentiated stem cells for LSCD treatment as reviewed by Sehic and colleagues (Sehic et al. 2015). However, there is still no successful engraftment of hiPSCs derived corneal epithelial lineage cells on any LSCD animal model reported to date especially for the advancement of cell-based therapy in ocular surface regenerative medicine.

GFP expressing cells were successfully generated using both hESCs (H9) and hiPSCs (SB-Ad3) lines via nucleofection of GFP plasmid, enabling the resulting cells to express GFP at all time. SB-Ad3 cells were chosen for transplant experiment to compare the engrafment of differentiated cells from the optimised (with SB431542 exposure) differentiation protocols with the H9 cells differentiated using the initial protocol (G5). The GFP cells maintained their pluripotency and similar baseline gene expression profile as the non-GFP cells (data not included). This is important as any changes in the cells' function or characteristics of the cells used in transplantation might pose a risk in future clinical setting (O'Callaghan and Daniels 2011). The GFP cells were successfully differentiated towards corneal epithelium lineages using the best and optimised protocols found and reported in the earlier Chapter 3, subsection

3.4.3 and Chapter 4, subsection 4.4.6. Those GFP cells could be easily observed during differentiation easily handled during transplantation and identified *in vivo* post-transplant.

Although the GFP cells used for transplant were successfully differentiated towards corneal epithelial lineages *in vitro,* those cells seemed not be able to engraft and proliferate on the cornea of LSCD mice after three transplant attempts. The reason behind this failure could be multiple and reflect the immaturity of hESCs and hiPSCs derived corneal epithelial cells, the location where the cells were transplanted or the unsuitability of the LSCD model. There are several improvements that can be done as part of future work and one of these includes addition of a positive control group (primary adult human limbal epithelial stem cells labelled with fluorescent dies) which would validate the suitability of LSCD mouse model for transplantation of human LSCs (Meyer-Blazejewska et al. 2011, Cotsarelis et al. 1989).

Another improvement could relate to identification of the most optimal stage for transplantation. Our results indicated that hESCs that were differentiated for less than 20 days survived for a longer time in the mouse model. This suggests that shorter differentiation period might result in a better cell engraftment as reported by some previously published studies (Zhang et al. 2017, Brzeszczynska et al. 2014, Cieslar-Pobuda et al. 2016). This improvement might be due to the different functional characteristic of the cells at different time point. At the earlier time point which corresponds to our early differentiation stage of day 9, the percentage of cells expressing putative limbal stem cells marker, ΔNp63 was higher when compared to day 20. In contrast, hiPSCs at later differentiation time point (eg: day 27) were found to also have a good survival following transplant. This suggests that the hiPSCs needed a longer differentiation time to transform into corneal epithelial-like cells, as previously reported by others (Hayashi et al. 2012, Mikhailova et al. 2014, Hayashi et al. 2016)

Another cells selection step that was not carried out in our setting is cell sorting. Since our differentiation protocols did not yield pure population of corneal epithelial-like cells or limbal epithelial stem cells, sorting the differentiated cells to select the cell of interest (e.g. ΔNp63 or CK3/12 positive) could result in a better cell engraftment, as reported by previous studies (Zhang et al. 2017, Hayashi et al. 2016). The differentiated cells could also be further functionally defined by inducing its stratification via air-lifting method (Zieske et al. 2004) during the second stage of differentiation prior to transplant.

Rho kinase inhibitor (ROCKi) (Y27632) was used during cell seeding and replating process as well as in the final incubation step before the second and third transplant in our setting. The supplementation of ROCKi in the media during cell seeding and replating has improved the cells' survival as the seeded and replated cells were disassociated into single cell suspension, a condition less favoured by pluripotent stem cells (Watanabe et al. 2007). Initial incubation of cells with ROCKi prior to transplant were also aimed to improve cell differentiation stability, survival and engraftment post-transplant, as the ROCKi was reported to be beneficial in limbal stem cell maintenance and corneal wound healing (Miyashita et al. 2013, Sun et al. 2015). Thus, another transplant outcome improvement strategy could include ROCKi to be applied to the cornea following the transplantation of differentiated cells (Okumura et al. 2013).

Transplanting cells as a sheet instead of cells suspension onto the mice cornea resulted in an improved cells' survival in our experiment. A few earlier studies also reported the advantages of the cell-sheet transplantation in human (Umemoto et al. 2013, Burillon et al. 2012) and rabbit LSCD model (Burillon et al. 2012, Gomes et al. 2010, Nishida et al. 2004) but no study was reported in mouse models. Another avenue that is closely related and might have a huge impact in the translational study is the use of biomaterials to assist cells differentiation, cells transfer as well as engraftment. The use of silk, hydrogels or extra cellular matrix substrates as cells' coating or surface for cells culture amongst others have been reported to have improved the outcome of cells differentiation, transfer and transplant (Wu et al. 2014, Krishnan et al. 2014, Meyer-Blazejewska et al. 2011, Gu et al. 2009). Thus this might be one of various ways to enhance the transplant outcome especially but not restricted for our setting.

In conclusion our data indicates that further improvement strategies are still needed with regard to length of differentiation, cell harvest prior to transplantation, mode of delivery and improvement of the animal model management in order to establish whether hESCs and hiPSCs derived epithelial cells can engraft into LSCD corneas as well as establishing proof-of-principle for the cells' therapeutic application in the future (ISSCR Guideline 2016).

# CHAPTER 6. OVERALL DISCUSSIONS AND CONCLUSION

## 6.1 Overall Discussion

The main aim of this project was to define efficient protocols that results in robust hESCs and hiPSCs differentiation to corneal epithelial progenitors. Then we tested the engraftment of hESCs and hiPSCs derived corneal epithelial-like cells in a mouse model of total LSCD. As described in Chapter 3, our project has successfully defined a feeder-free, two-step protocol that results in differentiation of hESCs to corneal epithelial cells with colony forming ability similar to limbal epithelial progenitors within 20 days. The differentiation protocol included growth factors and morphogens (BMP4, RA, EGF) that have been shown to promote non-neural ectodermal commitment (Gambaro et al. 2006, Aberdam et al. 2007, Metallo et al. 2008, Li and Lu 2005) and proliferation of corneal epithelial progenitors (Hayashi et al. 2016, Zhang et al. 2017). In the second window of differentiation, we attempted to replicate the LSCs niche by coating the cell culture surfaces with collagen-IV which was reported to be the key component of peripheral cornea basement membrane and limbal stroma (Schlotzer-Schrehardt et al. 2007, Blazejewska et al. 2009) and supplementing the cells with a defined media (CnT-PR 2D Diff) which is used to maintain the *ex vivo* expansion of human corneal epithelial progenitors (Gonzalez et al. 2017).

Our differentiated hESCs express high *ECADHERIN, CK8, ΔNp63, ABCG2,* and *CK3* markers which represent epithelial, corneal and limbal epithelial stem cells as well as terminally differentiated corneal epithelium respectively (Mikhailova et al. 2014, Zhang et al. 2017). In line with the advancement of stem cell therapy using autologous cells, our hESCs derived protocol was tested on two hiPSCs lines that have different transcriptional and epigenetic profiles. The differences in the hiPSCs lines resulted in different responses towards the two-step hESCs derived protocol. One of the hiPSC lines (SB-Ad2) responded well to the differentiation protocol, but the second one (SB-Ad3) still needed further adjustment for its corneal epithelial lineages differentiation. This discrepancy was especially observed in the colony forming ability of the differentiated SB-Ad3 hiPSCs, rather than gene expression analysis.

In Chapter 4 we assessed the differences in the two hiPSCs lines using quantitative PCR. Our quantitative PCR results were confirmed by a BMP reporter analysis which showed that the two hiPSCs lines have significantly different levels of endogenous BMP signalling activity. The non-responsive hiPSCs line (SB-Ad3) had a low level of BMP signalling activity which

was caused by low expression of receptors and effectors, which might have reduced its potential in corneal epithelial differentiation (Shalom- Feuerstein et al. 2012). Our findings on gene expression and signalling differences between the two hiPSCs lines used might have influenced the cells' differentiation potential and caused the different responses towards the hESCs derived protocol (Ortmann and Vallier 2017). To improve the corneal differentiation potential of the less responsive hiPSCs line (SB-Ad3), we tried to optimise the differentiation method by altering the co-SMAD/r-SMAD interaction in the cytoplasm. Since co-SMAD (SMAD4) is shared between the TGFβ and BMP pathways (Wrana & Attisano 2000, Wu & Hill 2009), we focused on the inhibition of the TGFβ pathway which should lead to an increase in the availability of SMAD4 for the BMP pathway (Figure 6.1). To achieve this, a selective TGFβ inhibitor, SB431542 which has been reported to drive differentiation away from neuro-ectoderm (Li et al. 2015) and to activate the BMP pathway (Zhu et al. 2016) was used.

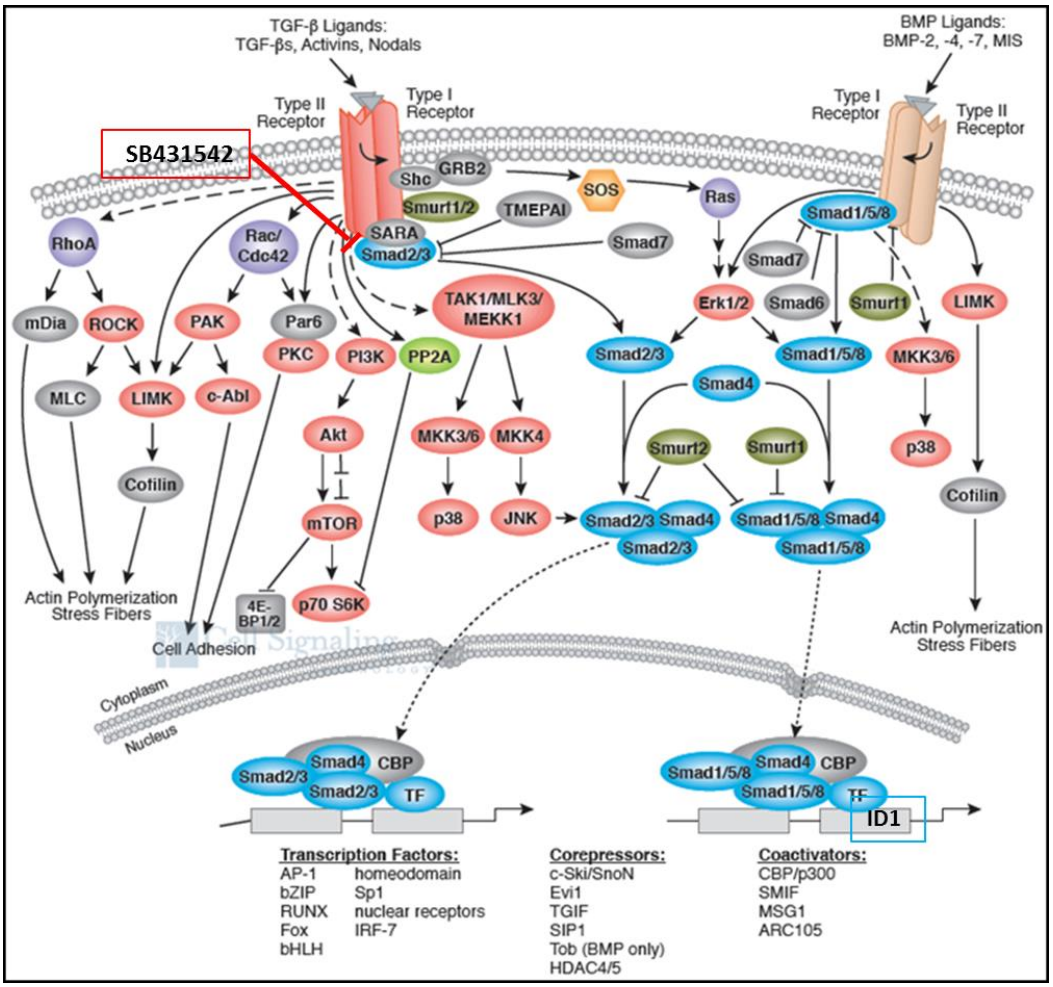


**Figure 6.1 : Schematic of TGFβ and BMP pathways interrelation (blue), showing the *ID1* gene used as a BMP pathway reporter and the action point for SB431542 inhibiting the TGFβ pathway. Adapted from www.cellsignal.com.**

The TGFβ pathway inhibition by SB431542 in our optimised protocol has increased the BMP pathway activity in the SB-Ad3 hiPSCs line and improved the corneal epithelial lineages differentiation as evident in the related genes and proteins expression analyses as early as the first differentiation window at day 9 (Figure 6.2). The optimised protocols also led to the generation of hiPSCs derived epithelial progenitor cells with higher colony forming efficiency, which was comparable to limbal epithelial progenitor cells obtained from adult human cornea (Figure 6.3).

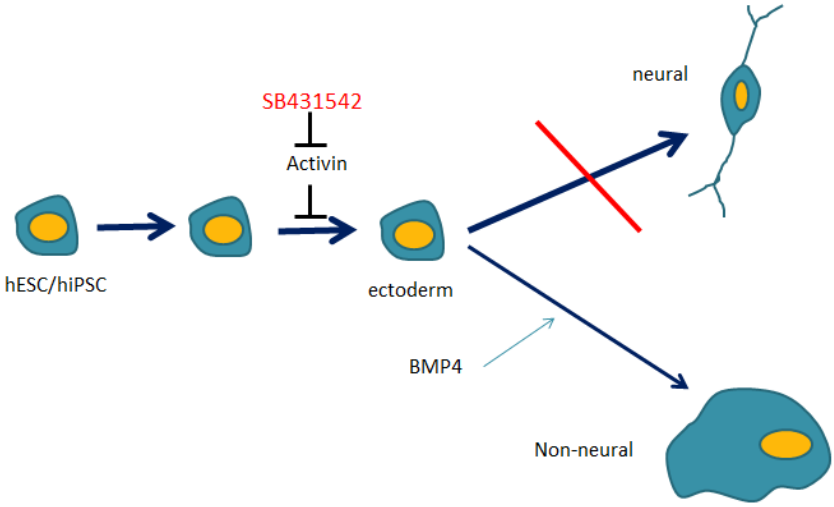


**Figure 6.2 : The effects of BMP4 and SB431542 in stem cell differentiation pathways toward neural and non-neural lineages.**

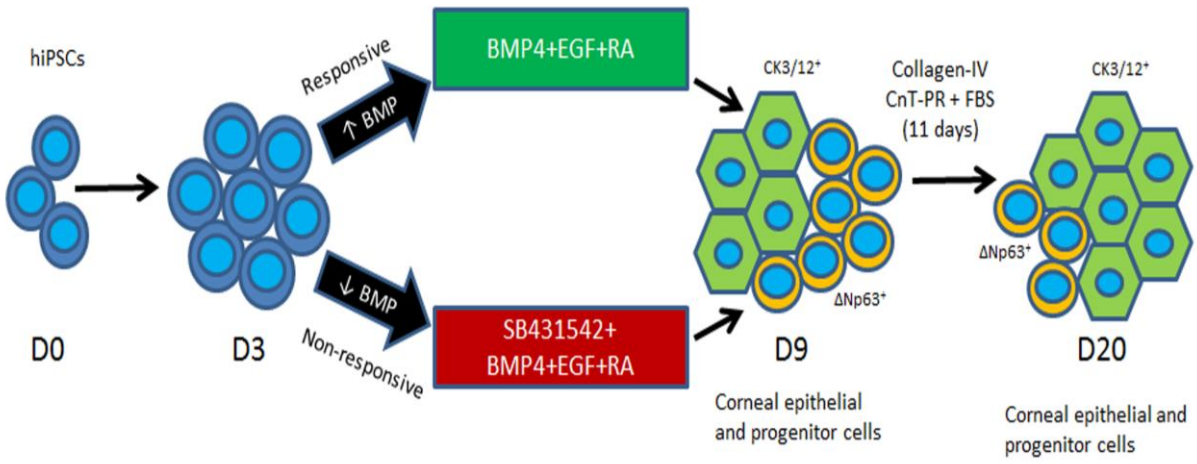


**Figure 6.3 : Graphical summary of the optimised differentiation protocol.**

We then used GFP expressing cells generated from both hESCs (H9) and hiPSCs (SB-Ad3) lines to test the engraftment of hiPSC derived corneal epithelial cells into a model of total LSCD. Our three transplant attempts using LSCD mice model indicated that SB-Ad3 hiPSCs at later

and H9 cells at earlier than day 20 of differentiation survived longer on the cornea. This suggests that shorter or longer differentiation period might result in a better cell engraftment as reported by most previous studies (Zhang et al. 2017, Brzeszczynska et al. 2014, Cieslar-Pobuda et al. 2016, Hayashi et al. 2016). This improvement might also be due to the different functional characteristic of the cells at the time of transplantation and the use of ROCKi in the cell preparation for transplants that survived the longest.

At the earlier time point which corresponds to our early differentiation stage of day 9, the percentage of cells expressing putative limbal stem cells marker, ΔNp63 was higher compared to day 20. This might indicate that at this early stage the differentiating cells were still having high proliferative potential, thus could survive longer on the cornea and limbus. In contrast, the cells transplanted at a later stage (day 27) might be more stable and have differentiated into CK3 or CK12 expressing cells that could also survive better on the corneal surface. Application of ROCKi (Y27632) to incubate the cells both before being harvested and before being transplanted have also improved the cells survival post-transplant as it was reported to be used in the maintenance of limbal epithelial progenitors (Miyashita et al. 2013). A recent report also found that the use of ROCKi with keratinocyte growth factor (KGF) could improve the gene expression in limbal epithelial cells (LECs) to be more similar to corneal epithelial cells (CECs) *in vivo* (Yoshihara et al. 2017). It would also be useful to try using ROCKi as an eye-drop for the mice after the transplant to improve the engraftment of the transplanted cells (Okumura et al. 2013).

Transplanting cells as a sheet instead of cells suspension onto the mice cornea also resulted in an improved cells' survival in our experiment, where the transplanted cells from the sheet were detected for 3 to 14 days longer after transplant. A few earlier studies also reported the advantages of the cell-sheet transplantation in human (Umemoto et al. 2013, Burillon et al. 2012) and rabbit LSCD model (Burillon et al. 2012, Gomes et al. 2010, Nishida et al. 2004) but this has not been done using mice. Despite less favourable transplantation outcomes obtained, our translational experiments suggest that transplantation of sorted cells sheet and cells from earlier or later differentiation time points might be able to improve the outcome.

Together our data suggest that establishment of a simple monolayer differentiation protocol for generation of corneal epithelial lineages that could be applied to both hESCs and hiPSCs. Despite the presence of corneal epithelial progenitor and cell markers and a comparable CFE

to human limbal epithelial cells, we were unable to maintain engraftment of these cells into the corneal of mice with total LSCD for longer than 14 days, which can be due to immaturity of corneal epithelial cells derived from hESC and hiPSC, the suitability of animal model or damage that may be caused to the cells during cell harvesting from tissue culture plates and transplantation into an inflamed cornea.

### 6.2 Implications of the Project and Recommendations for Future Work

Our project established a two-step protocol for corneal epithelial lineage differentiation in hESCs that could be applied to any responsive hiPSCs line. The differentiation protocol includes the supplementation of well-known ectodermal morphogens namely, RA, BMP4 and RA during differentiation induction period and adaptation towards corneal and limbal epithelial with collagen-IV coated surface with corneal epithelial specific medium, CnT-PR 2D. A non-responsive hiPSCs line with low BMP pathway activity could still make use of the protocol with an additional exposure of SB431542 in the first differentiation stage. Therefore, endogenous BMP pathway activity assessment of any candidate hiPSCs is important to help in the selection of appropriate differentiation protocol to be used.

Looking back at our transplant outcomes, there are many aspects that could be improved. The corneal inflammation that resulted following LSCD induction could be improved by the application of a steroid (e.g. prednisolone) or a special anti-inflammatory protein such as TNF-α–stimulated protein 6 (TSG-6) (Oh et al. 2010). This is particularly important as any on-going inflammatory reactions on the mice cornea might affect the engraftment efficiency (Polack 1965, Elliot 1971). Since we were lacking of positive control cells that should have been used for the transplant as the differentiated cells, fluorescence-labelled or magnetic nanoparticles loaded human LSCs could be used in future transplant. This will allow better assessment (via fluorescence miscoscopy and magneto-motive Optical Coherence Tomography (OCT) respectively) of the *in vivo* engraftment of LSCs and suitability of the animal model (Boadi et al. 2015). Differentiated cells at different stages of differentiation, for example cells at day 9, 14, 20, 27 and 40 could be used for the transplant in future. This will allow the assessment of the best differentiation stage at which the cells' have the characteristics that help their engraftment on the cornea. Another aspect is the cells' harvesting step, which could be optimised so that cell sheet could be made available for transplant rather than cells in suspension.

Another way of getting cell as a sheet is by modifying the cell culture method, where air-lifting techniques might be beneficial (Shimazaki et al. 2007) to promote stratification and produce more functional cells for transplant. Application of supplements that could improve cell survival such as ROCKi (Watanabe et al. 2007) could also be continued both during cell preparation prior to transplant, and as a post-transplant treatment. The post-transplanted LSCD mice eyeballs could also be collected and assessed by immunohistochemistry for any attached human cells on the cornea.

Although our protocol involves a short differentiation duration using monolayer culture method, it could only produce a mixture of differentiated cells. Therefore, the differentiated cells needed to be sorted prior to transplant to ensure better transplantation outcome in the future. Although markers that are specific for LSCs have yet to be defined (Chee et al 2006, Budak et al 2005), some markers (ABCG2 and ABCB5) that were reported to be useful in selecting stem cells from human limbal epithelial cells (Shaharuddin et al. 2017) could be used in the cell sorting. Those LCSs markers could be used together with a negative cell surface marker for corneal epithelial stem cells, connexin 43 (Cx43) (Chen et al. 2006) so that only the cells of interest are selected. In addition to the use of cell surface markers for sorting, generation of ΔNp63-GFP labelled hESCs and hiPSCs (Collin et al. 2016) prior the differentiation process could also be useful to help in the selection of ΔNp63 expressing differentiated cells. The cell sorting could be done at an earlier (day 9) or a later time point than day 20 to capture most of the differentiated cells for transplant. Additionally, the sorted cells could also be expanded either on collagen-IV coated plates or on a compatible biological scaffold. This step could improve cell transfer and transplant outcome.

As GFP expressing hESCs and hiPSCs were used in out translational study, verification on those GFP expressing cells' genomic stability would be a way to assess their safety for future clinical applications. In term of the hESCs and hiPSCs derived corneal epithelial-like cells, there are further studies that needed to be carried out to lay out their similarities and differences compared to the adult human corneal epithelial or limbal stem cells (eg: RNA-seq studies). This would enable both typing (in terms of understanding cell composition within each differentiation culture or in adult cornea) as well as gene expression for each progenitor subpopulation derived from the differentiation protocol.

# REFERENCES


Aberdam D, Gambaro K, Rostagno P, Aberdam E, De La Forest SD, Rouleau M. Key Role of p63 in BMP-4-Induced Epidermal Commitment of Embryonic Stem Cells. Cell Cycle. 2007; 6(3), pp : 291-294.

Aberdam E, Barak E, Rouleau M, de LaForest S, Berrih-Aknin S, Suter DM, Krause KH, Amit M, Itskovitz-Eldor J, Aberdam D. A Pure Population of Ectodermal Cells Derived from Human Embryonic Stem Cells. Stem Cells. 2008; 26 : 440–444. doi:10.1634/stemcells.2007-0588

Abeyta MJ, Clark AT, Rodriguez RT, Bodnar M., Pera RA, and Firpo MT. Unique gene expression signatures of independently-derived human embryonic stem cell lines. Hum. Mol. Genet. 2004; 13: 601–608.

Abudayyeh OO, Gootenberg JS, Essletzbichler P, Han S, Joung J, Belanto JJ, Verdine V, Cox DBT, Kellner MJ, Regev A, Lander ES, Voytas DF, Ting AY & Zhang F. RNA targeting with CRISPR–Cas13. Nature. 2017; 550 : 280 – 284. doi:10.1038/nature24049

Abujarour R and Ding S. Induced pluripotent stem cells free of exogenous reprogramming factors. Genome Biology. 2009; 10:220. https://doi.org/10.1186/gb-2009-10-5-220

Ahmad S, Kolli S, Lako M, FigueiredoF, Daniels JT. Stem cell therapies for ocular surface disease. Drug Discovery Today. 2010; 15(7-8), pp : 306-313. https://doi.org/10.1016/j.drudis.2010.02.001

Ahmad S, Osei-Bempong C, Dana R, Jurkunas U. The culture and transplantation of human limbal stem cells. Cell. Physiol. 2010a; 225: 15–19. doi:10.1002/jcp.22251

Ahmad S, Stewart R, Yung S, Kolli S, Armstrong L, Stojkovic M, Figueiredo F, Lako M. Differentiation of Human Embryonic Stem Cells into Corneal Epithelial-Like Cells by In Vitro Replication of the Corneal Epithelial Stem Cell Niche. Stem Cells. 2007; 25, pp : 1145–1155.

Ahmad S. Concise Review: Limbal Stem Cell Deficiency, Dysfunction, and Distress. Stem Cells Translational Medicine. 2012; 1 : 110–115. doi:10.5966/sctm.2011-0037

Amano S, Satoru Y, Tatsuya M, Saiko U, Seiichi Y. Corneal Stromal and Endothelial Cell Precursors. Cornea. 2006; 25: p. S73 – S77. doi:10.1097/01.ico.0000247218.10672.7e.

Amita M, Carpenter MK, Inokuma MS, Chiu CP, Harris CP, Waknitz MA, Itskovitz-Eldora J, Thomson JA. Clonally Derived Human Embryonic Stem Cell Lines Maintain Pluripotency and Proliferative Potential for Prolonged Periods of Culture.

Developmental Biology. 2000; 227(2), pp: 271-278. https://doi.org/10.1006/dbio.2000.9912

Anokye-Danso F, Trivedi CM, Juhr D, Gupta M, Cui Z, Tian Y, Zhang Y, Yang W, Gruber PJ, Epstein JA, Morrisey EE. Highly Efficient miRNA-Mediated Reprogramming of Mouse and Human Somatic Cells to Pluripotency. Cell Stem Cell. 2011; 8(4), pp : 376-388. https://doi.org/10.1016/j.stem.2011.03.001

Araújo AL, Ricardo JRS, Sakai VN, Barros JN & Gomes JÁP. Impression cytology and in vivo confocal microscopy in corneas with total limbal stem cell deficiency. Arquivos Brasileiros de Oftalmologia. 2013; 76(5), 305-308. https://dx.doi.org/10.1590/S0004-27492013000500011

Arber C, Precious SV, Cambray S, Risner-Janiczek JR, Kelly C, Noakes Z, Fjodorova M, Heuer A, Ungless MA, Rodríguez TA, Rosser AE, Dunnett SB, Li M. Activin A directs striatal projection neuron differentiation of human pluripotent stem cells. Development. 2015; 142: 1375-1386; doi: 10.1242/dev.117093

Auw-Haedrich C, Agrawal M, Gabbert HE, Meyer P, Arnold N, Reinhard T. Immunohistochemical expression of epithelial cell markers in corneas with congenital aniridia and ocular cicatrizing pemphigoid. Acta Ophthalmologica. 2011; 89 : 47–53. doi:10.1111/j.1755-3768.2009.01603.x

Avior Y, Sagi I and Benvenisty N. Pluripotent stem cells in disease modelling and drug discovery. NATURE REVIEWS. 2016; 17 : 170 – 182. doi:10.1038/nrm.2015.27

Baker CL and Pera MF. Capturing Totipotent Stem Cells. Cell Stem Cell. 2018; 22(1), pp : 25-34. https://doi.org/10.1016/j.stem.2017.12.011

Bao X, Zhu X, Liao B, Benda C, Zhuang Q, Pei D, Qin B, Esteban MA. MicroRNAs in somatic cell reprogramming. Current Opinion in Cell Biology. 2013; 25(2), pp : 208-214. https://doi.org/10.1016/j.ceb.2012.12.004

Baradaran-Rafii A, Delfazayebaher S, Aghdami N, Taghiabadi E, Bamdad S, Roshandel D. Midterm outcomes of penetrating keratoplasty after cultivated oral mucosal epithelial transplantation in chemical burn.. The Ocular Surface. 2017; Vol. 15: p 789 – 794.

Barrow KM, Perez-Campo FM, Ward CM. Use of the Cytomegalovirus Promoter for Transient and Stable Transgene Expression in Mouse Embryonic Stem Cells. In: Turksen K. (eds) Embryonic Stem Cell Protocols. Methods in Molecular Biology. 2006; vol 329. Humana Press.

Baud A, Wessely F, Mazzacuva F, McCormick J, Camuzeaux S, Heywood W, Little D, Vowles J, Tuefferd M, Mosaku O, Lako M, Armstrong L, Webber C, Cader M, Peeters

P, Gissen P, Cowley S, Mills K. Multiplex High-Throughput Targeted Proteomic Assay To Identify Induced Pluripotent Stem Cells. Anal. Chem. 2017; 89 : 2440−2448. DOI: 10.1021/acs.analchem.6b04368.

Bauwens CL, Peerani R, Niebruegge S, Woodhouse KA, Kumacheva E, Husain M, Zandstra PW. Control of Human Embryonic Stem Cell Colony and Aggregate Size Heterogeneity Influences Differentiation Trajectories. Stem Cells. 2008; 26: 2300–2310. doi:10.1634/stemcells.2008-0183

Behaegel J, Ní Dhubhghaill S, Koppen C, and Zakaria N. Safety of Cultivated Limbal Epithelial Stem Cell Transplantation for Human Corneal Regeneration. Stem Cells International. 2017; Volume 2017 (2017), Article ID 6978253, 11 pages. https://doi.org/10.1155/2017/6978253

Bershteyn M, Nowakowski TJ, Pollen AA, Lullo ED, Nene A, Wynshaw-Boris A, Kriegstein AR. Human iPSC-Derived Cerebral Organoids Model Cellular Features of Lissencephaly and Reveal Prolonged Mitosis of Outer Radial Glia. Cell Stem Cell. 2017; 20(4), pp : 435-449.e4. https://doi.org/10.1016/j.stem.2016.12.007

Bhalekar S, Basu S, Lal I, Sangwan VS. Successful autologous simple limbal epithelial transplantation (SLET) in previously failed paediatric limbal transplantation for ocular surface burns. BMJ Case Rep. 2013;2013.

Bhattacharya B, Miura T, Brandenberger R, Mejido J, Luo Y, Yang AX, Joshi BH, Ginis I, Thies RS, Amit M, Lyons I, Condie BG, Itskovitz-Eldor J, Rao MS, and Puri RK.. Gene expression in human embryonic stem cell lines: unique molecular signature. Blood . 2004; 103: 2956–2964.

Blazejewska E, Schlotzer-Schrehardt U, Zenkel M, Bachmann B, Chankiewitz E, Jacobi C, Kruse F. Corneal Limbal Microenvironment Can Induce Transdifferentiation of Hair Follicle Stem Cells into Corneal Epithelial-like Cells. Stem Cells. 2009; 27 : 642– 652.

Boadi J, Sangwal V, MacNeil S, Matcher SJ. System for tracking transplanted limbal epithelial stem cells in the treatment of corneal stem cell deficiency. Proceedings Volume 9328, Imaging, Manipulation, and Analysis of Biomolecules, Cells, and Tissues XIII; 93281D (2015); doi: 10.1117/12.2077921

Boergermann JH, Kopf J, Yu PB and Knaus P. Dorsomorphin and LDN-193189 inhibit BMP-mediated Smad, p38 and Akt signalling in C2C12 cells. The International Journal of Biochemistry & Cell Biology. 2010; 42, pp : 1802–1807.

Bothe I, Tenin G, Oseni A, Dietrich S. Dynamic control of head mesoderm patterning. Development. 2011; 138, pp : 2807 – 2821.

Bron AJ. The architecture of the corneal stroma. British Journal of Ophthalmology. 2001; 85:379-381. http://dx.doi.org/10.1136/bjo.85.4.379

Brons IGM, Smithers LE, Trotter MWB, Rugg-Gunn P, Sun B, de Sousa Lopes SMC, Howlett SK, Clarkson A, Ahrlund-Richter L, Pedersen RA, Vallier L. Derivation of pluripotent epiblast stem cells from mammalian embryos. Nature. 2007; 448, 191–195. doi:10.1038/nature05950

Brzeszczynska J, Samuel K, Greenhough S, Ramaesh K, Dhillon B, Hay DC, Ross JA. Differentiation and molecular profiling of human embryonic stem cell-derived corneal epithelial cells. Int J Mol Med. 2014;33:1597–1606.

Budak MT, Alpdogan OS, Zhou M, Lavker RM, Akinci MA, Wolosin JM. Ocular surface epithelia contain ABCG2-dependent side population cells exhibiting features associated with stem cells. J Cell Sci. 2005; 118 :1715-1724.

Buganim Y, Faddah DA and Jaenisch R. Mechanisms and models of somatic cell reprogramming. Nat Rev Genet. 2013; 14(6): 427–439. doi:10.1038/nrg3473.

Burillon C, Huot L, Justin V, Nataf S, Chapuis F, Decullier E, Damour O. Cultured Autologous Oral Mucosal Epithelial Cell Sheet (CAOMECS) Transplantation for the Treatment of Corneal Limbal Epithelial Stem Cell Deficiency. Invest Ophthalmol Vis Sci. 2012; 53 : 1325–1331.

Caestecker M. The transforming growth factor-β superfamily of receptors. Cytokine & Growth Factor Reviews. 2004; 15(1) : 1-11. https://doi.org/10.1016/j.cytogfr.2003.10.004

Chan AA, Hertsenberg AJ, Funderburgh ML, Mann MM, Du Y, Davoli KA, Mich-Basso JD, Yang L, Funderburgh JL. Differentiation of human embryonic stem cells into cells with corneal keratocyte phenotype. PLoS One. 2013;8:e56831.

Chang B, Smith RS, Peters M, Savinova OV, Hawes NL, Zabaleta A, Nusinowitz S, Martin JE, Davisson ML, Cepko CL, Hogan BLM and John SWM. Haploinsufficient Bmp4 ocular phenotypes include anterior segment dysgenesis with elevated intraocular pressure. BMC Genetics. 2001; 2:18. https://doi.org/10.1186/1471-2156-2-18

Chang YC, Chang WC, Hung KH, Yang DM, Cheng YH, LiaoYW, Woung LC, Tsai CY, Hsu CC, Lin TC, Liu JH, Chiou SH, Peng CH and Chen SJ. The generation of induced pluripotent stem cells for macular degeneration as a drug screening platform: identification of curcumin as a protective agent for retinal pigment epithelial cells against oxidative stress. Front. Aging Neurosci. 2014; Volume 6,Article 19, pp : 1 - 12. https://doi.org/10.3389/fnagi.2014.00191

Chee KY, Kicic A and Wiffen SJ. Limbal stem cells: the search for a marker. Clinical & Experimental Ophthalmology. 2006; 34 : 64–73. doi:10.1111/j.1442-9071.2006.01147.x

Chen H, Chen H, Lai J, Chen C, Tsai Y, Kuo M, Chu P, Sun C, Chen J, Ma D. Persistence of Transplanted Oral Mucosal Epithelial Cells in Human Cornea. Invest Ophthalmol Vis Sci. 2009; 50 : 4660–4668.

Chen IP, Fukuda K, Fusaki N, et al. Induced Pluripotent Stem Cell Reprogramming by Integration-Free Sendai Virus Vectors from Peripheral Blood of Patients with Craniometaphyseal Dysplasia. Cellular Reprogramming. 2013; 15(6) : 503-513. doi:10.1089/cell.2013.0037.

Chen JJY and Tseng SCG. Abnormal corneal epithelial wound healing in partial thickness removal of limbal epithelium. Invest Ophthalmol Vis Sci. 1991; 32 :2219-33.

Chen S, Borowiak M, Fox JL, Maehr R, Osafune K, Davidow L, Lam K, Peng LF, Schreiber SL, Lee L Rubin LL, Melton D. A small molecule that directs differentiation of human ESCs into the pancreatic lineage. Nature Chemical Biology. 2009; 5, 258–265. doi:10.1038/nchembio.154

Chen Z, Evans WH, Pflugfelder SC. and Li D.-Q. Gap Junction Protein Connexin 43 Serves as a Negative Marker for a Stem Cell-Containing Population of Human Limbal Epithelial Cells. Stem Cells. 2006; 24 : 1265–1273. doi:10.1634/stemcells.2005-0363

Chin MH, Mason MJ, Xie W, Volinia S, Singer M, Peterson C, Ambartsumyan G, Aimiuwu O, Richter L, Zhang J, Khvorostov I, Ott V, Grunstein M, Lavon N, Benvenisty N, Croce CM, Clark AT, Baxter T, Lowry WE. Induced Pluripotent Stem Cells and Embryonic Stem Cells Are Distinguished by Gene Expression Signatures. Cell Stem Cell. 2009; 5(1), pp : 111-123. https://doi.org/10.1016/j.stem.2009.06.008

Chow RL and Lang RA. Early Eye Development in Vertebrates. Annual Review of Cell and Developmental Biology. 2001; 17(1) : 255-296.

Chow RL, Altmann CR, Lang RA, Hemmati-Brivanlou A. Pax6 induces ectopic eyes in a vertebrate. Development. 1999; 126 : 4213-4222.

Cieślar-Pobuda A, Rafat M, Knoflach V, et al. Human induced pluripotent stem cell differentiation and direct transdifferentiation into corneal epithelial-like cells. Oncotarget. 2016;7(27) : 42314-42329. doi:10.18632/oncotarget.9791.

Cleutjens JPM, Havenith MG, Kasper M, Vallinga M, Bosman FT. Absence of type IV collagen in the centre of the corneal epithelial basement membrane. Histochem J. 1990; 22: 688. https://doi.org/10.1007/BF01047454

Collier AJ, Panula SP, Schell JP, Chovanec P, Reyes AP, Petropoulos S, Corcoran AE, Walker R, Douagi I, Lanner F, Rugg-Gunn PJ. Comprehensive Cell Surface Protein Profiling Identifies Specific Markers of Human Naive and Primed Pluripotent States. Cell Stem Cell. 2017; 20(6), pp : 874-890.e7. https://doi.org/10.1016/j.stem.2017.02.014

Collin J, Mellough CB, Dorgau B, Przyborski S, Moreno-Gimeno I, Lako M. Using Zinc Finger Nuclease Technology to Generate CRX-Reporter Human Embryonic Stem Cells as a Tool to Identify and Study the Emergence of Photoreceptors Precursors During Pluripotent Stem Cell Differentiation. Stem Cells. 2016; 34 :311–321.

Collinson JM, CQuinn JC, Hill RE, West JD. The roles of Pax6 in the cornea, retina, and olfactory epithelium of the developing mouse embryo. Developmental Biology. 2003; 255(2), pp : 303-312. https://doi.org/10.1016/S0012-1606(02)00095-7

Colman A and Dreesen O. Induced pluripotent stem cells and the stability of the differentiated state. EMBO reports. 2009; 10, pp: 714-721. DOI 10.1038/embor.2009.142

Colman A and Dreesen O. Pluripotent Stem Cells and Disease Modeling. Cell Stem Cell. 2009a; 5(3), pp: 244-247. https://doi.org/10.1016/j.stem.2009.08.010

Condic ML and Rao M. Regulatory Issues for Personalized Pluripotent Cells. Stem Cells. 2008; 26 : 2753–2758.

Cotsarelis G, Cheng SZ, Dong G, Sun TT, Lavker RM. Existence of slow-cycling limbal epithelial basal cells that can be preferentially stimulated to proliferate: Implications on epithelial stem cells. Cell. 1989; 57(2), pp: 201-209. https://doi.org/10.1016/0092-8674(89)90958-6

Cvekl, A. and Tamm, E. R. Anterior eye development and ocular mesenchyme: new insights from mouse models and human diseases. Bioessays. 2004; 26: 374–386. doi:10.1002/bies.20009

Cyranoski D. Japanese woman is first recipient of next-generation stem cells. Nature. 2014. doi:10.1038/nature.2014.15915

DaCosta Byfield S, Major C, Laping N, Roberts A. SB-505124 Is a Selective Inhibitor of Transforming Growth Factor-β Type I Receptors ALK4, ALK5, and ALK7. Mol Pharmacol. 2004; 65 : 744–752.

Davanger M dan Evensen A. Role of the Pericorneal Papillary Structure in Renewal of Corneal Epithelium. Nature. 1971; 229, pp: 560–561. doi:10.1038/229560a0

Davies SB, Chui J, Madigan MC, Provis JM, Wakefield D, Di Girolamo N. Stem cell activity in the developing human cornea. Stem Cells. 2009; 27(11), pp : 2781 – 2792.

De Paiva CS, Chen Z, Corrales RM, Pflugfelder S, Li DQ. ABCG2 transporter identifies a population of clonogenic human limbal epithelial cells. Stem Cells 2005; 23:63-73.

Di Iorio E., Barbaro V, Ruzza A, Ponzin D, Pellegrini G, De Luca M. Isoforms of DeltaNp63 and the migration of ocular limbal cells in human corneal regeneration. Proc Natl Acad Sci USA. 2005; 102 :9523-9528.

Dobrowolski D, Orzechowska-Wylegala B, Wowra B, Wroblewska-Czajka E, Grolik M, Szczubialka K, Nowakowska M, Puzzolo D, Wylegala EA, Micali A, Aragona P. Cultivated Oral Mucosa Epithelium in Ocular Surface Reconstruction in Aniridia Patients. BioMed Research International. 2015; Volume 2015, Article ID 281870, 7 pages. http://dx.doi.org/10.1155/2015/281870.

Dobrowolski D, Wylegala E, Wowra B And Orzechowska-Wylegala B. Cultivated oral mucosa epithelium transplantation (COMET) in bilateral limbal stem cell deficiency. Acta Ophthalmologica. 2011; 89: 0. doi:10.1111/j.1755-3768.2011.4374.x

Du J, Wu Y, Ai Z, Shi X, Chen L, Guo Z. Mechanism of SB431542 in inhibiting mouse embryonic stem cell differentiation. Cellular Signalling. 2014; 26(10), pp : 2107-2116.

Dua H and Azuara-Blanco A. Autologous limbal transplantation in patients with unilateral corneal stem cell deficiency. Br J Ophtalmol. 2000; 84 : 273 – 278.

Dua H, Saini J, Azuara-Blanco A, Gupta P. Limbal stem cell deficiency: concept, aetiology, clinical presentation, diagnosis and management. Indian Journal of Ophthalmology. 2000; 48(2), pp : 83-92.

Dua HS, Faraj LA, Said DG, Gray T, Lowe J. Human Corneal Anatomy Redefined: A Novel Pre-Descemet's Layer (Dua's Layer). Ophthalmology 2013;120:1778-1785.

Dua HS, Gomes JA, and Singh A. Corneal epithelial wound healing. Br J Ophthalmol. 1994; 78(5): 401–408.

Egbert PR, Lauber S, Maurice DM. A simple conjunctival biopsy. Am J Ophthalmol. 1977; 84 :798-801.

Elliott JH. Immune Factors in Corneal Graft Rejection. Invest. Ophthalmol. Vis. Sci. 1971; 10(3) :216-234.

Eslani M, Baradaran-Rafii A & Ahmad S. Cultivated Limbal and Oral Mucosal Epithelial Transplantation. Seminars in Ophthalmology. 2012; 27(3-4), pp : 80-93. https://doi.org/10.3109/08820538.2012.680641

Espana EM, Kawakita T, Romano A, Di Pascuale M, Smiddy R, Liu C, Scheffer C. G. Tseng SCG. Stromal Niche Controls the Plasticity of Limbal and Corneal Epithelial Differentiation in a Rabbit Model of Recombined Tissue. Invest. Ophthalmol. Vis. Sci. 2003; 44(12) : 5130-5135. doi: 10.1167/iovs.03-0584.

Figueira EC, Di Girolamo N, Coroneo MT, Wakefield D. The phenotype of limbal epithelial stem cells. Invest. Ophthalmol. Vis. Sci. 2007; 48(1), pp : 144-156. DOI: 10.1167/iovs.06-0346

Foster JW, Wahlin K, Adams SM, Birk DE, Zack DJ & Chakravarti S. Cornea organoids from human induced pluripotent stem cells. Scientific Reports. 2017; volume 7, Article number: 41286. doi:10.1038/srep41286

Fujiwara M, Yan P, Otsuji T, Narazaki G, Uosaki H, Fukushima H, Kuwahara K, Harada M, Matsuda H, Matsuoka S, Okita K, Takahashi K, Nakagawa M, Ikeda T, Sakata R, Mummery C, Nakatsuji N, Yamanaka S, Nakao K, Yamashita J. Induction and Enhancement of Cardiac Cell Differentiation from Mouse and Human Induced Pluripotent Stem Cells with Cyclosporin-A. PLoS ONE. 2011; 6(2): e16734. doi:10.1371/journal.pone.0016734

Funderburgh ML et al. PAX6 expression identifies progenitor cells for corneal keratocytes. The FASEB Journal express article 10.1096/fj.04-2770fje. Published online May 18, 2005.

Furukawa T, Kozak CA and Cepko CL. RAX, a novel paired-type homeobox gene, shows expression in the anterior neural fold and developing retina. Proc. Natl Acad. Sci. USA. 1997; 94 : 3088–3093.

Furuta Y and Hogan BLM. BMP4 is essential for lens induction in the mouse embryo. Genes Dev. 1998;12, 3764-3775. doi:10.1101/gad.12.23.3764

Fusaki N, Ban H, Nishiyama A, Saeki K, Hasegawa M. Efcient induction of transgene-free human pluripotent stem cells using a vector based on Sendai virus, an RNA virus that does not integrate into the host genome. Proc. Jpn. Acad., Ser. B. 2009; 85(8), pp: 348-362. https://doi.org/10.2183/pjab.85.348

Fussner E, et al. Constitutive heterochromatin reorganization during somatic cell reprogramming. EMBO J. 2011; 30:1778–89. [PubMed: 21468033]

Gaddipati S, Muralidhar R, Sangwan VS, Mariappan I, Vemuganti GK, Balasubramanian D. Oral epithelial cells transplanted on to corneal surface tend to adapt to the ocular phenotype. Indian J Ophthalmol. 2014; 62(5): 644–648. doi: 10.4103/0301-4738.109517

Gain P, Jullienne R, He Z, Aldossary M, Acquart S, Cognasse F, Thuret G. Global Survey of Corneal Transplantation and Eye Banking. JAMA Ophthalmol. 2016; 134(2) : 167-173. doi:10.1001/jamaophthalmol.2015.4776

Gambaro K, Aberdam E, Virolle T, Aberdam D, Rouleau M. BMP-4 induces a Smad-dependent apoptotic cell death of mouse embryonic stem cell-derived neural precursors. Cell Death and Differentiation. 2006; 13, pp: 1075-1087.

Garber K. RIKEN suspends first clinical trial involving induced pluripotent stem cells. Nature Biotechnology. 2015; 33(9) : 890 - 891. doi:10.1038/nbt0915-890

Golipour A, et al. A late transition in somatic cell reprogramming requires regulators distinct from the pluripotency network. Cell Stem Cell. 2012; 11:769–82. [PubMed: 23217423]

Gomes JA, Monteiro BG, Melo GB, et al. Corneal reconstruction with tissue-engineered cell sheets composed of human immature dental pulp stem cells. Invest Ophthalmol Vis Sci. 2010; 51, pp : 1408-1414.

Gomes JAP, Santos MS, Ventura AS. Amniotic Membrane With Living Related Corneal Limbal/Conjunctival Allograft for Ocular Surface Reconstruction in Stevens-Johnson Syndrome. Arch Ophthalmol. 2003; 121(10) :1369-1374. doi:10.1001/archopht.121.10.1369

González F, Boué S & Belmonte JCI. Methods for making induced pluripotent stem cells: reprogramming à la carte. Nature Reviews Genetics. 2011; 12 : 231–242.

González S, Chen L, Deng S. Comparative Study of Xenobiotic-Free Media for the Cultivation of Human Limbal Epithelial Stem/Progenitor Cells. Tissue Engineering Part C: Methods. 2017; 23(4), pp : 219-227.

Gordon KJ and Blobe GC. Role of transforming growth factor-β superfamily signalling pathways in human disease. Biochimica et Biophysica Acta. 2008; 1782 : 197–228. doi:10.1016/j.bbadis.2008.01.006

Gore A, Li Z, Fung HL, Young JE, Agarwal S, Antosiewicz-Bourget J, et al. Somatic coding mutations in human induced pluripotent stem cells. Nature. 2011; 471:63–7. doi:10.1038/nature09805

Goudreau G, Petrou P, Reneker LW, Graw J, Loster J, and Gruss P. Mutually regulated expression of Pax6 and Six3 and its implications for the Pax6 haploinsufficient lens phenotype. PNAS. 2002; 99 (13) : 8719–8724. www.pnas.orgcgidoi10.1073pnas.132195699

Graw J. Current topics in developmental biology, ISSN: 1557-8933, Vol: 90, Issue: C, Page: 343-86. Publisher(s): Elsevier BV. Publication Year: 2010. DOI:10.1016/s0070-2153(10)90010-0. PMID:20691855

Gu S, Xing C, Han J, Tso MOM, Hong J. Differentiation of rabbit bone marrow mesenchymal stem cells into corneal epithelial cells in vivo and ex vivo. Molecular Vision. 2009; 15 : 99-107.

Guenou H, Nissan X, Larcher F, Feteira J, Lemaitre G, Saidani M, Del Rio M, Barrault C, Bernard F, Peschanski M, Baldeschi C, Waksman G. Human embryonic stem-cell derivatives for full reconstruction of the pluristratified epidermis: a preclinical study. The Lancet. 2009; 374(9703), pp : 1745-1753.

Guha P, Morgan JW, Mostoslavsky G, Rodrigues NP, Boyd AS. Lack of immune response to differentiated cells derived from syngeneic induced pluripotent stem cells. Cell Stem Cell. 2013; 12:407–12. doi:10.1016/j.stem.2013.01.006

Guo X and Wang XF. Signaling cross-talk between TGF-β/BMP and other pathways. Cell Res. 2009; 19(1): 71–88. doi:10.1038/cr.2008.302.

Haagdorens M, Van Acker SI, Van Gerwen V, Dhubhghaill SN, Koppen C, Tassignon MJ, and Zakaria N. Limbal Stem Cell Deficiency: Current Treatment Options and Emerging Therapies. Stem Cells International. 2016; Volume 2016 , Article ID 9798374, 22 pages. http://dx.doi.org/10.1155/2016/9798374

Hamrah P, Liu Y, Zhang Q, Dana MR. The Corneal Stroma Is Endowed with a Significant Number of Resident Dendritic Cells. Invest. Ophthalmol. Vis. Sci. 2003; 44(2) :581-589. doi: 10.1167/iovs.02-0838.

Hanna JH, Saha K, and Jaenisch R. Pluripotency and Cellular Reprogramming: Facts, Hypotheses, Unresolved Issues. Cell. 2010; 143: pp: 508 – 525. DOI 10.1016/j.cell.2010.10.008

Hanson C, Hardarson T, Ellerström C, Nordberg M, Caisander G, Rao M, Hyllner J, Stenevi U. Transplantation of human embryonic stem cells onto a partially wounded human cornea in vitro. Acta Ophthalmologica. 2013; 91(2), pp: 127-130.

Hay ED. Development of the Vertebrate Cornea. Int. Rev. Cytol. 1980. 63: pp: 263-322. https://doi.org/10.1016/S0074-7696(08)61760-X

Hayashi R, Ishikawa Y, Ito M, Kageyama T, Takashiba K, Fujioka T, Tsujikawa M, Miyoshi H, Yamato M, Nakamura Y, Nishida K. Generation of Corneal Epithelial Cells from Induced Pluripotent Stem Cells Derived from Human Dermal Fibroblast and Corneal

Limbal Epithelium. PLoS ONE. 2012; 7(9): e45435. doi:10.1371/journal.pone.0045435.

Hayashi R, Ishikawa Y, Sasamoto Y, Katori R, Nomura N, Ichikawa T, Araki S, Soma T, Kawasaki S, Sekiguchi K, Quantock AJ, Tsujikawa M, Nishida K. Co-ordinated ocular development from human iPS cells and recovery of corneal function. Nature. 2016;Vol. 531: p 376 – 380.

Heldin CH, Miyazono K & ten Dijke P. TGF-β signalling from cell membrane to nucleus through SMAD proteins. Nature. 1997; 390: p 465–471. doi:10.1038/37284

Herbst RS. Review of epidermal growth factor receptor biology. Int. J. Radiation Oncology Biol. Phys. 2004; 59(2): Supplement, p. 21–26.

Hewitt K, Shamis Y, Carlson M, Aberdam E, Aberdam D, Garlick J. Three-Dimensional Epithelial Tissues Generated from Human Embryonic Stem Cells. Tissue Engineering Part A. 2009; 15(11), pp : 3417-3426.

Higa K, Shimmura S, Miyashida H, Shimazaki J, Tsubota K. Melanocytes in the corneal limbus interact with K19-positive basal epithelial cells. Exp Eye Res. 2005; 81:218-223.

Hildreth C. 2016. RIKEN Resuming World's First Ever Clinical Study of iPSC-Derived Cells in Humans. https://www.bioinformant.com/riken-resuming-first-ever-clinical-study-of-ipsc-derived-cells-in-humans/

Hinson JT, Chopra A, Nafissi N, Polacheck WJ, Benson CC, Swist S, Gorham J, Yang L, Schafer S, Sheng CC, Haghighi A, Homsy J, Hubner N, Church G, Cook SA, Linke WA, Chen CS, Seidman JG, Seidman CE. Titin mutations in iPS cells define sarcomere insufficiency as a cause of dilated cardiomyopathy. Science. 2015; 349(6251), pp : 982-986. DOI: 10.1126/science.aaa5458

Hirayama M, Satake Y, Higa K, Yamaguchi T, Shimazaki J. Transplantation of Cultivated Oral Mucosal Epithelium Prepared in Fibrin-Coated Culture Dishes. Invest Ophthalmol Vis Sci. 2012; 53 :1602–1609.

Hoffman, L. M., Hall, L., Batten, J. L., Young, H., Pardasani, D., Baetge, E. E., Lawrence, J., and Carpenter, M. K. (2005) X-Inactivation status varies in human embryonic stem cell lines. Stem Cells 23, 1468–1478.

Holmes D. Corneal Repair: A Clear Vision. Nature. 2017; 544, S1.

Hongisto H, Ilmarinen T, Vattulainen M, Mikhailova A, Skottman H. Xeno- and feeder-free differentiation of human pluripotent stem cells to two distinct ocular epithelial cell

types using simple modifications of one method. Stem Cell Research & Therapy. 2017; 8 :291. https://doi.org/10.1186/s13287-017-0738-4

http://cellntec.com/products/cnt-pr/#datasheet

http://www.rnib.org.uk/nb-online/eye-health-statistics

https://www.seeintl.org/corneal-blindness/

Hu S, Wilson KD, Ghosh Z, Han L, Wang Y, Lan F, Ransohoff,KJ, Burridge P, Wu JC. MicroRNA-302 Increases Reprogramming Efficiency via Repression of NR2F2. STEM CELLS. 2013;, 31: 259–268. doi:10.1002/stem.1278

Huang AJW and Tseng SCG. Corneal epithelial wound healing in the absence of limbal epithelium. Invest Ophthalmol Vis Sci. 1991; 32: 96-105.

Hunihan L, Brown J, Cacace A, Fernandes A, Weston A. Generation of a clonal induced pluripotent stem cell (iPSC) line expressing the mutant MECP2 allele from a Rett Syndrome patient fibroblast line. Stem Cell Research. 2017; 20, pp : 67-69. https://doi.org/10.1016/j.scr.2017.02.017

Ilic D, Devito L, Miere C, Codognotto S. Human embryonic and induced pluripotent stem cells in clinical trials. British Medical Bulletin. 2015; 116(1), pp : 19–27. https://doi.org/10.1093/bmb/ldv045

Imanishi J, Kamiyama K, Iguchi I, Kita M, Sotozono C, Kinoshita S. Growth Factors: Importance in Wound Healing and Maintenance of Transparency of the Cornea. Progress in Retinal and Eye Research. 2000; 19(1), pp : 113-129.

Inatomi T, Nakamura T, Koizumi N, Sotozono C, Yokoi N, Kinoshita S. Midterm Results on Ocular Surface Reconstruction Using Cultivated Autologous Oral Mucosal Epithelial Transplantation. Am J Ophthalmol. 2006; 141, pp : 267–275.

Inatomi T, Nakamura T, Kojyo M, Koizumi N, Sotozono C, Kinoshita S. Ocular surface reconstruction with combination of cultivated autologous oral mucosal epithelial transplantation and penetrating keratoplasty. Am J Ophthalmol. 2006a; 142: 757–764.

ISSCR Guideline For Stem Cell Research And Clinical Translation 2016. www.ISSCR.ORG

Itoh M, Kiuru M, Cairo MS and Christiano AM. Generation of keratinocytes from normal and recessive dystrophic epidermolysis bullosa-induced pluripotent stem cells. PNAS. 2011; 108(21) : 8797-8802. https://doi.org/10.1073/pnas.1100332108

Jean D, Ewan K, Grus P. Molecular regulators involved in vertebrate eye development. Mechanisms of Development. 1998; 76(1–2), pp: 3-18.

Jin ZB, Okamoto S, Xiang P and Takahashi M. Integration-Free Induced Pluripotent Stem Cells Derived from Retinitis Pigmentosa Patient for Disease Modeling. Stem Cells Translational Medicine. 2012; 1: 503–509. doi:10.5966/sctm.2012-0005

Joyce NC. Proliferative capacity of the corneal endothelium. Progress in Retinal and Eye Research. 2003; 22(3), pp : 359-389. https://doi.org/10.1016/S1350-9462(02)00065-4

Katikireddy KR, Dana R, Jurkunas UV. Differentiation Potential of Limbal Fibroblasts and Bone Marrow Mesenchymal Stem Cells to Corneal Epithelial Cells. Stem Cells. 2014; 32, pp : 717–729.

Kawakita T, Espana EM, He H, Li W, Liu CY,Tseng SCG. Intrastromal Invasion by Limbal Epithelial Cells Is Mediated by Epithelial-Mesenchymal Transition Activated by Air Exposure. The American Journal of Pathology. 2005; 167(2), pp : 381-393. https://doi.org/10.1016/S0002-9440(10)62983-5

Kawasaki S, Tanioka H, Yamasaki K, Connon CJ, Kinoshita S. Expression and tissue distribution of p63 isoforms in human ocular surface epithelia. Exp Eye Res. 2005; 82 :293-299.

Kenyon KR, Bulusoglu G, Ziske JD. Clinical pathologic correlations of limbal autograft transplantation. Am J Ophthalmol. 1990; 31 :l-12.

Kheirkhah A, Raju VK, and Tseng SCG. Minimal Conjunctival Limbal Autograft for Total Limbal Stem Cell Deficiency. Cornea. 2008; 27(6) : 730–733. doi: 10.1097/QAI.0b013e31815cea8b

Kheirkhah A, Casas V, Raju VK, Tseng SCG. Sutureless Amniotic Membrane Transplantation for Partial Limbal Stem Cell Deficiency. American Journal of Ophthalmology. 2008; 145(5), pp : 787-794. https://doi.org/10.1016/j.ajo.2008.01.009

Kilens S, Meistermann D, Moreno D, Chariau C, Gaignerie A et al. Parallel derivation of isogenic human primed and naive induced pluripotent stem cells. Nature Communications. 2018; 9:360. DOI: 10.1038/s41467-017-02107-w

Kim D, Kim CH, Moon JI, et al. Generation of Human Induced Pluripotent Stem Cells by Direct Delivery of Reprogramming Proteins. Cell Stem Cell. 2009; 4(6) :472-476. doi:10.1016/j.stem.2009.05.005.

King NMP and Perrin J. Ethical issues in stem cell research and therapy. Stem Cell Research & Therapy. 2014; 5 : 85. https://doi.org/10.1186/scrt474

Kitsberg D. Human Embryonic Stem Cells for Tissue Engineering. In: Hauser H., Fussenegger M. (eds) Tissue Engineering. Methods in Molecular Medicine™. 2007; vol 140. Humana Press. https://doi.org/10.1007/978-1-59745-443-8_3

Ko HC and Gelb BD. Concise Review: Drug Discovery in the Age of the Induced Pluripotent Stem Cell. Stem Cells Translational Medicine. 2014; 3: 500–509. doi:10.5966/sctm.2013-0162

Kocaba V, Thépot A, Yamato M, Daisuke M, Kellal M, Mojallal A, Damour O, and Burillon C. Long-Term Results of Cultured Autologous Oral Mucosa Epithelial Cell Sheet (CAOMECS) Graft for the Treatment of Blindness Due to Bilateral Limbal Stem Cell Deficiency. J Stem Cell Res Ther. 2014; 4:181. doi:10.4172/2157-7633.1000181

Koizumi N, Inatomi T, Suzuki T, Sotozono C, Kinoshita S. Cultivated Corneal Epithelial Stem Cell Transplantation in Ocular Surface Disorders. Ophthalmology. 2001; 108 :1569–1574.

Koizumi N, Rigby H, Fullwood NJ, Kawasaki S, Tanioka H, Koizumi K, Kociok N, Joussen AM, Kinoshita S. Comparison of intact and denuded amniotic membrane as a substrate for cell-suspension culture of human limbal epithelial cells. Graefe's Arch Clin Exp Ophthalmol. 2007; 245 :123–134. DOI 10.1007/s00417-005-0095-3

Kolli S, Ahmad S, Lako M, Figueiredo F. Successful Clinical Implementation of Corneal Epithelial Stem Cell Therapy for Treatment of Unilateral Limbal Stem Cell Deficiency. Stem Cells. 2010; 28, pp : 597 – 610. DOI: 10.1002/stem.276.

Kolli S, Ahmad S, Mudhar H S, Meeny A, Lako M, Figueiredo F. Successful Application of Ex Vivo Expanded Human Autologous Oral Mucosal Epithelium for the Treatment of Total Bilateral Limbal Stem Cell Deficiency. Stem Cells. 2014; 32, pp : 2135–2146. DOI: 10.1002/stem.1694.

Korchynskyi O and Dijke P. Identification and Functional Characterization of Distinct Critically Important Bone Morphogenetic Protein-specific Response Elements in the Id1 Promoter. The Journal Of Biological Chemistry. 2002; 277(7), pp : 4883–4891.

Koster MI. p63 in skin development and ectodermal dysplasias. J Invest Dermatol. 2010; 130(10), pp : 2352 – 2358.

Krishnan R, Alexander M, Robles L, Foster 3rd CE, Lakey JRT. Islet and Stem Cell Encapsulation for Clinical Transplantation. The Review of Diabetic Studies : RDS. 2014;11(1):84-101. doi:10.1900/RDS.2014.11.84.

Kruse V, Hamann C, Monecke S, Cyganek L, Elsner L, Hübscher D, et al. Human induced pluripotent stem cells are targets for allogeneic and autologous natural killer (NK) cells and killing is partly mediated by the activating NK receptor DNAM-1. PLoS One (2015) 10:e0125544. doi:10.1371/journal.pone.0125544

Lagarkova MA, Volchkov PY, Philonenko ES, Kiselev SL. Efficient differentiation of hESCs into endothelial cells in vitro is secured by epigenetic changes. Cell Cycle. 2008; 7(18), pp: 2929-2935. https://doi.org/10.4161/cc.7.18.6700

Lal I, Gupta N, Purushotham J, Sangwan VS. Limbal stem cell deficiency: Current management. Journal of Clinical Ophthalmology and Research. 2016; 4 : 3 – 12. DOI: 10.4103/2320-3897.174344

Lavker RM and Sun TT. Epidermal stem cells: Properties, markers, and location. PNAS. 2000; 97 (25), pp: 13473-13475. published ahead of print November 21, 2000, doi:10.1073/pnas.250380097

Lee JH, Laronde S, Collins TJ, et al. Lineage-Specific Differentiation Is Influenced by State of Human Pluripotency. Cell Reports. 2017; 19 : 20–35. https://doi.org/10.1016/j.celrep.2017.03.036

Lee JH, Lee JB, Shapovalova Z, et al. Somatic transcriptome priming gates lineage-specific differentiation potential of human-induced pluripotent stem cell states. Nature Communications. 2014; volume 5, Article number: 5605. doi:10.1038/ncomms6605

Lee MR, Kwon KW, Jung H, Kim HN, Suh KY, Kim K, Kim KS. Direct differentiation of human embryonic stem cells into selective neurons on nanoscale ridge/groove pattern arrays. Biomaterials. 2010; 31(15), pp: 4360-4366. https://doi.org/10.1016/j.biomaterials.2010.02.012

Leung AW, Morest DK, Li JYH. Differential BMP signalling controls formation and differentiation of Multipotent preplacodal ectoderm progenitors from human embryonic stem cells. Developmental Biology. 2013; 379, pp : 208 – 220.

Lewitzky M and Yamanaka S. Reprogramming somatic cells towards pluripotency by defined factors. Current Opinion in Biotechnology. 2007; 18(5), pp: 467-473.

Li C and Xiao Z. Regulation of p63 protein stability via ubiquitin-proteasome pathway. BioMed Research International. 2014; vol. 2014, Article ID 175721, 8 pages. doi:10.1155/2014/175721.

Li L and Xie T. Stem cell niche:structure and function. Annu Rev Cell Dev Biol. 2005; 21:605-631.

Li L, Song L, Liu C, Chen J, Peng G, Wang R, Liu P, Tang K, Rossant J, Jing N. Ectodermal progenitors derived from epiblast stem cells by inhibition of Nodal signalling. Journal of Molecular Cell Biology. 2015; 0(0), p : 1 – 11.

Li R, et al. A mesenchymal-to-epithelial transition initiates and is required for the nuclear reprogramming of mouse fibroblasts. Cell Stem Cell. 2010; 7:51–63. [PubMed: 20621050]

Li T and Lu L. Epidermal Growth Factor-induced Proliferation Requires Down-regulation of Pax6 in Corneal Epithelial Cells. The Journal of biological chemistry. 2005; 280(13), pp : 12988-95.

Li W, Hayashida Y, Chen YT, Tseng SCG. Niche regulation of corneal epithelial stem cells at the limbus. Cell Research. 2007; 17 :26-36. doi:10.1038/sj.cr.7310137.

Liang P and Du J. Human induced pluripotent stem cell for modeling cardiovascular diseases. Regenerative Medicine Research. 2014; 2:4. https://doi.org/10.1186/2050-490X-2-4

Lister R, Pelizzola M, Kida YS, Hawkins RD, Nery JR, Hon G, et al. Hotspots of aberrant epigenomic reprogramming in human induced pluripotent stem cells. Nature. 2011; 471:68–73. doi:10.1038/nature09798

Litwack G. Hedgehog Signaling. Academic Press. 2012; Volume 88 of Vitamins and hormones, ISSN 0083-6729.

Liu X, Li W, Fu X and Xu Y. The Immunogenicity and Immune Tolerance of Pluripotent Stem Cell Derivatives. Front. Immunol. 2017; 8:645. doi: 10.3389/fimmu.2017.00645

Liu Z, Cai Y, Wanget Y al. Cloning of Macaque Monkeys by Somatic Cell Nuclear Transfer. Cell. 2018. https://doi.org/10.1016/j.cell.2018.01.020

Livak KJ and Schmittgen TD. Analysis of Relative Gene Expression Data Using Real-Time Quantitative PCR and the 22DDCT Method. Methods. 2001; 25 : 402–408. doi:10.1006/meth.2001.1262

Lu B, Malcuit C, Wang S, Girman S, Francis P, Lernieux L, Lanza R, Lund R. Long-term safety and function of RPE from human embryonic stem cells in preclinical models of macular degeneration. Stem Cells. 2009;27:2126–2135.

Lu L, Reinach PS, Kao WWY. Corneal Epithelial Wound Healing. Exp Biol Med. 2001; 226(7), pp : 653–664.

Lwigale PY. Chapter Four - Corneal Development: Different Cells from a Common Progenitor. Progress in Molecular Biology and Translational Science. 2015; 134, pp : 43-59. https://doi.org/10.1016/bs.pmbts.2015.04.003.

Lyngholm M, Vorum H, Nielsen K, Østergaard M, Honoré B, Ehler N. Differences in the protein expression in limbal versus central human corneal epithelium – a search for stem cell markers. Experimental Eye Research. 2008; 87(2), pp : 96-105. https://doi.org/10.1016/j.exer.2008.05.001

Ma DHK, Kuo MT, Tsai YJ, Chen HCJ, Chen XL, Wang SF, Li L, Hsiao CH, Lin KK. Transplantation of cultivated oral mucosal epithelial cells for severe corneal burn. Eye. 2009; 23, 1442–1450; doi:10.1038/eye.2009.60

Ma XL and Liu HQ. Effect of calcium on the proliferation and differentiation of murine corneal epithelial cells in vitro. Int J Ophthalmol. 2011; 4(3): 247–249. doi: 10.3980/j.issn.2222-3959.2011.03.06

Maeder ML and Gersbach CA. Genome-editing Technologies for Gene and Cell Therapy. Molecular Therapy. 2016; 24(3), pp : 430-446. https://doi.org/10.1038/mt.2016.10

Mahendra Rao and Maureen L. Condic. Alternative Sources of Pluripotent Stem Cells: Scientific Solutions to an Ethical Dilemma. Stem Cells and Development. 2008; 17(1) : 1-10. https://doi.org/10.1089/scd.2008.0013

Maherali N, et al. Directly reprogrammed fibroblasts show global epigenetic remodeling and widespread tissue contribution. Cell Stem Cell. 2007; 1:55–70. [PubMed: 18371336]

Mandai M, Watanabe A, Kurimoto Y, Hirami Y, et al. Autologous Induced Stem-Cell–Derived Retinal Cells for Macular Degeneration. N Engl J Med. 2017; 376:1038-1046. DOI: 10.1056/NEJMoa1608368

Marolt D, Campos IM, Bhumiratana S, Koren A, Petridis P, Zhang G, Spitalnik PF, Grayson WL, Vunjak-Novakovic G. Engineering bone tissue from human embryonic stem cells. PNAS. 2012; 109 (22), pp : 8705-8709. doi:10.1073/pnas.1201830109

Martello G and Smith A. The Nature of Embryonic Stem Cells. Annual Review of Cell and Developmental Biology. 2014; 30:1, 647-675.

Martin GR. Isolation of a pluripotent cell line from early mouse embryos cultured in medium conditioned by teratocarcinoma stem cells. PNAS. 1981; 78 (12) : 7634-7638.

Martinez-Morales JR and Wittbrodt J. Shaping the vertebrate eye. Current Opinion in Genetics & Development. 2009; 19(5), pp : 511-517. https://doi.org/10.1016/j.gde.2009.08.003

Mascetti VL and Pedersen RA. Human-Mouse Chimerism Validates Human Stem Cell Pluripotency. Cell Stem Cell. 2016; 18(1), pp: 67-72. https://doi.org/10.1016/j.stem.2015.11.017

Massague´ J, Blain SW, and Lo RS. TGFb Signaling in Growth Control, Review Cancer, and Heritable Disorders. Cell. 2000; 103: 295–309. https://doi.org/10.1016/S0092-8674(00)00121-5

Massague J. Integration of Smad and MAPK pathways: a link and a linker revisited. Genes & development. 2003; 17(24), pp : 2993-7.

Matsushima D, Heavner W, Pevny LH. Combinatorial regulation of optic cup progenitor cell fate by SOX2 and PAX6. Development (Cambridge, England). 2011; 138(3) :443-454. doi:10.1242/dev.055178.

Matt N, Dupé V, Garnier JM, Dennefeld C, Chambon P, Mark M, Ghyselinck NB. Retinoic acid-dependent eye morphogenesis is orchestrated by neural crest cells. Development. 2005; 132: 4789-4800. doi: 10.1242/dev.02031

McCracken KW, Aihara E, Martin B, Crawford CM, Broda T, Treguier J, Zhang X, Shannon JM, Montrose MH & Wells JM. Wnt/β-catenin promotes gastric fundus specification in mice and humans. Nature. 2017; 541, 182–187. doi:10.1038/nature21021

Medvedev SP, Grigor'eva EV, Shevchenko AI, Malakhova AA, Dementyeva EV, Shilov AA, Pokushalov EA, Zaidman AM, Aleksandrova MA, Plotnikov EY, Sukhikh GT, and Zakian SM. Stem Cells and Development. Human Induced Pluripotent Stem Cells Derived from Fetal Neural Stem Cells Successfully Undergo Directed Differentiation into Cartilage. 2010; 20(6) : 1099-1112. https://doi.org/10.1089/scd.2010.0249

Melguizo-Sanchis D, Xu Y, Taheem D, Yu M, Tilgner K, Barta T1, Gassner K, Anyfantis G, Wan T, Elango R, Alharthi S, El-Harouni AA, Przyborski S, Adam S, Saretzki G, Samarasinghe S, Armstrong L and Lako M. iPSC modeling of severe aplastic anemia reveals impaired differentiation and telomere shortening in blood progenitors. Cell Death and Disease. 2018; 9:128 . DOI 10.1038/s41419-017-0141-1

Mellough CB, Sernagor E, Moreno-Gimeno I, Steel DHW and Lako M. Efficient Stage-Specific Differentiation of Human Pluripotent Stem Cells Toward Retinal Photoreceptor Cells. Stem Cells. 2012; 30 : 673–686. doi:10.1002/stem.1037

Menzel-Severing J. Emerging Techniques to Treat Limbal Epithelial Stem Cell Deficiency. Discov Med. 2011; 11(56), pp : 57 – 64.

Merjava S, Neuwirth A, Mandys V, Jirsova K. Cytokeratins 8 and 18 in adult human corneal endothelium. Experimental Eye Research. 2009; 89(3), pp : 426-431. https://doi.org/10.1016/j.exer.2009.04.009

Merjava S, Neuwirth A, Tanzerova M, Jirsova K. The spectrum of cytokeratins expressed in the adult human cornea, limbus and perilimbal conjunctiva. Histol Histopathol. 2011; 26 : 323-331.

Metallo CM, Ji L, De Pablo JJ, Palecek SP. Retinoic Acid and Bone Morphogenetic Protein Signaling Synergize to Efficiently Direct Epithelial Differentiation of Human Embryonic Stem Cells. Stem Cells. 2008; 26, pp : 372–380.

Meyer-Blazejewska, E. A., Call, M. K., Yamanaka, O., Liu, H., Schlötzer-Schrehardt, U., Kruse, F. E. and Kao, W. W. From Hair to Cornea: Toward the Therapeutic Use of Hair Follicle-Derived Stem Cells in the Treatment of Limbal Stem Cell Deficiency. Stem Cells. 2011; 29 : 57–66. doi:10.1002/stem.550.

Mikhailova A, Ilmarinen T, Ratnayake A, Petrovski G, Uusitalo H, Skottman H, Rafat M. Human pluripotent stem cell-derived limbal epithelial stem cells on bioengineerd matrices for corneal reconstruction. Experimental Eye Research. 2016; 146: 26 – 34.

Mikhailova A, Ilmarinen T, Uusitalo H, Skottman H. Small-Molecule Induction Promotes Corneal Epithelial Cell Differentiation from Human Induced Pluripotent Stem Cells. Stem Cell Reports. 2014; 2, pp : 219–231.

Mikkelsen TS, et al. Dissecting direct reprogramming through integrative genomic analysis. Nature. 2008; 454:49–55. [PubMed: 18509334]

Miyashita H, Yokoo S, Yoshida S, Kawakita T, Yamagami S, Tsubota K. and Shimmura S. Long-Term Maintenance of Limbal Epithelial Progenitor Cells Using Rho Kinase Inhibitor and Keratinocyte Growth Factor. STEM CELLS Translational Medicine. 2013; 2: 758–765. doi:10.5966/sctm.2012-0156

Moll R, Divo M, Langbein L. The human keratins: biology and pathology. Histochem Cell Biol. 2008; 129: 705 – 733. doi:10.1007/s00418-008-0435-6

Moll R, Franke WW, Schiller DL, Geiger B, Krepler R. The catalog of human cytokeratins: Patterns of expression in normal epithelia, tumors and cultured cells. Cell. 1982; 31(1), pp: 11-24. https://doi.org/10.1016/0092-8674(82)90400-7

Moon SY, Park YB, Kim DS, Oh SK, Kim DW. Generation, Culture, and Differentiation of Human Embryonic Stem Cells for Therapeutic Applications. Molecular Therapy. 2006; Vol. 13, No. 1, 5 – 14. doi:10.1016/j.ymthe.2005.09.008

Moore KA and Lemischka IR. Stem cells and their niches. Science. 2006; 311:1880-1885.

Morita M, Fujita N, Takahashi A, Nam ER, Yui S, Chung CS, Kawahara N, Lin HY, Tsuzuki K, Nakagawa T, Nishimura R. Evaluation of ABCG2 and p63 expression in canine cornea and cultivated corneal epithelial cells. Veterinary Ophthalmology. 2015; 18(1), pp : 59 – 68.

Morizane A, Doi D, Kikuchi T, Okita K, Hotta A, Kawasaki T, et al. Direct comparison of autologous and allogeneic transplantation of iPSC-derived neural cells in the brain of a nonhuman primate. Stem Cell Reports. 2013; 1:283–92. doi:10.1016/j.stemcr.2013.08.007

Mort RL et al. Stem cells and corneal epithelial maintenance – insights from the mouse and other animal models. Results Probl Cell Differ. 2012; 55: 357–394. doi: 10.1007/978-3-642-30406-4_19

Müller LJ, Pels E, Vrensen GFJM. The specific architecture of the anterior stroma accounts for maintenance of corneal curvature. British Journal of Ophthalmology. 2001; 85 : 437-443. http://dx.doi.org/10.1136/bjo.85.4.437

Nakamura T, Inatomi T, Sotozono C, Amemiya T, Kanamura N, Kinoshita S. Transplantation of cultivated autologous oral mucosal epithelial cells in patients with severe ocular surface disorders. Br J Ophthalmol. 2004; 88: 1280–1284.

Narsinh KH, Plews J, Wu JC. Comparison of Human Induced Pluripotent and Embryonic Stem Cells: Fraternal or Identical Twins?. Molecular Therapy. 2011; 19(4), pp : 635 – 638. doi:10.1038/mt.2011.41

Narsinh KH, Sun N, Sanchez-Freire V, Lee AS, Almeida P, Hu S, Jan T, Wilson KD, Leong D, Rosenberg J, Yao M, Robbins RC, Wu JC. Single cell transcriptional profiling reveals heterogeneity of human induced pluripotent stem cells. J Clin Invest. 2011a; 121(3) :1217–1221. doi:10.1172/JCI44635.

Nguyen HV, Li Y, Tsang SH. Patient-Specific iPSC-Derived RPE for Modeling of Retinal Diseases. J. Clin. Med. 2015; 4(4) : 567-578. doi:10.3390/jcm4040567

Nguyen M and Arnheiter H. Signaling and transcriptional regulation in early mammalian eye development: a link between FGF and MITF. Development. 2000; 127: 3581-3591.

Nichols J and Smith A. Naive and Primed Pluripotent States. Cell Stem Cell, 2009; 4:pp: 487 – 492. DOI 10.1016/j.stem.2009.05.015

Nishida K, Yamato M, Hayashida Y, Watanabe K, Yamamoto K, Adachi E, Nagai S, Kikuchi A, Maeda N, Watanabe H, Okano T, Tano Y. Corneal Reconstruction with Tissue Engineered Cell Sheets Composed of Autologous Oral Mucosal Epithelium. N Engl J Med. 2004; 351: 1187-1196.

Nishida K, Yamato M, HayashidaY, Watanabe K, Maeda N, Watanabe H, Yamamoto K, Nagai S, Kikuchi A, Tano Y, Okano T. Functional bioengineered corneal epithelial sheet grafts from corneal stem cells expanded ex vivo on a temperature-responsive cell culture surface. Transplantation. 2004. Vol. 77 (3): p 379-385. doi: 10.1097/01.TP.0000110320.45678.30.

Nishizawa M, Chonabayashi K, Nomura M, Tanaka A, Nakamura M, Inagaki A, Nishikawa M, Takei I, Oishi A, Tanabe K, Ohnuki M, Yokota H, Koyanagi-Aoi M, Okita K, Watanabe A, Takaori-Kondo A, Yamanaka S, Yoshida Y. Epigenetic Variation

between Human Induced Pluripotent Stem Cell Lines Is an Indicator of Differentiation Capacity. Cell Stem Cell. 2016; 19(3), pp : 341-354.

Niu X, He W, Song B, Ou Z, Fan D, Chen Y, Fan Y, and Sun X. Combining Single Strand Oligodeoxynucleotides and CRISPR/Cas9 to Correct Gene Mutations in β-Thalassemia-induced Pluripotent Stem Cells. J. Biol. Chem. 2016 291: 16576-. doi:10.1074/jbc.M116.719237

O'Callaghan AR and, Daniels JT. Concise Review: Limbal Epithelial Stem Cell Therapy: Controversies and Challenges. STEM CELLS. 2011; 29 : 1923–1932.

Oh JY, Lee RH, Yu JM, Ko JH, Lee HJ, Ko AY, Roddy GW and Prockop DJ. Intravenous Mesenchymal Stem Cells Prevented Rejection of Allogeneic Corneal Transplants by Aborting the Early Inflammatory Response. Molecular Therapy. 2012; 20(11) : 2143–2152. doi:10.1038/mt.2012.165

Oh JY, Roddy GW, Choi H, Lee RH, Ylöstalo JH, Rosa RH, Prockop DJ. Anti-inflammatory protein TSG-6 reduces inflammatory damage to the cornea following chemical and mechanical injury. Proceedings of the National Academy of Sciences. 2010; 107(39) : 16875-16880. DOI: 10.1073/pnas.1012451107

Ohgushi M and Sasai Y. Lonely death dance of human pluripotent stem cells: ROCKing between metastable cell states. Trends in Cell Biology. 2011; 21(5), pp : 274 – 282.

Ohgushi M et al. Molecular Pathway and Cell State Responsible for Dissociation-Induced Apoptosis in Human Pluripotent Stem Cells. Cell Stem Cell. 2010; 7(2) : 225-239. https://doi.org/10.1016/j.stem.2010.06.018

Okita K, Ichisaka T, Yamanaka S. Generation of germline-competent induced pluripotent stem cells. Nature. 2007; 448, 313–317. doi:10.1038/nature05934

Okumura N, Koizumi N, Kay EP, Ueno M, Sakamoto Y, Nakamura S, Hamuro J, Kinoshita S. The ROCK inhibitor eye drop accelerates corneal endothelium wound healing. Invest Ophthalmol Vis Sci. 2013; 54 :2439 – 2502. DOI:10. 1167/iovs.12-11320

Olariu V. Stem cell dynamics: naïve pluripotency and reprogramming. OA Biology. 2013; 01;1(1):4.

O'Rahilly R. The Prenatal Development of the Human Eye. Exp. Eye Res. 1975; 21, pp: 93-112.

O'Rahilly R. The timing and sequence of events in the development of the human eye and ear during the embryonic period proper. Anat Embryol. 1983; 168(1), pp : 87–99. https://doi.org/10.1007/BF00305401

Ortmann D and Vallier L. Variability of human pluripotent stem cell lines. Current Opinion in Genetics & Development. 2017; 46 :179–185.

Osei-Bempong C, Figueiredo FC and Lako M. The limbal epithelium of the eye – A review of limbal stem cell biology, disease and treatment. Bioessays. 2013; 35: 211–219. doi:10.1002/bies.201200086

Patel DV, McGhee CNJ. Mapping of the normal human corneal sub-Basal nerve plexus by in vivo laser scanning confocal microscopy. Invest Ophthalmol Vis Sci. 2005; 46(12) : 4485–4488. http://dx.doi.org/10.1167/iovs.05-0794.

Pfister RR. Corneal stem cell disease: Concepts, categorization, and treatment by auto and homotransplantation of limbal stem cells. CLAO J. 1994; 20 : 64-72.

Polack FM. The Effect of Ocular Inflammation on Corneal Grafts. American Journal of Ophthalmology. 1965; 60(2) : 259-269.

Pouton CW and Haynes JM. Embryonic stem cells as a source of models for drug discovery. Nature Reviews Drug Discovery. 2007; 6, 605–616. doi:10.1038/nrd2194

Prabhasawat P, Ekpo P, Uiprasertkul M, Chotikavanich S, Tesavibul N, Pornpanich K, Luemsamran P. Long-term result of autologous cultivated oral mucosal epithelial transplantation for severe ocular surface disease. Cell Tissue Bank. 2016; Vol. 17: p 491–503.

Pyle AD, Lock LF, Donovan PJ. Neurotrophins mediate human embryonic stem cell survival. Nature Biotechnology. 2006; 24, 344–350. doi:10.1038/nbt1189

Qian X, Nguyen HN, Song MM, Hadiono C, et al. Brain-Region-Specific Organoids Using Mini-bioreactors for Modeling ZIKV Exposure . Cell. 2016; 165(5), pp : 1238-1254. https://doi.org/10.1016/j.cell.2016.04.032

Quarto N, Li S, Renda A, Longaker M. Exogenous Activation of BMP-2 Signaling Overcomes TGFβ-Mediated Inhibition of Osteogenesis in Marfan Embryonic Stem Cells and Marfan Patient-Specific Induced Pluripotent Stem Cells. Stem Cells. 2012; 30(12), pp : 2709-2719.

Rama, P, Bonini, S, Lambiase, A, Golisano, O, Paterna, P, De Luca, M, Pellegrini, G. Autologous Fibrin-Cultured Limbal Stem Cells Permanently Restore The Corneal Surface Of Patients With Total Limbal Stem Cell Deficiency. Transplantation. 2001; 72(9), pp : 1478-1485.

Rao MS and Malik N. Assessing iPSC reprogramming methods for their suitability in translational medicine. J. Cell. Biochem. 2012; 113: 3061 – 3068. doi:10.1002/jcb.24183

Ren Y, Lee MY, Schliffke S, Paavola J, Amos PJ, Ge X, Ye M, Zhu S, Senyei G, Lum L, Ehrlich BE, Qyang Y. Small molecule Wnt inhibitors enhance the efficiency of BMP-4-directed cardiac differentiation of human pluripotent stem cells. Journal of Molecular and Cellular Cardiology. 2011; 51 : 280–287. doi:10.1016/j.yjmcc.2011.04.012

Resnikoff S, Pascolini D, Etya'ale D, Kocur I, Pararajasegaram R, Pokharel GP, & Mariotti SP. Global data on visual impairment in the year 2002. Bulletin of the World Health Organization. 2004; 82:844-851.

Reyes AP, Petrus-Reurer S, Antonsson L, Stenfelt S, Bartuma H, Panula S, Mader T, Douagi I, André H, Hovatta O, Lanner F, Kvanta A. Xeno-Free and Defined Human Embryonic Stem Cell-Derived Retinal Pigment Epithelial Cells Functionally Integrate in a Large-Eyed Preclinical Model. Stem Cell Reports. 2016; 6(1), pp : 9-17. https://doi.org/10.1016/j.stemcr.2015.11.008

Riken Press Releases 2013 at http://www.riken.jp/en/pr/press/2013/20130730_1/

Robinton DA and Daley GQ. The promise of induced pluripotent stem cells in research and therapy. Nature. 2012; 481, 295–305. doi:10.1038/nature10761

Romano RA, Smalley K, Liu S, Sinha S. Abnormal hair follicle development and altered cell fate of follicular keratinocytes in transgenic mice expressing DeltaNp63a. Development. 2010; 137, pp : 1431 – 1439.

Romero-Rangel T, Stavrou P, Cotter J, Rosenthal P, Baltatzis S, Foster CS. Gas-permeable scleral contact lens therapy in ocular surface disease. Am J Ophthalmol. 2000; 130:25-32.

Rubin LL and Haston KM. Stem cell biology and drug discovery. BMC Biology. 2011; 9:42. https://doi.org/10.1186/1741-7007-9-42

Ruiz S, Diep D, Gore A, Panopoulos AD, Montserrat N, Plongthongkum N, et al. Identification of a specific reprogramming-associated epigenetic signature in human induced pluripotent stem cells. Proc Natl Acad Sci U S A. 2012; 109:16196–201. doi:10.1073/pnas.1202352109

Sadler TW and Langman J. Langman's medical embryology. 11th ed. Publisher: Philadelphia : Wolters Kluwer Lippincott Williams & Wilkins, c2010.

Sadler TW. Langman's medical embryology. 13th ed. Publisher: Philadelphia : Wolters Kluwer Lippincott Williams & Wilkins, 2014.

Sancho-Martinez I, Izpisua Belmonte JC. Stem cells: Surf the waves of reprogramming. Nature. 2013; 493:310–1. [PubMed: 23325209]

Sanford LP, Ormsby I, Gittenberger-de Groot AC, Sariola H, et al. TGFbeta2 knockout mice have multiple developmental defects that are non-overlapping with other TGFbeta knockout phenotypes. Development .1997; 124: 2659-2670.

Sasaki M, Abe R, FujitaY, Ando S, Inokuma D, Shimizu H. Mesenchymal Stem Cells Are Recruited into Wounded Skin and Contribute to Wound Repair by Transdifferentiation into Multiple Skin Cell Type. The Journal of Immunology. 2008; 180 (4) 2581-2587. DOI: 10.4049/jimmunol.180.4.2581

Schatten G, Smith J, Navara C, Park JH, Pedersen R. Culture of human embryonic stem cells. Nature Methods. 2005; 2, 455–463. doi:10.1038/nmeth0605-455

Schlotzer-Schrehardt U and Kruse FE. Identification and characterization of limbal stem cells. Experimental Eye Research. 2005; 81, pp : 247–264.

Schlötzer-Schrehardt U, Dietrich T, Saito K, Sorokin L, Sasaki T, Paulsson M, Kruse F. Characterization of extracellular matrix components in the limbal epithelial stem cell compartment. Experimental Eye Research. 2007; 85(6), pp : 845-860.

Schuldiner M, Yanuka O, Itskovitz-Eldor J, Melton DA, Benvenisty N. Effects of eight growth factors on the differentiation of cells derived from human embryonic stem cells. PNAS. 2000; 97(21), pp : 11307 – 11312.

Schulz TC. Concise Review: Manufacturing of Pancreatic Endoderm Cells for Clinical Trials in Type 1 Diabetes. Stem Cells Translational Medicine. 2015; 4:927–931.

Schwartz SD, Hubschman JP, Heilwell G, Franco-Cardenas V, Pan CK, Ostrick RM, Mickunas E, Gay R, Klimanskaya I, Lanza R. Embryonic stem cell trials for macular degeneration: a preliminary report. Lancet. 2012; 379, pp: 713–20.

Sehic A, Utheim OA, Ommundsen K and Utheim TP. Pre-Clinical Cell-Based Therapy for Limbal Stem Cell Deficiency. J. Funct. Biomater. 2015; 6(3), 863-888. doi:10.3390/jfb6030863

Sevim DG and Acar U. Stem Cell-Based Treatment Modalities for Limbal Stem Cell Deficiency. Niche. 2013; 2: 25-30 • DOI : 10.5152/niche.2014.166

Shaharuddin B, Ahmad S, Md Latar N, Ali S, Meeson A. A Human Corneal Epithelial Cell Line Model for Limbal Stem Cell Biology and Limbal Immunobiology. Stem Cells Translational Medicine. 2017; 6:761–766.

Shalom-Feuerstein R, Serror L, Aberdam E, Muller FJ, van Bokhoven H, Wiman KG, Zhou H, Aberdam D, Petit I. Impaired epithelial differentiation of induced pluripotent stem cells from ectodermal dysplasia-related patients is rescued by the small compound APR-246/PRIMA-$1^{MET}$. PNAS. 2013; 110(6), pp : 2152–2156.

Shalom-Feuerstein R, Serror L, De La Forest Divonne S, Petit I, Aberdam E, Camargo L, Damour O, Vigouroux C, Solomon A, Gaggioli C, Itskovitz-Eldor J, Ahmad S, Aberdam D. Pluripotent Stem Cell Model Reveals Essential Roles for miR-450b-5p and miR-184 in Embryonic Corneal Lineage Specification. Stem Cells. 2012; 30(5), pp : 898-909.

Sharp J, Frame J, Siegenthaler M, Nistor G and Keirstead HS. Human Embryonic Stem Cell-Derived Oligodendrocyte Progenitor Cell Transplants Improve Recovery after Cervical Spinal Cord Injury . STEM CELLS. 2010; 28: 152–163. doi:10.1002/stem.245

Sheth R, Neale M, Shortt A, Massie I, Vernon A, Daniels J. Culture and Characterization of Oral Mucosal Epithelial Cells on a Fibrin Gel for Ocular Surface Reconstruction. Current Eye Research. 2015; 40(11), pp : 1077-1087.

Shimazaki, J, Higa K, Morito F, Dogru M, et al. Factors Influencing Outcomes in Cultivated Limbal Epithelial Transplantation for Chronic Cicatricial Ocular Surface Disorders. American Journal of Ophthalmology. 2007; 143(6) : 945 – 953. DOI: http://dx.doi.org/10.1016/j.ajo.2007.03.005

Shortt AJ, Bunce C, Levis HJ, Blows P, Doré CJ, Vernon A, Secker GA, Tuft SJ and Daniels JT. Three-Year Outcomes of Cultured Limbal Epithelial Allografts in Aniridia and Stevens-Johnson Syndrome Evaluated Using the Clinical Outcome Assessment in Surgical Trials Assessment Tool. STEM CELLS Translational Medicine. 2014; 3: 265–275. doi:10.5966/sctm.2013-0025

Shortt AJ, Secker GA, Notara MD, Limb GA, et al. Transplantation of Ex Vivo Cultured Limbal Epithelial Stem Cells: A Review of Techniques and Clinical Results. Survey of Ophthalmology. 2007; 52(5) : 483 – 502. DOI: http://dx.doi.org/10.1016/j.survophthal.2007.06.013

Shortt AJ, Tuft SJ, and Daniels JT. Corneal stem cells in the eye clinic. British Medical Bulletin. 2011; 100 : 209–225. DOI:10.1093/bmb/ldr041

Singh R, Shen W, Kuai D, Martin JM, Guo X, Smith MA, Perez ET, Phillips MJ, Simonett JM, Wallace KA, Verhoeven AD, Capowski EE, Zhang X, Yin Y, Halbach PJ, Fishman GA, Wright LS, Pattnaik BR, Gamm DM. iPS cell modeling of Best disease: insights into the pathophysiology of an inherited macular degeneration. Human Molecular Genetics. 2013; 22(3), pp: 593–607. https://doi.org/10.1093/hmg/dds469

Sinn R and Wittbrodt J. An eye on eye development. Mechanisms of Development. 2013; 130(6–8), pp : 347-358 . https://doi.org/10.1016/j.mod.2013.05.001

Sivak JM, Mohan R, Rinehart WB, Xu PX, Maas RL, Fini ME. Pax-6 Expression and Activity Are Induced in the Reepithelializing Cornea and Control Activity of the Transcriptional Promoter for Matrix Metalloproteinase Gelatinase B. Developmental Biology. 2000; 222, pp : 41 – 54.

Skottman H, Dilber MS, Hovatta O. The derivation of clinical-grade human embryonic stem cell lines. FEBS Lett. 2006; 580:2875–2878.

Skottman H, Mikkola M, Lundin K, Olsson C, Strömberg A-M, Tuuri T, Otonkoski T, Hovatta O and Lahesmaa R. Gene Expression Signatures of Seven Individual Human Embryonic Stem Cell Lines. Stem Cells. 2005; 23: 1343–1356. doi:10.1634/stemcells.2004-0341

Somers A, Jean JC, Sommer CA, Omari A et al. Generation of transgene-free lung disease-specific human induced pluripotent stem cells using a single excisable lentiviral stem cell cassette. Stem Cells. 2010; 28, 1728–1740. doi: 10.1002/stem.495

Sommer CA, Stadtfeld M, Murphy GJ, Hochedlinger K, Kotton DN, Mostoslavsky G. Induced Pluripotent Stem Cell Generation Using a Single Lentiviral Stem Cell Cassette. Stem Cells. 2009; 27: 543–549. doi:10.1634/stemcells.2008-1075

Sotozono C, Inatomi T, Nakamura T, Koizumi N, Yokoi N, Ueta M, Matsuyama K, Miyakoda K, Kaneda H, Fukushima M, Kinoshita S. Visual Improvement after Cultivated Oral Mucosal Epithelial Transplantation. Ophthalmology. 2013; 120 :193–200.

Stadtfeld M and Hochedlinger K. Induced pluripotency: history, mechanisms and applications. Gene & Development. 2010; 24 : 2239 – 2263. doi:10.1101/gad.1963910

Stepp MA and Zieske JD. The Corneal Epithelial Stem Cell Niche. The Ocular Surface. 2005; 3(1), pp : 15-26. https://doi.org/10.1016/S1542-0124(12)70119-2

Sterneckert JL, Reinhardt P,. Schöler HR. Investigating human disease using stem cell models. Nature Reviews Genetics . 2014; 15, pp: 625–639. doi:10.1038/nrg3764

Sugawara T, Nishino K, Umezawa A, Akutsu H. Investigating cellular identity and manipulating cell fate using induced pluripotent stem cells. Stem Cell Research & Therapy. 2012; 3:8. http://stemcellres.com/content/3/2/8.

Sun CC, Chiu HT, Lin YF, Lee KY, Pang JHS. Y-27632, a ROCK Inhibitor, Promoted Limbal Epithelial Cell Proliferation and Corneal Wound Healing. PLoSONE. 2015; 10(12): e0144571.

Swamynathan SK. Ocular Surface Development and Gene Expression. Journal of Ophthalmology. 2013; vol. 2013, Article ID 103947, 22 pages. doi:10.1155/2013/103947

Takahashi K and Yamanaka S. Induction of Pluripotent Stem Cells from Mouse Embryonic and Adult Fibroblast Cultures by Defined Factors. Cell. 2006; 126(4): pp: 663-676. https://doi.org/10.1016/j.cell.2006.07.024

Takahashi K, Tanabe K, Ohnuki M, Narita M, Ichisaka T, Tomoda K, Yamanaka S. Induction of Pluripotent Stem Cells from Adult Human Fibroblasts by Defined Factors. Cell. 2007; 131: p. 861–872.

Takasato M, Er PX, Becroft M, Vanslambrouck JM, Stanley EG, Elefanty AG, Little MH. Directing human embryonic stem cell differentiation towards a renal lineage generates a self-organizing kidney. Nature Cell Biology. 2014; 16, 118–126. doi:10.1038/ncb2894

Tesar PJ, Chenoweth JG, Brook FA, Davies TJ, Evans EP, Mack DL, Gardner RL, McKay RDG. New cell lines from mouse epiblast share defining features with human embryonic stem cells. Nature. 2007; 448, 196–199. doi:10.1038/nature05972

Theunissen TW, Powell BE, Wang H, Mitalipova M, Faddah DA, Reddy J, Fan ZP, Maetzel D, Ganz K, Shi L, Lungjangwa T, Imsoonthornruksa S, Stelzer Y, Rangarajan S, D'Alessio A, Zhang J, Gao Q, M. Dawlaty MM, Young RA, Gray NS, Jaenisch R. Systematic Identification of Culture Conditions for Induction and Maintenance of Naive Human Pluripotency. Cell Stem Cell. 2014; 15, 471–487. https://doi.org/10.1016/j.stem.2014.07.002

Thoft RA, Friend J. The X, Y, Z hypothesis of corneal epithelial maintenance. Invest. Ophthalmol. Vis. Sci. 1983; 24(10) :1442-1443.

Thomson JA, Itskovitz-Eldor J, Shapiro SS, Waknitz MA, Swiergiel JJ, Marshall VS, Jones JM. Embryonic Stem Cell Lines Derived from Human Blastocysts. Science. 1998; 282(5391), pp: 1145-1147. DOI: 10.1126/science.282.5391.11451998

Trosan P, Svobodova E, Chudickova M, et al. The key role of insulin-like growth factor I in limbal stem cell differentiation and the corneal wound-healing process. Stem Cells Dev. 2012; 21, pp : 3341-3350.

Trounson A and DeWitt N. Pluripotent stem cells progressing to the clinic. Nature Reviews Molecular Cell Biology. 2016; volume 17, pages 194–200. doi:10.1038/nrm.2016.10

Tsien RY. The green fluorescent protein. Annu. Rev. Biochem. 1998; 67:509–44.

Tucker BA, Mullins RF, Stone EM. Stem cells for investigation and treatment of inherited retinal disease. Human Molecular Genetics. 2014. R1–R8.

Tucker BA, Mullins RF, Streb LM, et al. Patient-specific iPSC-derived photoreceptor precursor cells as a means to investigate retinitis pigmentosa. eLife. 2013; 2:e00824. doi:10.7554/eLife.00824.

Umemoto T, Yamato M, Nishida K, Okano T. Regenerative medicine of cornea by cell sheet engineering using temperature-responsive culture surfaces. Chin. Sci. Bull. 2013; 58(35) : 4349–4356. https://doi.org/10.1007/s11434-013-5742-1

Vallier L, Reynolds D, Pedersen R. Nodal inhibits differentiation of human embryonic stem cells along the neuroectodermal default pathway. Developmental Biology. 2004; 275(2), pp: 403-421.

Van De Bunt M, Lako M, Barrett A, Gloyn A, Hansson M, McCarthy M, Beer N, Honoré C. Insights into islet development and biology through characterization of a human iPSC-derived endocrine pancreas model. ISLETS. 2016; 8(3) : 83–95. http://dx.doi.org/10.1080/19382014.2016.1182276.

Villapol S, Logan TT and Symes AJ. Role of TGF-β Signaling in Neurogenic Regions After Brain Injury. In Chapter 1 : Trends in Cell Signaling Pathways in Neuronal Fate Decision. 2013. InTech. DOI: 10.5772/53941

Walia B, Satija N, Tripathi RP, Gangenahalli GU. Induced Pluripotent Stem Cells: Fundamentals and Applications of the Reprogramming Process and its Ramifications on Regenerative Medicine. Stem Cell Rev and Rep. 2012; 8: 100-115. https://doi.org/10.1007/s12015-011-9279-x

Wang A et al. Induced pluripotent stem cells for neural tissue engineering. Biomaterials. 2011; 32(22) : 5023-5032. https://doi.org/10.1016/j.biomaterials.2011.03.070

Wang S and Gurdon JB. Therapeutic Somatic Cell Reprogramming by Nuclear Transfer. In: Gage F, Christen Y. (eds) Programmed Cells from Basic Neuroscience to Therapy. Research and Perspectives in Neurosciences. 2013; vol 20. Springer, Berlin, Heidelberg. https://doi.org/10.1007/978-3-642-36648-2_2

Wang W, Yang J, Liu H, Lu D, Chen X, Zenonos Z, Campos LS, Rad R, Guo G, Zhang S, et al. Rapid and efficient reprogramming of somatic cells to induced pluripotent stem cells by retinoic acid receptor gamma and liver receptor homolog 1. Proc. Natl. Acad. Sci. USA. 2011; 108, 18283–18288.

Waring GO, Bourne WM, Edelhauser HF, Kenyon KR. The Corneal Endothelium: Normal and Pathologic Structure and Function. Ophthalmology. 1982; 89(60), pp : 531-590. https://doi.org/10.1016/S0161-6420(82)34746-6

Warren L, Manos PD, Ahfeldt T, et al. Highly efficient reprogramming to pluripotency and directed differentiation of human cells using synthetic modified mRNA. Cell Stem Cell. 2010; 7(5) :618-630. doi:10.1016/j.stem.2010.08.012.

Warrier S, Van der Jeught M, Duggal G, Tilleman L, Sutherland E, Taelman J, Popovic M, Lierman S, De Sousa Lopes SC, Van Soom A, Peelman L, Van Nieuwerburgh F, De Coninck DIM, Menten B, Mestdagh P, Van de Sompele J, Deforce D, De Sutter P & Heindryckx B. Direct comparison of distinct naive pluripotent states in human embryonic stem cells. Nature Communications. 2016; DOI: 10.1038/ncomms15055

Watanabe K, Nishida K, Yamato M, et al. Human limbal epithelium contains side population cells expressing the ATP-binding cassette transporter ABCG2. FEBS Lett. 2004; 565 :6-10.

Watanabe K, Ueno M, Kamiya D, Nishiyama A, Matsumura M, Wataya T, Takahashi JB, Nishikawa S, Nishikawa SI, Muguruma K, Sasai Y. A ROCK inhibitor permits survival of dissociated human embryonic stem cells. Nature Biotechnology. 2007; 25(6), pp : 681 – 686.

Weinberger L, Ayyash M, Novershtern N, Hanna JH. Dynamic stem cell states: naive to primed pluripotency in rodents and humans. Nature Reviews Molecular Cell Biology. 2016; 17, pp: 155–169. doi:10.1038/nrm.2015.28

Wernig M, et al. In vitro reprogramming of fibroblasts into a pluripotent ES-cell-like state. Nature. 2007; 448:318–24. [PubMed: 17554336]

West-Mays JA and Dwivedi DJ. The keratocyte: Corneal stromal cell with variable repair phenotypes. The International Journal of Biochemistry & Cell Biology. 2006; 38(10), pp : 1625-1631. https://doi.org/10.1016/j.biocel.2006.03.010

Wiley L, Sunderaj N, Sun TT, Thoft RA. Regional heterogeneity in human corneal and limbal epithelia: An Immunohistochemical evaluation. Invest Ophthalmol Vis Sci. 1991; 32 :594-602.

Wilmut I. The First Direct Reprogramming of Adult Human Fibroblasts. Cell Stem Cell. 2007; pp: 593 – 594. DOI 10.1016/j.stem.2007.11.013

Wobus AM, and Boheler KR. Embryonic Stem Cells: Prospects for Developmental Biology and Cell Therapy. Physiol Rev. 2005; 85: pp: 635– 678. doi:10.1152/physrev.00054.2003.

Woltjen K, Michael IP, Mohseni P, Desai R, Mileikovsky M, Hämäläinen R, Cowling R, Wang W, Liu P, Gertsenstein M, Kaji K, Sung HK, Andras Nagy A. piggyBac transposition reprograms fibroblasts to induced pluripotent stem cells. Nature. 2009; 458, pp: 766–770. doi:10.1038/nature078632009

Wordinger RJ and Clark AF. Bone Morphogenetic Proteins and Their Receptors in the Eye. Exp Biol Med. 2007; 232:979–992. DOI: 10.3181/0510-MR-345

Wrana JL and Attisano L. The Smad pathway. Cytokine & Growth Factor Reviews. 2000. 11: p. 5-13.

Wu J, Okamura D, Li M, Suzuki K, Luo C, Ma L, He Y, Li Z, et al. An alternative pluripotent state confers interspecies chimaeric competency. Nature. 2015; volume 521, pages 316–321. doi:10.1038/nature14413

Wu J, Rnjak-Kovacina J, Du Y, Funderburgh ML, Kaplan DL, Funderburgh JL. Corneal stromal bioequivalents secreted on patterned silk substrates. Biomaterials. 2014; 35(12), pp : 3744-3755. https://doi.org/10.1016/j.biomaterials.2013.12.078

Wu MY and Hill CS. TGF-b Superfamily Signalling in Embryonic Development and Homeostasis. Developmental Cell. 2009; 16 : 329 – 343. DOI 10.1016/j.devcel.2009.02.012.

www.cellsignal.com

Xu N, Papagiannakopoulos T, Pan G, Thomson JA, Kosik KS. MicroRNA-145 Regulates OCT4, SOX2, and KLF4 and Represses Pluripotency in Human Embryonic Stem Cells. Cell. 2009; 137(4), pp: 647-658. https://doi.org/10.1016/j.cell.2009.02.038

Xu RH, Chen X, Li DS, Li R, Addicks GC, Glennon C, Zwaka TP, Thomson JA. BMP4 initiates human embryonic stem cell differentiation to trophoblast. Nature Biothechnology. 2002; 20, p: 1261 – 1264.

Xu RH, Peck RM, Li DS, Feng X, Tenneille Ludwig T, Thomson JA. Basic FGF and suppression of BMP signaling sustain undifferentiated proliferation of human ES cells. Nature Methods. 2005; 2 : 185–190. doi:10.1038/nmeth744

Yamanaka S. Induced Pluripotent Stem Cells: Past, Present, and Future. Cell Stem Cell. 2012; 10, pp : 678 – 684. DOI 10.1016/j.stem.2012.05.005

Yang C, Yang Y, Brennan L, Bouhassira EE, Kantorow M, and Cvekl A. Efficient generation of lens progenitor cells and lentoid bodies from human embryonic stem cells in chemically defined conditions. The FASEB Journal. 2010; 24:9, 3274-3283. https://doi.org/10.1096/fj.10-157255

Yang L, Soonpaa MH, Adler ED, Roepke TK, Kattman SJ, Kennedy M, Henckaerts E, Bonham K, Abbott GW, Linden RM, Field LJ, Keller GM. Human cardiovascular progenitor cells develop from a KDR+ embryonic-stem-cell-derived population. Nature. 2008; 453, 524–528. doi:10.1038/nature06894

Yao S, Chen S, Clark J, Hao E, Beattie GM, Hayek A, Ding S. Long-term self-renewal and directed differentiation of human embryonic stem cells in chemically defined conditions. PNAS. 2006; 103(18), pp: 6907 – 6912.

Yoshihara M, Sasamoto Y, Hayashi R, Ishikawa Y, Tsujikawa M, Hayashizaki Y, Itoh M, Kawaji H, Nishida K. High-resolution promoter map of human limbal epithelial cells cultured with keratinocyte growth factor and rho kinase inhibitor. Scientific Reports. 2017; 7(2845). doi:10.1038/s41598-017-02824-8

Yu J, Vodyanik MA, Smuga-Otto K, Antosiewicz-Bourget J, Frane JL, Tian S, Nie J, Jonsdottir GA, Ruotti V, Stewart R, Slukvin II, Thomson JA. Induced Pluripotent Stem Cell Lines Derived from Human Somatic Cells. Science. 2007; 318(5858) : 1917-1920. DOI: 10.1126/science.1151526

Yu M, Bojic S, Figueiredo GS, Rooney P, de Havilland J, Dickinson A, Figueiredo FC, Lako M. An important role for adenine, cholera toxin, hydrocortisone and triiodothyronine in the proliferation, self-renewal and differentiation of limbal stem cells in vitro. Experimental Eye Research . 2016; 152 : 113-122. http://dx.doi.org/10.1016/j.exer.2016.09.008

Zaragosi LE, Billon N, Ailhaud G and Dani C. Nucleofection Is a Valuable Transfection Method for Transient and Stable Transgene Expression in Adipose Tissue-Derived Stem Cells. STEM CELLS. 2007; 25: 790–797. doi:10.1634/stemcells.2006-0235

Zavala J, Jaime GRL, Barrientos CAR & Valdez-Garcia J. Corneal endothelium: developmental strategies for regeneration. Eye. 2013; volume 27, pages 579–588. doi:10.1038/eye.2013.15

Zhang C, Du L, Pang K, Wu X. Differentiation of human embryonic stem cells into corneal epithelial progenitor cells under defined conditions. PLoS ONE. 2017; 12(8): e0183303.

Zhang P, Li J, Tan Z, Wang C, Liu T, Chen L, Yong J, Jiang W, Sun X, Du L, Ding M and Deng H. Short-term BMP-4 treatment initiates mesoderm induction in human embryonic stem cells. Blood. 2008; 111 :1933-1941. doi: https://doi.org/10.1182/blood-2007-02-074120

Zhang X, Huang C T, Chen J, Pankratz M T, Xi J, Li J, Yang Y, LaVaute T M, Li X J, Ayala M, Bondarenko G I, Du Z W, Jin Y, Golos T G, Zhang S C. Pax6 Is a Human Neuroectoderm Cell Fate Determinant. Cell Stem Cell. 2010; 7, pp: 90–100. DOI 10.1016/j.stem.2010.04.017.

Zhou, W. & Freed, C. R. Adenoviral gene delivery can reprogram human fibroblasts to induced pluripotent stem cells. Stem Cells. 2009; 27, 2667–2674.

Zhu L, Gomez-Duran A, Saretzki G, Jin S, Tilgner K, Melguizo-Sanchis D, Anyfantis G, Al-Aama J, Vallier L, Chinnery P, Lako M, Armstrong L. The mitochondrial protein CHCHD2 primes the differentiation potential of human induced pluripotent stem cells to neuroectodermal lineages. The Journal of Cell Biology. 2016; 215(2) pp: 187 – 202.

Zieske JD. Corneal development associated with eyelid opening. Int. J. Dev. Biol. 2004; 48: 903-911. doi: 10.1387/ijdb.041860jz

Zieske JD, Chung EH, Guo X and Hutcheon AEK. Human corneal organotypic cultures. Journal of toxicology. Cutaneous and ocular toxicology. 2004; 23(1):19-28. DOI:10.1081/CUS-120027484

Zuba-Surma EK, Wojakowski W, Madeja Z, Ratajczak MZ. Stem Cells as a Novel Tool for Drug Screening and Treatment of Degenerative Diseases. Current Pharmaceutical Design. 2012; 18(18), pp: 2644 - 2656. DOI : 10.2174/138161212800492859

# APPENDIX

STEM CELLS®

EMBRYONIC STEM CELLS/INDUCED PLURIPOTENT STEM CELLS

# Differences in the Activity of Endogenous Bone Morphogenetic Protein Signaling Impact on the Ability of Induced Pluripotent Stem Cells to Differentiate to Corneal Epithelial-Like Cells

TATY ANNA KAMARUDIN,[a] SANJA BOJIC,[a] JOSEPH COLLIN,[a] MIN YU,[a] SAMEER ALHARTHI,[b] HARLEY BUCK,[c] ALEX SHORTT,[c] LYLE ARMSTRONG,[a] FRANCISCO C. FIGUEIREDO,[a,d] MAJLINDA LAKO [a]

**Key Words.** Human embryonic stem cell • Human induced pluripotent stem cell • Corneal epithelial progenitors • Corneal epithelial cells • Bone morphogenetic protein 4 • Retinoic acid • Epidermal growth factor

## ABSTRACT

**Cornea is a clear outermost layer of the eye which enables transmission of light onto the retina. The transparent corneal epithelium is regenerated by limbal stem cells (LSCs), whose loss/dysfunction results in LSCs deficiency (LSCD). Ex vivo expansion of autologous LSCs obtained from patient's healthy eye followed by transplantation onto the LSCs damaged/deficient eye, has provided a successful treatment for unilateral LSCD. However, this is not applicable to patient with total bilateral LSCD, where LSCs are lost/damaged from both eyes. We investigated the potential of human induced pluripotent stem cell (hiPSC) to differentiate into corneal epithelial-like cells as a source of autologous stem cell treatment for patients with total bilateral LSCD. Our study showed that combined addition of bone morphogenetic protein 4 (BMP4), all trans-retinoic acid and epidermal growth factor for the first 9 days of differentiation followed by cell-replating on collagen-IV-coated surfaces with a corneal-specific-epithelial cell media for an additional 11 days, resulted in step wise differentiation of human embryonic stem cells (hESC) to corneal epithelial progenitors and mature corneal epithelial-like cells. We observed differences in the ability of hiPSC lines to undergo differentiation to corneal epithelial-like cells which were dependent on the level of endogenous BMP signaling and could be restored via the activation of this signaling pathway by a specific transforming growth factor β inhibitor (SB431542). Together our data reveal a differential ability of hiPSC lines to generate corneal epithelial cells which is underlined by the activity of endogenous BMP signaling pathway.** STEM CELLS *2017; 00:000–000*

## SIGNIFICANCE STATEMENT

Directing differentiation of human induced pluripotent stem cells (hiPSC) to corneal epithelial progenitors could provide an autologous source for cell replacement therapy in patients with bilateral limbal stem cell deficiency, avoiding dependency on post-transplant immunosuppressant or donated cornea. This work describes a simple and efficient two-step method with the supplementation of growth factors and small molecules that results in differentiation of pluripotent stem cells to corneal epithelial cells in 20 days. There were cell line differences in capacity to differentiate to corneal epithelial progenitors which were underlined by the endogenous BMP signaling activity and could be restored using SB431542.

[a]Institute of Genetic Medicine, International Centre for Life, Newcastle University, Central Parkway, Newcastle upon Tyne, United Kingdom; [b]Princess Al Jawhara Al-Brahim Center of Excellence in Research of Hereditary Disorders, King Abdulaziz University, Saudi Arabia; [c]UCL Institute of Immunology and Transplantation, Royal Free Campus, London, United Kingdom; [d]Department of Ophthalmology, Royal Victoria Infirmary, Queen Victoria Road, Newcastle upon Tyne, United Kingdom

Correspondence to: Majlinda Lako, Ph.D., Institute of Genetic Medicine, International Centre for Life, Newcastle University, Central Parkway, Newcastle upon Tyne, United Kingdom. Telephone: 44-0191-2418-688; e-mail: majlinda.lako@newcastle.ac.uk

Received September 20, 2017; accepted for publication November 15, 2017; first published online in STEM CELLS *EXPRESS* December 11, 2017.

http://dx.doi.org/10.1002/stem.2750



## INTRODUCTION

Cornea is the transparent region at the front of the eye which enables transmission of light to the retina. It comprises the corneal epithelium, stroma, and endothelium. The corneal epithelium is continuously regenerated by limbal stem cells (LSCs) [1, 2], which migrate from peripheral to central region of the cornea and ascend from basal to superficial layer to differentiate and form a new stratified layer of non-keratinized squamous epithelium [3]. The corneal epithelium develops from surface ectoderm [4], while the stroma and endothelium developed from the mesenchymal tissue and neural crest cells [5].

LSCs deficiency (LSCD) is a disease caused by the loss or dysfunction of LSCs, leading to

loss of corneal epithelial integrity and function, often resulting in persistent pain and severe visual impairment [6]. Work done by our group and others have shown that the transplantation of ex vivo expanded autologous LSCs is able to reconstruct the corneal surface and to restore vision in patients with unilateral total LSCD [7–9]. However, this treatment is not applicable to a significant number of patients with total bilateral LSCD where patient's both eyes are devoid of LSCs which are needed for the ex vivo expansion and subsequently used for transplantation. Hence, alternative sources of cells that could be used to replace the missing LSCs in total bilateral LSCD are being sought after by many researchers. Of those, transplantation of ex vivo expanded autologous oral mucosa epithelial (OME) cells has been the most used cell source in clinical studies of bilateral LSCD treatment with a reported "success" rate of 48%–75% within follow-up times up to 34 months [10–17]. Our group provided proof of concept by transplanting autologous ex vivo expanded OME in two patients with histologically confirmed total bilateral LSCD which resulted in successful reversal of LSCD in the treated eye up to 24 months [18]. Notwithstanding, we also showed that cultured oral epithelial cells retained a gene expression profile that was attributed to epithelial stem cells in general, but they did not acquire a typical limbal expression pattern after 10–14 days in culture [18], thus indicating that the transplanted cells did not fully transdifferentiate into corneal epithelium.

Recent advances in somatic cell induced reprogramming have shown that it is possible to reprogram somatic cells back to an "embryonic-like cells" through overexpression of four key pluripotency factors. These are named induced pluripotent stem cells and like human embryonic stem cells (hESC), they are characterized by unlimited self-renewal and potential to differentiate into any cell type of the adult organism [19, 20]. The most important advantage of human induced pluripotent stem cells (hiPSC) is the ability to avoid post-transplantation rejection by patient's own immune system [21]. Traditionally, differentiation of hESC and hiPSC to corneal epithelial cells has relied on usage of feeder cells, undefined conditioned media, or amniotic membrane [22–26]. More recently, small molecule driven protocols have become available resulting in generation of corneal epithelial-like cells within 6 weeks [27]. Bioengineered medical grade collagen matrices have also been shown to provide an excellent carrier for pluripotent stem cell derived limbal epithelial cells, which retained their ability to proliferate when in contact with matrix as well as the ability to differentiate into epithelial cells [28]. In this article, we describe the development of a defined feeder-free monolayer differentiation method which results in differentiation of hESC and hiPSC to corneal epithelial progenitors and mature corneal epithelial cells within 20 days. Furthermore, we show differences in the ability of hiPSC lines to generate corneal epithelial-like cells which are dictated by the activity of endogenous bone morphogenetic protein (BMP) signaling pathway.

## Materials and Methods

### Cell Culture

Undifferentiated hESC (H9) and hiPSC that were generated and fully characterized in our group (SB-Ad2 and SB-Ad3 [29]) were maintained in BD Matrigel (growth factor reduced) (BD Biosciences, Belgium) with mTeSR1 (STEMCELL Technologies, Cambridge, MA) at 37°C and 5% $CO_2$. hESC and hiPSC were passaged every 3–4 days by using 0.02% EDTA (Versene, Belgium) at 1:3–1:6 ratio. 3T3 fibroblasts for feeder plate preparation were maintained in cell culture flasks in fibroblast medium at 37°C and 5% $CO_2$. 3T3 fibroblast medium was prepared by mixing 89% high glucose Dulbecco's modified Eagle medium + GlutaMAX; 10% fetal bovine serum (FBS); 1% Pen/Strep (Gibco, UK). 3T3 fibroblasts were passaged every 3 to 4 days using 0.05% Trypsin-EDTA (Gibco, UK). All cells used in this study were between passages 15 and 50 and assessed to be karyotypically normal through CytoSNP analysis.

### Differentiation of hESC and hiPSC to Corneal Epithelial Cells

A schematic representation of differentiation protocol is presented in Figure 1A. In brief, hESC and hiPSC were seeded at $1.7 \times 10^4$ cells per square centimeter [30] on BD Matrigel-coated plates and kept in mTeSR1 medium for two days. Rho kinase inhibitor, Y27632 (Chemdea, NJ, USA) [10 μM) was added to the mTeSR1 medium for the first 24 hours. Eight differentiation induction media listed in Figure 1B were introduced to the cells according to the respective groups on day 3 and maintained until day 9. The cells were then replated at $1.7 \times 10^4$ cells per square centimeter onto 0.05 mg/ml collagen-IV–coated plates [22] on day 9 and supplemented with CnT-Prime medium (CELLnTEC, Switzerland) and 10% serum for the next 11 days. Three technical and three biological repeats were set up for each differentiation group.

### Optimization of hiPSC Differentiation Using SB431542

hiPSC were seeded at $1.7 \times 10^4$ cells per square centimeter on BD Matrigel coated plates and kept in mTeSR1 medium for 2 days, with 10 μM Rho kinase inhibitor, Y27632 (Chemdea, NJ, USA) added for the first 24 hours. The SB431542 (10 μM) (Tocris, UK) was added to the differentiation media from day 3 for 1, 2, or 3 days. The cell were replated at $1.7 \times 10^4$ cells per square centimeter onto collagen-IV-coated plates at day 9 and supplemented with CnT-Prime medium (CELLnTEC, Switzerland) and 10% serum for the next 11 days. Three technical and three biological repeats were set up for each differentiation group.

### RNA Extraction, Reverse Transcription, and Quantitative Real-Time Polymerase Chain Reaction

RNA was extracted from the cells collected from differentiating hESC and hiPSC at days 0, 9, and 20 using the ReliaPrep RNA Cell Miniprep System (Promega, WI). The RNA quality was evaluated using the Nanodrop 2000 spectrophotometer (Thermo Fisher Scientific, MA). One microgram of extracted RNA was converted into cDNA using reverse transcription (GoScript Transcription System; Promega, WI) following the manufacturer's instructions. Quantitative real-time polymerase chain reaction (qRT-PCR) was carried out using the QuantStudio 7 Flex Real-Time PCR System (Thermo Fisher Scientific, MA) and GoTaq qPCR Master Mix (Promega, WI) according to manufacturer's instructions. The primer sequences used are listed in Supporting Information Table S1. The data were analyzed using the ΔΔCt calculation method.

 

A

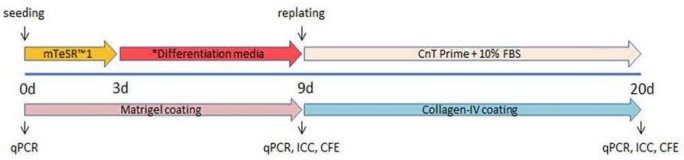


B

| Groups | *Differentiation media (3d – 9d) |
|---|---|
| G1 | Differentiation medium = DMEM-F12 (1:1), N2 (1%), B27 (2%), NEAA (1%), L-glutamine (1%), Pen-Strep (1%) |
| G2 | Differentiation medium + BMP4 (25 µg/ml) |
| G3 | Differentiation medium + All trans retinoic acid (10 mM) |
| G4 | Differentiation medium + EGF (0.5 mg/ml) |
| G5 | Differentiation medium + BMP4 (25 µg/ml), All trans retinoic acid (10 mM), EGF (0.5 mg/ml) |
| G6 | Differentiation medium + SB-505124 (10 mM), IWP-2 (10 mM) |
| G7 | Differentiation medium + SB-505124 (10 mM) , IWP-2 (10 mM), BMP4 (25 µg/ml) |
| G8 | Differentiation medium + LDN193189 (100 uM) |

C

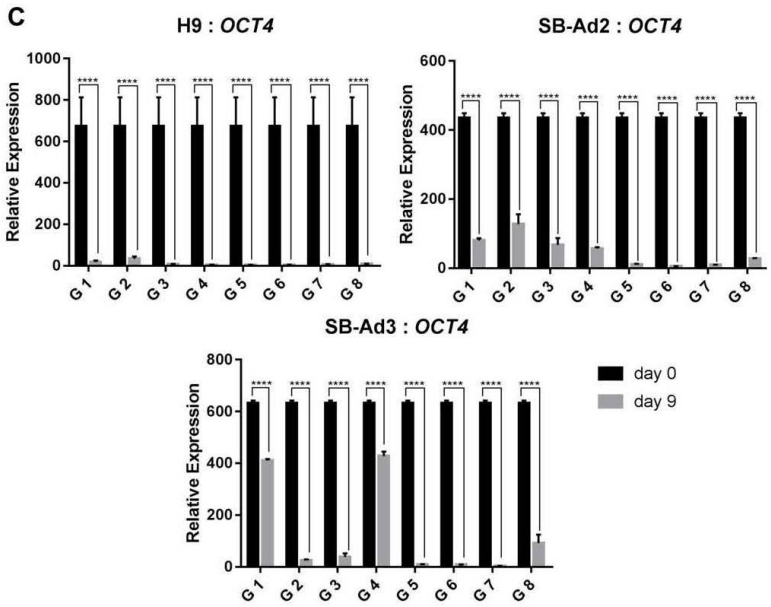


**Figure 1.** Schematic outline of the differentiation process. The differentiation process is divided into two stages, early (days 0–9) and advanced (days 10–20) **(A)**. Endpoint analyses included quantitative real-time polymerase chain reaction (qRT-PCR), immunocytochemistry, and colony forming efficiency. List of differentiation induction media components for each of the eight groups **(B)**. Downregulation of *OCT4* from days 0 to 9 for all the groups in the three cell lines used (H9, SB-Ad2, and SB-Ad3) assessed by qRT-PCR **(C)**. Data are presented as mean ± SEM, $n = 3$. *, statistically different compared with day 0. ****, $p < .0001$. Abbreviations: BMP4, bone morphogenetic protein 4; CFE, colony forming efficiency; EGF, epidermal growth factor; ICC, immunocytochemistry; IWP-2, Wnt antagonist II; qPCR, quantitative polymerase chain reaction.

### Colony Forming Efficiency Assay

3T3 cells were mitotically inactivated with mitomycin C (10 μg/ml) (Sigma-Aldrich, Germany) for 2 hours as described by Ahmad et al. [22]. Then $2.4 \times 10^4$ per square centimeter of the cells were added into each well of the six-well gelatin-coated plates containing fibroblast medium. The plated cells were incubated at 37°C in 5% $CO_2$. The feeder plates were used on the following day. On day 9 or day 20, 1,000 cells from each experimental group were added to each feeder well containing limbal epithelial medium [7]. The limbal epithelial medium was replaced after 3 days and every other day thereafter. The colony forming efficiency (CFE) plates were kept for 14 days. The CFE plates were fixed in 3.7% formaldehyde for 10 minutes at room temperature. The wells were washed with phosphate-buffered saline (PBS) once before enough volume of 1% Rhodamine B (Sigma-Aldrich, Germany) in methanol was added to each well and incubated for 10 minutes. Cell colonies were washed three times with PBS before being observed and counted with the aid of a dissection microscope.

### Immunofluorescence Staining

Cells on day 9 or day 20 of differentiation were dissociated using Tryple express (Gibco, UK) and kept in PBS supplemented with 2% FBS on ice. Cells were cytospun into poly-L-lysine-coated slides, fixed with 4% paraformaldehyde (Sigma-Aldrich, Germany) for 15 minutes. Nonspecific staining was inhibited by blocking in 5% normal goat serum for 1 hour at room temperature. Primary antibody was added overnight at 4°C followed by washes and incubation with a secondary antibody at room temperature in a dark humidified chamber for 1 hour. Slides were protected from light as much as possible after the addition of secondary antibody to avoid bleaching of the fluorescence signal. Following staining, cells were washed three times with PBS, with each wash lasting for 3 minutes. Vectashield mounting medium (Vector Laboratories, Burlingame, CA) with Hoechst (Thermo Fisher Scientific, UK) (1:2,000) was added carefully before mounting the coverslips. A list of antibodies used and all dilutions are presented in Supporting Information Table S2.

### Microscopy

Cell morphology was observed and digital images were taken using a microscope (Zeiss AxioVert 1, Germany). ImageJ software was then used to count the stained and unstained cells from the pictures. Five fields, each containing more than 100 cells, were counted for each group.

### Transfection of BMP Reporter Plasmid

Lipofectamine 3000 reagent (Thermo Fisher, Waltham, MA) was used for BMP reporter plasmid (Addgene, MA) transfection. Cells were disassociated by incubating with EDTA (0.02%) for 5 minutes. The disassociated cells were collected and centrifuged at 500*g* for 5 minutes. The cell pellet was resuspended into 2 ml of media and cell count was performed before replating cells at the density of $1.3 \times 10^5$ cells into one well of a BD Matrigel coated 24 well plate one day before lipofection. For plasmid lipofection, 500 ng of pGL3-Basic or pGL3 BRE Luciferase (Promega, Madison, WI) were used to transfect the cells in each well of 24-well plate following manufacturer's recommendations. Cells that were transfected with empty vector (pGL3-Basic) or BMP reporter (pGL3 BRE Luciferase) were cotransfected with empty Renilla vector (pRL-Null) (Promega, Madison, WI).

### Luciferase Assays

Transfected cells were cultured in mTeSR1 alone or mTeSR1 supplemented with BMP4 or BMP4 and SB431542. Cell extracts were prepared 48 hours after transfection using a passive lysis buffer. Luciferase activities were evaluated with a Dual-Luciferase Assay System (Promega, Madison, WI) according to the manufacturer's recommendations using Varioskan LUX plate reader (Thermo Fisher Scientific, Waltham, MA). Background luminescence was determined using untransfected cells and the background readings were then subtracted from the resulting luminescence readings before being normalized to Renilla luminescence and presented as relative luminescence unit.

### Statistical Analysis

Statistical analysis was performed with one-way analysis of variance analysis with GraphPad Prism 7 software. Unless otherwise stated in all figures data are shown as mean ± SEM ($n = 3$). *, $p < .05$; **, $p < .01$; ***, $p < .001$; ****, $p < .0001$.

## Results

### Differentiation of hESC and hiPSC to Corneal Epithelial Progenitors

One hESC (H9) and two hiPSC (SB-Ad2 and SB-Ad3) lines were directed to differentiate to corneal epithelial-like cells using a two stage differentiation protocol which aimed at generating corneal epithelial progenitors (days 0–9) and their further differentiation to mature corneal epithelial cells (days 10–20). In the first 9 days, the serum-free medium was supplemented with a range of growth factors and signaling molecules which included BMP4 and all-trans retinoic acid (RA) known to promote non-neural ectodermal differentiation [31, 32], and epidermal growth factor (EGF) which stimulates the proliferation of corneal epithelial progenitors [33]. Inhibition of Wnt and transforming growth factor (TGF) β pathway have been reported to be necessary for guiding differentiation of hESC and hiPSC to a ventral neural fate and eye field determination; hence, we included IWP-2, a Wnt/β-catenin pathway inhibitor, and SB505124, a selective TGFβ type 1 receptor inhibitor, either on their own or in combination with BMP4 in groups 6 and 7, respectively [27]. We also included one additional group with a BMP pathway inhibitor (LDN 193189) to control for the impacts of BMP4, which we used to induce commitment to non-neural ectoderm. A total of seven combinations of growth factors and signaling molecules were tested, along with the basal medium alone in three independent differentiation experiments for each cell line. The differentiation induction media and the plate coating were changed on day 9 to CnT-Prime with 10% fetal bovine serum and collagen-IV coating, respectively, to promote the differentiation of corneal epithelial progenitors into mature corneal epithelial-like cells. A Schematic outline of the differentiation protocol is detailed in Figure 1A and 1B.

We noticed similar morphological changes observed for both hESCs and hiPSC (Supporting Information Fig. S1A–S1C). The experimental groups 2, 3, and 5 showed the most

 

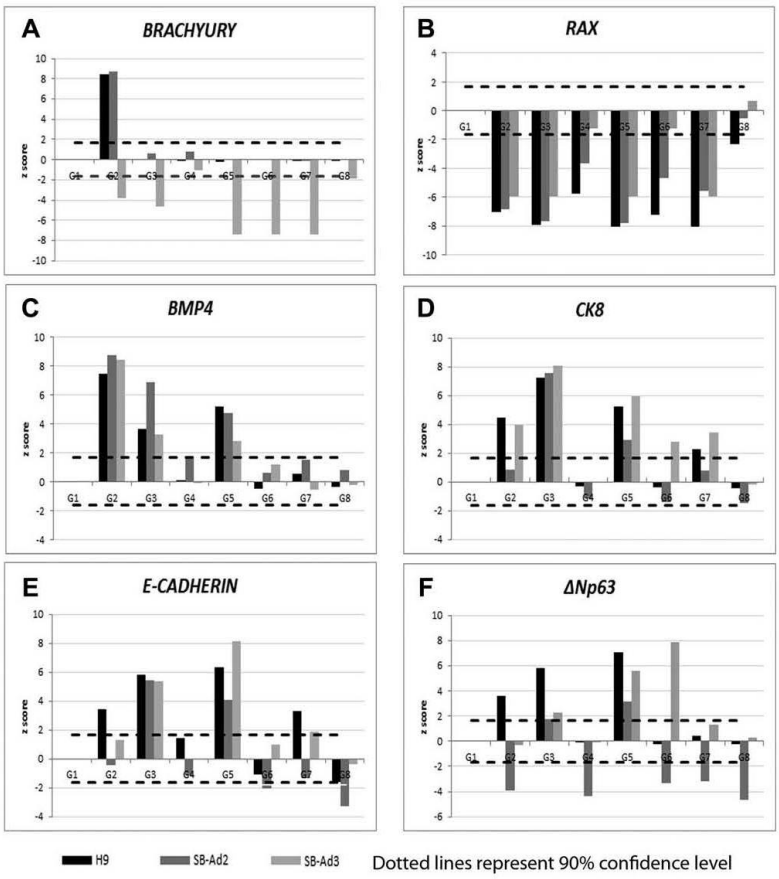


**Figure 2.** Bone morphogenetic protein 4 (BMP4), retinoic acid, and epidermal growth factor improve early corneal/limbal differentiation process. Quantitative real-time polymerase chain reaction analysis of *BRACHYURY, RAX, BMP4, CK8, ECADHERIN,* and *ΔNp63* genes for groups G2–G8 compared with control group (G1) presented as z scores **(A–F)**. z score was calculated using the following formula: z score = D/SEM where D is the difference between the two means and SEM is the standard error of mean (computed from the data). Dotted lines represent 90% confidence level. Abbreviation: BMP4, bone morphogenetic protein 4.

differentiated morphology typical of epithelial cells on day 9 for both hESC and hiPSC (Supporting Information Fig. S1A–S1C, black arrows). The differentiated cells grew into pockets of flatter and larger cells with higher cytoplasm to nucleus ratio in between the smaller undifferentiated stem cells, corroborating similar observations published by Xu et al. [34]. In contrast, most cells in the experimental groups 1, 4, 6, and 8 proliferated robustly and retained the small and compact cell appearance. qRT-PCR analysis indicated that on day 9, all experimental groups across hESC and hiPSC differentiations were associated with loss of the pluripotent phenotype as shown by a significant decrease in the expression of *OCT4* (Fig. 1C).

To assess the differentiation efficiency and compare the effects of media supplementation across the eight groups, qRT-PCR analysis was carried out at day 9 of differentiation. The results for each group were compared with the control group (G1) which contained no growth factors or small molecules supplementation and presented as z scores. Addition of BMP4 has been associated with differentiation of hESC and hiPSC to mesodermal lineages [35]; however, a significant increase in the expression of mesodermal marker, *BRACHYURY* was only observed in the hESC (H9) and one hiPSC line (SB-Ad2; Fig. 2A) upon BMP4 treatment (Group 2). The expression of *RAX*, a gene expressed in the eye primordia and required for retinal cell fate determination [36], was significantly downregulated in groups 2–7 for both hESC and hiPSC, thus indicating that in all these groups, the differentiation to neuroectodermal lineages was avoided (Fig. 2B). *BMP4* is expressed in early ectodermal tissue [32, 37] and is often used as marker of non-neural ectoderm, developing cornea and lens. Our qRT-PCR analysis indicated a significant upregulation of *BMP4* in experimental groups 2, 3, and 5 of hESC and two hiPSC (Fig. 2C), suggesting that the differentiation factors added to these three groups encouraged differentiation to non-neural ectoderm [30]. The expression of

 

ectodermal cytokeratin 8 (*CK8*), basal, and suprabasal corneal epithelium (*E-CADHERIN*) and putative LSCs (*ΔNp63*) markers were all significantly increased in experimental groups 3 and 5 of both hESCs and hiPSC (Fig. 2D–2F), indicating a likely commitment of these groups to corneal epithelial progenitors.

The z scores from the qRT-PCR analysis consistently indicated that the experimental groups that were supplemented with BMP4, RA, and a combination of BMP4, RA, and EGF showed a significant upregulation of non-neural ectoderm, epithelial, cell junction, and putative LSC markers. Therefore, we went on to analyze these groups by immunostaining for the expression of putative LSCs protein, ΔNp63. No significant differences between the control nonsupplemented groups and the ones that received BMP4, RA, and a combination of BMP4, RA, and EGF were found (Fig. 3A, 3B). These immunostaining results do not corroborate the qRT-PCR analysis and a possible reason for this may be the post-translational modifications already reported for the p63 protein [38]. Expression of PAX6, a marker of neuroectodermal [39], anterior placodal ectoderm, and developing eye and lens, was significantly highest in groups treated with RA and a combination of BMP4, RA, and EGF for the differentiating hESC and one of the hiPSC (Fig. 3B).

CFE was highest in experimental groups 2 and 5 of hESC and one of the hiPSC lines (SB-Ad2, Fig. 3C), suggesting that supplementation of basic media with BMP4 or a combination of BMP4, RA, and EGF provides an optimal combination for directing differentiation of hESC and hiPSC to corneal epithelial progenitor cells. Notwithstanding, no significant difference in CFE ability was observed between the four experimental groups tested in the second hiPSC line (SB-Ad3), indicating significant differences between the hiPSC lines in their response to our differentiation protocols and the need for further culture modifications for nonresponsive hiPSC lines.

### Differentiation of hESC and hiPSC to Corneal Epithelial-Like Cells

During the second differentiation window (days 10–20), we aimed at promoting the maturation of corneal epithelial progenitors to epithelial cells by replating on collagen-IV coated plates and feeding the cells with a specific corneal differentiation medium (CnT-Prime) supplemented with 10% serum (Fig. 1A). Similar morphological changes were observed in both hESC and hiPSC during this time window (Fig. 4A; Supporting Information Figs. 2A, 3A). Cells appeared larger and flatter and characterized by an epithelial-like morphology by the end of the experiment on day 20. qRT-PCR analysis showed that the combination of RA, BMP4, and EGF (group 5) was associated with the greatest upregulation of putative LSC marker (*ΔNp63*) across the cell lines (Fig. 4B; Supporting Information Figs. 2B, 3B). Expression of *ABCG2*, which was reported as another putative LSCs marker [40], was also consistently highest in groups supplemented with RA across the cells lines. Differentiated corneal epithelial cytokeratin, *CK3* expression was more variable across the cell lines, with the highest expression observed in BMP4 supplemented group for hESC, RA supplemented group for hiPSC-SB-Ad3 and RA and RA, BMP4, and EGF supplemented group for hiPSC-SB-Ad2. *CK12* expression was consistently highest in the groups supplemented with RA, BMP4, and EGF. Together, these data suggest some intra-line differences in the capacity to mature toward corneal epithelial-like cells.

Immunostaining analysis at day 20 revealed a significant upregulation of ΔNp63 expression in groups supplemented with BMP4, RA, and EGF across the hESC and hiPSC lines (Fig. 5A). It needs to be noted though that the expression of this marker decreased from day 9 of differentiation, indicating further differentiation of these cells to CK3 and CK12 expressing corneal epithelial cells as shown in Supporting Information Figure 4A and 4B. CFE assays also showed that the BMP4, RA, and EGF supplemented group in hESC resulted in the highest colony forming ability which was similar to human limbal epithelial progenitor cells (Fig. 5B). All the selected groups of one of the hiPSC lines (SB-Ad2) showed an increased CFE ability compared with control group; however, this was considerably lower than human limbal epithelial progenitor cells (Fig. 5B). In contrast, all the treated groups from the second hiPSC line (SB-Ad3) showed a very low CFE ability and no difference to the untreated control group, indicating a lack of response from this cell line to differentiation factors added during the 20 day time window.

### Differences in the Activity of Endogenous BMP Signaling Pathway Between Responsive and Nonresponsive hiPSC Lines

This study data and others indicate that BMP4 is a key driver of pluripotent stem cell differentiation toward non-neural ectoderm [41, 42]. Since one of the hiPSC lines was not responsive to the differentiation method, we investigated whether differences in the endogenous activity of BMP pathway between hiPSC lines could be the underlying mechanism. We first carried out qRT-PCR analysis which indicated that although the nonresponsive hiPSC line (SB-Ad3) expressed higher levels of endogenous *BMP4* when compared with the responsive hiPSC line, SB-Ad2 (Supporting Information Fig. S5), the expression of key receptors (*BMPR1A* and *BMPR1B*) and receptor activated *SMAD1* and *SMAD5* genes that mediate BMP signaling were significantly lower, suggesting that this hiPSC line may be characterized by a much lower level of endogenous BMP activity. This is further corroborated by low expression of two BMP target genes, *ID1* and *JUNB*, which were expressed at a lower level in the nonresponsive hiPSC line when compared with the responsive line. Since both the receptor and effector genes expressions are lower, addition of exogenous BMP4 alone (as in our differentiation methods), is unlikely to activate the pathway in the nonresponsive hiPSC line.

To confirm this further, a BMP reporter plasmid was transfected in both hiPSC lines causing a transient overexpression of BMP specific gene, *ID1* [43]. The reporter analyses showed that the SB-Ad3 iPSC line has a significantly lower endogenous BMP activity compared with SB-Ad2 iPSC (Supporting Information Fig. S6A). Addition of BMP4 increased the BMP activity of both hiPSCs; however, SB-Ad3 iPSC still lagged behind SB-Ad2 (Supporting Information Fig. S6B). Combined addition of BMP4 and SB435142 did not have a significant impact on SB-Ad2; however, it increased the endogenous BMP activity of Sb-Ad3 hiPSC to the same levels as SB-Ad3 (Supporting Information Fig. S6B).

### Specific TGFβ Inhibitor, SB431542, Induces the Differentiation of Nonresponsive hiPSC Lines to Corneal Epithelial Cells

Given the low level of BMP receptor and effector expression in the nonresponsive hiPSC line, we aimed to improve the

 

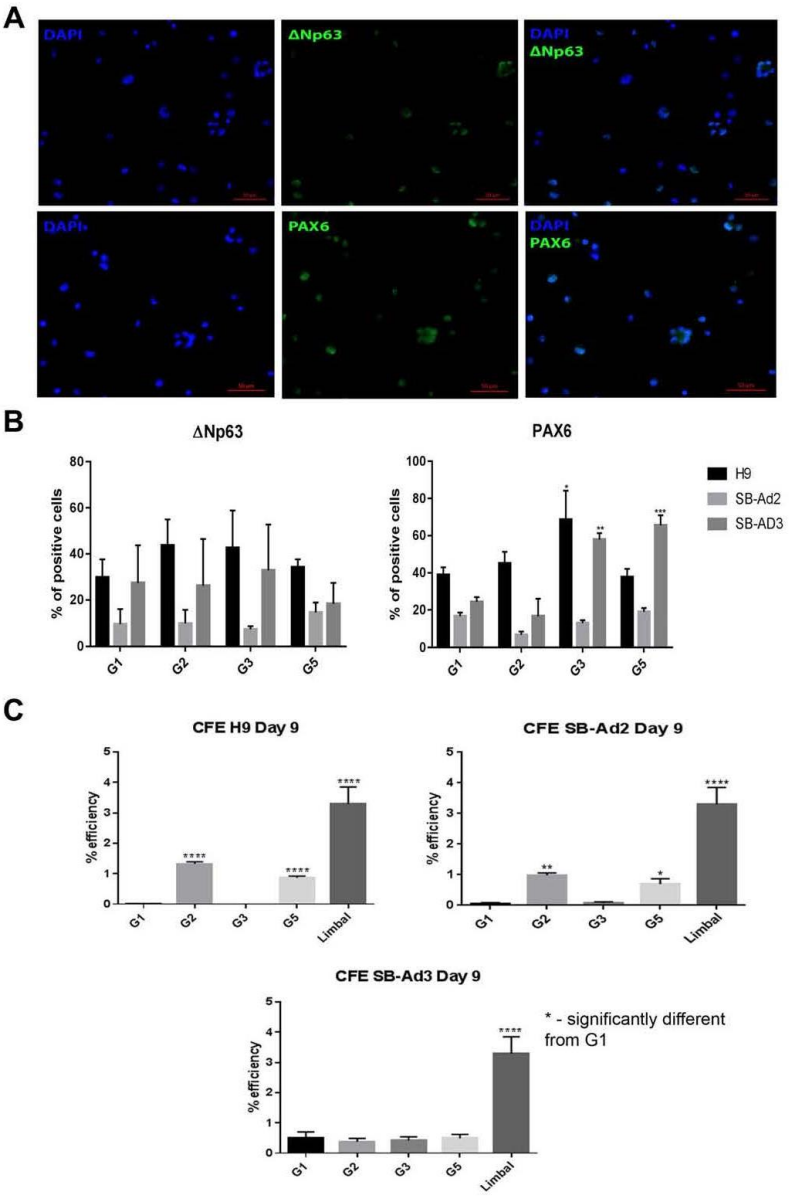


**Figure 3.** ΔNp63 protein expression and colony forming efficiency. Immunocytochemistry analyses for differentiated cells on day 9 for G1, G2, G3, and G5. Representative immunofluorescence images showing positive ΔNp63 and PAX6 nuclear staining in G3 of H9 cells **(A)** and percentage of ΔNp63 and PAX6 positive cells for H9, SB-Ad2, and SB-Ad3 **(B)**. Colony forming efficiency assays for the three cell lines on day 9 for G1, G2, G3 G5, and human limbal epithelium **(C)**. Scale bar = 50 μm. Data are presented as mean ± SEM, $n = 3$. *, statistically different compared with G1. *, $p < .05$; **, $p < .01$; ***, $p < .001$; ****, $p < .0001$. Abbreviations: CFE, colony forming efficiency; DAPI, 4′,6-diamidino-2-phenylindole.

differentiation method by altering the co-SMAD/r-SMAD interaction in the cytoplasm. Since co-SMAD (SMAD4) is shared between TGFβ and BMP pathways [44, 45], we focused on the inhibition of the TGFβ pathway which should lead to an increase in the availability of SMAD4 for the BMP pathway. To achieve this, a selective TGFβ inhibitor, SB431542, which has been reported to drive differentiation away from neuroectoderm [35] and to activate the BMP pathway [46], was

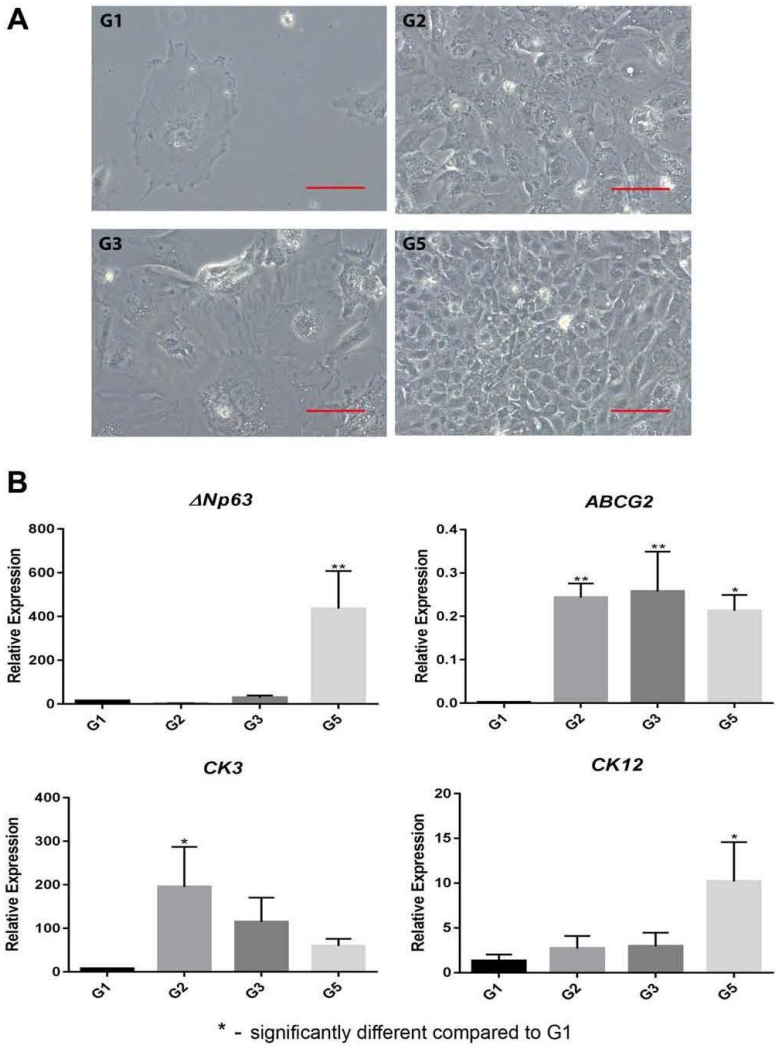


**Figure 4.** Cell morphology at advanced stage of differentiation and molecular characterization. Differentiated G1, G2, G3, and G5 of H9 cells morphological appearance on day 20 **(A)**, and quantitative real-time polymerase chain reaction analysis of corneal and limbal epithelial genes **(B)**. Data are presented as mean ± SEM, $n = 3$. Scale bar = 50 μm. *, statistically different compared with G1. *, $p < .05$; **, $p < .01$.

used. SB431542 (10 μM) was added for 1, 2, and 3 days to the differentiation media in combination with BMP4, RA, and EGF as detailed in Figure 6A. qRT-PCR analysis at day 20 indicated the highest expression of *ΔNp63* in groups treated for 2 and 3 days with SB431542 (Fig. 6B). Interestingly, only the group treated for 3 days with SB431542 showed enhanced CFE ability to similar levels observed with human limbal epithelial progenitor cells (Fig. 6C), suggesting that continuous inhibition of TGFβ pathway for 3 days with this specific TGFβ inhibitor, can result in differentiation of nonresponsive hiPSC lines to corneal epithelial progenitor cells (please refer to graphical abstract). It is of interest to note that SB431542 on its own was not able to achieve the upregulation of *ΔNp63* observed after combined addition of BMP4 and SB431542 (Fig. 6B).

## Discussion

Efficient differentiation of a large numbers of hESC and hiPSC for autologous cell replacement therapies using robust and fast protocols has become an important aim for most researchers in the field. In this paper, we report a feeder-free, two-step method that results in differentiation of hESC to corneal epithelial progenitors and mature corneal epithelial-like cells within 20 days. Previous studies in the field have

 

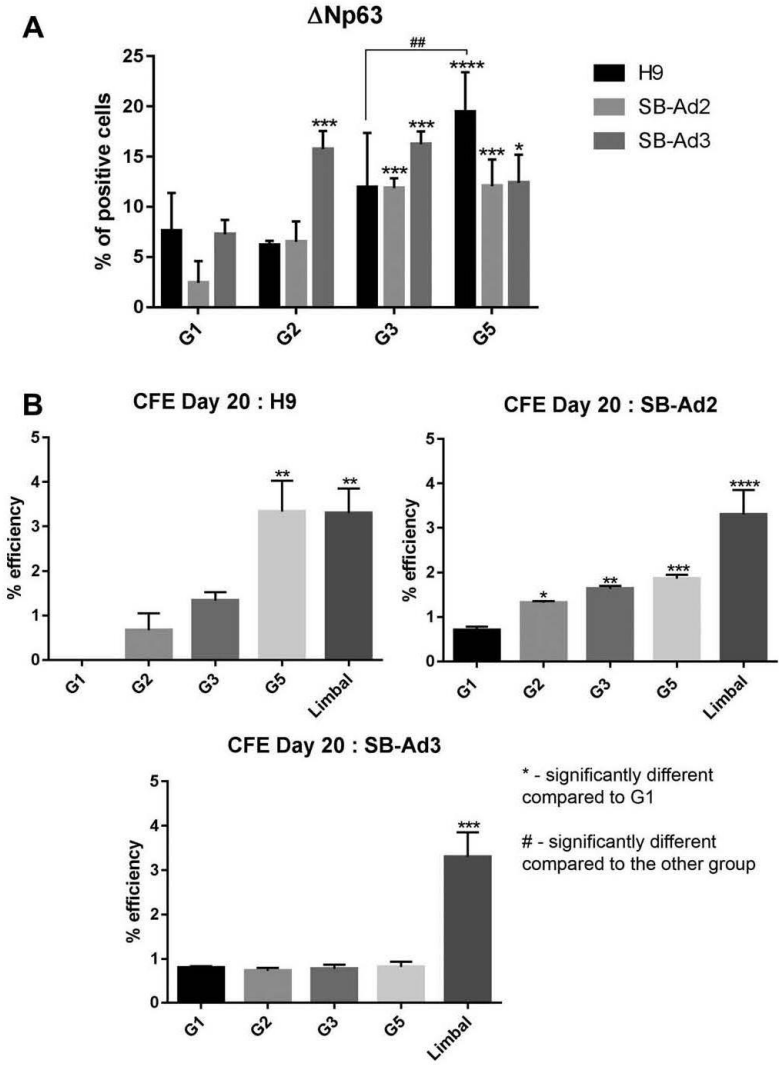


**Figure 5.** ΔNp63 protein expression and colony forming efficiency at day 20 of differentiation. Percentage of ΔNp63 positive cells for H9, SB-Ad2, and SB-Ad3 cells on day 20 for G1, G2, G3, and G5 **(A)**. Colony forming efficiency for the three cell lines on day 20 for G1, G2, G3 G5, and human limbal epithelium **(B)**. Data are presented as mean ± SEM, $n = 3$. *, statistically different compared with G1 of the same cell line. *, $p < .05$; **, $p < .01$; ***, $p < .001$; ****, $p < .0001$. #, statistically different compared with the other group; ##, $p < .01$. Abbreviation: CFE, colony forming efficiency.

replicated early developmental mechanisms by blocking the TGFβ and Wnt-signaling pathways with small-molecule inhibitors and activating fibroblast growth factor (FGF) signaling [27] to generate corneal epithelial-like progenitor cells capable of terminal differentiation toward mature corneal epithelial-like cells within 44 days. TGF-β pathway has been shown to play multiple roles in maintenance of pluripotency and early cell fate decisions. Work done by other groups [47] and this group [48] has shown that low activity of this pathway (either through application of inhibitors or low endogenous activity) results in neuroectodermal default pathway which skews pluripotent stem cells away from non-neural ectoderm and corneal epithelial differentiation. For this reason, we designed our differentiation protocol to include growth factors and morphogens (BMP4, RA, and EGF) that have been shown to promote non-neural ectodermal commitment [31, 32, 49, 50] and proliferation of corneal epithelial progenitors. In the second window of differentiation, we attempted to replicate the LSCs niche by coating the cell surfaces with collagen-IV shown to be the key component of limbal stroma and [51, 52] and

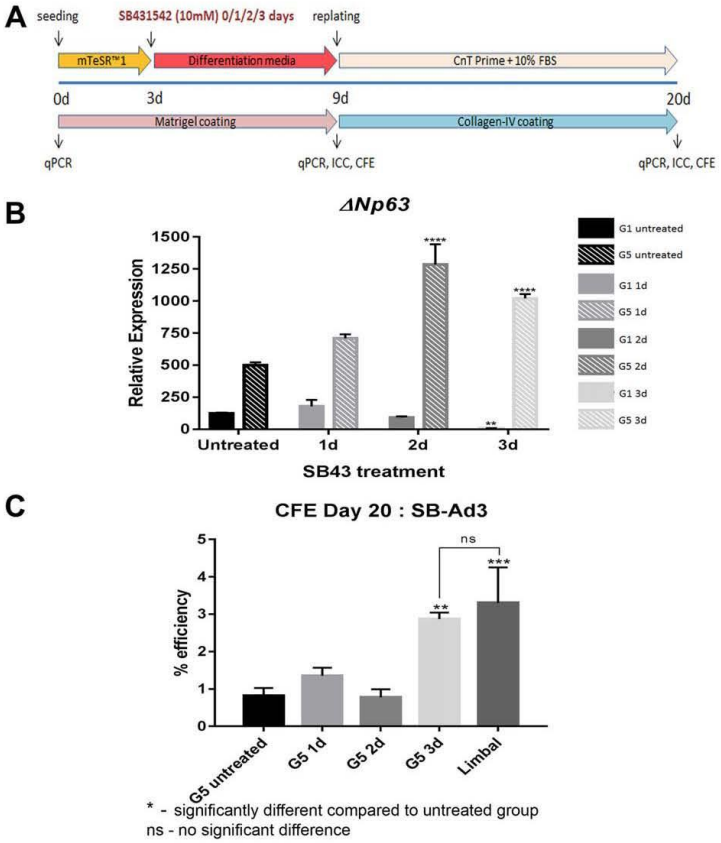


**Figure 6.** SB431542 exposure during early differentiation enhanced the hiPSC differentiation to corneal epithelial progenitors. Schematic outline for optimization experiment using SB431542 **(A)**. Quantitative real-time polymerase chain reaction analysis of the putative limbal stem cells (*ΔNp63*) gene for SB-Ad3 cells from G5 subgroups on day 20 of optimization experiment following different durations of SB431542 exposure **(B)**. Colony forming efficiency assays for the SB431542 exposed and unexposed G5 subgroups on day 20 **(C)**. Data presented as mean ± SEM, $n = 3$. *, statistically different compared with untreated group. **, $p < .01$; ***, $p < .001$; ****, $p < .0001$. ns, no significant difference. Abbreviations: CFE, colony forming efficiency; ICC, immunocytochemistry; FBS, fetal bovine serum; qPCR, quantitative polymerase chain reaction.

feeding the cells with a defined media (CnT-Prime) which is used to maintain the ex vivo expansion of human corneal epithelial progenitors [53]. This two-step differentiation protocol resulted in successful generation of hESC-derived corneal epithelial progenitors with colony forming ability similar to limbal epithelial progenitors within a window of 20 days.

Since the main aim of this study was to design robust differentiation protocols for differentiation of hiPSC to corneal epithelial-like cells for autologous cell replacement therapies, we tested the two-step differentiation protocol in two hiPSC lines generated and well characterized by our laboratory [54]. One of the hiPSC lines was able to generate corneal epithelial progenitors with colony forming ability in response to BMP4, RA, or combined addition of BMP4, RA, and EGF, although at lower levels than hESC. In contrast, the second tested hiPSC line was not able to respond to the step differentiation protocol resulting in low levels of corneal epithelial progenitor generation. Differences in transcriptional and epigenetic profiles between hiPSC lines which are linked to their differentiation capacity are commonly encountered, especially during directed differentiations, where specific molecules were used to alter the pathways of interest. A study published by our group indicated that hiPSC lines that possess higher level of mitochondrial protein CHCHD2, have a less active TGFβ signaling activity, making them more prone to neural differentiation [48]. A recent report by Nishizawa et al. also indicated that haematopoietic commitment of hiPSC lines depends on the expression of insulin-like growth factor 2 (IGF2) [55]. Earlier, Fujiwara et al. found variations in the basal cardiomyocyte differentiation efficiency of hiPSC lines which was overcomed by using Cyclosporin-A [56]. Together, these studies suggest that differentiation protocols may need to be adjusted to take into account the endogenous expression of key transcription and growth factors as well as signaling pathways that govern early differentiation steps.

 

Endogenous BMP signaling activity is different in various hiPSC lines and crosstalk between BMP and TGFβ signaling has also been reported [57], affecting the propensity of each cell line during differentiation process. Given the importance of BMP4 signaling in inhibiting neural differentiation and promoting epidermal commitment of embryonic stem cells [32, 58, 59], we investigated the level of endogenous BMP pathway activity using reporter based assays and qRT-PCR. These experiments indicated that the nonresponsive hiPSC line had lower level of BMP signaling activity which was caused by a lower expression of effectors and receptors, resulting in low expression of BMP target genes. To restore the differentiation potential we used a specific TGFβ inhibitor, SB431542, which changed the balance of co-SMADS into the favor of BMP signaling resulting in successful differentiation of the nonresponsive hiPSC to corneal epithelial progenitors. Our findings closely corroborate those published by Shalom-Feuerstein et al. [42] who reported improved differentiation of hiPSC to epidermal lineages upon addition of SB431542 to BMP4 and ascorbic acid supplemented media. A different small molecule TGFβ inhibitor was used by Mikhailova et al. to guide differentiation of hiPSC to corneal epithelial progenitor cells in combination with a Wnt inhibitor, IWP-2, and FGF [27]. Although SB505124 is reported to be more selective than SB431542 for inhibiting TGFβ signaling [60], the supplementation of the former inhibitor and IWP-2 alone or in combination with BMP4 in our setting failed to activate expression of key epithelial and LSCs markers, suggesting crosstalk between signaling pathways is essential for guiding differentiation of pluripotent stem cells to corneal epithelial lineages.

Similarly to other published studies in the field, our method generated a high percentage of ΔNp63-positive cells in the first window of differentiation which went on to further mature to CK3 and CK12 positive corneal epithelial cells. In addition, this study indicated that the hESC and hiPSC derived epithelial progenitors have a high colony forming efficiency which was comparable with limbal epithelial progenitor cells obtained from adult human cornea.

## Conclusion

In summary, this article describes a new two-step differentiation method with which minor modifications can be applied to generate corneal epithelial progenitor cells in a short time from a large range of hESC and hiPSC. However, further work in animal models of total LSCD needs to be carried out to test the engraftment and functionality of hESC- and hiPSC-derived corneal epithelial progenitor cells.

## Acknowledgments

This work was supported by FP7 Ideas: European Research Council (ERC) (614620), Medical Research Council (MRC UK) (G0900879), CiC (MC_PC_15030), Inovative Medicine Initiative (IMI) (115439: StemBANCC), studentship awarded from the Ministry of Education, Malaysia and Universiti Kebangsaan Malaysia (TAK). NHSBT provided the human corneal epithelial tissue.

## Author Contributions

T.A.K.: performed laboratory work, data analysis and interpretation, manuscript writing, final approval of manuscript, S.B., J.C., M.Y., S.A., and H.B.: performed laboratory work and collection and/or assembly of data, final approval of manuscript; A.S., L.A., and F.C.F.: conception/design and fund raising, final approval of manuscript; M.L.: conception/design,data analysis and interpretation,manuscript writing, final approval of manuscript.

## Disclosure of Potential Conflicts of Interest

The authors indicated no potential conflicts of interest.

## References

1 Schlotzer-Schrehardt U, Kruse FE. Identification and characterization of limbal stem cells. Exp Eye Res 2005;81:247–264.

2 Li W, Hayashida Y, Chen YT et al. Niche regulation of corneal epithelial stem cells at the limbus. Cell Res 2007;17:26–36.

3 Lu L, Reinach PS, Kao WWY. Corneal epithelial wound healing. Exp Biol Med 2001; 226:653–664.

4 Hay ED. Development of the vertebrate cornea. Int Rev Cytol 1980;63:263–322.

5 Amano S, Satoru Y, Tatsuya M et al. Corneal stromal and endothelial cell precursors. Cornea 2006;25:S73–S77.

6 Dua H, Saini J, Azuara-Blanco A, Gupta P. Limbal stem cell deficiency: Concept, aetiology, clinical presentation, diagnosis and management. Indian J Ophthalmol 2000;48: 83–92.

7 Kolli S, Ahmad S, Lako M et al. Successful clinical implementation of corneal epithelial stem cell therapy for treatment of unilateral limbal stem cell deficiency. Stem Cells 2010;28: 597–610.

8 Rama P, Bonini S, Lambiase A et al. Autologous fibrin-cultured limbal stem cells permanently restore the corneal surface of patients with total limbal stem cell deficiency. Transplantation 2001;72:1478–1485.

9 Dua H, Azuara-Blanco A. Autologous limbal transplantation in patients with unilateral corneal stem cell deficiency. Br J Ophtalmol 2000;84:273–278.

10 Inatomi T, Nakamura T, Koizumi N et al. Midterm results on ocular surface reconstruction using cultivated autologous oral mucosal epithelial transplantation. Am J Ophthalmol 2006;141:267–275.

11 Nishida K, Yamato M, Hayashida Y et al. Corneal reconstruction with tissue engineered cell sheets composed of autologous oral mucosal epithelium. N Engl J Med 2004; 351:1187–1196.

12 Burillon C, Huot L, Justin V et al. Cultured autologous oral mucosal epithelial cell sheet (CAOMECS) transplantation for the treatment of corneal limbal epithelial stem cell deficiency. Invest Ophthalmol Vis Sci 2012;53:1325–1331.

13 Hirayama M, Satake Y, Higa K et al. Transplantation of cultivated oral mucosal epithelium prepared in fibrin-coated culture dishes. Invest Ophthalmol Vis Sci 2012;53: 1602–1609.

14 Sotozono C, Inatomi T, Nakamura T et al. Visual improvement after cultivated oral mucosal epithelial transplantation. Ophthalmology 2013;120:193–200.

15 Chen H, Chen H, Lai J et al. Persistence of transplanted oral mucosal epithelial cells in human cornea. Invest Ophthalmol Vis Sci 2009;50:4660–4668.

16 Ma DHK, Kuo MT, Tsai YJ et al. Transplantation of cultivated oral mucosal epithelial cells for severe corneal burn. Eye 2009; 23:1442–1450.

17 Sheth R, Neale M, Shortt A et al. Culture and characterization of oral mucosal epithelial cells on a fibrin gel for ocular surface reconstruction. Curr Eye Res 2015;40:1077–1087.

18 Kolli S, Ahmad S, Mudhar HS et al. Successful application of ex vivo expanded

 

human autologous oral mucosal epithelium for the treatment of total bilateral limbal stem cell deficiency. Stem Cells 2014;32:2135–2146.
19 Takahashi K, Tanabe K, Ohnuki M et al. Induction of pluripotent stem cells from adult human fibroblasts by defined factors. Cell 2007;131:861–872.
20 Lewitzky M, Yamanaka S. Reprogramming somatic cells towards pluripotency by defined factors. Curr Opin Biotechnol 2007; 18:467–473.
21 Tucker BA, Mullins RF, Stone EM. Stem cells for investigation and treatment of inherited retinal disease. Human Mol Genet 2014;23:R9–R16.
22 Ahmad S, Stewart R, Yung S et al. Differentiation of human embryonic stem cells into corneal epithelial-like cells by in vitro replication of the corneal epithelial stem cell niche. Stem Cells 2007;25:1145–1155.
23 Hanson C, Hardarson T, Ellerström C et al. Transplantation of human embryonic stem cells onto a partially wounded human cornea in vitro. Acta Ophthalmol 2013;91: 127–130.
24 Hayashi R, Ishikawa Y, Ito M et al. Generation of corneal epithelial cells from induced pluripotent stem cells derived from human dermal fibroblast and corneal limbal epithelium. PLoS One 2012;7:e45435.
25 Hewitt K, Shamis Y, Carlson M et al. Three-dimensional epithelial tissues generated from human embryonic stem cells. Tissue Eng Part A 2009;15:3417–3426.
26 Shalom-Feuerstein R, Serror L, De La Forest Divonne S et al. Pluripotent stem cell model reveals essential roles for miR-450b-5p and miR-184 in embryonic corneal lineage specification. Stem Cells 2012;30:898–909.
27 Mikhailova A, Ilmarinen T, Uusitalo H et al. Small-molecule induction promotes corneal epithelial cell differentiation from human induced pluripotent stem cells. Stem Cell Rep 2014;2:219–231.
28 Mikhailova A, Ilmarinen T, Ratnayake A et al. Human pluripotent stem cell-derived limbal epithelial stem cells on bioengineerd matrices for corneal reconstruction. Exp Eye Res 2016;146:26–34.
29 Baud A, Wessely F, Mazzacuva F et al. Multiplex high-throughput targeted proteomic assay to identify induced pluripotent stem cells. Anal Chem 2017;89:2440–2448.
30 Leung AW, Morest DK, Li JYH. Differential BMP signalling controls formation and differentiation of Multipotent preplacodal ectoderm progenitors from human embryonic stem cells. Dev Biol 2013;379:208–220.
31 Aberdam D, Gambaro K, Rostagno P et al. Key role of p63 in BMP-4-induced epidermal commitment of embryonic stem cells. Cell Cycle 2007;6: 291–294.
32 Metallo CM, Ji L, De Pablo JJ et al. Retinoic acid and bone morphogenetic protein signaling synergize to efficiently direct epithelial differentiation of human embryonic stem cells. Stem Cells 2008;26:372–380.
33 Li T, Lu L. Epidermal growth factor-induced proliferation requires down-regulation of Pax6 in corneal epithelial cells. J Biol Chem 2005;280:12988–12995.
34 Xu RH, Chen X, Li DS et al. BMP4 initiates human embryonic stem cell differentiation to trophoblast. Nat Biothechnol 2002; 20:1261–1264.
35 Li L, Song L, Liu C et al. Ectodermal progenitors derived from epiblast stem cells by inhibition of nodal signalling. J Mol Cell Biol 2015;0:1–11.
36 Furukawa T, Kozak CA, Cepko CL. RAX, a novel paired-type homeobox gene, shows expression in the anterior neural fold and developing retina. Proc Natl Acad Sci USA 1997;94:3088–3093.
37 Bothe I, Tenin G, Oseni A et al. Dynamic control of head mesoderm patterning. Development 2011;138:2807–2821.
38 Li C, Xiao Z. Regulation of p63 protein stability via ubiquitin-proteasome pathway. BioMed Res Int 2014;2014:1. Article ID 175721, 8 pages, 2014.
39 Zhang X, Huang CT, Chen J et al. Pax6 is a human neuroectoderm cell fate determinant. Cell Stem Cell 2010;7:90–100.
40 Morita M, Fujita N, Takahashi A et al. Evaluation of ABCG2 and p63 expression in canine cornea and cultivated corneal epithelial cells. Vet Ophthalmol 2015;18: 59–68.
41 Schuldiner M, Yanuka O, Itskovitz-Eldor J et al. Effects of eight growth factors on the differentiation of cells derived from human embryonic stem cells. Proc Natl Acad Sci USA 2000;97: 11307–11312.
42 Shalom-Feuerstein R, Serror L, Aberdam E et al. Impaired epithelial differentiation of induced pluripotent stem cells from ectodermal dysplasia-related patients is rescued by the small compound APR-246/PRIMA-1MET. Proc Natl Acad Sci USA 2013;110:2152–2156.
43 Korchynskyi O, ten Dijke P. Identification and functional characterization of distinct critically important bone morphogenetic protein-specific response elements in the Id1 promoter. J Biol Chem 2002;277:4883–4891.
44 Wrana JL, Attisano L. The Smad pathway. Cytokine Growth Factor Rev 2000;11:5–13.
45 Wu MY, Hill CS. TGF-b superfamily signalling in embryonic development and homeostasis. Dev Cell 2009;16:329–343.
46 Du J, Wu Y, Ai Z et al. Mechanism of SB431542 in inhibiting mouse embryonic stem cell differentiation. Cell Signal 2014;26: 2107–2116.
47 Vallier L, Reynolds D, Pedersen R. Nodal inhibits differentiation of human embryonic stem cells along the neuroectodermal default pathway. Dev Biol 2004;275:403–421.
48 Zhu L, Gomez-Duran A, Saretzki G et al. The mitochondrial protein CHCHD2 primes the differentiation potential of human induced pluripotent stem cells to neuroectodermal lineages. J Cell Biol 2016;215:187–202.
49 Gambaro K, Aberdam E, Virolle T et al. BMP-4 induces a Smad-dependent apoptotic cell death of mouse embryonic stem cell-derived neural precursors. Cell Death Diff 2006;13:1075–1087.
50 Massague J. Integration of Smad and MAPK pathways: A link and a linker revisited. Genes Dev 2003;17:2993–2997.
51 Schlötzer-Schrehardt U, Dietrich T, Saito K et al. Characterization of extracellular matrix components in the limbal epithelial stem cell compartment. Exp Eye Res 2007;85:845–860.
52 Blazejewska E, Schlotzer-Schrehardt U, Zenkel M et al. Corneal limbal microenvironment can induce transdifferentiation of hair follicle stem cells into corneal epithelial-like cells. Stem Cells 2009;27:642–652.
53 González S, Chen L, Deng S. Comparative study of xenobiotic-free media for the cultivation of human limbal epithelial stem/progenitor cells. Tissue Eng Part C Methods 2017;23:219–227.
54 Van De Bunt M, Lako M, Barrett A et al. Insights into islet development and biology through characterization of a human iPSC-derived endocrine pancreas model. Islets 2016;8:83–95.
55 Nishizawa M, Chonabayashi K, Nomura M et al. Epigenetic variation between human induced pluripotent stem cell lines is an indicator of differentiation capacity. Cell Stem Cell 2016;19:341–354.
56 Fujiwara M, Yan P, Otsuji T et al. Induction and enhancement of cardiac cell differentiation from mouse and human induced pluripotent stem cells with cyclosporin-A. PLoS One 2011;6:e16734.
57 Quarto N, Li S, Renda A et al. Exogenous activation of BMP-2 signaling overcomes TGFβ-mediated inhibition of osteogenesis in marfan embryonic stem cells and marfan patient-specific induced pluripotent stem cells. Stem Cells 2012;30:2709–2719.
58 Aberdam E, Barak E, Rouleau M et al. A pure population of ectodermal cells derived from human embryonic stem cells. Stem Cells 2008;26:440–444.
59 Guenou H, Nissan X, Larcher F et al. Human embryonic stem-cell derivatives for full reconstruction of the pluristratified epidermis: A preclinical study. Lancet 2009;374: 1745–1753.
60 DaCosta Byfield S, Major C, Laping N et al. SB-505124 is a selective inhibitor of transforming growth factor-β type I receptors ALK4, ALK5, and ALK7. Mol Pharmacol 2004; 65:744–752.

See www.StemCells.com for supporting information available online.

 